



Homogeneous and heterogeneous Fenton and photo-Fenton processes : impact of iron complexing agent ethylenediamine-N,N'-disuccinic acid (EDDS)

Wenyu Huang

► To cite this version:

Wenyu Huang. Homogeneous and heterogeneous Fenton and photo-Fenton processes : impact of iron complexing agent ethylenediamine-N,N'-disuccinic acid (EDDS). Other. Université Blaise Pascal - Clermont-Ferrand II, 2012. English. NNT : 2012CLF22241 . tel-00788822

HAL Id: tel-00788822

<https://theses.hal.science/tel-00788822>

Submitted on 15 Feb 2013

HAL is a multi-disciplinary open access archive for the deposit and dissemination of scientific research documents, whether they are published or not. The documents may come from teaching and research institutions in France or abroad, or from public or private research centers.

L'archive ouverte pluridisciplinaire **HAL**, est destinée au dépôt et à la diffusion de documents scientifiques de niveau recherche, publiés ou non, émanant des établissements d'enseignement et de recherche français ou étrangers, des laboratoires publics ou privés.

Numéro d'Ordre : D.U. 2241

UNIVERSITE BLAISE PASCAL

U. F. R. Sciences et Technologies

ECOLE DOCTORALE DES SCIENCES FONDAMENTALES

N°: 715

THESE EN COTUTELLE

Avec l'Université de Wuhan (Chine)

Présentée pour obtenir le grade de

DOCTEUR D'UNIVERSITE

Spécialité : Chimie Physique et chimie de l'environnement

Par

Wenyu HUANG

Diplômée de Master

**Homogeneous and heterogeneous Fenton and photo-Fenton processes : Impact of iron complexing agent
Ethylenediamine-N,N'-disuccinic acid (EDDS)**

Soutenue publiquement le 25 mai 2012, devant la commission d'examen.

Président:

Pr. Hui ZHANG

Examineurs:

Dr. Marcello BRIGANTE

Pr. Jean-Marc CHOVELON

Dr. Gilles MAILHOT

Pr. Zongping WANG

Pr. Feng WU

Abstract

Advanced oxidation processes (AOPs) can be successfully used in the field of wastewater treatment to reduce toxicity, to convert toxic and biorecalcitrant contaminants into biodegradable by-products, to remove color or to reach the complete mineralization of organic pollutants. Fenton and photo-Fenton processes that employ hydrogen peroxide (H_2O_2) and iron species have been extensively studied over the last two decades.

However, under neutral pH conditions a low efficiency of such systems is observed. This low efficiency is mainly due to the presence of insoluble forms of Fe(III) under neutral pH conditions which produce very low yield in the presence of H_2O_2 . In fact, most of the iron in natural waters exists in the form of insoluble ferric oxides and (hydr)oxides. The concentration of dissolved iron is very low and most of the dissolved iron is associated with strong organic ligands in natural waters. Polycarboxylates such as citrate, malonate, and oxalate are common constituents of precipitation, fog, surface waters and soil solutions. Polycarboxylates can form strong complexes with Fe^{3+} and enhance the dissolution of iron in natural water through photochemical processes. Moreover, such polycarboxylate complexes undergo rapid photochemical reactions under sunlight irradiation leading to the formation of oxidative species. Therefore, research into the photochemistry of iron complexes is very important, since it substantially affects the speciation of iron in surface waters and the biogeochemical cycle of iron and other elements.

Aminopolycarboxylic acids (APCAs) may present behavior similar to that of polycarboxylic acid. Among the APCAs, ethylenediaminetetraacetic acid (EDTA) has been the most widely used chelating agent for these processes. The addition of EDTA was used to extend the useful range of the Fe(III)/ H_2O_2 system to neutral pH conditions preventing iron precipitation and so producing more oxidant species. But due to its low biodegradability, EDTA is emerging as a contaminant of concern. Very recently our group started to work with a new complexing agent of iron, the Ethylenediamine-*N,N'*-disuccinic acid (EDDS). EDDS is a structural isomer of EDTA, and exists as three stereo isomers, namely [S,S]-EDDS, [R,R]-EDDS and [R,S/S,R]-EDDS. Among them, [S,S]-EDDS is

readily biodegradable. It has been proposed as a safe and environmentally benign replacement for EDTA for environmental remediation products as it is also a strong complexing agent. Our laboratory has studied the physicochemical properties of the Fe(III)-EDDS complex. And the result demonstrates that this complex is stable in aqueous solution under neutral pH condition and photochemically efficient.

Bisphenol A (BPA) is a chemical widely used in production of epoxy resins and polycarbonates, and especially abundant in PVC plastics. The market of BPA has been growing with the increasing demand for polycarbonates and epoxy resins. It is one of the highest production-volume chemicals. The presence of BPA in food is of special concern since it constitutes the primary route to human exposure. Due to health risks it may pose to humans and other biota, BPA has engendered much controversy. BPA is classified as an endocrine disruptor and can be the cause of different diseases.

In this work, BPA was used as a model pollutant to investigate the homogeneous and heterogeneous Fenton and photo-Fenton process in the presence of Fe(III)-EDDS complex. Main experiment contents and conclusions of this dissertation are as follows:

In the first part, EDDS (Ethylenediamine-*N,N'*-disuccinic acid) was used in the homogeneous Fenton process. The effect of H₂O₂ concentration, Fe(III)-EDDS concentration, pH value and oxygen concentration on the homogeneous Fenton degradation of BPA used as a model pollutant, was investigated. Surprisingly, the performance of BPA oxidation in an EDDS-driven Fenton reaction was found to be much higher at near neutral or basic pH than at acidic pH. Inhibition and probe studies were conducted to ascertain the role of several radicals (e.g. $\cdot\text{OH}$, $\text{HO}_2\cdot/\text{O}_2\cdot^-$) on BPA degradation. These results suggested that this unexpected effect could be due to the formation of $\text{HO}_2\cdot$ or $\text{O}_2\cdot^-$ radicals as a function of pH, while the hydroxyl radical was shown to be mainly responsible for BPA degradation. Indeed, the reduction of Fe(III)-EDDS to Fe(II)-EDDS by superoxide radical anions is a crucial step that governs the efficiency of the proposed Fenton process. In addition to its ability to maintain iron in soluble form, EDDS acts as a -superoxide radical-promoting agent, enhancing the generation of Fe(II) (the rate limiting step) and therefore the production of $\cdot\text{OH}$ radicals.

In the second part of the work, the use of Fe(III)-EDDS in homogeneous photo-Fenton system as an iron source was reported. The performance of this system was followed through the formation of the $\bullet\text{OH}$ radical and the degradation of BPA. It was observed that Fe(III)-EDDS can enhance the efficiency of both $\bullet\text{OH}$ radical formation and BPA degradation especially near neutral pH. The effect of H_2O_2 concentration, Fe(III)-EDDS concentration, pH value and oxygen concentration on the BPA degradation during this photo-Fenton system was investigated. It was observed that O_2 is an important parameter affecting the efficiency of this process not only due to its reactivity with BPA but also because of its effect on the iron species present in solution. Comparison with iron complexes of oxalate, citrate and EDTA have demonstrated that Fe(III)-EDDS is a very efficient iron source for this photo-Fenton process. This work also demonstrates that Fe(III)-EDDS plays a positive role in the photo-Fenton system, especially at higher pHs, and makes this system an encouraging method for the treatment of organic pollutants in the natural environment.

In the third part, the effect of EDDS on heterogeneous Fenton and photo-Fenton system using goethite as iron source was tested. For this aim, batch experiments including adsorption of EDDS and BPA on goethite, H_2O_2 decomposition, dissolved iron measurement and BPA degradation were conducted. It was observed that the addition of EDDS inhibited the heterogeneous Fenton degradation of BPA but also the formation of hydroxyl radical. The presence of EDDS decreases the reactivity of goethite toward H_2O_2 , because EDDS adsorbs strongly onto the goethite surface and alters catalytic sites. However, the addition of EDDS can enhance the heterogeneous photo-Fenton degradation of BPA at low H_2O_2 concentration and pH around 6. The effect of goethite dose, H_2O_2 concentration, EDDS concentration and pH value on the heterogeneous photo-Fenton degradation of BPA was then evaluated. The impact of Fe-EDDS complex on iron cycling both in liquid phase and on the solid surface of iron oxide through generation of different kinds of radicals play the key role in determining the efficiency of heterogeneous Fenton oxidation.

Finally, the products of BPA degradation in homogeneous and heterogeneous systems were

detected respectively. It is found that BPA degradation in homogeneous system was initiated from the disconnection between two benzene rings, then a sequence of reactions followed and the degradation of BPA was achieved. Whereas in heterogeneous photo-Fenton system, besides the same scheme in homogeneous system, there is another possible degradation pathway proposed.

Key words: Fenton, photo-Fenton, Fe(III)-EDDS, BPA, OH radicals, Goethite

Acknowledgement

This project has been carried out within the framework of the cooperation program, between Wuhan University and Blaise Pascal University. One part of my work was performed in the Environmental photochemistry laboratory of Wuhan University directed by Prof. Feng WU and Prof. Nansheng DENG, the other part was carried out in the Laboratoire de Photochimie Moléculaire et Macromoléculaire UMR CNRS 6505 from Blaise Pascal University led by Dr. Claire RICHARD. I would sincerely like to thank them for providing the good experimental conditions, supervision, and help.

I would like to express my thanks to Prof. Feng WU and Prof. Nansheng DENG who directed my study in Wuhan University and gave me a lot of help and support during my whole study period. Their professional spirit gave me a lot of encouragement. Without them, I could not get this chance to study both in Wuhan and Clermont-Ferrand.

I want to say thank you to Dr. Gilles MAILHOT and Dr. Marcello BRIGANTE who directed my experiments in France and help me to finish all my papers and thesis. Both of them always gave me helpful suggestion and idea for the whole study, their hard-working gave me deep impression and influenced me very much. And they also help me a lot both in my application to study in France and in my life time during my stay in Clermont-Ferrand.

I also want to thank sincerely Mr. Xiaofei XUE, Ms. Yixin LIN, Ms. Beibei WANG, Ms. Jing LI, Mr. Xu ZHANG, Mr. Li GUO, Mr. Xuwei WU, Mr. Lijie BAI, Mr. Zhiping WANG, Ms. Li QIN, Ms. Yajie WANG, Ms. Chunyan DENG, Ms. Cong REN, Ms. Rui SHI, Ms. Yan WANG, Ms. Junhong HE, Mr. Xingwen WANG and Mr. Zhaohuan MAI who are my colleagues in the laboratory and friends in Wuhan University. I am very grateful to Mrs. Mei Xiao and Mrs. Lin Zhang, who give me many help in Wuhan University.

I also wish to express my thanks to all members of the laboratory in France Mr. Mohamed SARAKHA, Mr. Guillaume VOYARD, Mr. Jean-Philippe DEBOUT, Mr. Pascal WONG WAH CHUNG, Mrs. Alexandra TER HALLE, Mr. Ghislain GUYOT, Ms. Marie SIAMPIRINGUE, Ms. Sarka PAUSOVA, Ms. Shirin MONADJEMI, Ms. Rungsima

CHOLLAKUP, Ms. Eliana SILVA, Ms. Monica MABSILVA, and to the people that I forgot the name and that I have not mentioned. Thanks for their friendship and help for me when I stay in Blaise Pascal University. And I also take this opportunity to thank my friends who live in France for their kindly help. They are Yibo CHEN, Rui HUANG, Yuan WANG, Beilin LIU, Ying WANG, Weiyi SHI, Jian YANG et al.

Thanks for the fund support of China Scholarship Council (CSC) affiliated with the Ministry of Education of the P. R. China. Thanks also go to the Education Service of China Embassy in Paris.

Finally, I would like to express my deepest gratitude and love to my parents, without their supports and help, I cannot finish this thesis, I love you so much!

CONTENTS

A. Introduction.....	1
B. Bibliography study.....	4
B-1. Iron in water.....	4
B-1-1. Iron distribution in water.....	4
B-1-2. Iron species in water and their corresponding reactivity and photoreactivity.....	5
B-1-3. Chemical pollutants removal based on iron photoreactivity.....	7
B-2. Iron complexes.....	7
B-2-1. Iron-Polycarboxylates complexes.....	7
B-2-2. Iron-Aminopolycarboxylic acids complexes.....	10
B-3. Ethylenediamine-N,N'-disuccinic acid (EDDS).....	13
B-3-1. EDDS: one of naturally occurring APCAs.....	13
B-3-2. Fe(III)-EDDS.....	16
B-4. Iron Oxides.....	18
B-4-1. Structure and properties of iron oxides.....	18
B-4-2. Goethite.....	20
B-5. Reactivity and photoreactivity of iron oxides.....	22
B-5-1. Catalytic decomposition of hydrogen peroxide on iron oxide surface.....	22
B-5-2. Photoreactivity of iron oxides.....	23
B-6. Advanced oxidation processes (AOPs).....	28
B-6-1. General description of AOPs.....	28
B-6-2. Photochemistry related to AOPs.....	29
B-6-3. AOPs based on iron species.....	32
B-6-4. Fenton and photo-Fenton processes.....	32
B-6-5. Iron complex used in Fenton and photo-Fenton processes.....	36
B-6-6. Iron oxides used in Fenton and photo-Fenton processes.....	37
B-7. Endocrine disrupting compounds.....	40
B-7-1. Bisphenol A as a kind of typical EDCs.....	41
B-7-2. BPA degradation summary.....	44
C. Materials and Methods.....	45
C-1. Reagents.....	45
C-2. Preparation of Materials and Solutions.....	46
C-2-1. Synthesis of Goethite.....	46
C-2-2. Preparation of Stock Solutions.....	46
C-2-3. Preparation of reaction solution.....	49
C-3. Reaction Process.....	49
C-3-1. Actinometry.....	49
C-3-2. Fenton process using Fe(III)-EDDS complex.....	51

C-3-3. Photo-Fenton process using Fe(III)-EDDS complex.....	51
C-3-4. Heterogeneous Fenton process using goethite.....	52
C-3-5. Heterogeneous photo-Fenton process using goethite.....	53
C-4. Analysis methods.....	53
C-4-1. Goethite.....	53
C-4-2. Chemicals analysis.....	54
C-4-2-1. Spectroscopic methods.....	54
C-4-2-2. Chromatographic methods.....	54
C-4-2-3. Dosage methods.....	55
C-4-2-4. Cyclic voltammetry measurements.....	61
C-4-2-5. Products determination in different reaction system using GC-MS detection.....	62
D. Result and discussion.....	64
D-1. Physicochemical properties of BPA, Fe(III)-EDDS and Goethite.....	64
D-1-1. Properties of Bisphenol A.....	64
D-1-2. Properties of Fe(III)-EDDS complex.....	67
D-1-3. Characterization of goethite.....	71
D-1-4. Normalized of emission spectrum of the lamps.....	72
D-2. BPA degradation in homogeneous Fenton system using Fe(III)-EDDS.....	73
D-2-1. Effect of the Fe(III) complexation.....	73
D-2-2. Effect of H ₂ O ₂ concentration.....	75
D-2-3. Effect of Fe(III)-EDDS complex concentration.....	77
D-2-4. Effect of oxygen.....	78
D-2-5. Effect of pH value.....	79
D-2-6. Implication of radical species in the Fenton process.....	82
D-2-7. Comparison with other Fe(III) complex.....	86
D-2-8. Effect of EDDS concentration.....	88
D-2-9. Conclusion.....	89
D-3. BPA degradation in homogeneous photo-Fenton process.....	90
D-3-1. Photochemical degradation of BPA in the presence of Fe(III).....	90
D-3-2. Degradation of BPA in traditional photo-Fenton process.....	91
D-3-3. Photochemical degradation of BPA in the presence of Fe(III)-EDDS.....	91
D-3-3-1. Effect of pH value.....	92
D-3-3-2. Effect of Fe(III)-EDDS concentration.....	93
D-3-4. Degradation of BPA in photo-Fenton process in the presence of Fe(III)-EDDS.....	94
D-3-4-1. Photodegradation of BPA experiments in different systems.....	94
D-3-4-2. OH radical production comparison at pH 6.2.....	97
D-3-4-3. Effect of H ₂ O ₂ concentration.....	99
D-3-4-4. Effect of Fe(III)-EDDS concentration.....	101
D-3-4-5. Effect of oxygen.....	102
D-3-4-6. Effect of pH value.....	104
D-3-4-7. Comparison of Fenton and Photo-Fenton process.....	106
D-3-4-8. Comparison with different organic ligands.....	109
D-3-4-9. Implication of HO ₂ •/O ₂ •- and •OH radicals in the photo-Fenton process.....	112
D-3-5. Conclusion.....	114

D-4. BPA degradation in heterogeneous Fenton and photo-Fenton process.....	115
D-4-1. Heterogeneous Fenton process.....	115
D-4-1-1. Effect of EDDS on heterogeneous Fenton reaction.....	115
D-4-1-2. Effect of H ₂ O ₂ concentration on this Fenton system in the presence of EDDS.....	123
D-4-2. Heterogeneous photo-Fenton process.....	124
D-4-2-1. Effect of EDDS on the kinetic of heterogeneous photochemical system in the presence of goethite.....	124
D-4-2-2. Effect of goethite-EDDS complexation on the heterogeneous photo-Fenton process.....	126
D-4-2-3. Optimization of heterogeneous photo-Fenton system in the presence of EDDS.....	132
I. Effect of goethite dosage.....	132
II. Effect of H ₂ O ₂ concentration.....	133
III. Effect of EDDS concentration.....	135
IV. Effect of pH value.....	136
V. Comparison of different systems.....	140
D-4-3. Conclusion.....	141
D-5. Products analysis in different systems.....	142
D-5-1. Product of BPA degradation analysis in homogeneous Fenton and photo-Fenton process.....	143
D-5-2. Product of BPA degradation analysis in heterogeneous photo-Fenton process.....	148
D-5-3. Conclusion.....	154
E. Conclusion.....	155
Reference.....	158

A. Introduction

Advanced oxidation processes (AOPs) can be successfully used in the field of wastewater treatment, to convert toxic and biorecalcitrant contaminants into biodegradable by-products, to remove color or to reach the complete mineralization of organic pollutants. AOPs that employ hydrogen peroxide (H_2O_2) and iron species have extensively studied over the last two decades. Under acidic conditions ($\text{pH} \leq 3.0$), Fenton-like process converts H_2O_2 into stoichiometric amount of hydroxyl radical ($\bullet\text{OH}$)

However, under neutral pH conditions a low efficiency of such systems is observed. This low efficiency is mainly due to the presence of insoluble forms of Fe(III) under neutral pH conditions which produce very low yield of $\bullet\text{OH}$ in the presence of H_2O_2 . In fact, iron is present under a variety of forms in water ranging from soluble to colloidal and particulate species. But, most of the iron in natural waters exists in the form of insoluble ferric oxides and (hydr)oxides. The concentration of dissolved iron is very low and most of the dissolved iron is associated with strong organic ligands in natural waters.

Ethylenediamine-*N,N'*-disuccinic acid (EDDS) is a structural isomer of Ethylenediaminetetraacetic acid (EDTA). It has been proposed as a safe and environmentally benign replacement for EDTA for environmental remediation products as it is also a strong complexing agent. Our laboratory has studied the physicochemical properties of the Fe(III)-EDDS complex. Fe(III) is complexed by EDDS with a ratio 1:1. As a contrary of other iron-complexes, the quantum yield of $\bullet\text{OH}$ radical formation was higher at higher pHs between 3.0 and 9.0. This result demonstrates that this complex is stable in aqueous solution under neutral pH condition and photochemically efficient.

Bisphenol A (BPA) is a chemical widely used in production of epoxy resins and polycarbonates, and especially abundant in PVC plastics. The market of BPA has been growing with the increasing demand for polycarbonates and epoxy resins. It is one of the highest production-volume chemicals. The presence of BPA in food is of special concern since it constitutes the primary route to human exposure. Due to health risks it may pose to

humans and other biota, BPA has engendered much controversy. BPA is classified as an endocrine disruptor and could be the cause of different diseases. As a result, the research of BPA degradation in environment is of great importance.

The objective of this work is to understand the effect of EDDS on homogeneous and heterogeneous Fenton and photo-Fenton process in the degradation of BPA and the generation of $\bullet\text{OH}$ radical, in order to enhance the efficiency of Fenton and photo-Fenton processes especially at neutral pH condition and prevent from the iron precipitation in the whole system.

In the first part of our work, use of Fe(III)-EDDS in homogeneous Fenton process was investigated. We used BPA as a model pollutant to investigate the efficiency of Fenton process. The main influencing factors, such as pH, the concentrations of Fe(III)-EDDS, H_2O_2 and O_2 were examined. Our research work of this part was also focused on the formation of reactive species and more particularly on the reactivity of $\bullet\text{OH}$ and $\text{HO}_2\bullet/\text{O}_2^{\bullet-}$ radicals. And the generation of $\bullet\text{OH}$ radicals was also detected in order to further understand the effect of the Fe(III)-EDDS complex on the efficiency of Fenton system.

Secondly, we investigated the efficiency of the photo-Fenton process using Fe(III)-EDDS complex/ H_2O_2 system through $\bullet\text{OH}$ generation and the degradation of BPA. The effects of parameters such as pH and the concentrations of H_2O_2 , Fe(III)-EDDS complex and oxygen have been studied. The effects of Fe(III)-oxalate, Fe(III)-citrate and Fe(III)-EDTA complexes were also measured and compared with those of the Fe(III)-EDDS complex.

Thirdly, the effect of EDDS on heterogeneous Fenton and photo-Fenton system using goethite as iron source was tested. For this aim, batch experiments including adsorption of EDDS and BPA on goethite, H_2O_2 decomposition, dissolved iron measurement and BPA degradation were conducted. And the generation of $\bullet\text{OH}$ radicals in Fenton system was evaluated in order to further detect the effect of EDDS. The effects of goethite dose, H_2O_2 concentration, EDDS concentration and pH value on the heterogeneous photo-Fenton degradation of BPA were then evaluated and the optimum condition in the heterogeneous photo-Fenton system for BPA degradation was determined.

Finally, the products of BPA degradation in homogeneous Fenton/photo-Fenton and

heterogeneous photo-Fenton processes were evaluated by GC-MS system, and the possible pathways for this degradation were then determined using the products detected in the systems.

B. Bibliography study

B-1. Iron in water

B-1-1. Iron distribution in water

Table B-1 Iron species in natural water

Site	Sample	Iron concentration ($\mu\text{mol/L}$)	Reference
Dübendorf, CH	Fog water	Dissolved Fe(III): 1.7, Fe(II): 14	2
Dübendorf, CH	Fog water	Dissolved Fe(III): 3.2~134.3	3
San Joaquin, Los Angeles, US	Fog water	Dissolved Fe(III): 1.6~115	4
Po Valley, IT	Fog water	Dissolved Fe(III): 1.0~29	5
Leeds, UK	Rain water	Dissolved Fe(III): 0.3~23, mean: 5	6
Birmendorf, CH	Fog water	Total Fe(dissolved): 0.3~91.1	7
Windermere	Surface water	Total Fe (dissolved): 0.04~0.2	8
catchment, UK	of lake (0.5m)	Total Fe (particle): 0.2~0.7	
Cunsey Beck rive, UK	River water	Total Fe (dissolved): 0.3~2.4	8
		Total Fe (particle): 1.4~4.2	
Northwest Atlantic	Sea water	Ferric ions: 4.5×10^{-3}	9
Amazon estuary,	Sea water	Ferric ions: 1.4	9
Atlantic seacoast			
Greifense lake, CH	Lake water	Total Fe: 0.1-0.2, dissolved Fe: 0.03-0.05	10
<i>Ein Ashlag, Il</i>	Spring water	Fe(II): 2.1×10^{-3}	11

As it is known to all, iron is a kind of rich element that distributes in different phases of the earth. In the Earth crust, iron is the second abundant metal following aluminum; iron also exists in living creature, and exhibits as one of the most important trace elements in human body which is essential for health; after all, iron is also one of the common compositions in natural aqueous phase, including rain, cloud water, fog, other atmospheric water and surface water. There were a lot of related reports about the iron detection in natural aqueous phase, which was partly shown in Table B-1 [1].

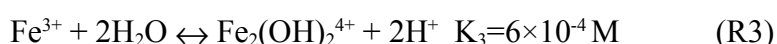
In Table B-1, it is shown that dissolved iron exists generally in several different kinds of atmospheric and surface waters; as a result, it can influence the migration and

transformation of other chemicals in the environment significantly.

B-1-2. Iron species in water and their corresponding reactivity and photoreactivity

Dissolved metal ions, especially soluble iron species, are rather common in natural water and industrial wastewater with considerable high concentration [12]. There is a large amount of related researches about the detection of total iron concentration in the atmosphere and the marine sediments [13-15]. However, the distribution of iron species in different medium hasn't been clarified in many researches yet [16]. It has been known that the iron species including Fe^{3+} , $\text{Fe}(\text{OH})^{2+}$, $\text{Fe}(\text{OH})_2^+$ and $\text{Fe}_2(\text{OH})_2^{4+}/\text{Fe}_2\text{O}^{4+}$ exist in aqueous Fe(III) salt solution [17], however, actual species in natural water depend on different conditions. Faust and Hoigné reported that based on the available equilibrium constants for Fe(III)-hydroxy complexes, $\text{Fe}(\text{OH})^{2+}$ is the dominant monomeric Fe(III)-hydroxy complex between pH 2.5 and 5 in rain, clouds, fog and probably in some acidic surface waters [18]. Furthermore, the major Fe(III) species in atmospheric water droplets, investigated by Weschler et al., which generated from $\text{Fe}(\text{OH})^{2+}$ are $[\text{Fe}(\text{OH})(\text{H}_2\text{O})_5]^{2+}$, $[\text{Fe}(\text{OH})_2(\text{H}_2\text{O})_4]^+$, and $[\text{Fe}(\text{SO}_3)(\text{H}_2\text{O})_5]^+$; the partitioning among these complexes is a function of pH [19]. And in natural water, whose pH value is in the range of 5-9, hydrated Fe(III) and Fe(II) ions are the dominant and stable form of iron, whereas when the concentration of dissolved oxygen is high enough, hydrated Fe(III) is the only inorganic form in water and other dissolved iron may exists as complexation with organic chemicals [16, 20].

In the aqueous solutions at $\text{pH} < 5$, there are at least four kinds of Fe(III) complexes with different forms, including Fe^{3+} , $\text{Fe}(\text{OH})^{2+}$, $\text{Fe}(\text{OH})_2^+$ and $\text{Fe}_2(\text{OH})_2^{4+}$. The distribution of these complex forms is described by the following equilibriums [21]:



In fact, the hydroxy complex of the oxidation state $[\text{Fe}(\text{OH})]^{2+}$, which is the abbreviated form of $[\text{Fe}(\text{OH})(\text{H}_2\text{O})_5]^{2+}$, can play the role of an oxidation reactant, because of its redox

potential of $E_h = 600-900$ mV at pH 4 [22]. As a result, the concentration ratio between $[Fe^{2+}]$ and $[Fe^{3+}]$ could be used to determine the redox potential in hydrometeors when taking the limited ranges of pH (about 3.5-6.5) and E_h (200-500 mV) in atmosphere aqueous samples into account [22-26]. On the other hand, as Fe^{2+} and Fe^{3+} could be easily complex with water, ammonia, sulfate and some organic compounds such as format, acetate and oxalate as a dominant central atom, especially, Fe^{3+} in acidic environments is octahedrally coordinated [17], iron could influence the chemical behavior by chelating forms [19, 27, 28]. The presence of iron (e.g. $Fe(OH)_2^+$) may increase the oxidation rate of some chemicals such as from S(IV) to S(VI) in complex catalytical chain reactions [26, 29]. Meanwhile, iron ions, especially Fe^{2+} , could react with H_2O_2 and produce $\bullet OH$ radicals, the mechanism of which is already quite well known, and this part will be discussed in detail in later chapter.

As long as it is known that iron is photosensitive, the effect of iron in environmental chemistry through photochemistry process is of great importance. The different products from hydrolysis of iron salts have different photochemical property. The governing hydroxy complex of iron salts at pH 2.5-5 is $Fe(OH)^{2+}$, it can generate $\bullet OH$ radicals through photolysis, and the quantum yield of $\bullet OH$ radicals is determined to be 0.075 at 360 nm [30], whereas the photochemical reduction could be shown as following:



And $Fe(II)$, photoreduced from $Fe(III)$, can be oxidized again to $Fe(III)$. Except the most reactive $Fe(OH)^{2+}$ [30], other $Fe(III)$ -OH complexes are also photosensitive.

The basic redox cycle of $Fe(III)/Fe(II)$ in aqueous solutions is shown as following:

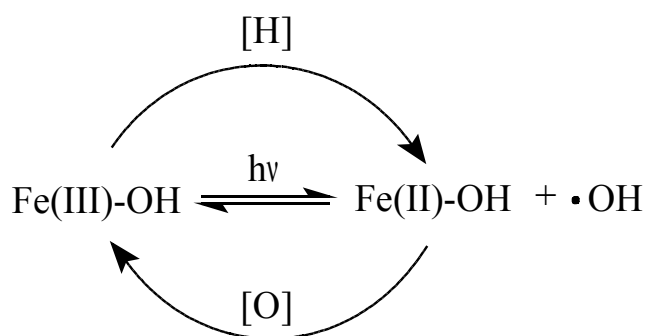


Figure B-1 $Fe(III)/Fe(II)$ -OH complex redox cycle [30]

Where [H] represents reducing agent, and [O] represents oxidant.

B-1-3. Chemical pollutants removal based on iron photoreactivity

Based on the reactivity and photoreactivity of iron in aquatic environment, removal and treatment of some organic and heavy metal pollutants were taken into researches. And it is found to be effective especially in the presence of UV irradiation, as Fe(III) aquacomplexes as a source of $\bullet\text{OH}$ radicals were proved to be efficient to induce the complete mineralization of pollutants [31]. Bolte et al. have deeply investigated photodegradation of different kinds of organic chemicals in the presence of iron salt [32-39], and proved to be effective in organic chemicals degradation/mineralization and quantum yield of $\bullet\text{OH}$ radicals formation. Meanwhile, in related researches about atmospheric chemistry, it is found that the photolysis of Fe(III)-OH complexes in atmospheric waters can lead to the production of $\bullet\text{OH}$ radicals and hydrogen peroxide (H_2O_2). H_2O_2 is the predominant source of the $\bullet\text{OH}$ radicals and hence initiate the secondary photochemical reaction, which would affect the oxidation-reduction reaction in the whole atmospheric environment and the degradation of environmental pollutants significantly.

B-2. Iron complexes

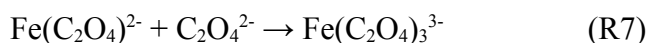
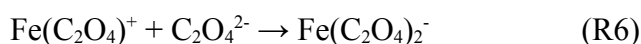
B-2-1. Iron-Polycarboxylates complexes

The carboxylate group $[\text{R}-\text{C}(\text{O})\text{O}^-]$ is one of the most common functional groups of the dissolved organic compounds, the organic chemicals that include carboxylate group called carboxylic acid and its corresponding salt usually present in natural waters [40-42]. Polycarboxylates, which contains molecules that have more than one carboxylate functional group, such as citrate, malonate, and oxalate are common constituents of precipitation, fog and surface waters and soil solutions [43-46]. Polycarboxylates can form strong complexes with Fe^{3+} and enhance the dissolution of iron in natural water through photochemical

processes.

The photolysis of Fe(III)-polycarboxylates affects the speciation of iron in atmospheric and surface waters. Moreover, such polycarboxylate complexes undergo rapid photochemical reactions under sunlight irradiation leading to the formation of oxidative species [41, 47]. As it is concluded by Martin et al., that binding of Fe^{3+} by excess citrate is already well described including $[\text{Fe}(\text{citH}_2)]^+$, $[\text{Fe}(\text{citH})]$ and $[\text{Fe}(\text{cit})]^-$ at low pH, whereas $[\text{Fe}(\text{citH})_2]^{3-}$ and $[\text{Fe}(\text{cit})]^-$ are the only species at pH 5-6 and only the latter one is present at pH 7-8 [48, 49]. However, only the $[\text{Fe}(\text{cit})_2]^{5-}$ seems to be stable in the form of $[\text{Fe}(\text{citH})_2]^{3-}$ or $[\text{Fe}(\text{cit})(\text{citH})]^{4-}$ with protonation of the uncoordinated carboxyl groups according to the precise pH [49].

As for oxalate, stable complexes formed between Fe^{3+} and oxalate in acidic atmospheric water following the reactions as [50]:



And the iron(III)-oxalate complexes species at pH range 1.5-5.5 are shown in Figure B-2:

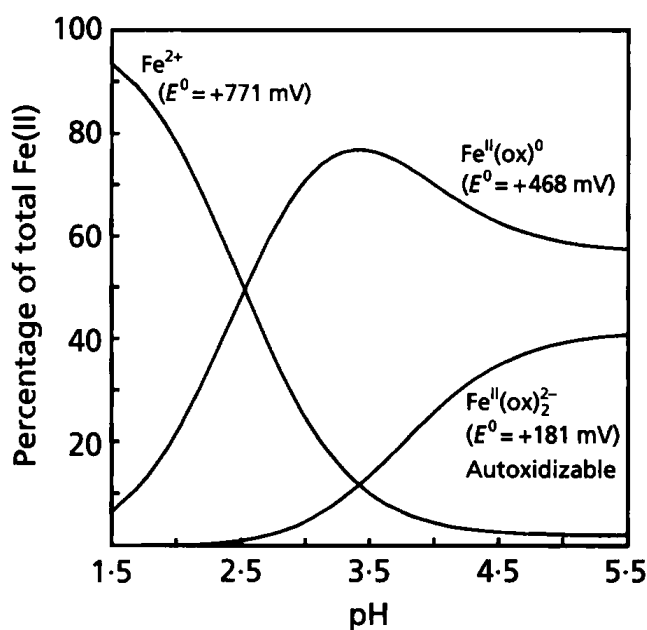
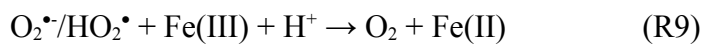
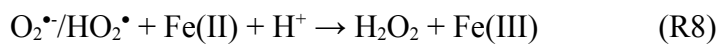


Figure B-2 Mole-fraction distribution of the Fe(III)-oxalate complexes at pH 1.5-5.5 [51]

In the presence of oxalate or citrate, the speciation of dissolved Fe(III) in aqueous solution

is found to depend on the competition between Fe(III)-oxalate/citrate complexes and Fe(III) aquacomplexes.

This complexation between iron and polycarboxylates, especially the photoreactivity of these complexes, plays important role in the movement and transformation of iron in natural environment and in organism. The photochemical behavior of these complexes has been of great interest in related research field. Faust et al declared that the photochemical redox reactions of Fe(III)-polycarboxylates in sunlight are potentially important sources of Fe(II), $O_2^{\bullet-}/HO_2^{\bullet}$, H_2O_2 and $\bullet OH$ in atmospheric water drops and surface waters [42]. It is also found that the efficiency of the Fe(III)-polycarboxylates photoreduction reaction in solution depends strongly on two factors including pH values and initial Fe to polycarboxylates ratio, and the quantum yield are in the order as: oxalate > tartrate > malate > citrate > isocitrate > succinate > formate at acidic pH [52]. At acidic pH in atmospheric water, the reduction of oxygen by intermediates formed from photoreactions of Fe(III)-oxalate complexes can produce H_2O_2 [50]. The reaction can be expressed as following:



Hence, the photochemical redox cycle of Fe(III)-polycarboxylates (oxalate as example) complexes is shown in Figure B-3:

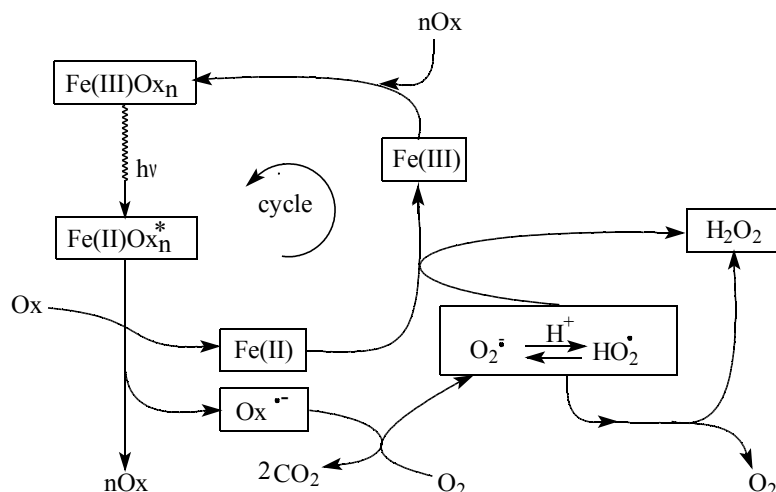


Figure B-3 Photochemical redox cycle of Fe(III)-oxalate complexes

Therefore, research into the photochemistry of iron complexes is very important, since it

substantially affects the speciation of reactive radicals in surface waters and the biogeochemical cycle of iron and other elements. And the organic chemicals degradation and heavy metal transformation in the presence of Fe(III)-polycarboxylates complexes has already been investigated by many researchers. Zuo and Hoigné announced that the presence of iron-organic compounds complexes are involved in the photochemical formation of hydrogen peroxide and other photooxidants in atmospheric waters, and depletion of dissolved organic matter and sulfur dioxide [53]. Wu et al. investigated the environmental endocrine disruptors photodegradation in the presence of Fe(III)-oxalate complexes, and found that the presence of this complex can lead to the formation of $\bullet\text{OH}$ radical and hence enhance the degradation of organic compounds [54, 55]. Hug and Laubscher investigated the photochemical reduction of chromium(VI) in the presence of Fe(III)-oxalate or Fe(III)-citrate complexes [56].

B-2-2. Iron-Aminopolycarboxylic acids complexes

Aminopolycarboxylic acids (APCAs) are a class of organic compounds that contain more than one carboxylate groups, which act as bonds to one or more than one nitrogen atoms. In fact, similar stable and water-soluble complex could be formed between iron and APCAs as the complex between iron and polycarboxylates [57], the most typical and widely used examples of which are nitrilotriacetate (NTA) and ethylenediaminetetraacetate (EDTA). Due to the complexes formed between iron and APCAs, APCAs can also solubilize and inactivate metal ions by complex formation [58]. Both NTA and EDTA can be found in sewage treatment plants [59-60] and natural water, especially in European rivers the concentration of NTA and EDTA are in the range of 0-20 and 0-60 $\mu\text{g/L}$, respectively [61-63].

NTA can form 1:1 complexes with metal ions by establishing three chelate rings with four co-ordination sites of the metal occupied by NTA, since it contains four donor atoms and is so-called quadridentate chelating ligand [64]. Whereas EDTA can form an octahedral complex ideally as EDTA contains six donor atoms and acts as a hexadentate ligand [65].

Since the reactivity, especially photoreactivity of iron-NTA/EDTA can play important impact on the movement and transformation of chemicals in the environment; there are already done many related researches reported. For Fe(III)-NTA complex, it is reported to be photosensitive and the half-life of which under the irradiation of sunlight is determined to be approximately 1.5 h, the photodegradation products of this complexes are verified to be iminodiacetic acid (IDA) as intermediate whereas CO₂ and HCHO as final products [66-68], this decomposition may result from the charge transfer from metal to ligand, which lead to the metal reduction and ligand radical formation [57].

Among the complexes formed between EDTA and metals, Fe(III)-EDTA is obviously proved to be the most photosensitive [69]. Related researches revealed that the decay of Fe(III)-EDTA under UV irradiation depends strongly on the wavelength of irradiation and the pH value of environment, as it is reported that the half-life of Fe(III)-EDTA in surface waters ranges from 11.3 min to more than 100 h, which depend on the different light conditions employed [70-72]. And the intermediate and decay pathways of photodegradation of Fe(III)-EDTA complex depends significantly on the oxygen of the system [73]. The mechanism pathway of the secondary thermal reactions proceeding in deoxygenated (i) and oxygenated (ii) solutions of [FeEDTA(H₂O)]⁻ in a consequence of the LMCT excitation is shown in Figure B-4.

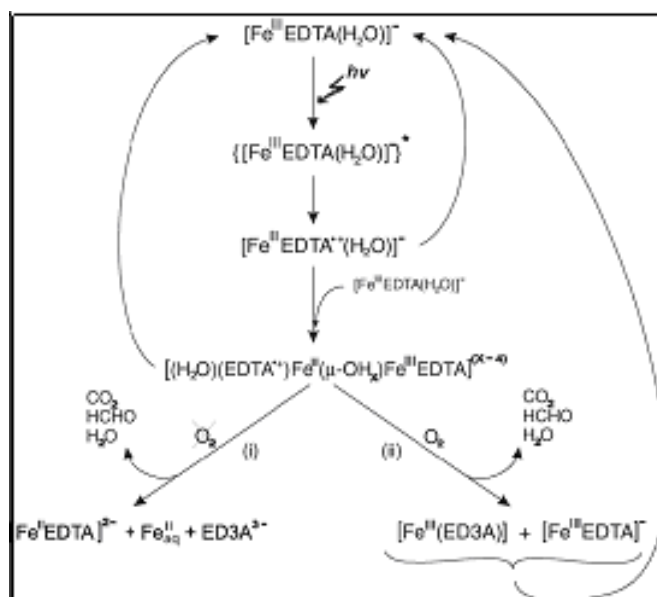
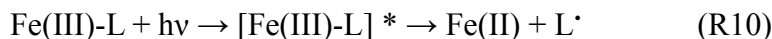


Figure B-4 Mechanistic pathways of the secondary thermal reactions proceeding in deoxygenated

(i) and oxygenated (ii) solutions of $[\text{FeEDTA}(\text{H}_2\text{O})]^-$ in a consequence of the LMCT excitation.

(Mechanism of the reactions in the case of the $[\text{Fe}(\text{OH})\text{EDTA}]^{2-}$ complex is supposed to be analogous.) [73]

It has also been certificated that the presence of Fe(III)-EDTA complex can enhance the production of reactive radicals in aqueous solutions especially at neutral pH [74]. As the photolysis of Fe(III)-EDTA is initiated by the ligand-to-metal charge transfer (LMCT) reactions (reaction (10)), which is followed by the reaction (reaction (11)) that the reducing radical reacts with Fe(III) species or O_2 to form Fe(II) species or $\text{O}_2^{\bullet-}$ [73], and the following reaction sequence between Fe(III)/Fe(II) and $^{\bullet}\text{O}_2^-/\text{HO}_2^{\bullet}$ lead to more reactive species generation [75].



As it is achieved from above that the complexes of metal ions and different APCAs would have different stability. The stability constant of 1:1 complexes of NTA, EDTA and [S, S]-Ethylenediamine-N,N'-disuccinic acid (EDDS) (for details see next chapter) with di- and trivalent metal ions was shown in Table B-2.

Table B-2 Stability constants (log K) of 1:1 complexes of NTA, EDTA and [S, S]-EDDS with di- and trivalent metal ions determined for an ionic strength of 0.1 mol/L [57]

	NTA	EDTA	EDDS
Mg^{2+}	5.5	8.8	5.8
Ca^{2+}	6.4	10.6	4.2
Mn^{2+}	7.5	13.8	9.0
Zn^{2+}	10.7	16.4	13.5
Co^{2+}	10.4	16.3	14.1
Cu^{2+}	12.9	18.7	18.4
Pb^{2+}	11.3	17.9	12.7
Cd^{2+}	9.8	16.4	10.8
Al^{3+}	11.4	16.5	
Fe^{2+}	8.3	14.3	
Fe^{3+}	15.9	25.0	22.0
Ni^{2+}	11.5	18.5	16.8

It is demonstrated that Fe(II)/Fe(III)-EDTA complexes have a significant role in producing

harsh oxidants from dissolved oxygen [76]. And there is also previous research certifying that pH adjustment would be not necessary in a Fe(III)-EDTA system compared to traditional Fenton reagent [77], which means photochemical system using Fe(III)-EDTA is available in wider pH range. Based on the reasons knowing from above, several previous researches focused on the photodegradation of different organic chemicals and phototransformation of heavy metals in the presence of Fe(III)-EDTA especially at neutral pH were carried out. Noradoun et al. investigated the photodegradation of 4-chlorophenol and 4-chlorophenol mixture in the presence of Fe(III)-EDTA complex [78], whereas the coexisting system in the presence of organics and different heavy metals was investigated, and it is found that both organics and heavy metals could be efficiently removed [79]. However, neither conventional chemical nor biological wastewater treatment removes effectively EDTA [80], so it is not so easy to remove it from aqueous solution. Same kinds of work were performed very recently by Dao and De Latt [81] with Fe(III)-nitrolotriacetate (NTA) complex. They demonstrated the efficiency of such system for the degradation of organic pollutant at pH = 7.0. Some other groups used inorganic complexing agent of Fe(III) like phosphotungstate ($\text{PW}_{12}\text{O}_{40}^{3-}$) to extend the working pH range until 8.5 [82]. The advantage of such complexing agent is to avoid the oxidant species scavenged that could be observed with the use of organic ligand.

B-3. Ethylenediamine-N,N'-disuccinic acid (EDDS)

B-3-1. EDDS: one of naturally occurring APCAs

Very recently our group started to work with a new complexing agent of iron EDDS. EDDS is a structural isomer of EDTA, has two chiral centers and exists as three stereoisomers, namely [S,S]-EDDS, [R,R]-EDDS and [R,S/S,R]-EDDS. As it is reported in the previous research, [S,S]-EDDS is readily biodegradable, while the [R,S/S,R] and [R,R] stereoisomers are less biodegradable [83].

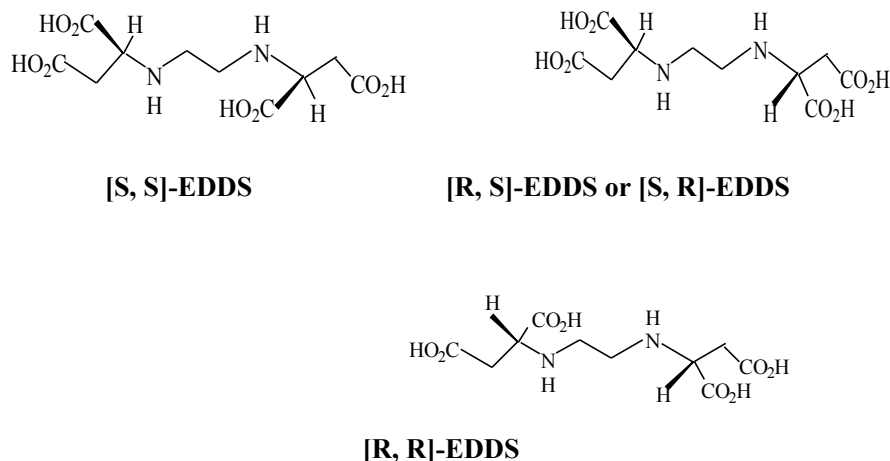


Figure B-5 Chemical structures of three different stereoisomers of EDDS [84]

As shown in Figure B-5, the molecule of EDDS contains four carboxyl functional groups, consequently, EDDS ionization equilibrium in the solutions is described as following reactions (R12)-(R15). For simplification, EDDS molecules were represented as H_4A .



So EDDS has four pK_a (25°C, 0.1 mol/L KNO_3) achieved in previous research [85].

Using the following equations (E1)-(E5) and the equilibrium constants showing above, the distribution diagram is calculated and shown in Figure B-6. It is found that $[H_3A^-]$, $[H_2A^{2-}]$ and $[HA^{3-}]$ are the dominate species at pH ranging from 2.4 to 3.9, 3.9 to 6.8 and 6.8 to 9.8, respectively [85]. The other properties of EDDS are shown in Table B-3.

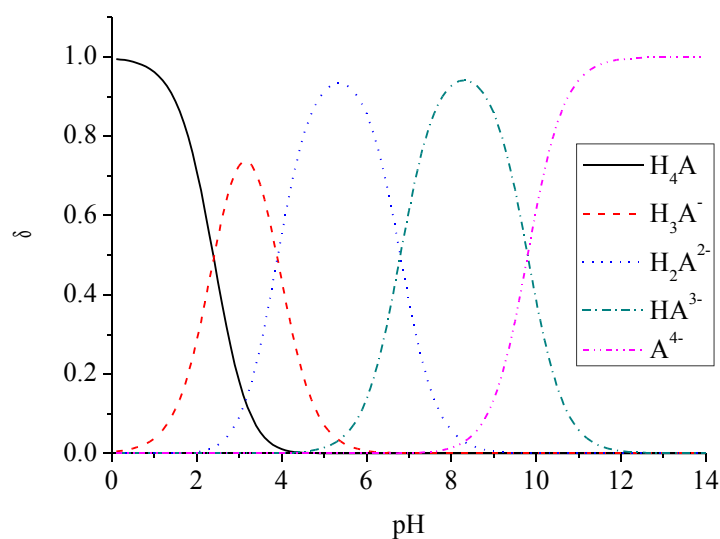


Figure B-6 Distribution diagram of EDDS aqueous solution as a function of pH values range from 0 to 14, calculated with equilibrium constants at 25°C [86].

$$\delta_0 = \frac{[H_4A]}{C} = \frac{[H^+]^4}{[H^+]^4 + K_1[H^+]^3 + K_1K_2[H^+]^2 + K_1K_2K_3[H^+] + K_1K_2K_3K_4} \quad (E1)$$

$$\delta_1 = \frac{[H_3A^-]}{C} = \frac{K_1[H^+]^3}{[H^+]^4 + K_1[H^+]^3 + K_1K_2[H^+]^2 + K_1K_2K_3[H^+] + K_1K_2K_3K_4} \quad (E2)$$

$$\delta_2 = \frac{[H_2A^{2-}]}{C} = \frac{K_1K_2[H^+]^2}{[H^+]^4 + K_1[H^+]^3 + K_1K_2[H^+]^2 + K_1K_2K_3[H^+] + K_1K_2K_3K_4} \quad (E3)$$

$$\delta_3 = \frac{[HA^{3-}]}{C} = \frac{K_1K_2K_3[H^+]}{[H^+]^4 + K_1[H^+]^3 + K_1K_2[H^+]^2 + K_1K_2K_3[H^+] + K_1K_2K_3K_4} \quad (E4)$$

$$\delta_4 = \frac{[A^{4-}]}{C} = \frac{K_1K_2K_3K_4}{[H^+]^4 + K_1[H^+]^3 + K_1K_2[H^+]^2 + K_1K_2K_3[H^+] + K_1K_2K_3K_4} \quad (E5)$$

Table B-3 Chemical and physical properties of EDDS

ethylenediamine-N,N'-disuccinic acid	
CAS number	20846-91-7
Molecular formula	C ₁₀ H ₁₆ N ₂ O ₈
Molecular weight	292.24 g/mol

Melting point	516.68 °C at 760 mmHg
Boiling point	220-222 °C
λ_{max}	none
Intensity	1.44 g/cm ³ (25°C)
logK _{ow}	-5.44 (KowWin est.)
Solubility in water	slightly soluble
Flash point	38 °C

B-3-2. Fe(III)-EDDS

EDDS has been proposed as a safe and environmentally benign replacement of EDTA for environmental remediation products as it is also a strong complexing agent [87, 88]. Our laboratory has studied the physicochemical properties of the Fe(III)-EDDS complex. Fe(III) is complexed by EDDS with a ratio 1:1 [89]. Studies of the crystal structure of the $\text{Fe}[(S,S)\text{-EDDS}]^-$ complex showed that the two five-membered NC_3OFe rings project out of the plane of the complex, reducing the equatorial ring strain that exists in the $\text{Fe}[\text{EDTA}]^-$ complex [90]. The structure of Fe(III)-EDDS complex is shown in Figure B-7 [89]:

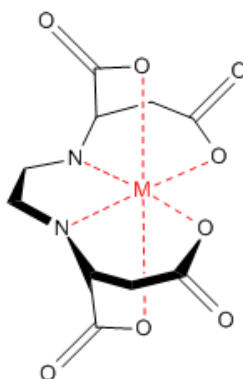


Figure B-7 Structure of Fe(III)-EDDS complex (M = Fe)

As the speciation of EDDS is different versus the change of pH, the species of Fe(III)- [S, S]-EDDS complexes at different pH is also different. The distribution of complexes is shown in Figure B-8:

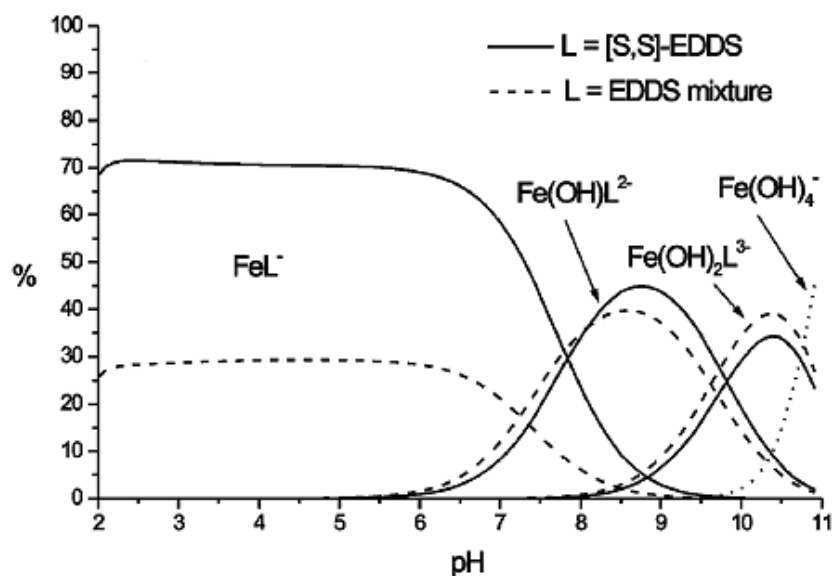


Figure B-8 Percentage distribution of different complexes versus pH for Fe(III) [91]

And the stability of Fe(III)- [S, S]-EDDS complexes at different pH comparing with different metal-[S, S]-EDDS complexes is shown in Figure B-9. The suitable pH value for Fe(III)-EDDS complex is approximately from 3 to 9.

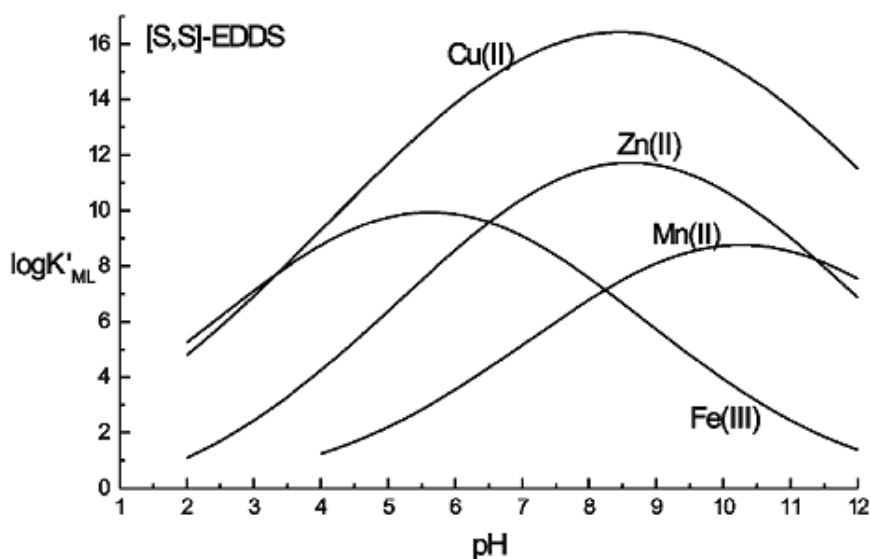


Figure B-9 Conditional stability constants for ML complexes of [S,S]-EDDS versus pH [91]

Under irradiation, Fe(III)-EDDS was easily photolyzed and the quantum yields of $\cdot\text{OH}$ formation were evaluated in different experimental conditions [92]. As a contrary of other

iron-complexes, the quantum yield of $\bullet\text{OH}$ radical formation was higher at higher pHs ranging from 3.0 to 9.0. This result demonstrates that Fe(III)-EDDS complex is photochemically efficient under neutral pH condition.

B-4. Iron Oxides

B-4-1. Structure and properties of iron oxides

It has been certificated that iron is one of the most abundant metal in the earth's crust, second after aluminum, which largely exists in the form of iron oxide, the minerals that was produced by the oxidation of Fe. Figure B-10 shows the normal distribution of iron oxides in nature and their commom roles.

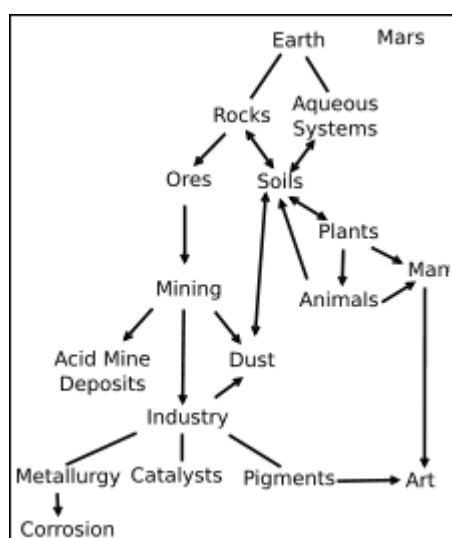


Figure B-10 distribution and role of iron oxides [93]

As composed of iron and oxygen, there are sixteen kinds of known iron oxides and hydroxides [92], since hydroxides can be expressed as the solid state of iron hydroxides, and the class of iron(III) oxide-hydroxide are oxide-hydroxides of iron, and may occur in anhydrous ($\text{FeO}(\text{OH})$) or hydrated ($\text{FeO}(\text{OH}) \cdot n\text{H}_2\text{O}$) forms. It is concluded that as far as we know iron oxides can be divided into these three sorts [93]. The sixteen natural occurring iron oxides are presented in Table B-4.

Natural iron oxides include a combination of one or more ferrous or ferric oxides, and impurities, such as manganese, clay, or organics. Synthetic iron oxides can be produced in various ways, including thermal decomposition of iron salts; precipitation to produce yellow, red, brown, and black oxides; and reduction of organic compounds by iron to produce yellow and black oxides [94]. And different kinds of iron oxides could transform into each other through hydration-dehydration and/or partial oxidation-reduction by thermal or pressure way.

As it is known from previous research that octahedron is the basic mineralogical structure of iron oxides, in this structure each iron atom is surrounded by O and/or OH ions [95]. As it is shown in Table B-4 iron(III) oxides and iron(III) oxide-hydroxides are distinguished by different Greek letters including α , β , γ , ε and δ , which symbolize different various polymorphs.

Table B-4 Natural occurring iron oxides [96]

Class	name	formula
Iron(II) oxide	wüstite	FeO
iron(II,III) oxide	magnetite	Fe ₃ O ₄
alpha phase iron(III) oxide	maghemite	α -Fe ₂ O ₃
beta phase iron(III) oxide		β -Fe ₂ O ₃
gamma phase iron(III) oxide		γ -Fe ₂ O ₃
epsilon phase iron(III) oxide		ε -Fe ₂ O ₃
iron(II) hydroxide		Fe(OH) ₂
iron(III) hydroxide	bernalite	Fe(OH) ₃
iron(III) oxide-hydroxide	goethite	α -FeOOH
	akaganéite	β -FeOOH
	lepidocrocite	γ -FeOOH
	feroxyhyte	δ -FeOOH
	ferrihydrite	FeOOH•0.4H ₂ O
		high-pressure FeOOH
	schwertmannite	Fe ₈ O ₈ (OH) ₆ (SO) ₄ ·nH ₂ O
green rusts		(Fe ^{III} _x Fe ^{II} _y (OH) _{3x+2y-z} (A ⁻) _z)

where A⁻ is Cl⁻ or 0.5SO₄²⁻

As the size of most natural occurring iron oxides is among the size less than 2 μ m, the existing forms of iron oxides in nature are usually dust in atmosphere and colloid in surface water [93]. Most of these iron oxides exist in crystal structures, and at the same time they can absorb light up to 600 nm, many of them have the properties of semiconductors and can

play the role as photocatalysts in many chemical reactions [97, 98]. When iron oxides exist in the aqueous phase, there are complex interaction including the dissolution of iron into liquid phase and adsorption of chemicals present in solution onto solid surface [99]. While there is the effect of protons, organic and inorganic ligands in liquid phase, the iron can be more easily dissolved into water and oxidized/reduced by the reaction combining with various factors [100].

According to their properties and widely distribution in the nature, iron oxides play significant effect on the chemical and biological process in the environment, and are widely utilized by humans, such as iron ores; catalysts; inexpensive, durable pigments in paints; coatings and colored concretes. At the same time, Fe(III)/Fe(II) in such kind of catalysts is quite stable and immobilized in the structure or between the interlayer of the solids, this characteristic makes the catalysts be able to maintain its ability to generate $\cdot\text{OH}$ radical and be easy to separate them from solution after treatment, and also makes catalysts reusable.

B-4-2. Goethite

Among these iron oxides, the most common used is goethite, which is one of the most thermodynamically stable iron oxides, and can be formed through the weathering of other iron-rich minerals; therefore, it is the most widespread iron oxide in soils and sediments [101]. Goethite is an iron bearing oxide mineral found in soil and other low-temperature environments. It is a kind of oxyhydroxide, and its mineral form is prismatic needle-like crystal but more typically massive [102]. The structure of Goethite including natural occurring and man-made synthesis is shown in Figure B-11[95]. And the chemical and physical properties of Goethite are shown in following Table B-5.

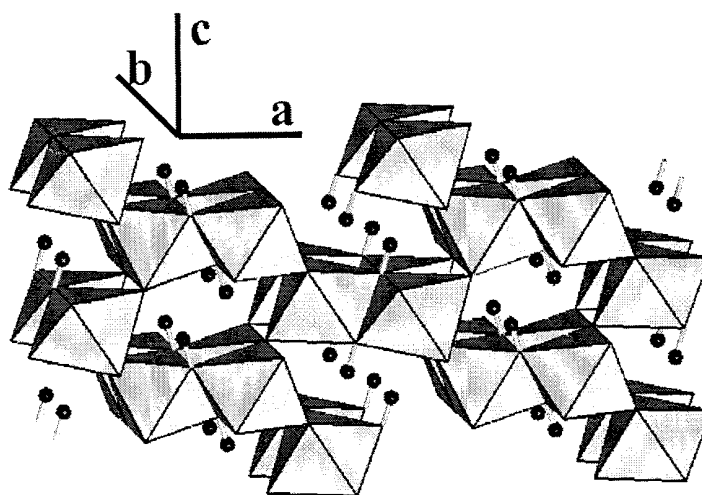


Figure B-11 Structure of Goethite (Dots represent H atoms) [95]

Table B-5 Chemical and physical properties of Goethite [103-106]

Properties	Goethite
Category	Oxide minerals
Chemical formula	α -FeO(OH)
Strunz classification	04.FD.10
Color	Yellowish to reddish to dark brown
Crystal system	Orthorhombic
Fracture	Uneven to splintery
Mohs scale hardness	5 - 5.5
Luster	Adamantine to dull
Streak	Brown, brownish yellow to orange
	yellow
Specific gravity	3.3 - 4.3
Refractive index	Opaque to sub-translucent
Fusibility	Fusible at 5 - 5.5

Like most other iron oxides, goethite is able to have affinity with anions and cations such as Cl^- , SO_4^{2-} , Al^{3+} , Zn^{2+} , Cu^{2+} , this affinity is pH dependent, because the surface charging is pH dependent [107-110].

Based on the properties of goethite shown above, it can play significant role in the biogeochemical activities such as the absorption/desorption of heavy metals, transformation of organic chemicals, cycling of micro-nutrients and uptake of toxic or nontoxic elements by fauna and flora from environment. As a result, researches about goethite have attracted great interest. Parida and Das synthesized goethite from precipitation of ferrihydrites in $\text{Fe}(\text{NO}_3)_3$ solution by the slow addition of ammonia, and made related characterization

[111], whereas goethite preparation from aerial oxidative precipitation of iron (hydrous) oxides from aqueous solutions of ferrous salts was reported by Domingo and Rodriguez-Clemente [112]. Dong et al. investigated the reduction of Fe(III) from goethite by microbial utilization to further study its impact on the iron geochemical cycling [113]. As the adsorption of organic and inorganic compounds onto Goethite was of great importance, a series of experiments were carried out. Nowack and Sigg determined the adsorption characteristics of a variety of divalent and trivalent metal–EDTA complexes onto goethite in aqueous solution [114]. Simultaneously, The adsorption and stability of arsenite [As(III)] on goethite (α -FeOOH) at varying pH and As(III) concentration was investigated [115]. Wiederhold et al. reported the dissolution of iron from goethite including proton-promoted, ligand-controlled and reductive dissolution mechanism [116]. In addition to the related researches above, a very interesting property of goethite is photoreactivity, since goethite can act as semiconductor and at the same time it contains large amount of iron, which is proved to be photosensitive and can produce reactive oxidant species under irradiation.

B-5. Reactivity and photoreactivity of iron oxides

B-5-1. Catalytic decomposition of hydrogen peroxide on iron oxide surface

The reaction between Fe(II)/Fe(III) species and H_2O_2 plays important role in the biogeochemical process in the environment, iron oxides containing Fe could also have interaction with chemicals adsorbed onto their surface and hence affect the movement and transformation of chemicals in nature.

According to the radical mechanism between iron oxides and H_2O_2 proposed by Lin and Gurol [117, 118], the reaction is initiated by the formation of an inner-sphere complex between hydrogen peroxide (H_2O_2) and $\equiv\text{Fe(III)-OH}$ groups at the oxide surface (Table B-6, Reaction (R16)), and the following mechanisms are also showed in Table B-6.

Table B-6 Radical mechanism proposed by Lin and Gurol [117]

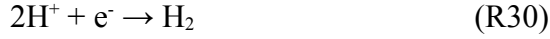
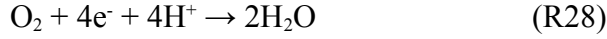
$\equiv\text{Fe(III)}\text{-OH} + \text{H}_2\text{O}_2 \leftrightarrow (\text{H}_2\text{O}_2)_s$	(R16)
$(\text{H}_2\text{O}_2)_s \leftrightarrow (\equiv\text{Fe(II)}\text{ }\bullet\text{O}_2\text{H}) + \text{H}_2\text{O}$	(R17)
$(\equiv\text{Fe(II)}\text{ }\bullet\text{O}_2\text{H}) \leftrightarrow \text{Fe(II)} + \text{HO}_2\bullet$	(R18)
$\equiv\text{Fe(II)} + \text{H}_2\text{O}_2 \xrightarrow{K_4} \equiv\text{Fe(III)}\text{-OH} + \bullet\text{OH} + \text{H}_2\text{O}$	(R19)
$\text{Fe(II)} + \text{O}_2 \xrightarrow{K_{4a}} \text{Fe(III)}\text{-OH} + \text{HO}_2\bullet$	(R20)
$\text{HO}_2\bullet \leftrightarrow \text{H}^+ + \text{O}_2^{\bullet-}$ pKa=4.8	(R21)
$\equiv\text{Fe(III)}\text{-OH} + \text{HO}_2\bullet / \text{O}_2^{\bullet-} \xrightarrow{K_6} \equiv\text{Fe(II)} + \text{H}_2\text{O} / \text{OH}^- + \text{O}_2$	(R22)
$\bullet\text{OH} + \equiv\text{Fe(II)} \xrightarrow{K_7} \equiv\text{Fe(III)}\text{-OH}$	(R23)
$\bullet\text{OH} + (\text{H}_2\text{O}_2)_s \xrightarrow{K_8} \text{Fe(III)}\text{-OH} + \text{HO}_2\bullet + \text{H}_2\text{O}$	(R24)
$(\text{H}_2\text{O}_2)_s + \text{HO}_2\bullet / \text{O}_2^{\bullet-} \xrightarrow{K_9} \equiv\text{Fe(III)}\text{-OH} + \text{H}_2\text{O} / \text{OH}^- + \bullet\text{OH} + \text{O}_2$	(R25)
$\text{HO}_2\bullet + \text{HO}_2\bullet \xrightarrow{K_{10}} (\text{H}_2\text{O}_2)_s + \text{O}_2$	(R26)
$\bullet\text{OH} + \text{HO}_2\bullet / \text{O}_2^{\bullet-} \xrightarrow{K_{11}} \text{H}_2\text{O}_2 + \text{O}_2$	(R27)

From the mechanisms above it is known that the oxidation-reduction cycle of Fe(III)/Fe(II) could enhance the efficiency of reactive radicals including $\bullet\text{OH}$ and $\text{HO}_2\bullet/\text{O}_2^{\bullet-}$ radicals. Based on this mechanism, several researches focusing on the removal and transformation of organic chemicals and heavy metals were carried out [101, 119-121].

B-5-2. Photoreactivity of iron oxides

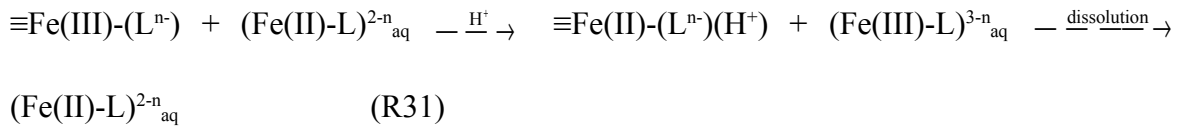
It is known that most of iron oxides have the semiconductor properties and can behave as photocatalyst though a very efficient positive holes-electrons recombination takes place [97]. As the photochemical properties of semiconductors are related to the charge transfer process, researches about the direct electron transfer of iron oxides under irradiation are implemented. Leland and Bard investigated photogenerated charge production and transfer of different iron oxides including $\alpha\text{-Fe}_2\text{O}_3$, $\alpha\text{-FeOOH}$, $\beta\text{-FeOOH}$, $\delta\text{-FeOOH}$, $\gamma\text{-Fe}_2\text{O}_3$, and $\gamma\text{-FeOOH}$, and it is found that this efficiency did not correlate with particle size and band gap [97]. Whereas the result observed from the experiments carried out by Sherman demonstrated that the band gap between the valence and conduction bands need to be less than 3.1 eV (400 nm) when photochemical reactivity can take place [122]. When the wavelength of light source is less than 400 nm, a hole (h^+) and electron (e^-) pair will be

produced in the surface of iron oxides. And the following reactions take place [122]:



If the reaction (R29) is more feasible, following oxidation of other chemicals in the system may take place.

While iron oxides solid exists in the liquid phase, there is obviously interaction between solid and aqueous solution. One of the most important parts in this process is iron dissolution from solid surface, since the dissolved iron ions can greatly enhance the reaction between iron and other compositions in liquid solutions [123]. Litter et al summarized that in the thermal dissolution, iron oxides surface Fe(III) complex are slowly transferred and dissolved into liquid phase by acid and reductive pathway until Fe(II)-L complex was built up and then strong acceleration was produced. This process could be shown as following [123-127]:



Related researches about iron photochemical dissolution from iron oxides were reported, and it is found that the presence of UV irradiation can accelerate the dissolution process, and the effect of some organic ligands such as oxalate and EDTA was also investigated [123]. Faust and Hoffmann investigated the photoinduced reductive dissolution of $\alpha\text{-Fe}_2\text{O}_3$ in colloidal suspension, the effect of bisulfite was taken into account, and it is found that Fe(III)-S(IV) complex was formed and hence affected the photoassisted charge-transfer reaction [128]. Cornell and schindler [129] explored the dissolution of iron from goethite in photochemical process and acidic oxalate solution. In this investigation a two stages reaction was concluded, as the first stage was a slow stage, whereas the second one was much faster. The iron species in the photodissolution process was detected, and the dissolution efficiency enhanced due to the increase of oxalate concentration and also depended on the pH values, the optimum condition was at pH 2.6. Wu and Deng concluded the process of photoreductive iron dissolution from FeOOH in the system containing

organic ligands as following Figure B-12 [130]:

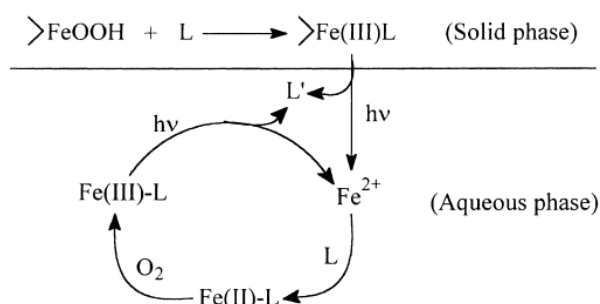
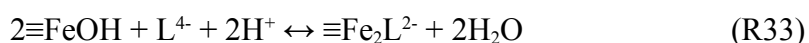
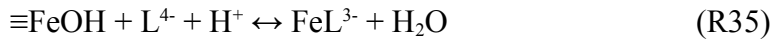


Figure B-12 Model on photoreductive dissolution of FeOOH in the system containing organic ligand. where >FeOOH represents Fe(III) oxides; L organic ligands; L' oxidized product of L [130]

The interaction of different compositions in the solid-liquid interface is quite complicated, which may be due to the migration or transformation of most chemical compounds in aqueous solutions, as a result, photodegradation of several organic compounds and phototransformation of heavy metals were investigated. First of all, investigation of adsorption of different organic chemicals and heavy metals onto the surface of iron oxides was of great importance, since this adsorption would affect the photodegradation of the target chemicals significantly. Gu et al. [131] investigated the interaction mechanism between natural organic matters and iron oxides surface, and results indicated that the dominant interaction mechanism was ligand exchange between NOM with carboxyl/hydroxyl functional group and iron oxides surface. And it is supported that a modified Langmuir model was defined to account for a decreasing adsorption affinity, which was also confirmed by other researches [97, 98, 101]. Usually, when the photodegradation of chemicals in the presence of iron oxides was investigated, adsorption researches were necessary before photodegradation examination in order to better understand the whole degradation processes.

Theoretically, the adsorption of EDTA^{4-} onto the surface of an iron(III) oxyhydroxide was generally described by Nowack and Sigg as following [114]:





$$K = \frac{[\equiv \text{Fe}_2\text{L}^{2-}]}{[\equiv \text{FeOH}]^2 \times [\text{L}^{4-}] \times [\text{H}^+]^2} \text{ or } K = \frac{[\equiv \text{Fe}_2\text{L}^{2-}]}{[(\equiv \text{FeOH})_2] \times [\text{L}^{4-}] \times [\text{H}^+]^2} \quad (\text{E6})$$

In the researches of Noren et al. [132], the adsorption of EDTA onto goethite was studied as a function of pH, time, and background electrolyte concentration at 25.0 °C experimentally. In this process, no direct interactions of these complexes with surface Fe(III) ions were detected, since it was found that two surface complexes consisting of HEDTA³⁻ and H₂EDTA²⁻ predominate at the water-goethite interface within the pH range of 3-9. And hence, most likely the surface complexes are stabilized at the interface by electrostatic and hydrogen-bonding forces.

The photocatalytic degradation and the influence of photocatalytic pretreatment on the biodegradability of 2-aminophenol using iron oxides are reported by Pulgarin and Kiwi [133]. And it seemed that the α -Fe₂O₃ reaction with aminophenol, which has electron-donating character, was only through the formation of surface complex. It is concluded in the paper that the mechanism of 2-aminophenol degradation in the presence of aerated iron oxides suspension can be attributed to the following reasons: (1) a ligand-to-metal charge transfer process on the surface of iron oxide; (2) photo Kolbe type reaction that 2-aminophenol scavenges holes and surface iron reacts with electrons; (3) •OH radicals resulting from the oxidation of surface -OH groups.

Different kinds of halogenated acetic acids affecting photoinduced reduction of a series of iron oxides including ferrihydrite (am-Fe₂O₃·3H₂O), lepidocrocite (γ-FeOOH), goethite (α-FeOOH), hematite (α-Fe₂O₃) and maghemite (γ-Fe₂O₃) were investigated by Pehkonen et al. [134], when ferrihydrite acted as electron acceptor and fluoroacetic acid as electron donor, the best efficiency was achieved.

Lei et al. reported the photodegradation of orange I in the presence of iron oxide-oxalate complex, and it is found that photodegradation of orange I depended strongly on the types of iron oxides, the initial pH value, the initial concentration of oxalate and orange I [135].

The photodegradation of bisphenol A (BPA) at the interface of iron oxides under UV irradiation was conducted by Li et al. [136]. Four different kinds of iron oxides were prepared and the results demonstrated that the photodegradation of BPA depends strongly on the properties of iron oxides and oxalate, and pH values. Furthermore, it is concluded that the dependence of BPA degradation should be also attributable to the formation of the dissolved Fe–oxalate in the solution and the adsorbed Fe–oxalate on the surface of iron oxides.

Mazellier and Sulzberger reported the diuron degradation under UV irradiation, aerated suspensions containing goethite (α -FeOOH) and oxalate [137]. And the light-induced iron cycling on goethite surface due to the presence of oxalate in this degradation process was concluded as following:

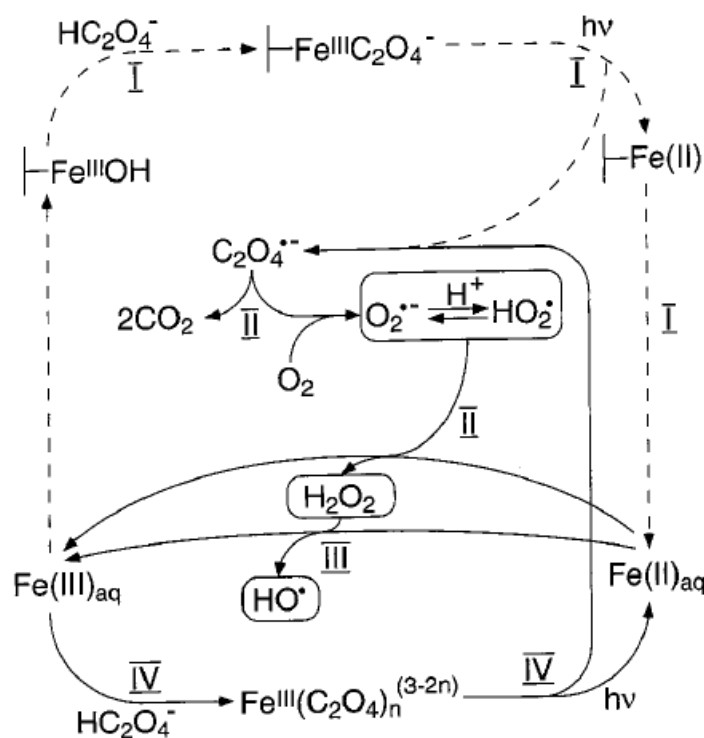


Figure B-13 Iron cycle on goethite surface in the presence of UV irradiation and oxalate [136]

It is concluded by Wu and Deng [130] that the reaction kinetics of organic compounds adsorbed onto iron oxides surface was generally in accordance with the Langmuir-Hinshelwood (L-H) equation, which was firstly concluded by Fox and Dulay that the adsorption of many organic chemicals onto solid surface was in accordance with this

equation [138]:

$$\frac{1}{r} = \frac{1}{k} + \frac{1}{(k + K) \times C} \quad (E7)$$

Where r represents photodegradation rate of the substrate, k the rate constant of pseudo-first-order reaction, K the adsorption constant, and C the concentration of the substrate.

B-6. Advanced oxidation processes (AOPs)

B-6-1. General description of AOPs

In the last few decades, the explosive development of modern industry produces quite strong negative impacts on the natural environment. The pollutants in water exhibit great changes, emerging pollutants attract great attention, which lead to fast evolution of the research activities devoted to wastewater treatments.

As a kind of safe and promising way for wastewater treatment, AOPs is attracting many interest of researches, which are defined as the processes that generate hydroxyl radicals in sufficient quantities to be able to oxidize majority of chemicals present in the effluent water. $\bullet\text{OH}$ radical is known as a kind of powerful oxidizing radical with an oxidation potential of 2.33V and demonstrates strong oxidation ability comparing to the oxidation capability of using conventional oxidants such as hydrogen peroxide or KMnO_4 [139]. And in previous research it was observed that $\bullet\text{OH}$ radical can react with most organic compounds and many inorganic chemicals with high rate constants [140-142]. For the source of $\bullet\text{OH}$ radical in AOPs, a combination of conventional strong oxidants such as ozone, oxygen or hydrogen peroxide and catalysts (e.g., transition metal, iron and copper), semiconductor solid (e.g., TiO_2 and Fe_2O_3) together with energy sources of UV-visible irradiation, ultrasound, electricity or ionizing radiation was used. The classification of AOPs is shown in Table B-7. As the emerging pollutants especially the persistent organic pollutants (POPs) emerge in the environment increasingly, there is a big challenge to the conventional biological wastewater treatment. So AOPs attract great attention in related

research field to degrade these complicated refractory molecules. In previous researches, typical AOPs including UV/O₃ [143-145], UV/TiO₂ [146-148], UV/H₂O₂ [149-151], UV/Fenton [152-154] and Electro-Fenton [155-157] processes, were investigated in the field of degradation of several chemical compounds, especially those non-biodegradable compounds including organic dyes [158-160], antibiotics [161-163], pesticides [164-166] and landfill leachates [167] in lab scale, in many cases these typical AOPs were also used as the pre-treatment to enhance the biodegradability of the compounds and followed by conventional methods [168-171]. Furthermore, some attempts of this technology application in pilot-plant scale for the removal of toxic and non-biodegradable chemicals were carried out since many years ago [172], in recent years, the work of applying this kind of technologies into actual production was taken into research [173, 174].

Table B-7. Classification of AOPs

Reaction Phase	Classification		Process
	External Energy	Generation of Hydroxyl radical	
Homogeneous	Light	Photochemical process	UV/O ₃ UV/H ₂ O ₂ UV/ H ₂ O ₂ /O ₃ UV/Fe ²⁺ (Fe ³⁺)/ H ₂ O ₂
		Sonochemical process	US/H ₂ O ₂ US/O ₃ UV/US
	Light/Ultrasound	Photochemical process	
	High-energy electron	Ionising radiation process	Electron Beam
	None	Chemical process	H ₂ O ₂ /O ₃ O ₃ / H ₂ O ₂ /high pH Fe ²⁺ /H ₂ O ₂ (Fenton)
	Electricity	Electrochemical/Chemical process	Electro-Fenton
Heterogeneous	Light	Photochemical process	UV/TiO ₂ /O ₂ UV/TiO ₂ / H ₂ O ₂
	None	Chemical process	Iron Oxide/ H ₂ O ₂

B-6-2. Photochemistry related to AOPs

Since light is a kind of green and sustainable energy, the application of light irradiation into wastewater treatment is of great interest in related research field. The basic and popular

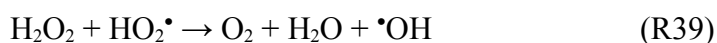
systems of this kind, excluding the application of iron, include UV/H₂O₂, UV/O₃, UV/semiconductor and photoelectrochemical processes.

The UV/H₂O₂ oxidizing ability can be attributed to the formation of •OH, O₂•⁻ and HO₂•, the reaction process is shown as following [175]:

Initiation [176]



Propagation [177, 178]

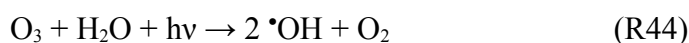


Termination [179, 180]



The reactive radicals produced in the reactions above could attack the molecules of chemicals and oxidize them. The application of UV/H₂O₂ in the removal of many different kinds of contaminants, especially azo dyes [180, 181] is common in research field and proved to be efficient.

Similarly, reactive radicals could be generated in the process of UV/O₃ as following processes and hence react with chemical molecules [182-184].



As O₃ is one compound of the composition of atmosphere, the oxidation and removal of organic chemicals in UV/O₃ system both in gas [185, 186] and liquid phase [187, 188] were investigated.

The most commonly used semiconductor in photocatalytic process is TiO₂. The photocatalytic process including TiO₂ is known to be initiated by the charge transfer process excited by UV irradiation (wavelength < 320 nm), and an electron-hole pair is produced, then the subsequent oxidation/reduction reaction is induced. The basic mechanism is shown as following Figure B-14 [189]:

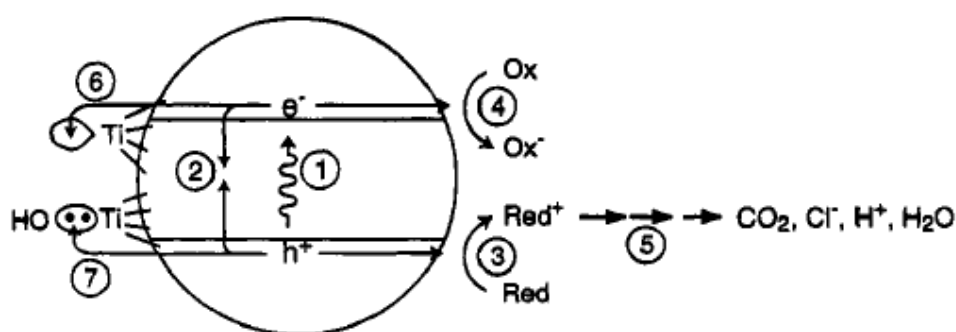


Figure B-14 basic mechanism of TiO_2 photocatalytic process [189]

In fact, photoelectrochemical process is a combination of photochemical and electrochemical processes. In the process of semiconductor photocatalysis, the high efficiency of electron-hole recombination is a major limiting factor. In order to overcome this limiting factor, photoelectrochemical process is taken into account. An external anodic bias is applied to drive the photogenerated electrons and holes in different directions so that the charge recombination is decreased [190-194]. K. Vinodgnpal et al. revealed the utilization of a porous nanocrystalline semiconductor thin film for the electrochemically assisted photocatalytic degradation of organic contaminants. The principle of this reaction is shown in Figure B-15 [195]:

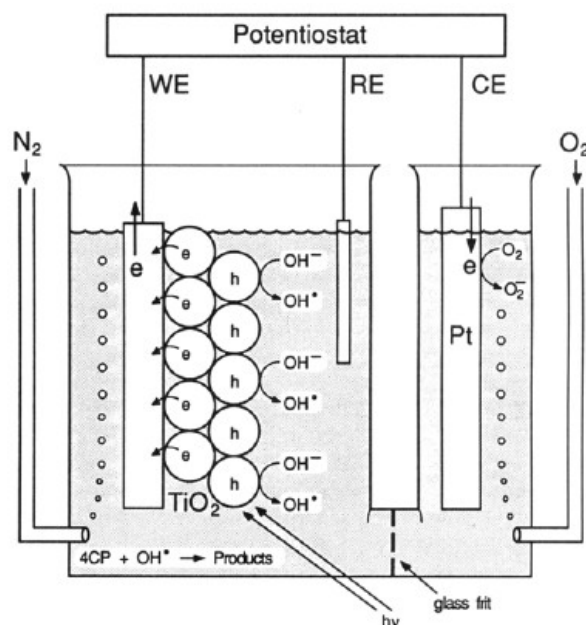


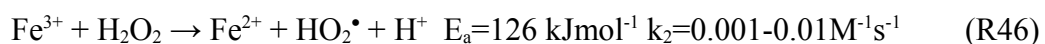
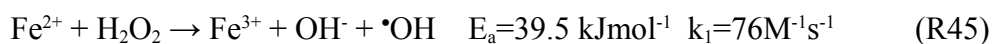
Figure B-15 Schematic Diagram of the Two-Compartment Cell Employed in the

B-6-3. AOPs based on iron species

As it is known from previous research that iron species are photosensitive and can enhance the cycling and transformation of reactive radicals in the environment, hence it could obviously be expected that iron species can be used in AOPs to participate in wastewater treatment. The processes including photochemical process employing Fe(III)/Fe(II) species, photocatalytic processes in the presence of iron oxides, Fenton and photo-Fenton processes have already been widely investigated and proved to be efficient somehow. Among all these processes, Fenton and photo-Fenton processes are the most promising and attracting methods, since this kind of process is proved to be efficient, easy to operate and low-cost.

B-6-4. Fenton and photo-Fenton processes

Among this various forms of AOPs, there is a group of typical techniques based on the Fenton reaction, including Fenton, Fenton-like, electro-Fenton and photo-Fenton systems. Fenton mainly based on the a series of chain reactions between Fe(II)/Fe(III) species and peroxide (H₂O₂) especially at acidic pH value, which is initiated by the reactions showed in Reaction (R45) and (R46) [196-198]:



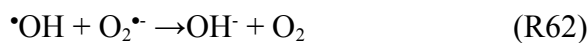
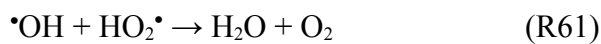
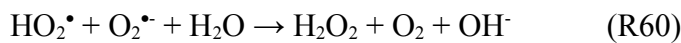
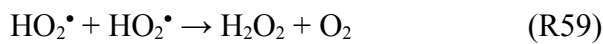
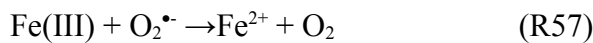
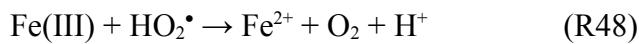
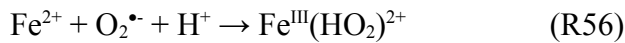
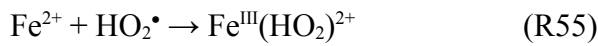
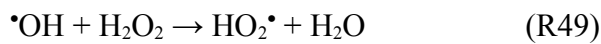
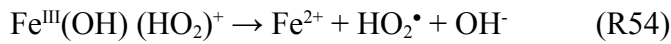
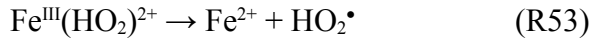
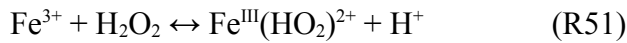
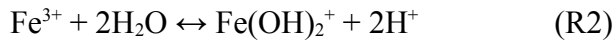
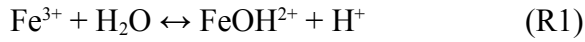
And more reactive radicals are generated or consumed by the following Reaction (R47)-(R50):



However, this mechanism is only preliminary one that could be approved by most of the researches; mechanism in detail is complicated especially at different pH and under the

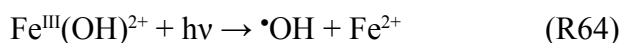
impact of many inorganic or organic ligands of iron. Many researches about the specific mechanism are still being carried out.

De Laat and Gallard investigated the mechanism of H_2O_2 catalytic by Fe(III) at acidic pH ($\text{pH} < 3$) [199]. Taking Fe(III) -hydroperoxy complexes ($\text{Fe(III)}-(\text{HO}_2)^{2+}$ and $\text{Fe(III)}(\text{OH})(\text{HO}_2)^+$) into account, a more precise mechanism was proposed. In this report, a kinetic model was used to accurately predict the decomposition of H_2O_2 by Fe(III) [199].



And at pH 3 to 7, the iron aquacomplex species changed significantly, which accounts for the coagulation capability of Fenton's reagent. Dissolved suspended solids are captured and precipitated [200], hence the whole Fenton process is retarded to a large extent.

In some researches, UV-irradiation was introduced into Fenton process, which is called as photo-Fenton system. Due to the introduction of light, there is also some supplement to the Fenton mechanism [201, 202].



As it is known to all, Fenton process was found more than 100 years ago [203], and application to destroy the structure of toxic organic compounds was started from late 1960s [204]. It is found that the Fenton reaction could be very efficient in the removal of many hazardous organic pollutants from water and could completely degrad the contaminants to harmless compounds such as CO_2 , H_2O and inorganic salts [200]. In recent decades, the mechanism of Fenton process has been widely used in inclusive number of wastewater treatments research such as (1) homogeneous Fenton and Fenton-like systems using different kinds of $\text{Fe}(\text{II})$ and/or $\text{Fe}(\text{III})$ salt and peroxide in acidic medium; (2) homogeneous photo-Fenton system by using UV irradiation to reduce $\text{Fe}(\text{III})$ to $\text{Fe}(\text{II})$; (3) heterogeneous Fenton and Fenton-like system using clay or iron oxides; (4) electro-Fenton or photo-electro-Fenton system.

So far, homogeneous Fenton and photo-Fenton systems have been widely investigated and proved to be efficient in removal of many kinds of organic chemical, especially many non-biodegradable chemicals in aqueous phase, soil and sediment. Furthermore, Fenton process can be used to actual wastewater treatment such as dye wastewater and landfill leachate due to its nonselectivity to organic chemicals [205-216]. The effect of variables such as temperature, pH value, initial concentration and inorganic ions was also determined in these related researches. The advantages and disadvantages of different homogenous Fenton system are concluded and shown in Table B-8.

Table B-8 Advantages and disadvantages in different homogeneous Fenton systems

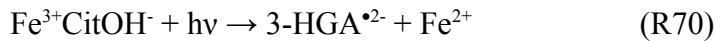
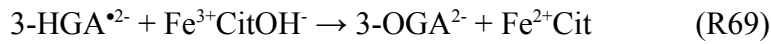
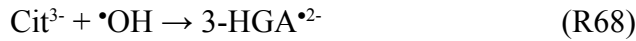
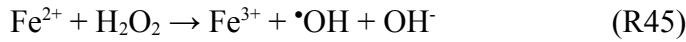
System	Advantage	Disadvantage
Fenton/Fenton-like	Simplicity: commonly available and inexpensive chemicals, no need for special equipment	Strict pH demand, easy production of iron containing sludge
Photo-Fenton	Lower chemical dosage demand, faster degradation, inexpensive	Strict pH demand, strict wavelength of light usable

Electro-Fenton	equipment Lower chemical dosage demand, faster degradation	Special and quite expensive equipments demand
Photo-electro-Fenton	Wide application pH value range, Lower chemical dosage demand, high degradation efficiency	Special and quite expensive equipments demand

When the UV irradiation is introduced into Fenton system, some of the drawbacks could be overcome due to the lower concentration of iron salt needed. Pignatello [205] compared the degradation of Chlorophenoxy Herbicides in the presence of Fe(III)/H₂O₂ with and without UV irradiation respectively, and it has been proved that the presence of UV irradiation could obviously enhance the efficiency of Fenton process in Chlorophenoxy Herbicides degradation, and photo-Fenton is a promising way for wastewater treatment. Zepp et al. reported the kinetic studies of hydroxyl radical generation promoted by photo-Fenton process (UV/Fe(III)/H₂O₂) at pH ranging from 3 to 8. And it is found that Fe²⁺ reacted with H₂O₂ under UV irradiation could produce •OH radicals at pH ranging from 3 to 8, and proved that such reactions provide a generally important pathway for oxidation in the environment and possibly for the treatment of contaminated waters [217]. Bauer and Fallmann [218] compared the efficiency of different AOPs systems including TiO₂/UV, Fe²⁺/H₂O₂/UV, Fe²⁺/O₂/UV and Fe²⁺/O₃/UV, and Fe²⁺/H₂O₂/UV system was proved to be most efficient. In this study, pilot plant experiments with industrial wastewaters treatment and with sunlight irradiation were carried out, and proved to be efficient. Finally, cost estimation showed the superiority of photo-Fenton system in wastewaters treatment. Besides, many studies of organic pollutants treatment based on photo-Fenton process were carried out, and it was practical to apply photo-Fenton system into actual wastewater treatment if the problems such as pH limitation and iron precipitation can be solved.

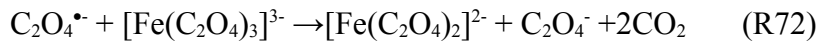
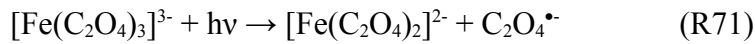
B-6-5. Iron complex used in Fenton and photo-Fenton processes

As it is mentioned above, several defects especially pH limitation and iron precipitation are involved in the traditional Fenton and photo-Fenton system. In order to solve these problems, different attempts were carried out in related researches, among which the introduction of organic and inorganic ligands for iron is one of the most attractive method. Hug et al. proposed the mechanism of Fenton and photo-Fenton reaction in the presence of Fe(II)-citrate complex as following [219, 220]:



Where Cit^{3-} represents citrate, $3\text{-HGA}\bullet^{2-}$ represents 3-hydroxo-glutarate radical and 3-OGA^{2-} represents 3-oxo-gulutarate respectively.

Similarly, the mechanism of complement of photo-Fenton process in the presence of Fe(III)-oxalate was concluded by Silva et al. [221]:



And the traditional photo-Fenton processes will be initiated following the reactions above.

In previous researches, citrate and oxalate are the most commonly used ligands in Fenton and photo-Fenton processes for organic chemicals removal especially in aqueous phase. In many cases it was proved to be quite efficient comparing with traditional Fenton and photo-Fenton system. This improvement in efficiency is mainly due to the high quantum yield of Fe(II) generation in the presence of ligands, and hence the $\bullet\text{OH}$ radical generation is promoted [221]. Besides citrate and oxalate, other ligands including EDTA, phosphate, glutamate and so on were also reported in modified Fenton and photo-Fenton systems. According to Sun and Pignatello paper, up to 50 compounds were used as the ligands of iron(III) and to catalyze the oxidation of 2,4-dichlorophenoxyacetic acid (2,4-D) by H_2O_2

in aerated aqueous solution at pH 6.0, some were found to be efficient [222].

Table B-9 Examples of different iron complexes used in Fenton and photo-Fenton system

Iron species	Ligands	System	pH range	Effect	Reference
humic acids	Fe(II)	Fenton	neutral pH favorable at 7.0	favorable	[223] [227]
			no effect at 3.5		
glutamate	Fe(II)	Fenton	5-7	improved	[224]
cross-linked chitosan	Fe(II)	Fenton	neutral pH	favorable	[225]
phosphotungstate	Fe(III)	Fenton	neutral pH	active	[226]
oxalate	Fe(III)	photo-Fenton	2.5	acceleration	[221]
citrate	Fe(III)	photo-Fenton	2.5-7.5	favorable	[219]
	Fe(II)	photo-Fenton	5.0	favorable	[220]

As it is achieved from previous researches that when many kind of ligands for iron such as citrate, oxalate, glutamate and humic acid were added into Fenton or photo-Fenton system respectively, the efficiency of organic compounds degradation and $\cdot\text{OH}$ radical generation were promoted, at the same time, iron in the solution was comparatively stable and precipitation was prevented at quite a wide pH range. For example, Fe(III)-EDTA was known to be stable in solution at pH ranging from 2 to 11. Table B-9 shows the typical application of iron complexes in Fenton and photo-Fenton processes.

B-6-6. Iron oxides used in Fenton and photo-Fenton processes

On the other hand, several kinds of heterogeneous catalysts, such as transition metal-exchanged zeolites, pillared interlayered clays containing iron or copper and iron-oxide minerals [198], are used for the oxidation of organic compounds through Fenton or photo-Fenton processes, since it is proved that these catalysts can act as the iron source in Fenton and photo-Fenton processes at a wide range of pH values [228, 229]. The iron species in such catalysts is quite stable in the structure or interlayer and the iron sludge could be prevented.

Among these catalysts, iron oxides, including goethite, hematite, magnetite, ferrihydrite, pyrite, and lepidocrocite are widely applied in heterogeneous Fenton and photo-Fenton systems. He et al reported the possible surface and solution reaction in heterogeneous

photo-Fenton reaction using goethite and summarized in Figure B-16 [230]:

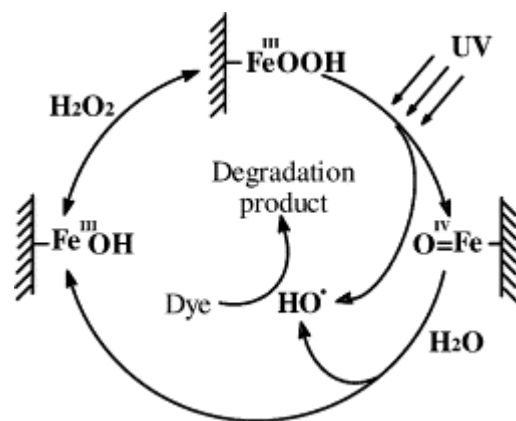


Figure B-16 Fe cycle under UV light irradiation in goethite surface [230]

As it is shown above, the reactions are initiated by the formation of a precursor surface complex of H₂O₂ with the oxide surface metal centers similar with the first step of dark reaction [231], different from the iron ion in solution, the surface Fe is immobilized and octahedrally coordinated by O²⁻ and OH⁻ [232]. The surface Fe may react with peroxides, dioxygen, or other oxidants to form a high-valent oxoiron (ferryl) moiety, where iron is formally in the +IV or +V oxidation state. Such reactions may generate •OH radical concurrently [233, 234]. At the same time, the O-O bond of the surface complex undergoes a cleavage under UV irradiation leading to the generation of a high-valent iron-oxo species and •OH radical [235]. Hence the •OH radical formatted will attack the target molecules and oxidize them.

The application of different kinds of iron oxides into Fenton and photo-Fenton processes for the removal of organic compounds in aqueous phase is already well documented as shown in Table B-10.

Table B-10 Application of iron oxides in Fenton and photo-Fenton processed for the oxidation of organic compounds in aqueous phase

Organic compound	Catalyst	System	Reference
9 kinds of synthetic dyes such as Reactive Orange	Magnetic mixed iron oxides (MO–Fe ₂ O ₃); M=Fe, Co, Cu, Mn	Fenton	[236]
16 Methyl red (MR)	Quartz/amorphous iron(III) oxide,	Fenton	[237]

	quartz/maghemite,		
	quartz/magnetite,		
	and quartz/goethite		
2,4,6-Trinitrophenol and ammonium picrate	Goethite	Fenton	[238]
2,4,6-Trinitrotoluene	Ferrihydrite, hematite, goethite, lepidocrocite, magnetite and pyrite	Fenton	[239]
2-Chlorophenol	Ferrihydrite, goethite and hematite	Fenton	[240]
2-Chlorophenol	Goethite	Fenton	[241]
Benzoic acid	[gamma]-FeOOH	Fenton	[242]
3,4-Dihydroxybenzoic acid	Goethite	Hydrogen peroxide in aqueous slurry	[243]
Petroleum-contaminated soils (diesel and kerosene)	Goethite and magnetite	Fenton	[244]
Aromatic hydrocarbons and chloroethylenes	Goethite	Fenton	[245]
Atrazine	Ferrihydrite	Fenton	[246]
Aromatic substrates	Goethite	Hydrogen peroxide in aqueous slurry	[247]
Aromatic substrates	Goethite	Fenton	[248]
Mordant Yellow 10 phenol	Goethite	Photo-Fenton	[230]
	Amorphous SiO ₂ -Fe ₂ O ₃ mixed oxide	Photo-Fenton	[249]
Mordant Yellow 10	hematite, goethite and akaganeite	Photo-Fenton	[250]
Orange II	novel nanocomposite of iron oxide	Photo-Fenton	[251]
Reactive Black 5	iron oxide on a activated alumina support	Photo-Fenton	[252]
17 β -estradiol (E2)	α -FeOOH-coated resin (α -FeOOHR)	Photo-Fenton	[253]
Reactive Black 5 (RB5)	Fe ₃ O ₄ -poly(3,4-ethylene-dioxythiophene) (PEDOT) core-shell nanoparticles	Photo-Fenton	[254]
linear alkylbenzene sulphonic acids	Iron(II, III) oxide (Fe ₃ O ₄), Iron(III) oxide (Fe ₂ O ₃), Iron(III) oxide hydrated (goethite)	Photo-Fenton	[255]
Reactive black 5	activated alumina-supported iron oxide	Photo-Fenton	[256]
Benzoic acid	oxide-composite nanocomposite material of crystalline iron oxides supported over mesostructured SBA-15	Photo-Fenton	[257]

B-7. Endocrine disrupting compounds

Table B-11 Classification of EDCs and their examples

Industrial solvents		polychlorinated biphenyls, dioxins
Plastics, plasticizers		bisphenol A, phthalates
Pesticides	use to kill insect pests	methoxychlor, chlorpyrifos, DDT
Fungicides	used to kill fungus	vinclozolin
Herbicides	used to kill unwanted plants	atrazine
Antibacterials		triclosan

Endocrine disrupting compounds (EDCs), which can also called as environmental estrogens or environmental hormones, are chemicals with the potential to elicit negative effects on the endocrine systems of humans and wildlife [258]. Since the publication of the book “Our Stolen Future” pushed our attention and researches into EDCs [259]. Environmental Protection Agency defines an EDC as “An exogenous” agent that interferes with the synthesis, secretion, transport, binding, action, or elimination of natural hormones in the body that are responsible for the maintenance of homeostasis, reproduction, development, and/or behavior [260]. Many related researches have been carried out by different countries and organizations such as WHO, IPCS, IUPAC, and the results observed have been published [261-266]. According to the related researches, various types of natural and synthetic chemical compounds have been identified as EDCs, such as pharmaceuticals, pesticides, industrial chemicals, personal care products and heavy metals, more than 70 chemicals have already been defined as EDCs so far [267]. Classes of these chemicals and some specific examples are shown in Table B-11 [268].

EDCs could be released to environment through various ways especially sewage treatment systems [269]. Humans come into contact with EDCs in many different ways. It can be through contact with soil, water, or air contaminated by such chemicals. Food can be also a source of EDCs for humans [268].

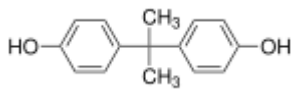
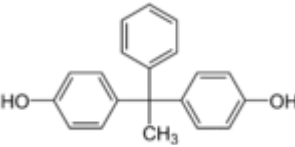
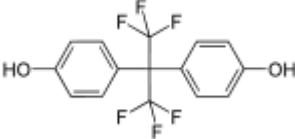
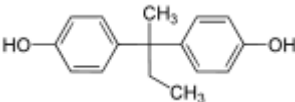
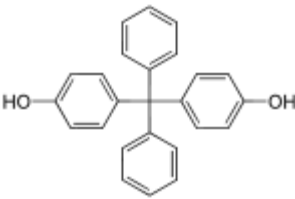
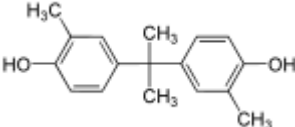
High level of EDCs can cause too many human health problems including endocrine, reproductive, or neurological problems. For example, in 1976 an industrial accident in Seveso, Italy exposed local populations to high levels of dioxins. Long-term studies showed

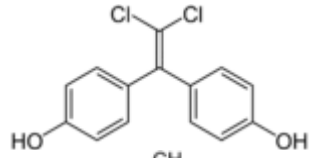
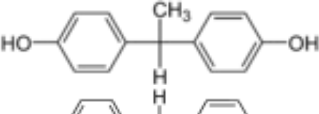
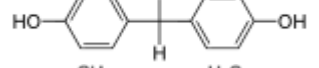
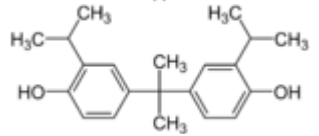
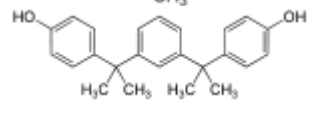
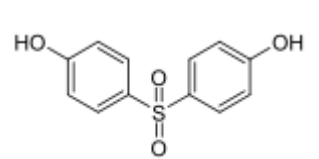
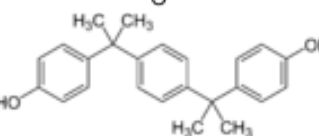
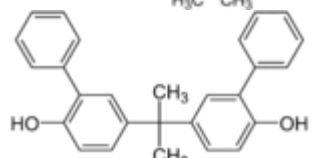
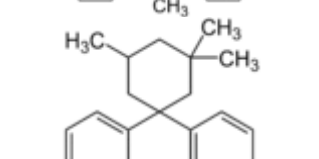
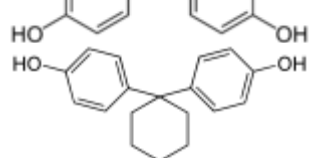
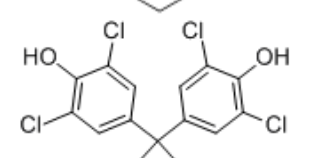
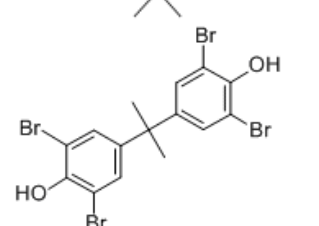
an increase in diabetes and certain types of cancer, among other health effects, in people living in highly contaminated areas. Whereas low level of EDCs impact to human is still not well known, but studies of low-dose exposure in animals show definite harm to health, and scientists suspect similar effects in humans [268]. Since EDCs is widespread in the environment and can do harm to human and animal health, it is very important to investigate the release and distribution of EDCs in environment, and study the technologies to remove or degrade them in environment.

B-7-1. Bisphenol A as a kind of typical EDCs

The bisphenols are a group of typical chemical compounds with two hydroxyphenyl functionalities, and a kind of typical EDCs. Such substances are shown in Table B-12 [270]:

Table B-12 Key substances as a class of Bisphenol

Structural formula	Name	CAS	Systematic name
	Bisphenol A	80-05-7	2,2-Bis(4-hydroxyphenyl)propane
	Bisphenol AP	1571-75-1	1,1-Bis(4-hydroxyphenyl)-1-phenyl-ethane
	Bisphenol AF	1478-61-1	2,2-Bis(4-hydroxyphenyl)hexafluoro propane
	Bisphenol B	77-40-7	2,2-Bis(4-hydroxyphenyl)butane
	Bisphenol BP	1844-01-5	Bis-(4-hydroxyphenyl)diphenylm ethane
	Bisphenol C	79-97-0	2,2-Bis(3-methyl-4-hydroxyphenyl)propane

	Bisphenol C	14868-03-2	Bis(4-hydroxyphenyl)- 2,2-dichlorethylene
	Bisphenol E	2081-08-5	1,1-Bis(4- hydroxyphenyl)ethane
	Bisphenol F	87139-40-0	Bis(4- hydroxydiphenyl)methane
	Bisphenol G	127-54-8	2,2-Bis(4-hydroxy-3- isopropyl-phenyl)propane
	Bisphenol M	13595-25-0	1,3-Bis(2-(4- hydroxyphenyl)-2- propyl)benzene
	Bisphenol S	80-09-1	Bis(4- hydroxyphenyl)sulfone
	Bisphenol P	2167-51-3	1,4-Bis(2-(4- hydroxyphenyl)-2- propyl)benzene
	Bisphenol PH	24038-68-4	5,5'-(1-Methylethyliden)- bis[1,1'-(bisphenyl)-2- ol]propane
	Bisphenol TMC	129188-99-4	1,1-Bis(4-hydroxyphenyl)- 3,3,5-trimethyl- cyclohexane
	Bisphenol Z	843-55-0	1,1-Bis(4- hydroxyphenyl)- cyclohexane
	Tetrachlorobisp henol A	79-95-8	2,2-Bis(4-hydroxy-3,5- dichlorophenyl)propane
	Tetrabromobisp henol A	79-94-7	2,2-bis(2,6-Dibromo-4- hydroxyphenyl)propane

It has been shown that Bisphenol substances distributed in our daily life, among which

Bisphenol A is one of the most typical and widespread chemical. BPA was firstly reported to be synthesized by Thomas Zincke of the University of Marburg, Germany [271]. The use of BPA commercially was started in the 1950s by Dr. Hermann Schnell of Bayer in Germany and Dr. Dan Fox of General Electric in the United States independently. The production of a new plastic material, polycarbonate, using BPA as the starting material was developed in 1953. Now BPA has already been an important industrial chemical that is used primarily to make polycarbonate plastic and epoxy resins, both of which are used in a wide variety of applications such as eyeglass lenses, medical equipment, water bottles, digital media, cell phones, consumer electronics, computers and other business equipment, electrical equipment, household appliances, safety shields, construction glazing, sports safety equipment, and automobiles [272].

Since the commercial usage of BPA is widespread, BPA release and distribution was estimated to be wide-ranging in the environment, and this is also confirmed by several experiments. The related results of BPA detection are shown in Table B-13.

Table B-13 Results of BPA detection in environment in related researches

Place	Phase	Concentration	Reference
Japan	River water	0.01-0.09 µg/L	[274]
Germany	Surface water	0.0005-0.41 µg/L	[275]
	Sewage effluents	0.018-0.702 µg/L	
	Sediments	0.01-0.19 mg/kg	
	Sewage sludge	0.004 to 1.363 mg/kg dw	
Japan	leaching from the plastic wastes	from undetectable to 139µg/g	[276]
Japan	Air	2.9-3.6 ng/m	[277]
Beijing, China	effluent and sludge in a sewage treatment plant	up to 825 µg/L	[278]

Since BPA is detectable in the environment, it is important to study its effect on environment and human health. It is found that long time exposure to low level of BPA would affect the survival, growth and reproductive fitness of animals [279-281]. For human health, BPA causes not only endocrine disruption [282], but also cancer [283, 284].

B-7-2. BPA degradation summary

The movement and transformation of BPA in the environment varied from different condition. It can be removed and degraded by adsorption, volatilization, hydrolysis, photolysis, bioaccumulation, and biodegradation. And the photoinduced degradation was also found to be important in the transformation of BPA.

At the same time, different AOPs technologies are also used for the removal of BPA in aqueous solutions (Table B-14). BPA degradation has been well documented in many researches and proved to be a good probe for detection of method efficiency for wastewater treatment.

Table B-14 Some reported methods for BPA degradation

Classification	System	Example reference
Biological degradation	laccase from basidiomycetes with the	[285]
	aid of extracellular polymers	
AOPs	UV irradiation/ultrasound/Fe(II)	[286-287]
	Fenton	[288]
	Sono/Fenton	[288]
	UV irradiation/Fenton	[290]
	UV/TiO ₂	[291]
	ozonization	[292]

C. Materials and Methods

C-1. Reagents

S, S'-Ethylenediamine-N, N'-disuccinic acid trisodium salt solution, (EDDS), 35% in water, Sigma-Aldrich.

Ferric perchlorate ($\text{Fe}(\text{ClO}_4)_3 \cdot 9\text{H}_2\text{O}$), $\geq 97\%$, Fluka.

Bisphenol A (BPA), $\geq 99\%$, Sigma-Aldrich.

Hydrogen peroxide (H_2O_2), 30%, Fluka, not stabilized (7722-84-1).

Nitrobenzene, $>99.5\%$, Fluka.

Chloroform, For HPLC, Carlo Erba.

2-propanol, For HPLC, 99.9%, Sigma-Aldrich.

Disodium terephthalate (TA), $> 99\%$, Alfa Aesar GmbH & Co KG.

2-Hydroxyterephthalic acid (TAOH), $> 98\%$, Atlantic.

$\text{FeSO}_4 \cdot (\text{NH}_4)_2\text{SO}_4 \cdot 6\text{H}_2\text{O}$, 99%, Aldrich.

Sodium hydroxide, $> 97\%$, Prolabo.

Sulfuric acid, $> 95\%$, Merck.

Perchloric acid, $> 97\%$, Merck.

Copper(II) sulfate pentahydrate, $> 99\%$, Merck.

Tetrabutylammonium hydrogen sulfate, $> 98\%$, Acros Organics.

Acetic acid, 96%, Carlo Erba reagent.

Sodium acetate, 99%, Merck.

5,6-Diphenyl-3-(2-pyridyl)-1,2,4-triazine-4,4'-disulfonic acid disodium salt hydrate (Ferrozine), 98%, Alfa Aesar.

Ethylenediaminetetraacetic acid disodium salt (EDTA), 99%, Sigma Aldrich.

Citric acid, 99%, Prolabo.

Sodium oxalate, 99.5%, Riedel de Haen.

Hydrochloric acid (HCl), 37%, Sigma Aldrich.

Hydroxylamine hydrochloride, 99%, Fluka.

Ammonium acetate, 97%, Fluka.

Ammonia, 28-30%, JT Baker.

P-hydroxyphenylacetic acid, 98%, Sigma Aldrich.

Sodium bicarbonate, 99.5%, Fluka.

Sodium Carbonate, 99.5%, Fluka.

C-2. Preparation of Materials and Solutions

C-2-1. Synthesis of Goethite

Goethite (α -FeOOH) sample was prepared in laboratory LCPME by air oxidation of a hydrolyzed FeSO₄ solution following a procedure described by Schwertmann and Cornell [293]. This process could be briefly described as following: appropriate amount of FeSO₄ and NaOH solutions were mixed together, and pH was adjusted by H₂SO₄ to pH 6, and then goethite was achieved by drying under 40°C condition.

C-2-2. Preparation of Stock Solutions

(a) Bisphenol A (BPA) stock solution (200 μ mol/L)

0.0114 g of BPA was diluted to 250 mL by adding an appropriate volume of Milli-Q water and then magnetic stirring was used for several hours to make BPA completely dissolved.

(b) S, S'-Ethylenediamine-N, N'-disuccinic acid trisodium salt (EDDS) stock solution (10 mmol/L)

1.0234 g of EDDS was diluted in appropriate volume of Milli-Q water to 100 mL to get the desired concentration of EDDS.

(c) Fe(III) stock solution (10 mmol/L)

When this solution was prepared, great care need to be taken into account in order to avoid reduction and/or precipitation of Fe(III). 0.5164g of Fe(ClO₄)₃·9H₂O was diluted into 100 mL Milli-Q water to get desired amount of Fe(III) stock solution and at the same time

appropriate amount of perchloric acid was added into the solution to adjust the pH at 2.0. Usually Fe(III) stock solution was newly prepared every time while needed.

(d) Fe(III)-EDDS complex stock solution (2 mmol/L)

50 mL of 10 mmol/L EDDS stock solution and 50 mL of 10 mmol/L $\text{Fe}(\text{ClO}_4)_3 \cdot 9\text{H}_2\text{O}$ were mixed together and diluted to 250 mL by adding an appropriate volume of Milli-Q water. And the mixture was put in dark for a period of time before used in order to make sure total complexation.

(e) H_2O_2 stock solution (500 mmol/L)

1.53 mL of H_2O_2 (30%) was diluted to 100 mL by adding an appropriate volume of Milli-Q water. However, every time before used, accurate concentration of H_2O_2 solution must be determined again because of the instability of H_2O_2 .

(f) Fe(II) stock solution (0.5 mmol/L)

0.0490 g of $\text{FeSO}_4 \cdot (\text{NH}_4)_2\text{SO}_4 \cdot 6\text{H}_2\text{O}$ was diluted to 250 mL by adding an appropriate volume of Milli-Q water.

(g) Ferrozine stock solution (0.01 mol/L)

0.4925 g of 5,6-Diphenyl-3-(2-pyridyl)-1,2,4-triazine-4,4'-disulfonic acid disodium salt hydrate was dissolved in appropriate volume of Milli-Q water to 100 mL to get the desired concentration of Ferrozine.

(h) Hydroxylamine hydrochloride stock solution (1.4 mol/L)

9.729 g of hydroxylamine hydrochloride was diluted in appropriate volume of 2 mol/L HCl solution to 100 mL to get desired amount of solution.

(i) EDTA stock solution (10 mmol/L)

0.3722 g of Ethylenediaminetetraacetic acid disodium salt was diluted to 100 mL by adding an appropriate volume of Milli-Q water to get desired amount of solution.

(j) Peroxidase stock solution (167 units/100mL)

About 0.001 g of peroxidase was diluted to 100 mL by adding an appropriate volume of Milli-Q water to get desired amount of solution.

(k) P-hydroxyphenylacetic acid stock solution (0.15 mol/L)

2.282 g of p-hydroxyphenylacetic acid was diluted to 100 mL by adding an appropriate

volume of Milli-Q water to get desired amount of solution.

(l) Buffer

For H₂O₂ detection

Firstly, 2.1 g of NaHCO₃ and 2.65 g of Na₂CO₃ was diluted in appropriate volume of Milli-Q water respectively, and then these two parts were mixed together and adjusted to 250 mL to get the desired concentration.

For iron detection

Firstly, 10 mol/L of ammonium acetate solution was prepared, and then, ammonium hydroxide solution was used to adjust the pH of ammonium acetate solution to 9.5.

(m) Fe(III)-citrate stock solution (2 mmol/L)

Firstly, 10 mmol/L of Fe(III) solution and 10 mmol/L of citrate solution were prepared respectively, and then 50 mL of each were mixed together and adjusted to 250 mL.

(n) Fe(III)-oxalate stock solution (2 mmol/L)

Firstly, 10 mmol/L of Fe(III) solution and 10 mmol/L of oxalate solution were prepared respectively, and then 50 mL of each were mixed together and adjusted to 250 mL.

(o) Nitrobenzene stock solution (1 mmol/L)

0.1 mL of nitrobenzene was diluted to 1000 mL by adding an appropriate volume of Milli-Q water to get desired amount of solution.

(m) TA stock solution (10 mmol/L)

0.2101 g of Disodium terephthalate was dissolved to 100 mL by adding an appropriate volume of Milli-Q water.

(n) TAOH stock solution (0.1 mmol/L)

0.00183 g of 2-Hydroxyterephthalic acid was diluted to 100 mL by adding an appropriate volume of Milli-Q water.

(o) Cu(II) stock solution (10 mmol/L)

0.25 g of CuSO₄·5H₂O was diluted to 100 mL by adding an appropriate volume of Milli-Q water to get desired amount of solution.

C-2-3. Preparation of reaction solution

All the reaction solutions were prepared using the stock solutions mixed together, and Milli-Q water was used to adjust to desired volume. And then the pH value was adjusted using Cyberscan 510 pH meter, and proper amount of HClO_4 and NaOH . Finally, H_2O_2 was added just before the beginning of the reaction.

The suspensions of goethite were dispersed by using magnetic stirring for 10 min. After the irradiation, the mineral suspensions were centrifuged at 12000 rpm for 30 min.

When deaerated or oxygenated reaction solutions were needed, argon, nitrogen or oxygen was purged into the reaction solutions before reaction for 30 min and during the whole reaction process.

C-3. Reaction Process

C-3-1. Actinometry

To calculate the photon flux of the irradiation system used, we used the method based on the photolysis of para-nitroanisole (PNA) in the presence of pyridine (Figure B-1) (Dulin and Mill (1982)) [294].

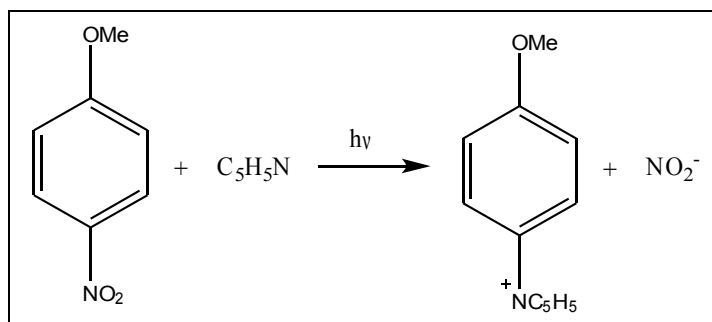


Figure C-1 Photolysis of PNA in the presence of pyridine

Irradiation of solutions of PNA (10^{-5} mol/L) in the presence of pyridine (10^{-4} mol/L) are performed for 4 hours with regular sampling every 15 minutes in the first one hour and every hour later on. To monitor the disappearance of PNA with time, samples were

analyzed by HPLC/UV-Visible detection under the following conditions:

- Zorbax C18 column, 4.6×250 mm, $5 \mu\text{m}$
- Flow rate: 0.5 mL/min
- Injection volume: 50 μL
- Analysis of Wavelength: 254 nm
- Retention time of PNA: 17 minutes
- Mobile phase: 60/40 methanol/Milli-Q water

The photolysis rate of PNA depends on the concentration of pyridine (Dulin and Mill (1982)) [294]. The quantum yield for the degradation of PNA ($\Phi_{\text{PNA/pyr}}$) in the presence of pyridine is expressed in the equation (1):

$$\Phi_{\text{PNA/pyr}} = 0.44 \times [\text{pyridine}] + 0.00028 \quad (1)$$

Knowing the rate of degradation of PNA according to HPLC analysis, one can determine ΔN_{PNA} which is the number of PNA molecules degraded per unit area and time ($\text{molecules.m}^{-2}.\text{s}^{-1}$). According to equation (2), we can then determine the number of photons absorbed (I_a) by the solution $\text{photon.cm}^{-2}.\text{s}^{-1}$:

$$I_a = \frac{\Delta N_{\text{PNA}}}{\Phi_{\text{PNA/pyr}}} \quad (2)$$

The value of I_a corresponding to a sum over the entire absorption spectrum of the PNA, the intensities of the photon flux for each wavelength ($I_o(\lambda)$) are determined from the equation (3):

$$I_a = \sum_{\lambda} I_o(\lambda) \times (1 - 10^{-\text{DO}_{\lambda}}) \quad (3)$$

With $I_o(\lambda)$ the actual intensity of photon flux for a given wavelength λ ($\text{photon.cm}^{-2}.\text{s}^{-1}$) and the absorbance of the solution DO_{λ} of PNA (10^{-5} mol/L). This experience has allowed us to calculate the energy of the photon flux received in the chamber of irradiation used. The shape of the emission spectrum of the lamp is obtained using an optical fiber (Ocean Optics SD 2000) and calibrated using a DH-2000-CAL Deuterium Tungsten Halogen reference lamp. This emission spectra is then normalized energy from the results obtained in the chemical actinometry PNA / pyridine.

C-3-2. Fenton process using Fe(III)-EDDS complex

All the homogeneous Fenton experiments were carried out in brown reaction flask with constant magnetic stirring at room temperature (293 ± 2 K). Appropriate amount of BPA solution was mixed with Fe(III)-EDDS complex solution, and the pH value was adjusted using Cyberscan 510 pH meter. The reaction started when H_2O_2 was added to the solution. At the same time the pH value was detected again, and it was found that the variation of pH value after H_2O_2 addition was less than 0.1. Samples were taken from the reaction flask at fixed time period. Control experiments were conducted without addition of iron complex or hydrogen peroxide and it was found that no BPA degradation occurred in such condition during typical experimental time.

C-3-3. Photo-Fenton process using Fe(III)-EDDS complex

Photo-Fenton experiments were carried out in a home-made Pyrex photoreactor placed in a cylindrical stainless steel container. Around the reactor four fluorescent tubes (Philips TL D 15W/05), having a continuous emission in the 300-500 nm range were placed. The solutions were magnetically stirred with a magnetic bar during irradiation. Appropriate amount of BPA solution was mixed with Fe(III)-EDDS complex solution, and the pH value was adjusted using Cyberscan 510 pH meter. The reaction started when appropriate amount of H_2O_2 was added into the solution. At the same time the pH value was detected again, and it was found that the variation of pH value before and after H_2O_2 adding was less than 0.1. All the experiments were carried out at room temperature (293 ± 2 K). Samples were taken from the photoreactor at fixed time period. The BPA direct photodegradation was checked and results showed its stability under adopted irradiation conditions.

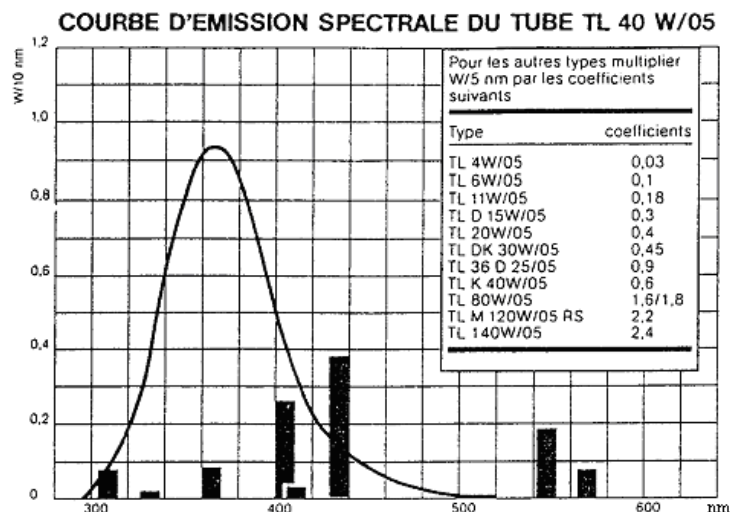


Figure C-2 Emission spectra of tube Philips, TLD 15W/05.

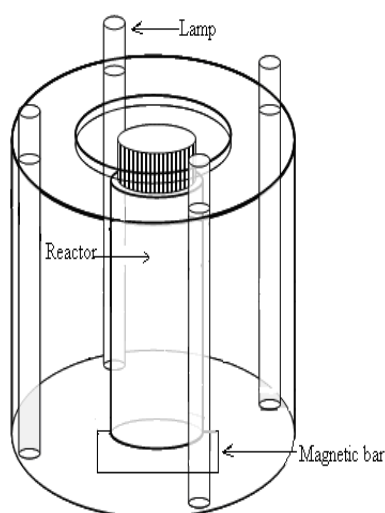


Figure C-3 Home-made photoreactor with four tubes (Philips TLD 15W/05)

C-3-4. Heterogeneous Fenton process using goethite

All the experiments were carried out in brown reaction flask with constant magnetic stirring at room temperature (293 ± 2 K). Appropriate amount of BPA solution was mixed with EDDS solution, and the pH value was adjusted using Cyberscan 510 pH meter. Then appropriate amount of goethite was added and magnetically stirred for 30 min. Finally, the reaction started when H_2O_2 was added to the solution. At the same time the pH value was

detected again, and it was found that the variation of pH value after H₂O₂ addition was less than 0.1. Samples were taken from the reaction flask at fixed time period.

C-3-5. Heterogeneous photo-Fenton process using goethite

Photo-Fenton experiments were carried out in a home-made Pyrex photoreactor placed in a cylindrical stainless steel container. Around the reactor, four fluorescent tubes (Philips TL D 15W/05), with a continuous emission in the 300-500 nm range, were placed. The solutions were magnetically stirred with a magnetic bar during irradiation. An appropriate amount of BPA solution was mixed with the EDDS solution and the pH value was adjusted using a Cyberscan 510 pH meter. The reaction started when an appropriate amount of goethite and H₂O₂ was added to the solution. At the same time the pH value was measured again, and it was found that the variation of pH value before and after adding H₂O₂ was less than 0.1. Before irradiation, the suspension was stirred in dark for 30 min in order to make sure the uniformity of the suspension. All the experiments were carried out at room temperature (293 ± 2 K). Samples were taken from photoreactor at fixed intervals.

C-4. Analysis methods

C-4-1. Goethite

In order to identify the crystal structure of the synthesized mineral, solid sample was analyzed by X-ray powder diffraction (XRD). The XRD data were collected with a D8 Bruker diffractometer, equipped with a monochromator and a position-sensitive detector. The X-ray source was a Co anode ($\lambda = 0.179$ nm). The diffractograms were recorded in the 3–64° 2 θ range, with a 0.0359° step size and a collection of 3 s per point.

The morphology of goethite particles was visualized using transmission electron microscopy (TEM). TEM observations were carried out with a Philips CM20 TEM (200 kV) coupled with an EDAX energy dispersive X-ray spectrometer. The solid powder was

re-suspended in 2 mL ethanol under ultrasonication, and a drop of suspension was evaporated on a carbon-coated copper grid which was placed on filter paper.

The point of zero charge (PZC) of minerals was determined at 293 K in 0.01, 0.1 and 1 mol/L NaCl solutions by the potentiometric method of Parks and de Bruyn (1962) [295]. The potentiometric titrations were performed in a 200 mL jacketed reaction vessel under an atmosphere of CO₂-free nitrogen.

C-4-2. Chemicals analysis

C-4-2-1. Spectroscopic methods

I. UV-vis spectrophotometer

The UV–visible spectra of the solutions including BPA, Fe(III)-EDDS, H₂O₂ and Fe(III) were recorded on a Cary 300 double beam spectrophotometer.

II. Fluorescence spectrometer

The fluorescence spectra of the solutions were recorded on a MPF-3L Fluorescence Spectrophotometer (Perkin Elmer).

For the detection of H₂O₂, the excitation wavelength was set at 320 nm and the emission wavelength at 400 nm, and the scan sensitivity was set at 0.3.

For the detection of TAOH, the excitation wavelength was set at 320 nm and the emission wavelength at 420 nm, and the scan sensitivity was set at 0.3.

C-4-2-2. Chromatographic methods

Three HPLC systems were used for product analysis:

HPLC Alliance chromatograph equipped with waters 2475 Multi λ Fluorescence detector, waters 2998 Photodiode Array detector and waters 2695 separations Module.

HPLC chromatograph equipped with waters 717plus Autosampler, waters 515 HPLC Pump and waters 996 Photodiode Array Detector.

HPLC 1050 HP (Hewlett Packard)

Three HPLC columns were used in the work:

A NUCLEODUR 100-5 C18 of 4.6 mm (ID) \times 250 mm (length) with a particle diameter of 5 μ m.

A zorbax C8 column of 4.6 mm (ID) \times 250 mm (length) with particle diameter of size 5 μ m.

An Agilent C8 column of 4.6 mm (ID) \times 150mm (length) with a particle diameter of 5 μ m.

The conditions of HPCL for the analysis are the following:

For the analysis of BPA, the experiments were performed by HPLC with UV detection at 225 and 275 nm. The flow rate was 1 mL/min and the mobile phase was a mixture of water and methanol (35/65, v/v). The retention time of BPA was 3.9 min.

For the analysis of Nitrobenzene, the experiments were performed by HPLC with UV detection at 210 nm and 267 nm. The flow rate was 1mL/min and the mobile phase was a mixture of water and acetonitrile (50/50, v/v). The retention time of nitrobenzene was 4.6 min.

For the analysis of EDDS, the experiments were performed by HPLC with UV detection at 254 nm. The flow rate was 1.0 mL/min and the mobile phase was a mixture of methanol and formate buffer (2 mmol/L tetrabutylammonium hydrogen sulfate and 15 mmol/L sodium acetate, pH adjusted to 4.0 with acetic acid) (20/80, v/v).

C-4-2-3. Dosage methods

I. Total iron concentration detection

The detection of total iron concentration was carried out by using 5,6-Diphenyl-3-(2-pyridyl)-1,2,4-triazine-4,4'-disulfonic acid disodium salt hydrate (Ferrozine), which can reacts with divalent Fe to form a stable magenta complex between pH 4 and 9 [296]. The maximum absorbance is recorded at 562 nm with a molar absorption coefficient close to 30,000 M⁻¹ cm⁻¹ [297]. While a mixture of dissolved Fe(II) and Fe(III) was detected, appropriate amount of hydroxylamine hydrochloride was used to reduce the Fe(III) ions

and the total iron concentration was then determined by complexation with Ferrozine. Buffer solution of ammonium acetate and ammonium hydroxide was used to maintain the pH value in the solution to make sure the stability of Fe(II)-Ferrozine complex. Different concentration of $\text{FeSO}_4 \cdot (\text{NH}_4)_2\text{SO}_4 \cdot 6\text{H}_2\text{O}$ solution was used as Fe(II) sources to make a calibration curve (as shown in Figure C-4). The molar absorption coefficient was $30,807 \text{ M}^{-1} \text{ cm}^{-1}$, which is nearly the same as the reference value $\epsilon_{562 \text{ nm}} = 30,000 \text{ M}^{-1} \text{ cm}^{-1}$. At the same time, from the calibration curve it was checked and concluded that when BPA and/or EDDS was present in the solution, no interference was observed in the determination of total iron concentration. However, when the concentration of Fe(II) is higher than $30 \mu\text{mol/L}$, no linear relationship was observed in this method anymore. So, when the concentration in the solution is supposed to be higher than $30 \mu\text{mol/L}$, a dilution must be carried out before analysis.

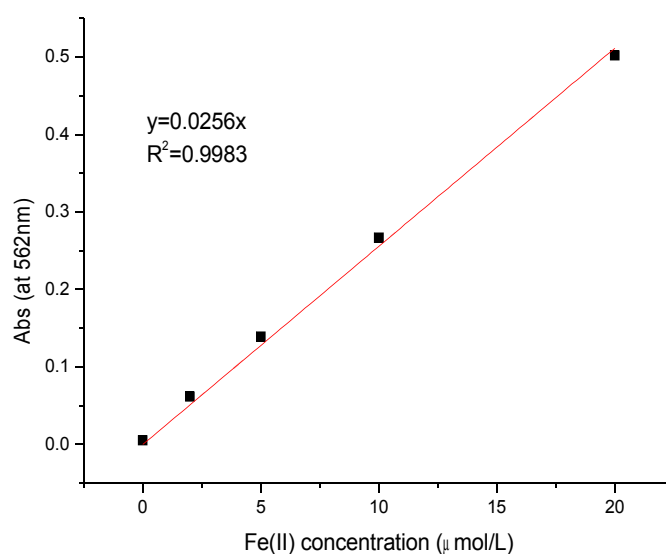


Figure C-4 Calibration curve of Fe(II) concentration

II. H_2O_2 concentration detection

Peroxidase is a kind of enzyme characterized by selectivity toward hydroperoxides. In the presence of a hydrogen donor molecule such as p-hydroxyphenylacetic acid (POPHA), this enzyme peroxidase could catalyze the reduction of H_2O_2 through the following reaction

[298, 299]:

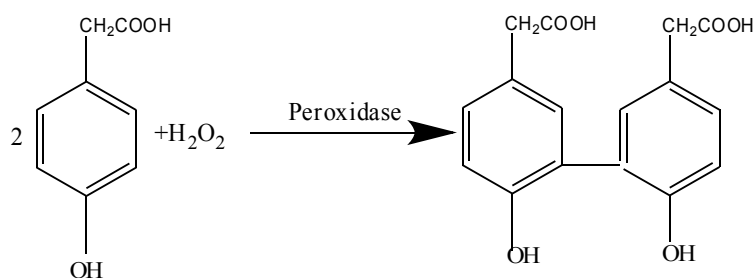


Figure C-5 enzyme peroxidase catalyzing reduction of H₂O₂

The production p-hydroxyphenylacetic acid dimers can product florescence with a peak excitation wavelength of 320 nm and peak emission wavelength of 400 nm [299]. Previous studies also proved this determination method to be reliable and free from interferences typically present in precipitation samples [300]. Potential interferences are masked by the use of EDTA to complex the transition metals such as iron and HCHO to reduce interference from hydroxymethanesulfonate [300]. In our research, EDTA was added in order to keep away from the interference of iron, whereas HCHO was not necessary. While the concentration of H₂O₂ to be detected is assumed to be higher than 100 μmol/L, dilution is necessary before detection.

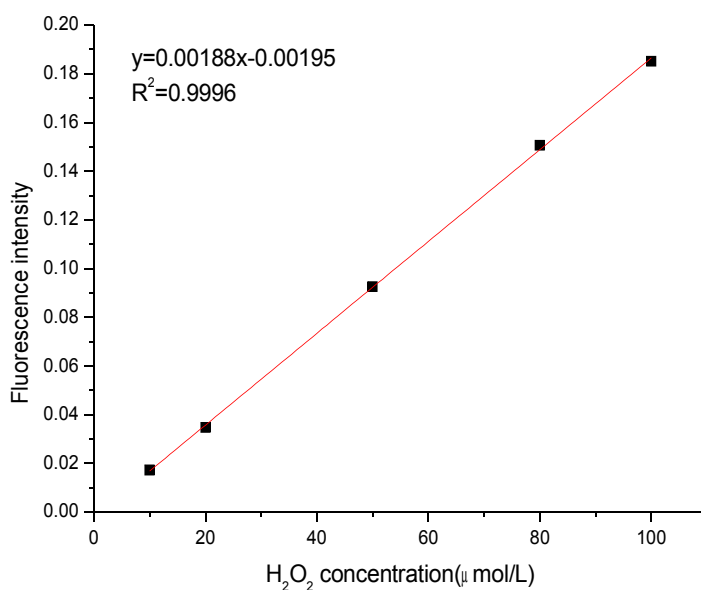


Figure C-6 Calibration curve of H₂O₂ concentration

III. Hydroxyl radicals

Nitrobenzene used as scavenger of $\cdot\text{OH}$ radicals

The detection of $\cdot\text{OH}$ during the photo-Fenton processes was performed using nitrobenzene (NB) as the trapping molecule. Nitrobenzene reacts directly with $\cdot\text{OH}$ to produce different nitrophenols and 1,3-dinitrobenzene [301]. The kinetic model used to estimate the hydroxyl radical formation rate is obtained from the following equation

$$R_{NB}^d = R_{OH}^f \frac{k_{NB,\cdot OH} [NB]}{k_{NB,\cdot OH} [NB] + \sum_i k_i [S_i]} \quad (4)$$

where R_{NB}^d is the degradation rate of nitrobenzene (M s^{-1}), R_{OH}^f is the rate of formation of

the hydroxyl radical (M s^{-1}), $k_{NB,\cdot OH}$ the second order rate constant between nitrobenzene

and the hydroxyl radical ($3.9 \times 10^9 \text{ M}^{-1} \text{ s}^{-1}$) [302] and $\sum_i k_i [S_i]$ is the pseudo-first-order rate

constant (s^{-1}) for $\cdot\text{OH}$ scavenging by all constituents (i.e. Fe-complexes, BPA, H_2O_2 , and EDDS) of the solution except for the probe NB. This $\cdot\text{OH}$ radicals detection method was used in homogeneous Fenton and photo-Fenton system where iron species existed in great amount. In previous research discussing the participation of iron species, it is found that their reactivity towards nitroaromatic compounds is negligible compared with that of $\cdot\text{OH}$ radicals [303]. In our research, $200 \mu\text{mol/L}$ of NB was used and it could be assumed that

$k_{NB,\cdot OH} [NB] \gg \sum_i k_i [S_i]$. From equation (4) and after rearrangement we deduce that the

initial formation rate of $\cdot\text{OH}$ is equal to the initial degradation rate of the probe (

$R_{NB}^d = R_{OH}^f$), as a result, the generation of $\cdot\text{OH}$ radicals could be detected through the detection of nitrobenzene degradation.

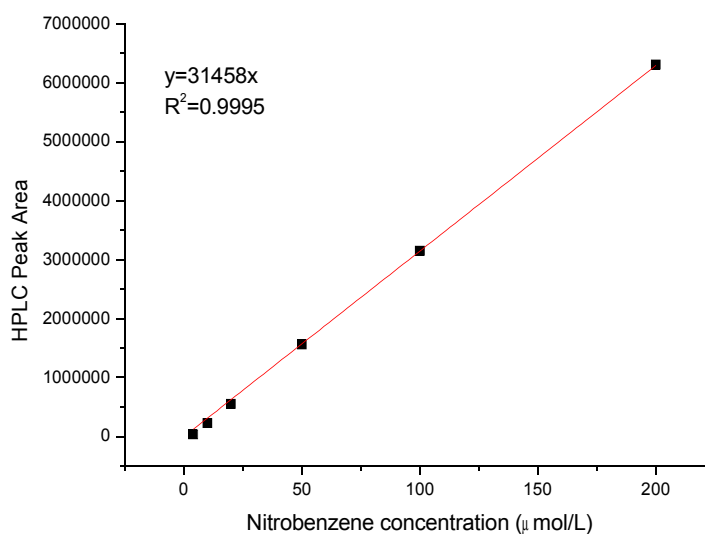


Figure C-7 Calibration curve of Nitrobenzene concentration at 267 nm

Disodium terephthalate (TA) used as scavenger of $\cdot\text{OH}$ radicals

As it is reported in previous research, terephthalic acid (TA) could trap $\cdot\text{OH}$ radicals and produce 2-hydroxyterephthalic acid (TAOH) [304, 305], the reaction was represented as following:

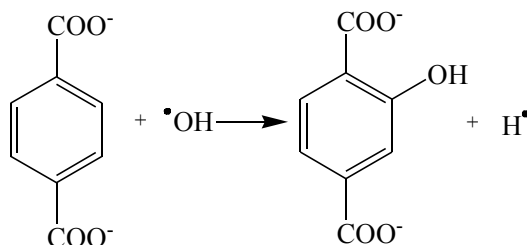


Figure C-8 Reaction between TA and $\cdot\text{OH}$ radicals

The TAOH product, which is the only form of the monohydroxylated adduct because of the symmetrical structure of TA [306], is a fluorescent product with a peak excitation wavelength at 320 nm and peak emission wavelength at 420 nm, while TA cannot give any fluorescence. Reaction of TA to form TAOH is highly specific towards $\cdot\text{OH}$ radicals, other common oxygen radical species, such as the superoxide anion and organic hydroperoxides, have failed to produce TAOH directly [305]. As a result, TA is proved to be an effective hydroxyl radical scavenger, which can be used to estimate relative amount of hydroxyl

radicals formed under varying conditions [304, 305].

In order to be sure that all the $\cdot\text{OH}$ radicals produced in the system is trapped by TA, high concentration of TA was used in our experiments. The concentrations of hydroxyl radicals formed in the system were determined as following:

$$C_{\text{OH}} = C_{\text{TAOH}} / f \quad (5)$$

f is the yield of TAOH produced in the reaction of $\cdot\text{OH}$ radicals with TA. In oxygen-containing solutions and oxygen-free solutions f is equal to 35% and 84% respectively [304, 306].

The concentration of TAOH was detected by fluorescence spectrometer. It should be noticed that when using the fluorescence spectrophotometer, the fluorescence intensity of TAOH was influenced by the pH, so calibration curves of TAOH at different pH values were detected. The Calibration curve of TAOH using fluorescence spectrophotometer detected was shown in Figure B-9.

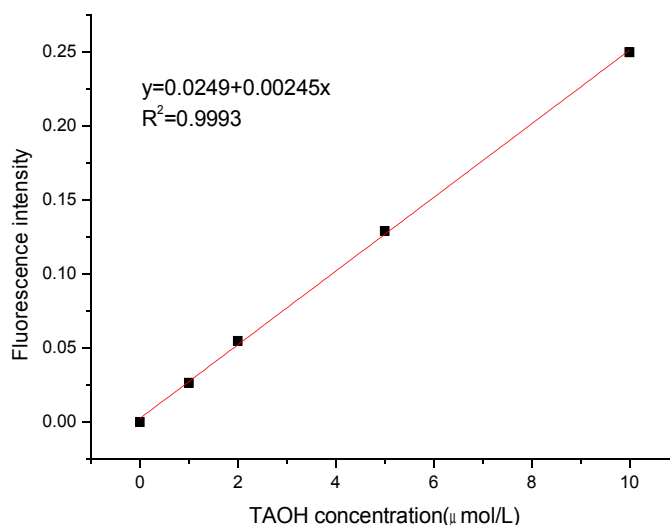


Figure C-9 Calibration curve of TAOH concentration at pH 6.2

IV. EDDS detection

Based on the fact which has been proved in previous researches that the complex formed between Cu(II) and EDDS is stable and EDDS could enhance the extraction of Cu(II) from contaminated soils [85, 307], the detection of EDDS was the method using the formation of

Cu(II)-EDDS complex followed by HPLC equipped with a UV detector. Firstly, A 10 mM of a CuSO_4 stock solution was prepared, then, metal complex solutions were prepared by mixing the desired proportions of Cu(II) and appropriate complexing agents and diluting with Milli-Q water. The concentration of Cu(II) was kept at 0.5 mM. The solutions were kept in a refrigerator and left to stand overnight to ensure complete complexation. The Calibration curve of EDDS was shown in Figure C-10.

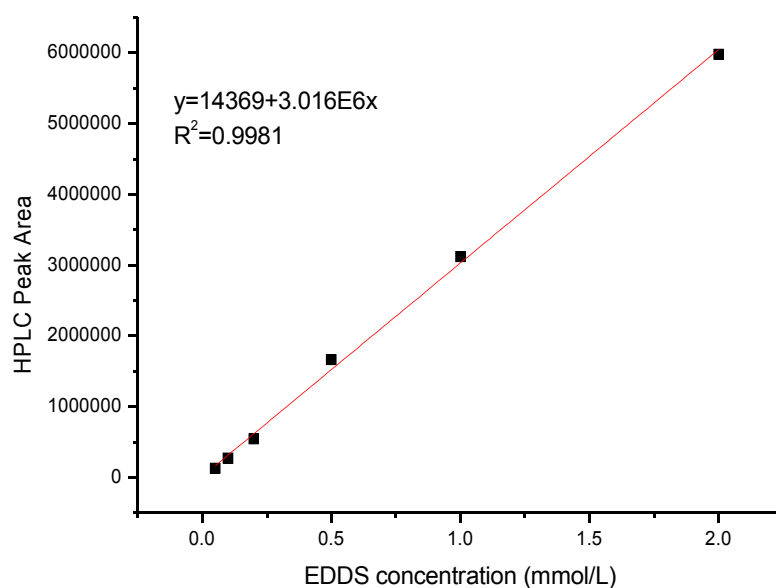


Figure C-10 Calibration curve of EDDS concentration

C-4-2-4. Cyclic voltammetry measurements

Electrochemical experiments were carried out with a potentiostat Autolab PGSTAT100 using a three-electrode cell, including an saturated calomel reference electrode (SCE), a platinum auxiliary electrode and a glassy carbon disk electrode (GCE, 3 mm diameter). Prior to each cyclic voltammetric run, the glassy carbon electrode was polished with alumina slurry paste (0.05 $\mu\text{mol/L}$) and rinsed with ethanol and distilled water in a sonicator for 1 min. Cyclic voltammograms were recorded at a scan rate (ν) of 5 mV s^{-1} in 0.05 mol/L KCl solution (pH 6.2) containing 1 mmol/L Fe(III)-EDDS, Fe(III)-citrate or Fe(III)-EDTA, Fe(III)-oxalate was also attempted, however it was unsuccessful because of

the instability of Fe(III)-oxalate complex at neutral pH and the generation of precipitation. At the same time, cyclic voltammograms of 1 mmol/L Fe(III)-EDDS at pH 3.7 and 8.7 was also carried out. These electrolyte solutions were purged with argon for 30 min before starting the measurements to remove dissolved oxygen. Redox potentials are reported vs NHE (-0.244 V/SCE).

C-4-2-5. Products determination in different reaction system using GC-MS detection

I. Preparation of Samples

The BPA degradation experiments were carried out as described before. For each system, one experiment was carried out in optimum condition. And two samples, 100 mL for each, were taken in different time interval for each system. For heterogeneous system, samples were centrifuged at the speed of 12000 rate/min for 20 min and the filtered by 0.22 μ m microporous membrane to make sure all the solid particles were removed. After that, all the samples were freeze-dried by and solved into 0.5 mL of dichloromethane solvent. Then, 200 μ L of BSTFA+TMCS(99:1) derivatization reagent was added into each sample and derivatization was carried out at 70°C for 1 h. After all these steps, all the samples were kept in 4°C refrigerator and prevented from light for determination.

II. GC-MS process

The detection process was carried out in the GC-MS equipment Agilent 7890/5975C.

The temperature programmed method:

Heating rate (°C /min)	Temperature (°C)	Retention time (min)	Keep time (min)
10	40	3	3
5	200	0	35
10	280	5	48

Finally the temperature was kept at 290 °C for detection.

Injection port:

Heater: 280°C

Pressure: 11.521 psi

Spacer blowing hot sweep flow: 3 mL/min

Mode: without shunting

Stream outlet purge flow: 50 mL/min at 0.75 min

Ion detector of MS:

Solvent delay: 9 min

Mode of EMV: relative value

Relative voltage: 0 = 2282 V

Acquisition mode: full scan

Time window: 42 min

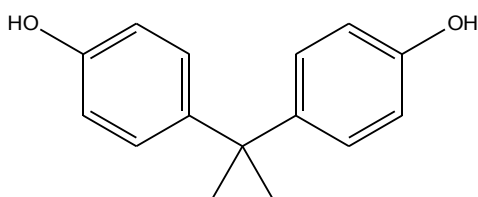
EI energy: 70 eV

m/z range: 40-650

D. Result and dicussion

D-1. Physicochemical properties of BPA, Fe(III)-EDDS and Goethite

D-1-1. Properties of Bisphenol A



Bisphenol A (BPA)

Bisphenol A, namely 4,4'-(1-Methylethyliden)bisphenol, is a typical chemical that has two phenol functional groups, with the chemical formula $(\text{CH}_3)_2\text{C}(\text{C}_6\text{H}_4\text{OH})_2$. The UV-visible spectrum of the solutions with different concentrations of BPA is presented in Figure D-1. It can be observed from the UV-visible spectrum that there is no absorption at $\lambda > 300$ nm, and there are two maximum of absorption are at 225 and 275 nm. The molar absorption coefficients are equal to $14422 \text{ M}^{-1} \text{ cm}^{-1}$ at 225 nm and $2691 \text{ M}^{-1} \text{ cm}^{-1}$ at 275 nm (Figure D-2).

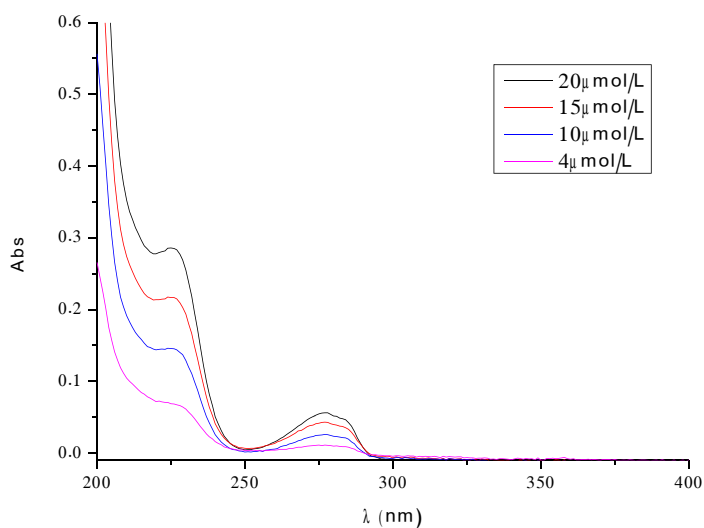


Figure D-1 UV-Visible absorption spectrum of BPA solution at different concentrations

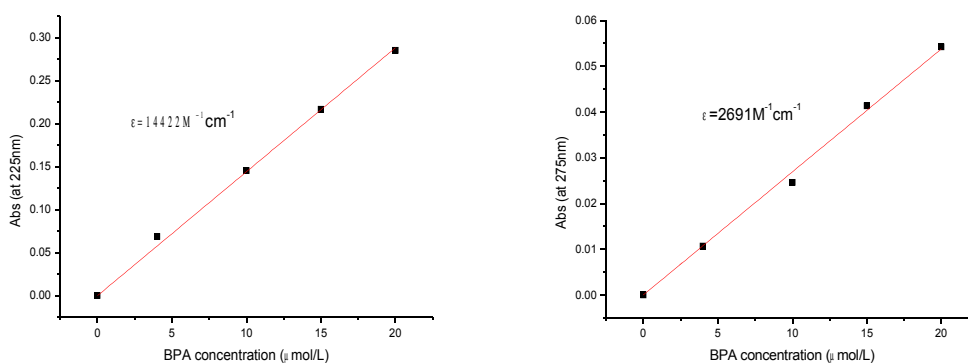


Figure D-2 Molar absorption coefficients of BPA at 225 nm and 275nm respectively

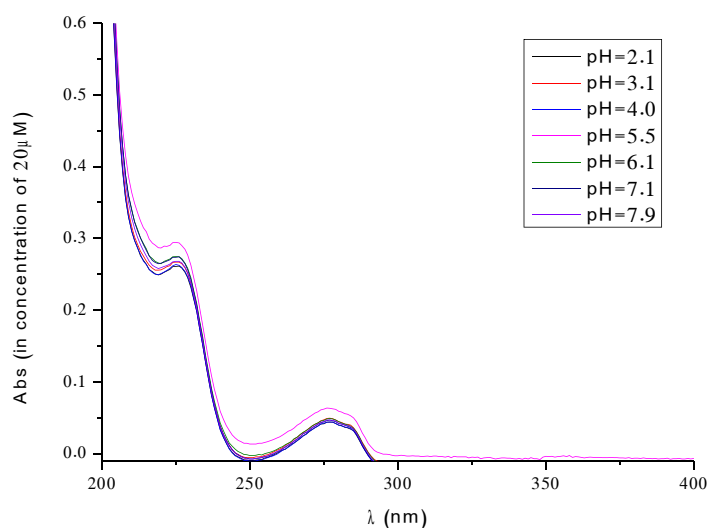


Figure D-3 UV-visible absorption spectrum of BPA at different pH values

The UV-visible absorption spectrum of BPA at different pH values is shown in Figure D-3. It is observed that there is no significant difference among the spectrums at different pHs. The other important chemical and physical properties of BPA are shown in Table D-1. The BPA solubility in water is not high. In this work, no organic solutions are used to help the dissolution of BPA in water solution. The maximal concentration of BPA in water can be reached to 400 $\mu\text{mol/L}$ after magnetic stirring for few hours.

Table D-1 Chemical and physical properties of BPA

Bisphenol A	
CAS number	80-05-7
Molecular formula	C ₁₅ H ₁₆ O ₂
Molecular weight	228.29
Melting point	158-159 °C, 431-432 K, 316-318 °F
Boiling point	220 °C (493 K) / 4mmHg
Appearance	White solid
λ_{max}	225 nm
Intensity	1.195g/cm ³ (25°C)
logK _{ow}	3.0-4.0
pKa	9.73
Solubility in water	120-300ppm (at 21.5 °C)
Flash point	227°C

D-1-2. Properties of Fe(III)-EDDS complex

As it is known from previous research of our group the stoichiometry between Fe(III) and EDDS in Fe(III)-EDDS complex is 1:1 [89], and it is observed that Fe(III)-EDDS complex in water solution is stable for at least 10 days.

The UV-visible spectrum of Fe(III)-EDDS complex solution with different concentration at pH 6.2 is shown in Figure D-4.

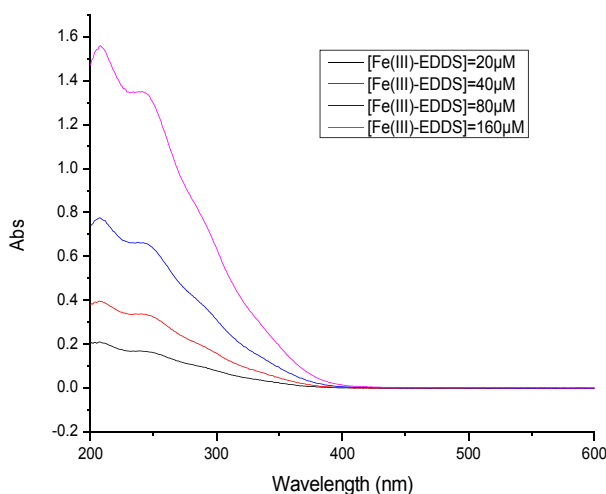


Figure D-4 UV-visible spectrum of Fe(III)-EDDS complex at different concentrations

It is observed that there is no absorption at $\lambda > 400$ nm. The molar absorption coefficient is equal to 8401 M⁻¹ cm⁻¹ at 239 nm as shown in Figure D-5.

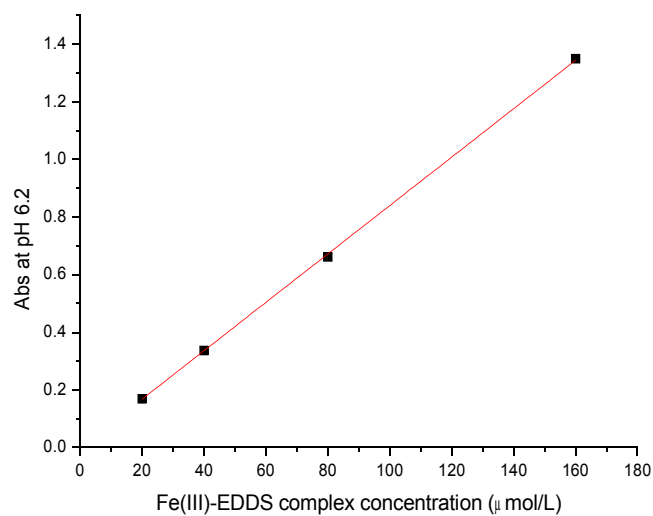


Figure D-5 Molar absorption coefficients of Fe(III)-EDDS complex at 239 nm

The Figure D-6 shows the UV-visible adsorption spectrum at pH 3.7, 6.2 and 8.7 respectively.

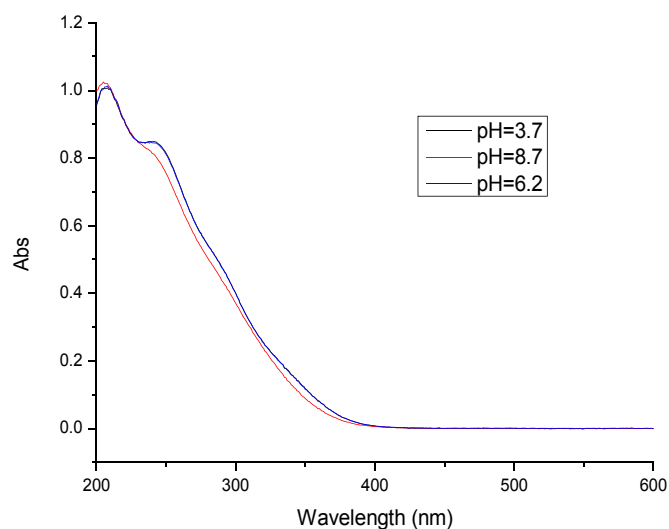


Figure D-6 UV-visible spectrum of Fe(III)-EDDS complex at different pH values

The stability constants of Fe(III)-EDDS complex in aqueous 0.1 mol/L NaCl at 25 °C are given Table D-2 [90].

Table D-2 Stability constants of Fe(III)-EDDS complex in aqueous 0.1 mol/L NaCl at 25 °C.

Reaction	Log (K+3σ) [S,S]-EDDS
$\text{Fe}^{3+} + \text{L}^{4-} \rightarrow \text{FeL}^-$	20.6 ± 0.2
$\text{FeL}^- + \text{H}_2\text{O} \rightarrow \text{Fe(OH)L}^{2-} + \text{H}^+$	7.9 ± 0.1
$\text{Fe(OH)L}^{2-} + \text{H}_2\text{O} \rightarrow \text{Fe(OH)}_2\text{L}^{3-} + \text{H}^+$	9.9 ± 0.1

In a previous research it is demonstrated that the redox potential of the system has significant effect on the oxidation/reduction efficiency of the chemicals. Figure D-7 shows the cyclic voltammogram of 1 mmol/L Fe-EDDS in 0.05 mol/L of KCl at different pH values. Following Figure D-8 shows the cyclic voltammogram of 1 mmol/L of Fe-EDDS, Fe-EDTA and Fe-Citrate in 0.05 mol/L of KCl at pH 6.2 respectively. The redox potentials obtained experimentally during my work from cyclic voltammogram, are presented in Table D-3.

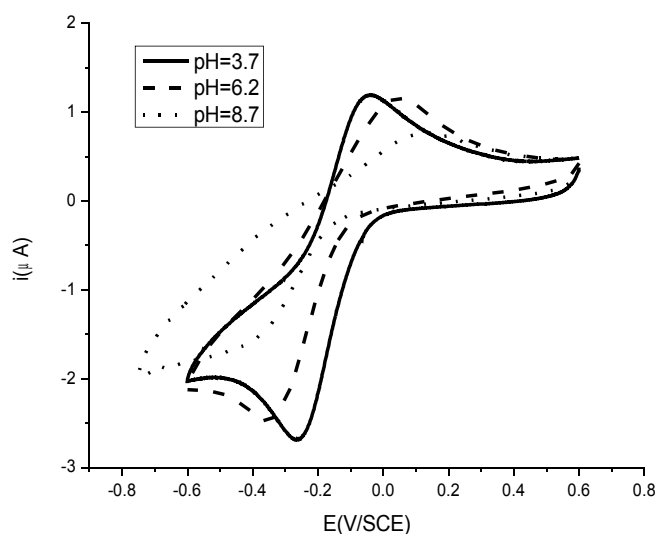


Figure D-7 Cyclic voltammogram of 1 mmol/L of Fe-EDDS in aqueous solution with 0.05 mol/L of KCl at different pH ($\nu = 5 \text{ mV/s}$).

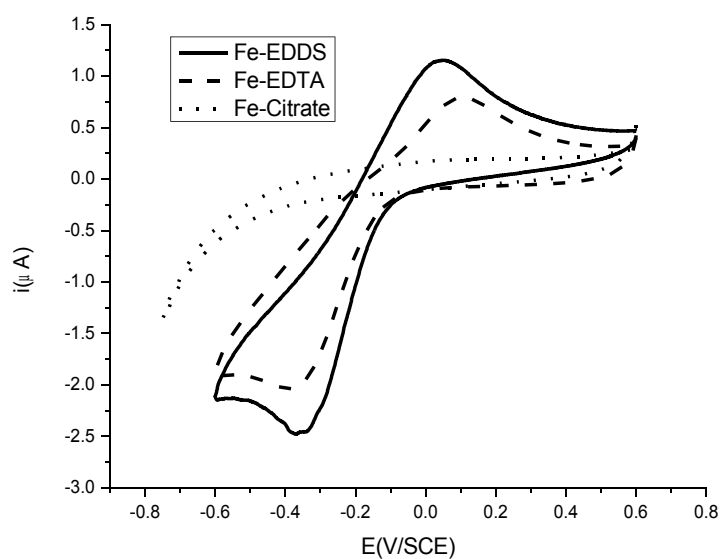


Figure D-8 Cyclic voltammogram of 1mmol/L Fe-EDDS, Fe-EDTA or Fe-Citrate in aqueous solution with 0.05 mol/L KCl at pH 6.2 ($\nu = 5$ mV/s)

The redox potential of Fe(III)/Fe(II)-EDDS complex was evaluated by cyclic voltammetry. At pH 6.2, the cyclic voltammogram is characterized by a quasi-reversible signal with a half-wave potential ($E_{1/2}$) of 0.069 V/NHE (see Figure D-7). This value is slightly lower (29 mV) than the $E_{1/2}$ value obtained under the same pH condition for Fe(III)/Fe(II)-EDTA complex (0.098 V/NHE), and it is significantly lower than $E^{\circ'}$ of free iron couple Fe(III)/Fe(II) (0.700 V/NHE).

Table D-3 Redox parameters obtained from the voltamograms of Fe-EDDS (at different pHs) and Fe-EDTA

	pH	E_{pc} (mV)	E_{pa} (mV)	DEP (mV)
Fe-EDDS	3.7	-251	-54	197
	6.2	-371	21	392
	8.7	-471	105	576
Fe-EDTA	6.2	-390	93	483

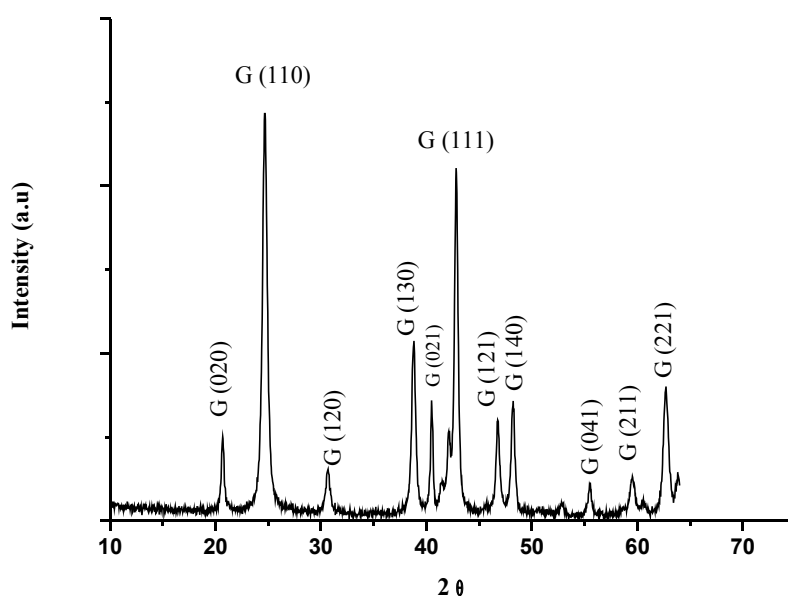
D-1-3. Characterization of goethite

XRD diffractogram confirmed the identity of the expected Fe^{III} oxihydroxide i.e. goethite (Figure D-9). The d-space values of the main peaks of goethite (Figure D-9) were 4.98, 4.19, 3.39, 2.69, 2.59, 2.45, 2.25, 2.19, 1.92, 1.80 and 1.72 Å which correspond to the more intense lines of goethite 020, 110, 120, 130, 021, 111, 121, 140, 041, 211 and 221 respectively [293].

Figure D-9 displays also the TEM pictures of goethite, where typical acicular needle shapes were identified. These crystals vary between 300 and 400 nm in length.

The specific surface area of synthesized solids was determined by multipoint N_2 -BET analysis using a Coulter (SA 3100) surface area analyzer and was found $38\text{m}^2/\text{g}$ for goethite.

The density of singly coordinated site was determined on the basis of AFM images and was found $3.59\text{sites}/\text{nm}^2$ as reported in previous report [317]. The PZC value was found about 9, which is consistent with those reported in the literature [239, 293, 308].



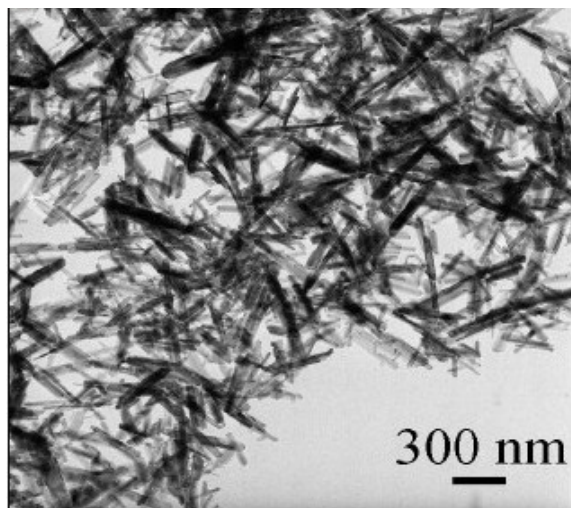


Figure D-9 XRD of individual goethite particles. Bright field TEM images showing goethite particles.

D-1-4. Normalized of emission spectrum of the lamps

Emission spectra of Philips tubes which was used during the irradiation experiments is shown in previous Figure C-2. The emission spectrum of the four Philips TL D 15W/05 tubes, which was normalized by actinometry of PNA/Pyr is shown in Figure D-10. Over the wavelength range 300-350 nm, a total flux of 76 W m^{-2} was measured.

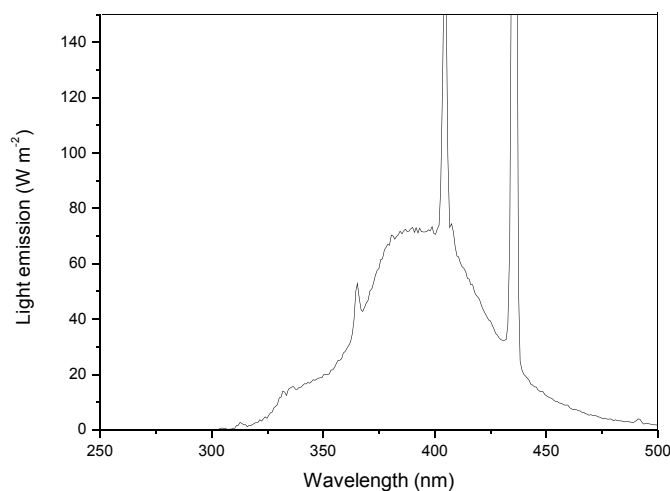


Figure D-10 Emission spectrum of the four Philips TL D 15W/05 tubes.

D-2. BPA degradation in homogeneous Fenton system using Fe(III)-EDDS

D-2-1. Effect of the Fe(III) complexation

In order to check the influence of EDDS in the homogeneous Fenton system, the degradation of BPA in the system of Fe(III), H₂O₂, Fe(III)/H₂O₂ and Fe(III)-EDDS/H₂O₂ respectively was detected and is reported in Figure D-11.

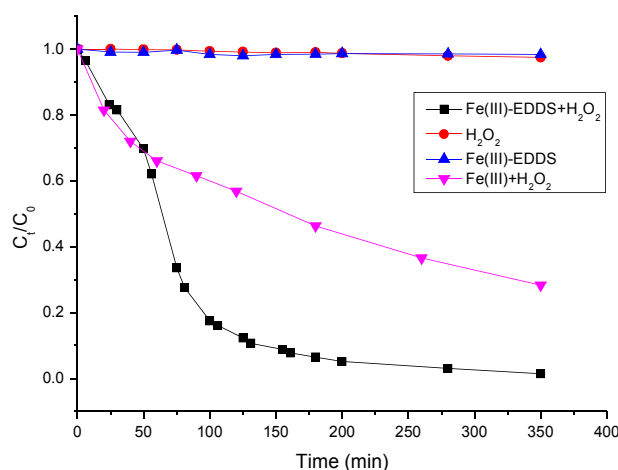


Figure D-11 Comparison between Fe(III) aquacomplex and Fe(III)-EDDS complex during the Fenton process ([Fe(III)-EDDS] = 1mmol/L, [Fe(III)] = 1 mmol/L, [H₂O₂] = 5 mmol/L)

In the presence of hydrogen peroxide or Fe(III)-EDDS alone, the BPA degradation is negligible. When Fe(III) aquacomplexes and hydrogen peroxide are present about 70 % of BPA is removed after 350 minutes. However, due to the precipitation observed in this system at pH 6.2 during the whole reaction process, the BPA degradation in Fe(III)/H₂O₂ system can not be totally attributed to Fenton process, indeed part of BPA disappearance may be due to the coprecipitation with Fe(III) precipitation at neutral pH. This phenomenon of precipitation is hard to be repeated experimentally, but we can estimate that in the presence of Fe(III) alone the BPA disappearance was about 40% in this system. Moreover, in the last oxidation system (Fe(III)-EDDS and H₂O₂) the BPA degradation is faster and the complete BPA transformation is reached after 300 minutes. In this latter oxidation system

(Fe(III)-EDDS and H₂O₂), the removal of BPA has a two-steps behavior: the first step comparable to that observed in the Fe(III)/H₂O₂ system, and then a fall of residual concentration leading to complete BPA removal after 300 minutes.

The interactions between oxidants and Fe(III)-EDDS complexes can be explained by homogeneous reactions analogous to those occurred for free Fe(III) ion with H₂O₂. In fact, superoxide radical anions or hydroperoxide radical together with Fe(II)-EDDS could be generated as described in the following reactions (R3) and (R4). In the Haber-Wiess cycle, the generation of Fe(II) species is the rate-limiting step, and any factor that can raise the corresponding rate constant (R3) would probably accelerate the formation rate of •OH radical (R4) [205, 318].

The higher efficiency observed with Fe(III)-EDDS complex may be due to the complexation of iron by EDDS (i) leading to higher solubility and stabilization of iron in aqueous solution at pH = 6.2, preventing iron precipitation, which could be obviously observed from the appearance of the reaction solution and the total iron concentration in the solution; and/or (ii) advantageously modifying the redox potential of iron, allowing the soluble complex to participate in both the oxidative and reductive step of Fenton-like chemistry. Indeed, two conditions must be simultaneously filled, the ferric complex must be reducible into its ferrous state and the ferrous complex must be able to transfer one electron to hydrogen peroxide. This is thermodynamically allowed when redox potentials of iron complexes are in the range $-324 < E^\circ < 460$ mV.



To determine the redox potential of Fe(III)-EDDS/Fe(II)-EDDS in this study, cyclic voltammetry was performed for EDDS and EDTA systems. At pH 6.2, the cyclic voltammogram is characterized by a quasi-reversible signal with a half-wave potential ($E_{1/2}$)

of 0.069 V/NHE (see Figure D-7). This value is slightly lower (29 mV) than the $E_{1/2}$ value obtained under the same pH condition for the Fe(III)/Fe(II)-EDTA complex (0.098 V/NHE, that is identical to the value reported in ref [319]), and is significantly lower than E° of the free iron couple Fe(III)/Fe(II) (0.700 V/NHE). As previously shown in the case of EDTA-iron complex, the thermodynamic condition is also filled for the reducibility of Fe(III)-EDDS by superoxide [319-321]. This result makes the Fenton reaction more thermodynamically favourable in the presence of EDDS and can explain the higher reduction ability of Fe(III)-EDDS to Fe(II)-EDDS.

D-2-2. Effect of H_2O_2 concentration

In order to elucidate the effect of H_2O_2 concentration on the BPA degradation, three experiments were conducted at pH 6.2 and room temperature by using different concentration of H_2O_2 (1 mmol/L, 5 mmol/L and 10 mmol/L) and 1 mmol/L Fe(III)-EDDS.

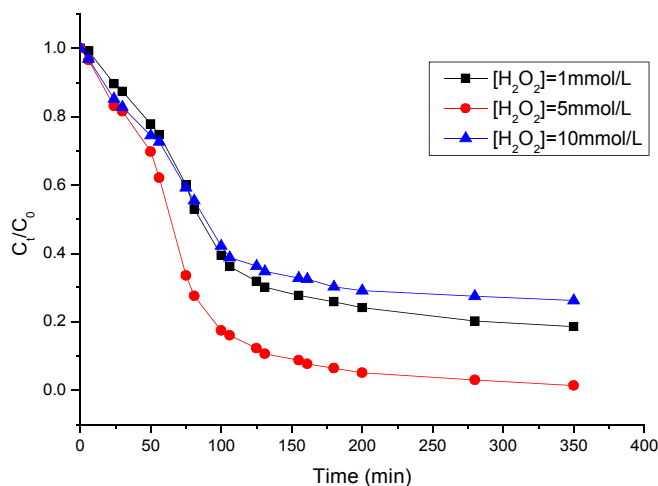
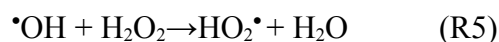


Figure D-12 degradation of BPA with different H_2O_2 concentration
 ([Fe(III)-EDDS]=1mmol/L, [BPA]=20 μ mol/L, pH=6.2)

From Figure D-12 it is evident that BPA remove increases from 1 to 5 mmol/L of H_2O_2 and decreases drastically in the presence of 10 mmol/L of H_2O_2 . Such trend could be explained by the scavenging effect of hydrogen peroxide toward generated hydroxyl radicals via

reaction (R5) with a second order rate constant $k_{\text{H}_2\text{O}_2, \bullet\text{OH}} = 2.7 \times 10^7 \text{ M}^{-1} \text{ s}^{-1}$ [199] and so decreased the efficiency of BPA removal:



Compared with the second order rate constant between BPA and $\bullet\text{OH}$ radicals

$k_{\text{BPA}, \bullet\text{OH}} = 6.9 \times 10^9 \text{ M}^{-1} \text{ s}^{-1}$ and taking the value for the second order rate constant between

Fe(III)-EDDS (considering all complexed iron forms) and $\bullet\text{OH}$ $k_{\text{Fe}_{\text{tot}}\text{EDDS}, \bullet\text{OH}}$ equal to that of the reactivity of $\bullet\text{OH}$ on EDDS alone ($2.0 \times 10^8 \text{ M}^{-1} \text{ s}^{-1}$). With these values, in the presence of the highest H_2O_2 concentration, 44% of the hydroxyl radicals generated will be scavenged by H_2O_2 , 33% by Fe(III)-EDDS and only 23 % by BPA. These percentages were calculated from the pseudo-first order rate constant of $2.7 \times 10^5 \text{ s}^{-1}$, $2.0 \times 10^5 \text{ s}^{-1}$ and $1.38 \times 10^5 \text{ s}^{-1}$ for H_2O_2 (10 mmol/L), Fe(III)-EDDS (1 mmol/L) and BPA (20 $\mu\text{mol/L}$) respectively. In the presence of 1 mmol/L of H_2O_2 , 38% of $\bullet\text{OH}$ radicals react with BPA.

Table D-4 Percentages of OH radical reacting on different compounds as a function of their concentration.

	Concentration (mmol/L)	Reactivity of $\bullet\text{OH}$ (%)
BPA	0.02	29.2
Fe(III)EDDS	1.0	42.3
H_2O_2	5.0	28.5
BPA	0.02	37.8
Fe(III)EDDS	1.0	54.8
H_2O_2	1.0	7.4
BPA	0.02	22.7
Fe(III)EDDS	1.0	32.9
H_2O_2	10.0	44.4
BPA	0.02	37.0
Fe(III)EDDS	0.5	26.8
H_2O_2	5.0	36.2

BPA	0.02	42.7
Fe(III)EDDS	0.25	15.5
H ₂ O ₂	5.0	41.8
BPA	0.02	47.1
Fe(III)EDDS	0.1	6.8
H ₂ O ₂	5.0	46.1

D-2-3. Effect of Fe(III)-EDDS complex concentration

The degradation of BPA in the presence of different Fe(III)-EDDS complex concentrations was determined using 0.1 mmol/L, 0.25 mmol/L, 0.5 mmol/L and 1 mmol/L of Fe(III)-EDDS complex and 5 mmol/L of H₂O₂, at pH 6.2.

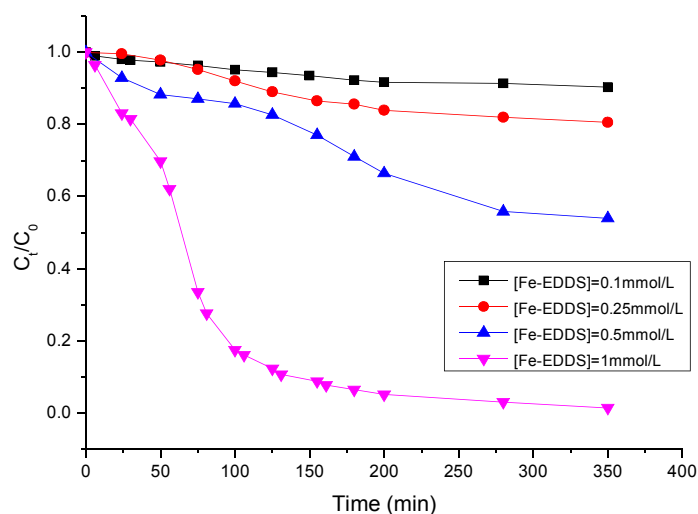


Figure D-13 Degradation of BPA with different Fe(III)-EDDS complex concentrations ([H₂O₂] = 5 mmol/L, [BPA] = 20 μ mol/L, pH =6.2)

The results in Figure D-13 shown obviously a close correlation between the BPA degradation and the Fe(III)-EDDS complex concentration. The degradation rate in case of 1 mmol/L of Fe(III)-EDDS reached 99% in 350 min, while, in case of 0.1 mmol/L of Fe(III)-EDDS, was less than 10%. However, when Fe(III)-EDDS concentration decreases from 1 mmol/L to 0.1 mmol/L, the percentage of \cdot OH radical reacting on Fe(III)-EDDS strongly

decreases also from 42.3% to 6.8%. These observations lead to the conclusion that in our experimental conditions although the reactivity of $\bullet\text{OH}$ is more important on a 1 mmol/L of Fe(III)-EDDS, high concentration of Fe(III)-EDDS complex can enhance the formation of $\text{HO}_2\bullet/\text{O}_2\bullet^-$ and $\bullet\text{OH}$ radicals, and ultimately BPA removal.

At higher concentration of Fe(III)-EDDS, the analysis of BPA was impossible by HPLC due to a very intense peak of the complex Fe(III)-EDDS. In any case, at higher concentration of Fe(III)-EDDS, which can not be implemented in this experiments, the competition for the $\bullet\text{OH}$ reactivity between EDDS ($k_{\text{EDDS},\bullet\text{OH}} = 2.0 \times 10^8 \text{ M}^{-1}\text{s}^{-1}$ [85]) and BPA will cause the decrease of the BPA degradation like in the presence of H_2O_2 as discussed before. This phenomenon was observed during the degradation of 17 β -estradiol photoinduced by Fe(III)-EDDS complex [92].

D-2-4. Effect of oxygen

The effect of oxygen on BPA degradation ($[\text{Fe(III)-EDDS}] = 1 \text{ mmol/L}$, $[\text{H}_2\text{O}_2] = 5 \text{ mmol/L}$, $[\text{BPA}] = 20 \text{ }\mu\text{mol/L}$) using the Fenton-like process at pH 6.2 was investigated by supplying proper gas in the reaction solution (oxygen or argon).

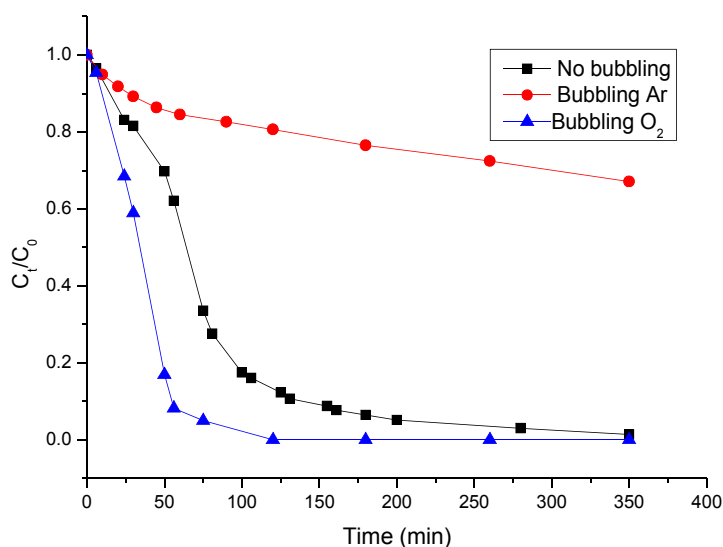


Figure D-14 Effect of Oxygen on the degradation of BPA ([Fe(III)-EDDS] = 1mmol/L, [H₂O₂] = 5 mmol/L, [BPA] = 20 μmol/L, pH = 6.2)

As reported in Figure D-14 at higher oxygen concentration (bubbling oxygen) a faster decay of BPA was noticed while in the absence of oxygen (bubbling argon) the transformation was strongly retarded. This effect could be mainly attributed to the reactivity of oxygen on the BPA radical formed subsequently by the hydroxyl radical attack. In fact, Torres and coworkers [310] investigated the BPA reactivity with photogenerated hydroxyl radical via ultrasound and UV-Fe(III) treatment suggesting that monohydroxylated BPA products could be formed via the first $\cdot\text{OH}$ attack and subsequent formation of peroxy radical in the presence of oxygen.

The BPA degradation in oxygen free solution could be accounted by an insufficient removal of oxygen from the solution and/or *via* oxygen-free pathways could not be excluded. The low degradation of BPA in the absence of oxygen, could be also explained by the reduction of BPA radical with Fe(II) species giving back BPA without net BPA degradation and secondly by the possible oxidation of BPA radical with Fe(III)-EDDS or H₂O₂.

D-2-5. Effect of pH value

In order to better understand the applicable pH value during Fenton process in the presence of Fe(III)-EDDS complex, experiments at pH 3.7, 6.2 and 8.7 were conducted. The initial concentration were the following: 1 mmol/L Fe(III)-EDDS and 5 mmol/L H₂O₂.

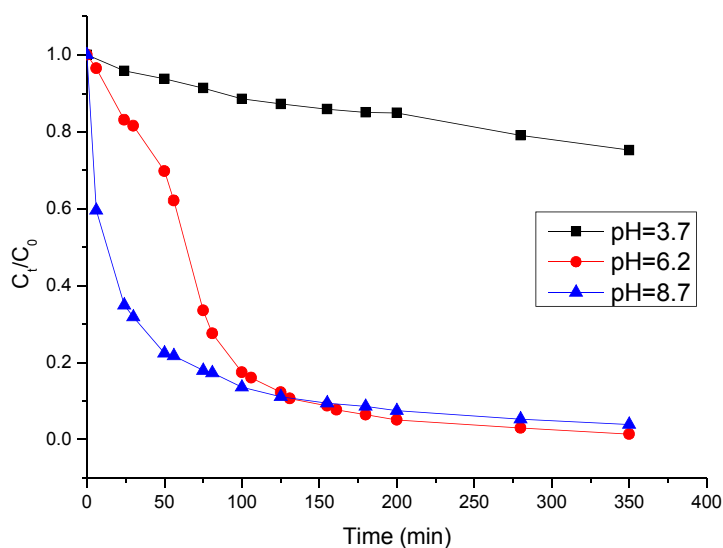
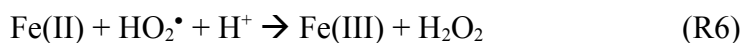


Figure D-15 Degradation of BPA in different pH ([Fe(III)-EDDS] = 1mmol/L, [H₂O₂] = 5 mmol/L, [BPA] = 20 μmol/L)

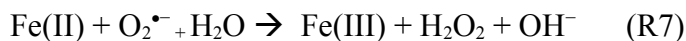
The results reported in Figure D-15 shown, although the initial reaction rate was different, a fast BPA degradation at both pH 8.7 and 6.2 was achieved, reaching the complete transformation at around 350 minutes, whereas, the slow degradation rate at pH 3.7 was noticed. The effect of pH can be explain mainly by two reasons, the different speciation of Fe(III)-EDDS complex as function of pH and the reactivity of generated radical species.

Orama et al. [91] suggested the presence of different forms, Fe(III)-EDDS⁻ at lower pH and hydrolyzed complex species at higher pH: Fe(OH)EDDS²⁻ and Fe(OH)₂EDDS³⁻ with a logarithmic stability constant K_{ML} of 7.9 and 9.9 respectively. They suggested also that the suitable pH range for the use of EDDS as chelating agent of Fe(III) is 3 to 9. Under such hypotheses we can estimate that at pH 3.7 iron complex is on the form Fe(III)-EDDS⁻, while at circumneutral or basic pHs the main forms are Fe(OH)EDDS²⁻ and Fe(OH)₂EDDS³⁻.

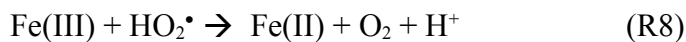
The increase of BPA degradation at higher pH could be explained by taking into account the effect of HO₂•/O₂•⁻ on the Fe(III)/Fe(II) cycle:



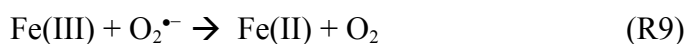
$$k_{\text{Fe(II),HO}_2^\bullet} = 1.2 \times 10^6 \text{ M}^{-1} \text{ s}^{-1} \quad [311]$$



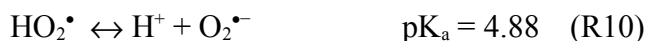
$$k_{\text{Fe(II),O}_2^{\bullet-}} = 1.0 \times 10^7 \text{ M}^{-1} \text{ s}^{-1} \quad [312]$$



$$k_{\text{Fe(III),HO}_2^\bullet} < 1.0 \times 10^3 \text{ M}^{-1} \text{ s}^{-1} \quad [312]$$



$$k_{\text{Fe(III),O}_2^{\bullet-}} = 5.0 \times 10^7 \text{ M}^{-1} \text{ s}^{-1} \quad [313]$$



For reactions (R6) and (R7), the formation of an Fe(III)-hydroperoxy complex with a form of $\text{Fe(III)(HO}_2)_2^{2+}$ has been previously suggested, on the basis of spectroscopic studies at acid pHs (between 1.0 and 3.0) [314].

In fact at pH 3.7, the main form present in solution (94%) is the hydroperoxyl radical (HO_2^\bullet) that could shift the equilibrium to the formation of Fe(III) (see equations R6 and R8) while at pHs 6.2 and 8.7 the main form (respectively 95 and 100%) is the superoxide radical anion ($\text{O}_2^{\bullet-}$). In the presence of $\text{O}_2^{\bullet-}$ the equilibrium is displaced to the formation of Fe(II) (see equations R7 and R9). We can expect a similar trend in the case of the EDDS complex and, as reported in the literature for EDTA and glutamate-iron complexes the reactivity of superoxide radical could be higher compared to those with free iron [224, 309].

In such scenario it is clear that the pH plays a crucial role on the Fe(III)/Fe(II) cycle and could accelerate the oxidation of Fe(III) into Fe(II) and as consequence increase the hydroxyl radical formation via Fenton reaction from equations R4 and R2. Such trend was supported by the measurement of hydroxyl radical formation in different pH conditions. We estimated the initial formation rate of hydroxyl radical by using nitrobenzene as trapping molecule for $\bullet\text{OH}$ radical. Indeed, the hydroxyl radical formation rate at pH 3.7 was

measured equal to $R_{\cdot\text{OH}}^f = 3.8 \times 10^{-9} \text{ M s}^{-1}$, while at pH 6.2 the value was 2.5 times higher and equal to $9.7 \times 10^{-9} \text{ M s}^{-1}$.

Table D-5 $\cdot\text{OH}$ radical formation rate at different pH

	pH = 3.7	pH = 6.2
$R_f(\cdot\text{OH}) (\text{M s}^{-1})$	3.8×10^{-9}	9.7×10^{-9}

D-2-6. Implication of radical species in the Fenton process

In order to have a better understanding of the $\cdot\text{OH}$ and $\text{HO}_2\cdot/\text{O}_2^{\cdot-}$ radicals role and impact during Fenton process 2-propanol and chloroform were used as scavenger of radicals. 2-propanol ($k_{2\text{propanol},\cdot\text{OH}} = 1.9 \times 10^9 \text{ M}^{-1}\text{s}^{-1}$ [302]) was used as $\cdot\text{OH}$ scavenger to check the effect on the BPA degradation. In the presence of 1 mmol/L of Fe(III)-EDDS complex, 5 mmol/L of H_2O_2 and 20 $\mu\text{mol/L}$ of BPA at pH 6.2, effect of 2-propanol was reported in Figure D-16. The results indicated that the addition of 2-propanol obviously inhibited the degradation of BPA playing a competitive role toward the hydroxyl radical reactivity. When the concentration of 2-propanol increased, the degradation of BPA decreased significantly. At 2 mmol/L of 2-propanol, the degradation of BPA was completely inhibited demonstrated that the degradation of BPA is mainly due to the reactivity with $\cdot\text{OH}$ radical.

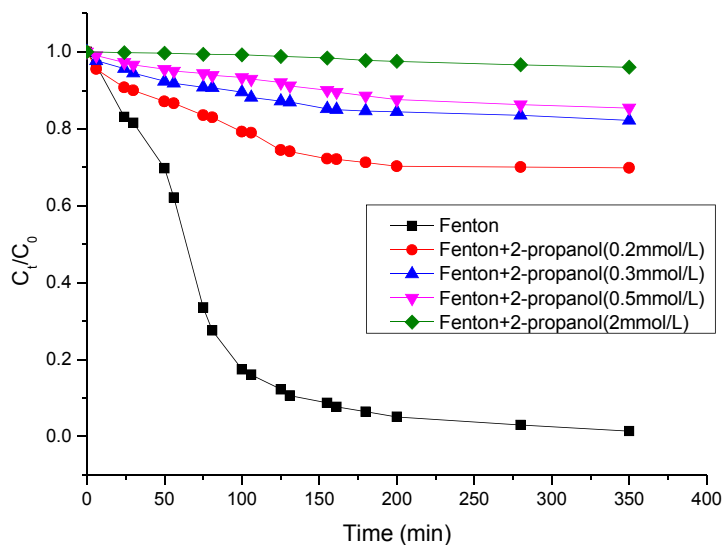
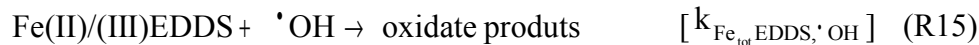


Figure D-16 Effect of different concentration of 2-propanol on the degradation of BPA ([Fe(III)-EDDS] = 1 mmol/L, [H₂O₂] = 5 mmol/L, [BPA] = 20 μmol/L, pH = 6.2)

To calculate the initial hydroxyl radical formation rate from Fenton reaction the following reactions (R11-R15) were included in the kinetic treatment of data:



Where $R_{\cdot\text{OH}}^f$ is the initial formation rate of hydroxyl radical produced via different sources

(mainly reaction of Fe(II)-EDDS with H₂O₂), $k_{\text{BPA},\cdot\text{OH}}$, $k_{2\text{Pr},\cdot\text{OH}}$ and $k_{\text{H}_2\text{O}_2,\cdot\text{OH}}$ the second

order rate constants between hydroxyl radicals and BPA, 2-propanol and hydrogen peroxide respectively. $k_{\text{Fe}_{\text{tot}}\text{EDDS}, \cdot\text{OH}}$ was varied between 2.0×10^8 and $5.2 \times 10^8 \text{ M}^{-1} \text{ s}^{-1}$, the reactivity of $\cdot\text{OH}$ with EDDS and Fe(II)-EDTA respectively.

The initial degradation rate of BPA ($R_{\text{BPA}}^{\text{d}}$) (M s^{-1}) as function of the isopropanol (2Pr) concentration was fitted using the following equation obtained from the application of the steady-state approximation to $\cdot\text{OH}$:

$$R_{\text{BPA}}^{\text{d}} = \frac{R_{\cdot\text{OH}}^{\text{f}} k_{\text{BPA}, \cdot\text{OH}} [\text{BPA}]}{k_{\text{BPA}, \cdot\text{OH}} [\text{BPA}] + k_{\text{H}_2\text{O}_2, \cdot\text{OH}} [\text{H}_2\text{O}_2] + k_{\text{Fe}_{\text{tot}}\text{EDDS}, \cdot\text{OH}} [\text{Fe}_{\text{tot}}\text{EDDS}] + k_{2\text{Pr}, \cdot\text{OH}} [2\text{Pr}]} \quad (\text{E1})$$

The data reported in Figure were fitted with an equation type: $y = \frac{1}{a + bx}$ where

$$a = \frac{k_{\text{BPA}, \cdot\text{OH}} [\text{BPA}] + k_{\text{H}_2\text{O}_2, \cdot\text{OH}} [\text{H}_2\text{O}_2] + k_{\text{Fe}_{\text{tot}}\text{EDDS}, \cdot\text{OH}} [\text{Fe}_{\text{tot}}\text{EDDS}]}{R_{\cdot\text{OH}}^{\text{f}} k_{\text{BPA}, \cdot\text{OH}} [\text{BPA}]}, \quad b = \frac{k_{\cdot\text{OH}, 2\text{Pr}}}{R_{\cdot\text{OH}}^{\text{f}} k_{\cdot\text{OH}, \text{BPA}} [\text{BPA}]} \text{ and } x \text{ the}$$

concentration of isopropanol [2Pr]. From the data fitted we can obtain from the fit, the formation rate of $\cdot\text{OH}$ from Fenton reaction $R_{\cdot\text{OH}}^{\text{f}}$ is comprised between 7.5×10^{-9} and $1.2 \times$

10^{-8} M s^{-1} considering $k_{\cdot\text{OH}, \text{Fe}_{\text{tot}}\text{EDDS}} = 2.0 \times 10^8$ and $5.2 \times 10^8 \text{ M}^{-1} \text{ s}^{-1}$ respectively. The value of $R_{\cdot\text{OH}}^{\text{f}}$ obtained by the kinetic model is in agreement with calculated one by using nitrobenzene as probe molecule of $9.7 \times 10^{-9} \text{ M s}^{-1}$.

Following reaction 1 the first radical produced during Fe(III) species reactivity toward hydrogen peroxide is the $\text{HO}_2\cdot/\text{O}_2^{\cdot-}$ radical. At pH 6.2, the radical is mainly (95%) present under the superoxide radical anion form ($\text{O}_2^{\cdot-}$), $\text{pK}_a(\text{HO}_2\cdot/\text{O}_2^{\cdot-}) = 4.8$. In order to investigate the role of $\text{O}_2^{\cdot-}$ during the BPA degradation, chloroform (CHCl_3) was used as an $\text{O}_2^{\cdot-}$ scavenger. Indeed, the second-order reaction rate constant between hydrated electrons and organic compounds is a general indicator of reducibility by the $\text{O}_2^{\cdot-}$. So, chloroform is

highly reactive with $O_2^{\bullet-}$ ($k_{CHCl_3 \cdot e^-} = 3 \times 10^{10} \text{ M}^{-1}\text{s}^{-1}$) and poorly reactive with hydroxyl radical $k_{CHCl_3 \cdot OH} = 5 \times 10^6 \text{ M}^{-1}\text{s}^{-1}$. [302].

In Figure D-17 we reported the BPA degradation in the presence of 1 mmol/L of Fe(III)-EDDS complex and 5 mmol/L of H_2O_2 at pH 6.2 using different $CHCl_3$ concentrations. The degradation of BPA strongly decreases in the presence of $CHCl_3$ until a concentration of 400 $\mu\text{mol/L}$. At higher concentration of $CHCl_3$, 1 mmol/L, the inhibition is significantly the same, corresponding to an inhibition of 80%. This observation shows that, as a contrary of experiments performed with 2-propanol, the inhibition is not complete.

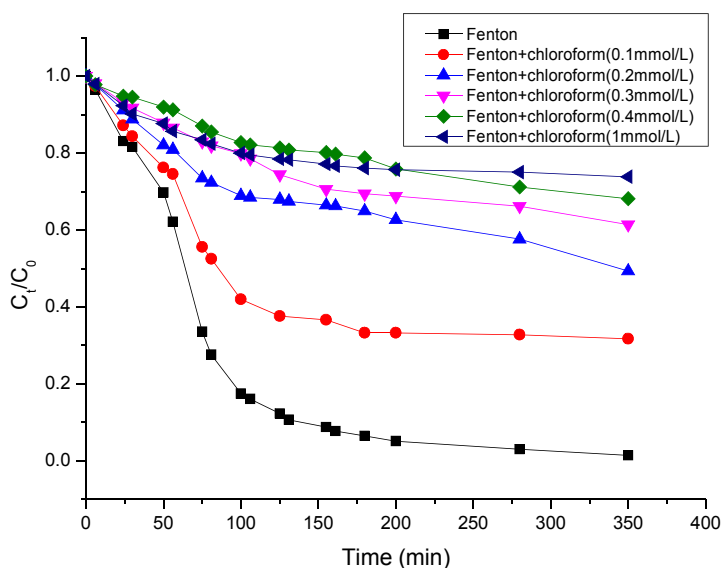


Figure D-17 Effect of different concentration of chloroform on the degradation of BPA ([Fe(III)-EDDS] = 1 mmol/L, [H_2O_2] = 5 mmol/L, [BPA] = 20 $\mu\text{mol/L}$, pH = 6.2)

These two sets of experiments with both scavengers leads to important conclusions about the mechanism involved in Fenton process with Fe(III)-EDDS complex in our experimental conditions:

$\bullet OH$ radicals are mainly responsible of the BPA degradation. But their formation, from the Fenton process, depends strongly (80%) of the presence of superoxide radical anion. Indeed, 20% of the $\bullet OH$ radical formation comes from the classical reactions R3 and R4 without need of superoxide radical anion and the other 80% comes also from Fenton

process but through the reduction of Fe(III)-EDDS complex (reaction R9 adapted to Fe(III)-EDDS) into Fe(II)-EDDS complex with superoxide radical anion (Figure D-18).

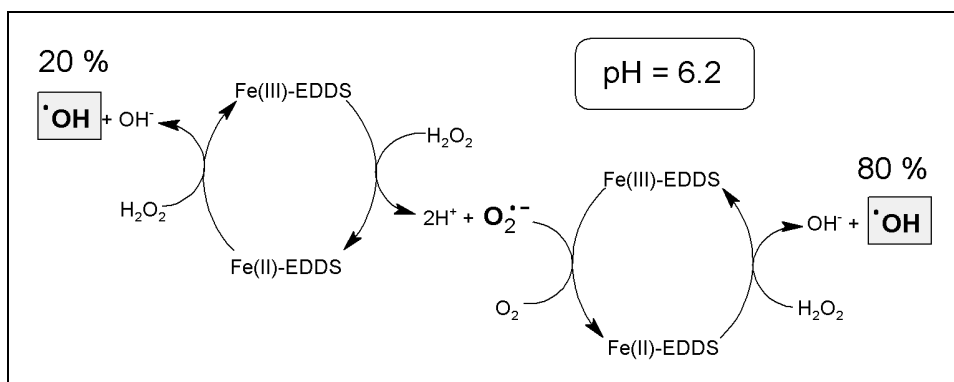


Figure D-18 Mechanism scheme in Fenton system

With the experiments performed with a specific scavengers (2-propanol and chloroform), we have clearly demonstrated the predominant role of the superoxide radical anion for the formation of the radical hydroxyl and so in the process of BPA degradation.

D-2-7. Comparison with other Fe(III) complex

In order to better understand the positive effect of EDDS in this Fenton system, other different kinds of organic ligands were used to complex Fe(III) and work as iron source in Fenton system. The BPA degradation in different iron complex Fenton system was observed and shown in Figure D-19.

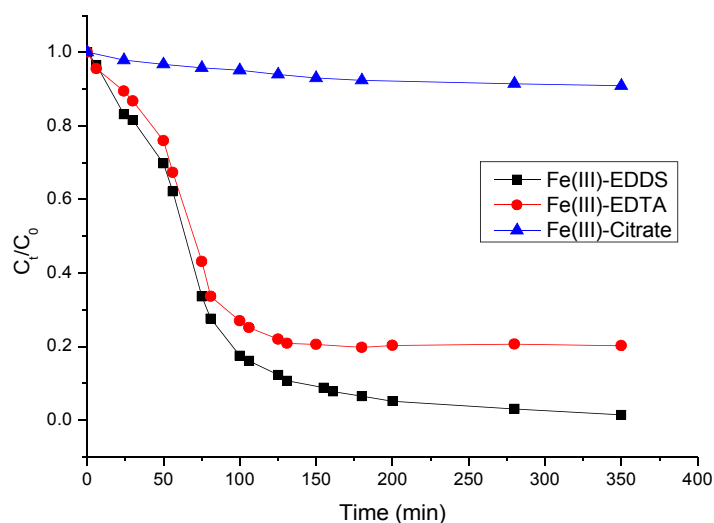


Figure D-19 BPA degradation in different Fenton systems using different iron complexes ([Fe(III)-complex] = 1 mmol/L, [H₂O₂] = 5 mmol/L, [BPA] = 20 μ mol/L, pH = 6.2)

It is obviously that the highest efficiency of BPA degradation at pH 6.2 was observed in the Fenton system when Fe(III)-EDDS was used as iron source. The degradation of BPA in the presence of Fe(III)-citrate in this Fenton system was very low and negligible. As in Fenton-like process, the reaction rate of reduction from Fe(III) to Fe(II) is important to the whole reaction process, the redox potential of Fe(III)/Fe(II) plays important role in the efficiency of Fenton-like process. Corresponding to the results of redox potentials gained in the cyclic voltammetry measurements, it can be sure again that the addition of EDDS can reduce the Fe(III)/Fe(II) redox potential effectively, and therefore enhance the efficiency of Fenton system and also the degradation of BPA. At the same pH condition, the $E_{1/2}$ value of Fe(III)/Fe(II)-EDTA (0.098 V/NHE) (0.096 V/NHE at pH = 7.2 and 25°C in previous research), is a little lower than that of Fe(III)/Fe(II)-EDDS (0.069V/NHE). From previous research, it is also found that the redox potential of Fe(III) /Fe(II)-citrate at pH = 7.0 and 25°C is 0.372 V/NHE [315], which is also much higher than that of Fe(III)/Fe(II)-EDDS, and this could explain the low BPA degradation in presence of Fe(III)-citrate. As reported in previous research [101], the redox potential of Fe(III)/Fe(II)-oxalate, which could not be used in our work due to the instability of Fe(III)-oxalate solution at pH 6.2, was varying at pH ranging from 1.5 to 5.5, and the values are higher than that of Fe(III)/Fe(II)-EDDS. This

confirmed again that the positive effect of EDDS on the efficiency of Fenton system is mainly due to its influence on the redox potential of the system.

D-2-8. Effect of EDDS concentration

From the results shown in Figure D-20, it is obviously that the excess addition of EDDS can totally inhibit the degradation of BPA. The reason of this phenomenon can be simply due to the reaction of $\bullet\text{OH}$ radicals on EDDS. When the concentration of EDDS is too high, almost all $\bullet\text{OH}$ radicals produced in Fenton system are scavenged by EDDS, so almost no BPA is degraded. It is known from previous research that the complexation ratio between Fe(III) and EDDS was 1:1. When the concentration of EDDS used is higher than that of Fe(III), the excess of EDDS is in the solution, and there is a competition of $\bullet\text{OH}$ radicals reaction between EDDS and BPA. When the concentration of EDDS is high enough, almost all of $\bullet\text{OH}$ radicals were trapped by EDDS, and hence the degradation of BPA was totally inhibited. Comparing the rate constant between $\bullet\text{OH}$ radical and BPA ($k_{(\bullet\text{OH},\text{BPA})} = 6.9 \times 10^9 \text{ M}^{-1} \text{ s}^{-1}$) with that between $\bullet\text{OH}$ radical and EDDS ($k_{(\bullet\text{OH},\text{EDDS})} = 2 \times 10^8 \text{ M}^{-1} \text{ s}^{-1}$ [86]), with 10 mmol/L of EDDS and with a concentration of BPA of 20 μM , the pseudo-first order rate constant for BPA and EDDS is $1.38 \times 10^5 \text{ s}^{-1}$ and $2 \times 10^6 \text{ s}^{-1}$ respectively. So it is observed that in this condition more than 90% of $\bullet\text{OH}$ radical was trapped by EDDS.

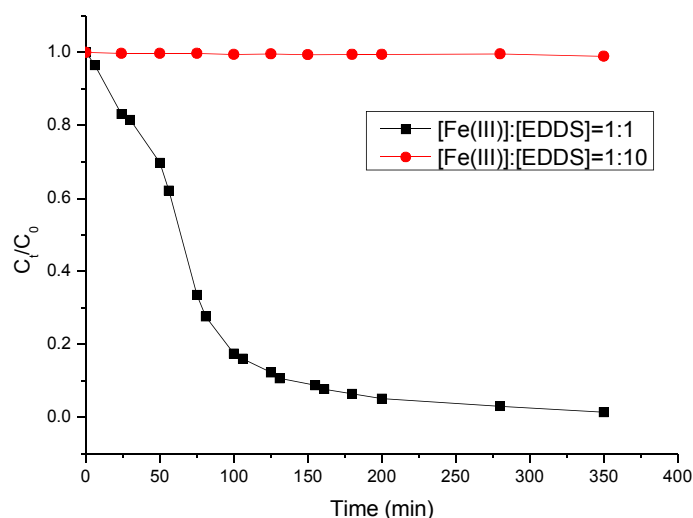


Figure D-20 BPA degradation using different concentrations of EDDS in complex preparation

([Fe(III)] = 1 mmol/L, [H₂O₂] = 5 mmol/L, [BPA] = 20 μmol/L, pH = 6.2)

D-2-9. Conclusion

The use of Fe(III)-EDDS complex as iron source in the Fenton process was evaluated during the BPA degradation. The main positive effect of Fe(III)-EDDS complex is the fact that Fe(III)-EDDS into Fenton reaction can extend and strongly improve the degradation of BPA at neutral and alkaline pH. The first important role of EDDS is the stabilization of Fe(III) in a large range of pH (3 to 9) preventing its precipitation. The increase of H₂O₂ and Fe(III)-EDDS concentrations leads to a higher efficiency of BPA degradation. However, beyond a certain concentration the competition of OH radical reactivity between BPA and H₂O₂ or Fe(III)-EDDS is detrimental for the efficiency of the process. The effect of oxygen was also determined and it was shown that oxygen is an important parameter for the oxidation of BPA. The experiments performed at different pH demonstrated that pH is an influent parameter. As a contrary, of a classical Fenton process using iron ions, the efficiency is much higher at near neutral and slightly basic pH than in acidic pH. This effect is due to the presence of HO₂[•] or O₂^{•-} as a function of pH (pK_a = 4.86).

The formation and the role of two main radical species ([•]OH and HO₂[•]/O₂^{•-}) involved in such system were demonstrated. The hydroxyl radical is mainly responsible of organic compound (BPA) degradation but its formation is strongly dependant of the presence of superoxide radical anion (O₂^{•-}). Indeed, the presence of this radical species accelerates the cycling between Fe(III) and Fe(II), avoid the decomposition of H₂O₂ for the reduction of Fe(III) species and so increase the production of [•]OH radical. For the first time, the results of this study demonstrate that the reduction of Fe(III)-EDDS by superoxide radical anion is a crucial reaction which govern the efficiency of the Fenton process involving iron complexes. These results are very encouraging for the application of the Fenton process under conditions of pH closer natural conditions encountered in the environment.

D-3. BPA degradation in homogeneous photo-Fenton process

D-3-1. Photochemical degradation of BPA in the presence of Fe(III)

In order to better understand the effect of Fe(III) in the photodegradation of BPA, experiments in the presence of 0.1 mmol/L Fe(III) under UV irradiation were conducted at pH 3.7, 6.2 and 8.7 respectively.

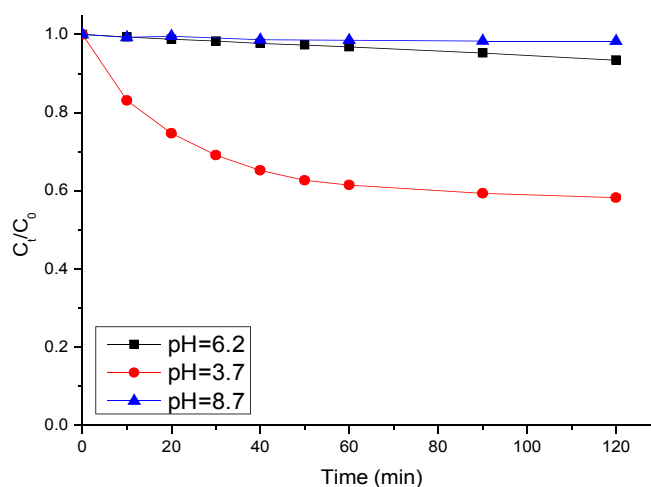


Figure D-21 BPA degradation in photochemical process in the presence of Fe(III) at different pH
([Fe(III)] = 0.1 mmol/L, [BPA] = 20 μ mol/L)

From the results shown in Figure D-21, it is obviously that the BPA degradation was effective in the presence of Fe(III) only at pH 3.7, BPA degradation reaches 40% in 120 min of irradiation, while at pH 6.2 and 8.7 the degradation of BPA can be neglected. This result is in agreement with the results of previous research [31] where iron species are much more stable in solution and photosensitive at acidic pH value. Usually at neutral and alkaline pH, iron species are not stable in the solution and lead to the formation of precipitate. So, the properties of Fe(III) species in solution will be weakened and the production of reactive species at neutral or basic pH due to the photosensitized reaction of Fe(III) in solution will be quite low and resulting in the low efficiency of BPA degradation.

D-3-2. Degradation of BPA in traditional photo-Fenton process

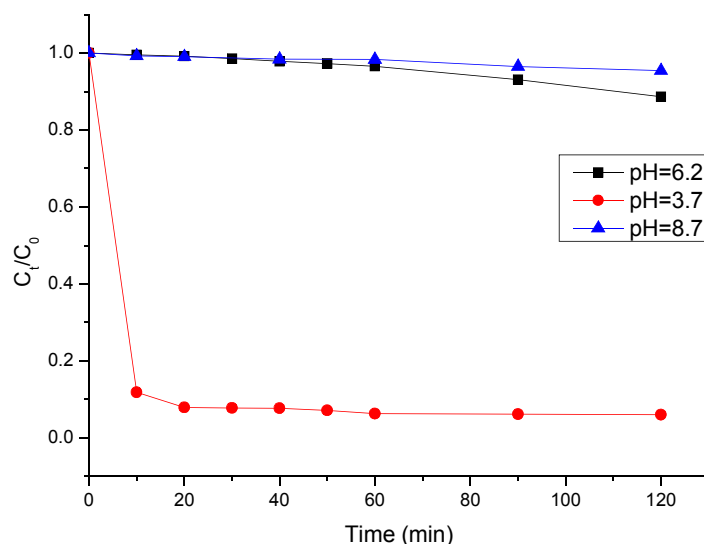


Figure D-22 BPA degradation in photo-Fenton process at different pH ([Fe(III)] = 0.1 mmol/L, [H₂O₂] = 0.1 mmol/L, [BPA] = 20 μ mol/L)

This part of experiments was conducted in order to show the efficiency of photo-Fenton at different pH value. We can read from the results showed in Figure D-22 that in traditional photo-Fenton process, BPA can be degraded very fast at pH 3.7 and the degradation reached over 90% in 20 min of irradiation. As the contrary, the BPA degradation at pH 6.2 and 8.7 was very low, and the degradation rate at both pHs was less than 10%, which could almost be neglected. In previous research, there are also same results that traditional photo-Fenton process can only get high efficiency at acidic pH values, which is due to the presence of high reactive iron species at acidic pH values. At neutral and alkaline pH, the interaction between iron species and H₂O₂ will be weakened due to the precipitation of iron. This reason can be easily confirmed by our observation that in the reaction solution at pH 6.2 and 8.7, there was yellow-brown precipitation formed.

D-3-3. Photochemical degradation of BPA in the presence of Fe(III)-EDDS

In previous research of our group, it is confirmed that the presence of Fe(III)-EDDS can

enhance the photodegradation of organic compounds in solutions [86, 92]. In this part, BPA was used as model substance to further confirm the photochemical reactivity of Fe(III)-EDDS complex. The effect of different parameters including pH values and Fe(III)-EDDS complex concentration was studied.

D-3-3-1. Effect of pH value

The BPA photodegradation in the presence of Fe(III)-EDDS complex at pH 3.7, 6.2 and 8.7 was detected. From the results showed in Figure D-23, it is demonstrated that the photochemical properties of Fe(III)-EDDS at pH 3.7, 6.2 and 8.7 are almost the same. The degradation rate of BPA is around 60% at all three pHs. At the same time, through the observation during the whole reaction process, there was no precipitation in solution, which means that in the presence of EDDS, iron species are stable in aqueous solution at neutral and alkaline pH due to the complexation between Fe(III) and EDDS. At the same time, the quantum yield of $\cdot\text{OH}$ radical formation is higher when the pH value of the system increases from 3.0 to 9.0 [92]. Anyway, the $\cdot\text{OH}$ radicals required for BPA degradation are produced photochemically at pH ranging from 3.0 to 9.0.

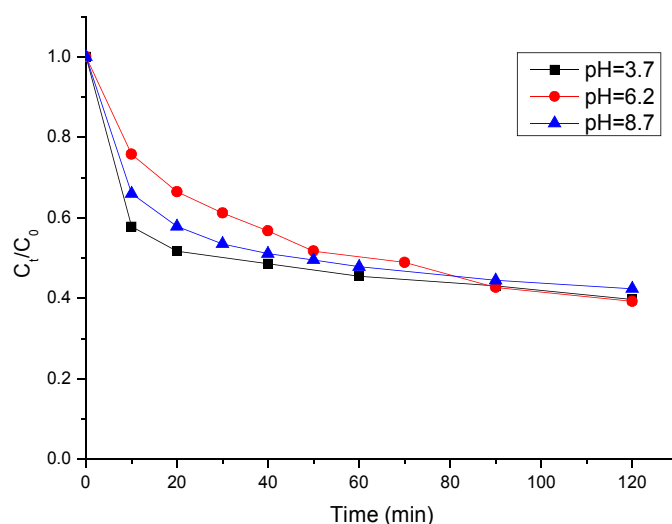


Figure D-23 BPA degradation in photochemical process in the presence of Fe(III)-EDDS at different pH ([Fe(III)-EDDS] = 0.1 mmol/L, [BPA] = 20 $\mu\text{mol/L}$)

D-3-3-2. Effect of Fe(III)-EDDS concentration

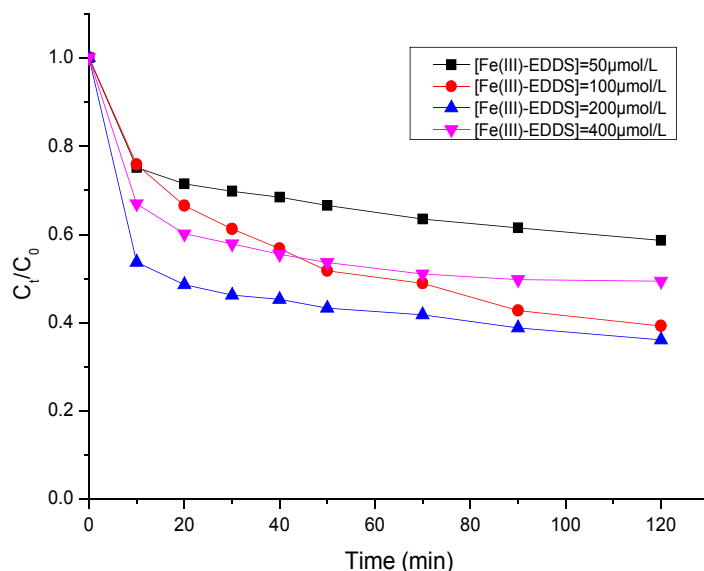


Figure D-24 BPA degradation in photochemical process in the presence of different Fe(III)-EDDS concentration ([BPA]= 20 μmol/L, pH = 6.2)

The effect of Fe(III)-EDDS complex concentration on the BPA photodegradation was also examined. The experiments of BPA photodegradation in the presence of Fe(III)-EDDS complex using the concentration including 0.05 mmol/L, 0.1 mmol/L, 0.2 mmol/L and 0.4 mmol/L. From the results shown in Figure D-24 it can be concluded that when the concentration of Fe(III)-EDDS complex increases from 0.05 mmol/L to 0.2 mmol/L, the photodegradation efficiency of BPA in 120 min enhances from 41.5% to 64%, and the initial reaction rate also follow the same tendency.

However, when the concentration of Fe(III)-EDDS complex used in the system increases to 0.4 mmol/L, the trend of BPA degradation changed. The degradation of BPA in 120 min reduces to 51.5%, which is slower than in the case of Fe(III)-EDDS concentrations at 0.1 mmol/L and 0.2 mmol/L. So with this experiment, it can be demonstrated that the existence of Fe(III)-EDDS complex can enhance the degradation of BPA through enhancing the

generation of $\bullet\text{OH}$ radical, however, if the concentration of this complex added is too high, the BPA degradation will be inhibited due to the competition reaction with $\bullet\text{OH}$ radical between BPA and EDDS. Indeed, it is known that EDDS can also react with $\bullet\text{OH}$ radical with high reaction constant ($k_{(\bullet\text{OH},\text{EDDS})} = 2 \times 10^8 \text{ M}^{-1}\text{s}^{-1}$ [86]).

The conclusion of the photochemical study of the complex Fe(III)-EDDS was the description of the photochemical cycle of Fe(III)/Fe(II) in the presence of EDDS. EDDS stabilizes iron in solution and increases the oxidation of Fe(II), which the limiting step, by complexation (Figure D-25) and increases the $\bullet\text{OH}$ radical production [92].

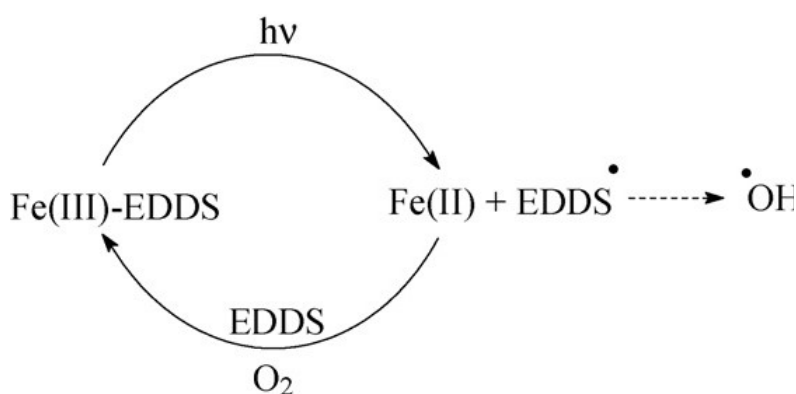


Figure D-25 The cycle of photochemical process of Fe(III)-EDDS [92]

D-3-4. Degradation of BPA in photo-Fenton process in the presence of Fe(III)-EDDS

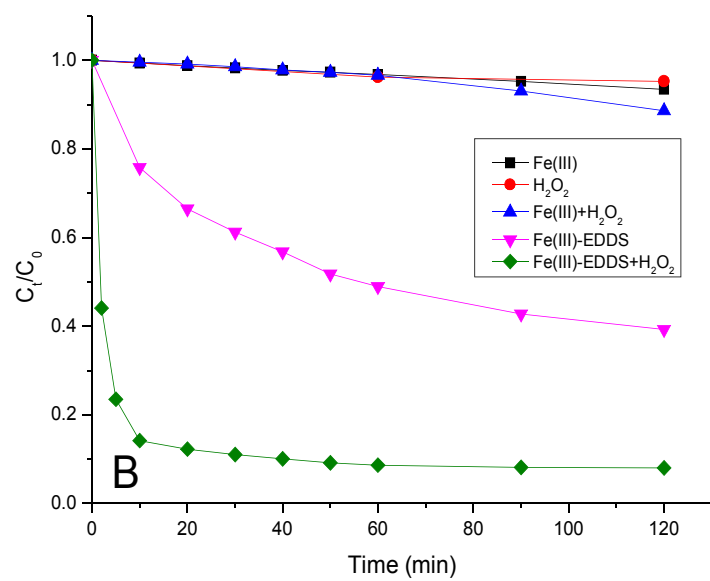
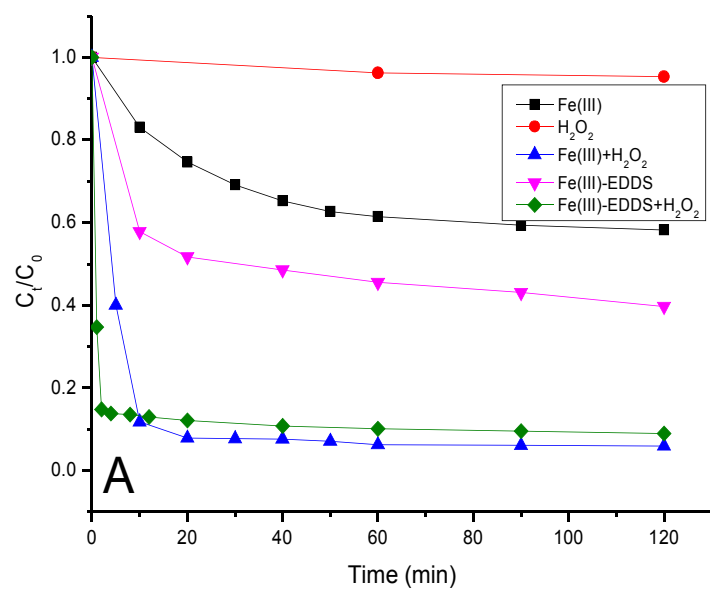
D-3-4-1. Photodegradation of BPA experiments in different systems

The degradation of BPA at pH 3.7, 6.2 and 8.7 in the presence of light using Fe(III), H₂O₂, Fe(III)/ H₂O₂, Fe(III)-EDDS and Fe(III)-EDDS/H₂O₂, is shown in Figures D-26. It is obviously that at all three pHs, the best condition of BPA degradation was achieved in the system of Fe(III)-EDDS/H₂O₂.

At pH 3.7 (Figure D-26 A), although the BPA degradation in the system of Fe(III)/ H₂O₂ was almost the same as in the system of Fe(III)-EDDS/H₂O₂, the initial reaction rate in the system of Fe(III)-EDDS/H₂O₂ was obviously faster, which may be due to the high photoreactivity of Fe(III)- EDDS leading to the faster $\bullet\text{OH}$ radical generation in Fe(III)-EDDS/H₂O₂ system.

In the case of pH 6.2 (Figure D-26 B), in the presence of hydrogen peroxide (0.1 mmol/L) or Fe(III) (0.1 mmol/L) alone or a mixture of both, the BPA degradation is less than 10% after 120 min of irradiation. However, in the presence of Fe(III)-EDDS, over 60% of the BPA was transformed, due to the rapid photochemical reactions involving Fe(III)-EDDS complexes under UV light. Moreover, with the addition of H₂O₂ to the Fe(III)-EDDS complex, the BPA degradation reached 92% after 120 min of irradiation. The positive effect of the EDDS can be attributed to several reasons. First of all, the complex formed between Fe(III) and EDDS enhances the dissolution and stability of iron in aqueous solution at neutral pH, which leads to higher activity of iron in solution. Secondly, we demonstrated in previous work that the Fe(III)-EDDS complex is stable and photochemically efficient at neutral pH, which means that higher quantum yields for the formation of •OH can be achieved, due to rapid photochemical reactions of Fe(III)-EDDS ($\phi_{\bullet OH} \approx 2.5 \times 10^{-2}$ at pH = 6.0) [92].

While in the case of pH 8.7 (Figure D-26 C), the results observed were similar with that at pH 6.2. As it is normally accepted that Fe(III)-EDDS complex is stable at pH ranging from 3 to 9, and the rapid photochemical reaction of Fe(III)-EDDS was also achieved at basic pH, it is easy to be explained that the reactivity of this complex at pH 8.7 is the same than at pH 6.2.



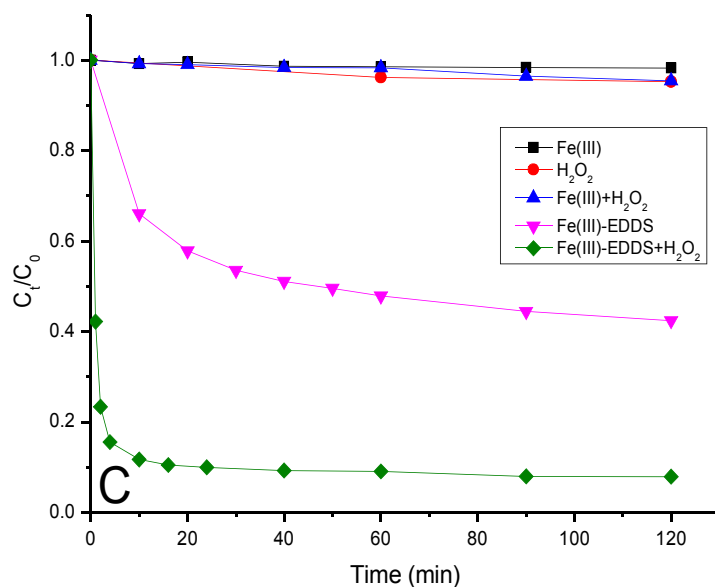


Figure D-26 BPA degradation in different photo-oxidation systems at different pH (pH = 3.7 (A), pH = 6.2 (B) and pH = 8.7 (C)). Initial concentrations were 20 μ M BPA, 0.1 mmol/L Fe(III)-EDDS, 0.1 mmol/L Fe(III), and 0.1 mmol/L H₂O₂.

D-3-4-2. OH radical production comparison at pH 6.2

In order to understand if the complexation of iron by EDDS really impacts the BPA degradation through an increase of the hydroxyl radical formation, we compared the \bullet OH radical formation in different systems, using nitrobenzene (NB) as the trapping molecule for the photogenerated \bullet OH radical. The kinetic model to estimate the hydroxyl radical formation rate is obtained from the following equation

$$R_{NB}^d = R_{OH}^f \frac{k_{NB,\bullet OH}[NB]}{k_{NB,\bullet OH}[NB] + \sum_i k_i[S_i]} \quad (E2)$$

where R_{NB}^d is the degradation rate of nitrobenzene (M s⁻¹), R_{OH}^f is the formation rate of

hydroxyl radical (M s⁻¹), $k_{NB,\bullet OH}$ the second order rate constant between nitrobenzene and

hydroxyl radical ($3.9 \times 10^9 \text{ M}^{-1} \text{ s}^{-1}$) [311] and $\sum_i k_i[S_i]$ is the pseudo-first-order rate constant (s^{-1}) for $\bullet\text{OH}$ scavenging by all constituents (i.e. Fe-complexes, BPA, H_2O_2 , EDDS) of the solution except for the probe. Using $200 \text{ }\mu\text{mol/L}$ of NB we can assume that $k_{\text{NB},\bullet\text{OH}}[\text{NB}] \gg \sum_i k_i[S_i]$. From equation (E2) and after rearrangement we deduce that the initial

formation rate of $\bullet\text{OH}$ is equal to the initial degradation rate of the probe ($R_{\text{NB}}^d = R_{\text{OH}}^f$).

After a few minutes, the approximation used to simplify equation (E2) is not valid and the NB concentration reaches a plateau due to competition for $\bullet\text{OH}$ radicals between NB and the other constituents present in the aqueous solution.

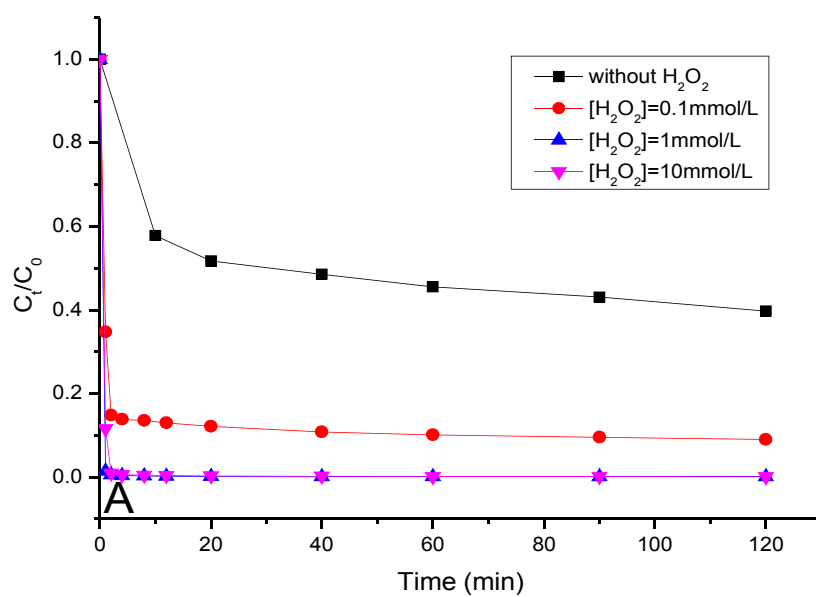
In Table D-6 the R_{OH}^f values in different aqueous solutions ($\text{pH} = 6.2$) are reported. In the presence of 0.1 mmol/L of Fe(III)-EDDS and 0.1 mmol/L of H_2O_2 the initial hydroxyl radical formation rate explains the fast BPA degradation reported in Figure D-26B. From the results shown in Figure D-26B it can be seen that the trend of $\bullet\text{OH}$ radical formation in different solutions is consistent with the trend of BPA degradation. On one hand, this illustrates that the BPA degradation is due to the production of $\bullet\text{OH}$ radicals, and on the other hand, this demonstrates that EDDS can enhance the $\bullet\text{OH}$ radical formation in the photo-Fenton process. In fact, in the presence of EDDS as the complexing agent, the initial formation rate of $\bullet\text{OH}$ from Fe(III) species in the photo-Fenton process increases by approximately 20 times.

Table D-6 Initial rates of formation of $\bullet\text{OH}$ radicals R_{OH}^f in different solutions ($\text{pH} = 6.2$) under irradiation. Initial concentrations were 0.1 mmol/L H_2O_2 , 0.1 mmol/L Fe(III), and 0.1 mmol/L Fe(III)-EDDS. The errors represent $\pm 1\sigma$, based on a linear fit of the experimental data.

Solution composition	H_2O_2	Fe(III) + H_2O_2	Fe(III)-EDDS	Fe(III)-EDDS + H_2O_2
$R_{\text{OH}}^f (\text{M s}^{-1})$	$3.4 \pm 0.6 \times 10^{-9}$	$4.4 \pm 0.1 \times 10^{-9}$	$1.2 \pm 0.3 \times 10^{-8}$	$8.0 \pm 3.8 \times 10^{-8}$

D-3-4-3. Effect of H_2O_2 concentration

In order to investigate the effect of H_2O_2 concentration during the photo-Fenton system, experiments in the presence of 0.1 mmol/L of Fe(III)-EDDS with three different H_2O_2 concentrations (0.1, 1 and 10 mmol/L) at pH = 3.7, 6.2 and 8.7 were carried out.



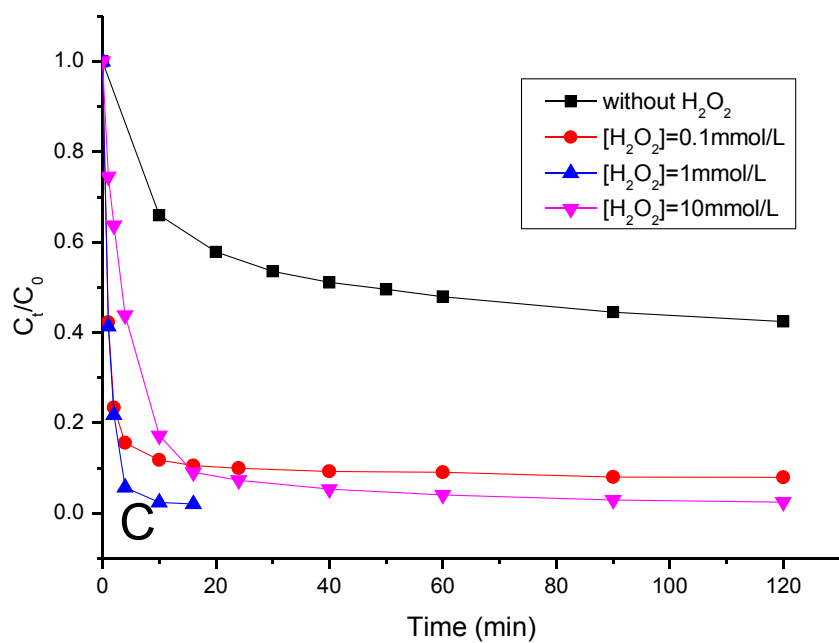
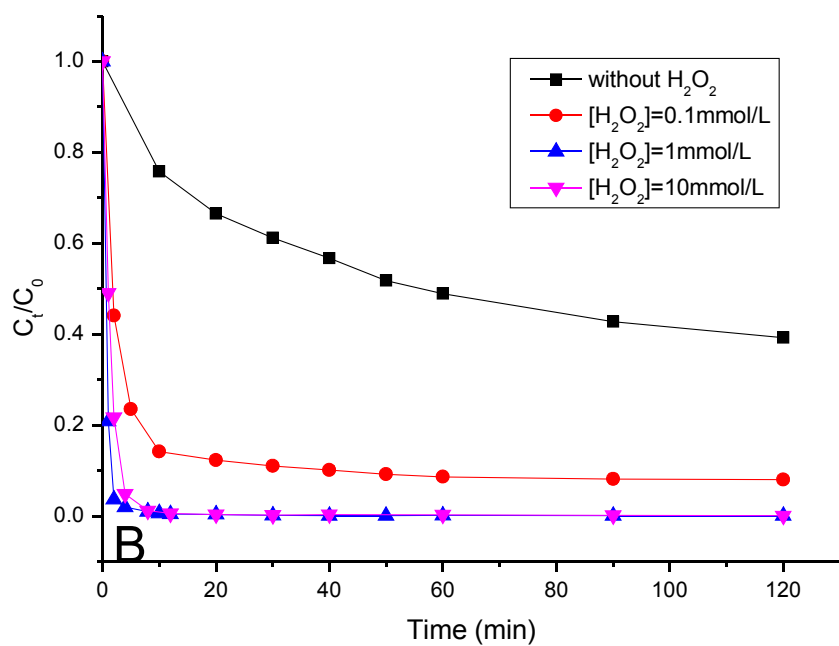


Figure D-27 BPA degradation in the presence of different H_2O_2 concentrations. Initial concentrations were 20 $\mu\text{mol/L}$ BPA and 0.1 mmol/L Fe(III)-EDDS. Initial pH was 3.7 for A figure,

6.2 for B figure and 8.7 for C figure.

It can be seen from the results in Figure D-27, that the presence of H_2O_2 whatever the pH condition, up to 1 mmol/L, enhances the degradation of BPA. Whereas at higher H_2O_2 concentration (10 mmol/L) the rate of BPA degradation is lower. In fact, H_2O_2 is able to increase the regeneration of Fe(III) from Fe(II) via the Fenton reaction (R2) and consequently the formation of $\bullet\text{OH}$ radicals, but is also able to scavenge photogenerated hydroxyl radicals ($k_{\text{H}_2\text{O}_2, \bullet\text{OH}} = 2.7 \times 10^7 \text{ M}^{-1} \text{ s}^{-1}$ [302]) and so decrease their reactivity with BPA. However, with the highest H_2O_2 concentrations (1 and 10 mmol/L) the BPA completely disappeared after 10 min of irradiation. It is achieved from the results that the change trends at three different pH conditions were similar.

D-3-4-4. Effect of Fe(III)-EDDS concentration

A similar trend is observed in Figure D-28 showing results of experiments with five different Fe(III)-EDDS concentrations (0.01, 0.05, 0.1, 0.2 and 0.4 mmol/L) in the presence of 0.1 mmol/L H_2O_2 , at pH = 6.2 and room temperature. The BPA degradation is enhanced by the increase of Fe(III)-EDDS concentration from 0.01 mmol/L to 0.2 mmol/L. However, at higher concentration, when the Fe(III)-EDDS concentration is 0.4 mmol/L, the degradation of BPA is reduced. This inhibition can not be attributed to the competitive absorption of the light between Fe(III)-EDDS and hydrogen peroxide because its contribution to the $\bullet\text{OH}$ radical production via direct photolysis can be neglected (see table D-6). However, the photogenerated $\bullet\text{OH}$ radicals could react with both BPA and Fe(III)-EDDS complex. When the concentration of Fe(III)-EDDS is high, the role of Fe(III)-EDDS as a competitor for the $\bullet\text{OH}$ reaction is much more important, and as a consequence inhibits the BPA degradation.

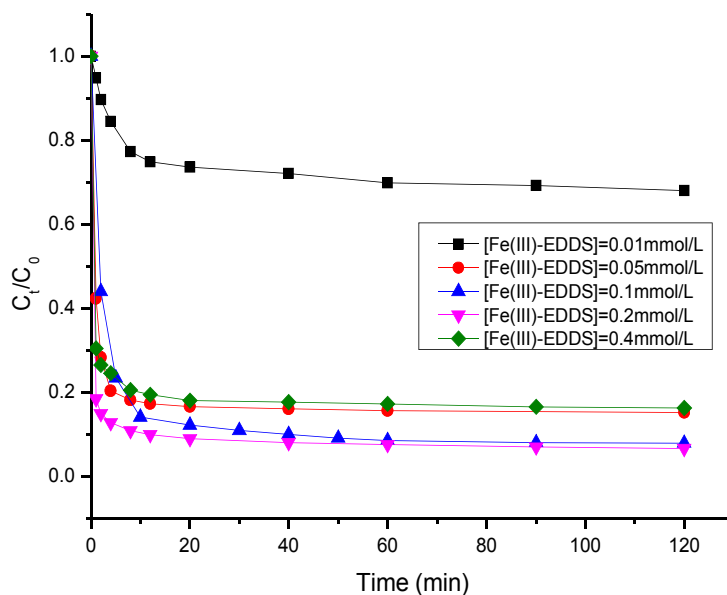


Figure D-28 BPA degradation in photo-Fenton system in the presence of different Fe(III)-EDDS concentrations. Initial concentrations were 20 $\mu\text{mol/L}$ of BPA and 0.1 mmol/L of H_2O_2 at pH 6.2.

D-3-4-5. Effect of oxygen

In order to understand the effect of oxygen in this photo-Fenton process, experiments in 0.1 mmol/L of Fe(III)-EDDS and 0.1 mmol/L of H_2O_2 at pH 6.2 in different oxygen condition were performed. These experiments were carried out with bubbling of O_2 or N_2 for 30 min before and during the photo-Fenton process.

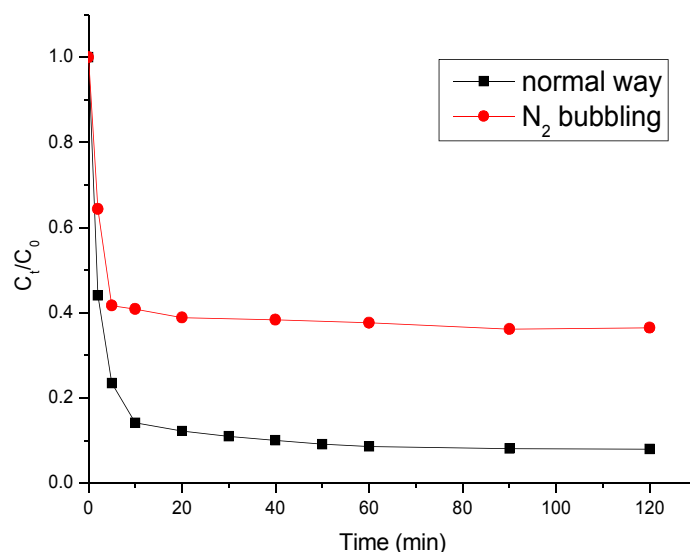
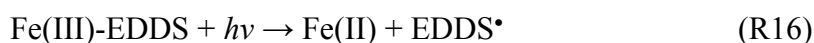


Figure D-29 BPA degradation in photo-Fenton process in anaerobic and aerated condition. Initial concentrations were 20 $\mu\text{mol/L}$ BPA, 0.1mmol/L Fe(III)-EDDS and 0.1mmol/L H_2O_2 at pH 6.2.

As can be seen from the results reported in Figure D-29, the BPA degradation is much lower (in terms of rate) under anaerobic conditions. In oxygen saturated solution, complete degradation of BPA is achieved in 5 min while in the case of aerated and nitrogen saturated solution, plateaus are present at around 90% and 60% degradation, respectively. Such a trend indicates that the oxygen can enhance the degradation of BPA but it rules out a possible oxygen effect on the direct $\bullet\text{OH}$ radical formation because of the non-negligible degradation of BPA observed in the nitrogen saturated solution.

However, it is clear that the reactivity of O_2 with the iron ligand produced via reactions R16 and R17 can affect the Fe(III)/(II) cycle.



In fact, considering the ratio between the second order rate constants of the Fe species with

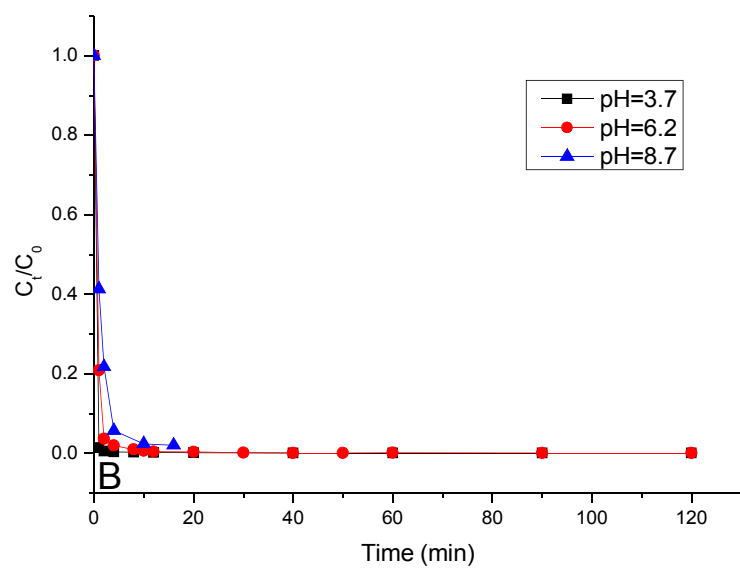
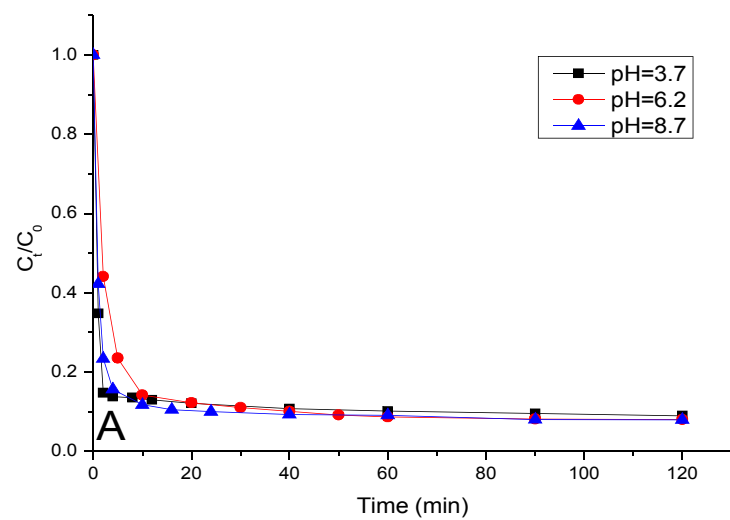
$\text{HO}_2^\bullet/\text{O}_2^{\bullet-}$ we obtain $k_{\text{Fe(III),HO}_2^\bullet} / k_{\text{Fe(II),HO}_2^\bullet} < 8.3 \times 10^{-5}$ for HO_2^\bullet [311, 312], while for $\text{O}_2^{\bullet-}$

we obtain $k_{Fe(III),O_2^{\cdot-}} / k_{Fe(II),O_2^{\cdot-}} = 5.0$ [312, 313]. These data give clear evidence that at pH 6.2 the Fe(III) reduction into Fe(II) is promoted and hence the Fenton process enhanced, so the efficiency of the BPA degradation is increased.

Moreover, oxygen is expected to play a role in the BPA degradation by reacting with BPA radical which is generated from hydroxyl radical attack, in agreement with previously reported work [310].

D-3-4-6. Effect of pH value

In order to better understand what is a suitable pH value for the photo-Fenton process with the Fe(III)-EDDS complex, experiments at pH 3.7, 6.2 and 8.7 were carried out and compared with those obtained with Fe(III). From the results, as reported in Figure D-30, the photo-Fenton reaction with Fe(III) is efficient only at pH 3.7. Indeed, due to the precipitation of iron at (and close to) neutral and basic pH values, the efficiency of photo-Fenton process with Fe(III) is quite low comparing to that with Fe(III)-EDDS complex whatever the H₂O₂ concentration used. However, complexation with EDDS produces a double effect by increasing the stability of iron in aqueous solution at higher pH and increasing the efficiency of the Fenton process by formation of hydroperoxyl/superoxide radicals as shown in reactions R4 and R5.



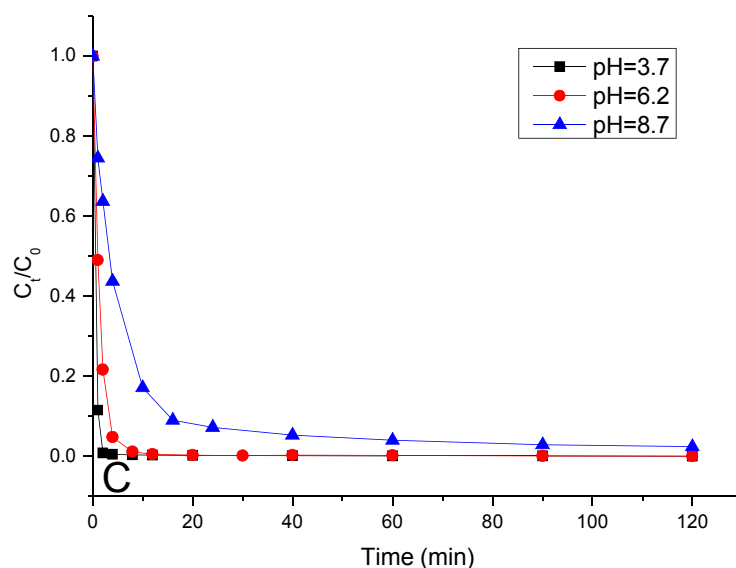


Figure D-30 BPA degradation in photo-Fenton process at different pH values. Initial concentrations were 20 $\mu\text{mol/L}$ BPA, 0.1 mmol/L Fe(III)-EDDS and 0.1 mmol/L H_2O_2 for A, 1 mmol/L H_2O_2 for B, 10 mmol/L H_2O_2 for C.

D-3-4-7. Comparison of Fenton and Photo-Fenton process

In order to better understand the effect of UV irradiation on the degradation of BPA, experiments in Fenton and photo-Fenton processes in the same condition (0.1 mmol/L and 1 mmol/L of H_2O_2 , 0.1 mmol/L of Fe(III)-EDDS complex at pH 6.2) were conducted.

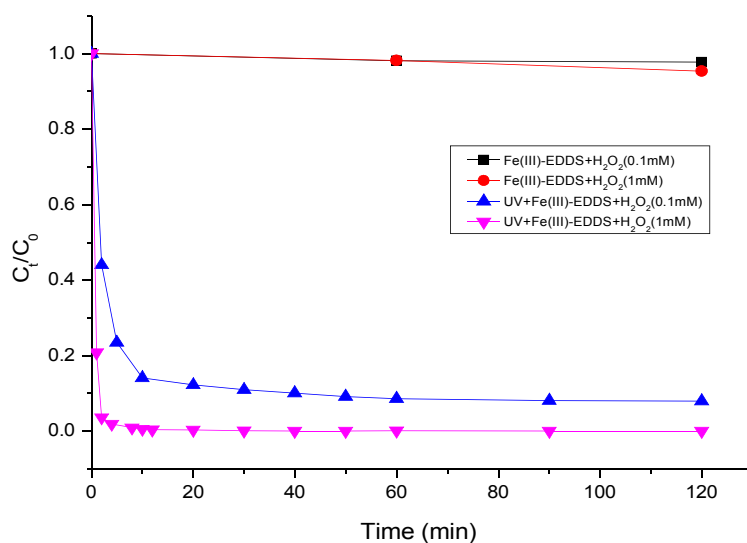


Figure D-31 BPA degradation in Fenton and photo-Fenton process. Initial concentrations were 20 $\mu\text{mol/L}$ BPA, 0.1 mmol/L Fe(III)-EDDS and 0.1 or 1.0 mmol/L H_2O_2 at pH 6.2.

From the results showed in Figure D-31 it is found that the presence of UV irradiation could obviously enhance the degradation of BPA. As it is achieved in previous part of research about Fenton process using Fe(III)-EDDS complex, it is found that the concentration of Fe(III)-EDDS complex and H_2O_2 needs to be up to 1 mmol/L and 5 mmol/L respectively to make sure the BPA could be degraded with high efficiency and the reaction time needs to be much longer. This detection indicated that the UV irradiation could effectively enhance the efficiency of reaction between Fe(III)-EDDS and H_2O_2 due to the photosensitivity of Fe(III)-EDDS complex. As in photo-Fenton process, use of 0.1 mmol/L of Fe(III)-EDDS complex and 1 mmol/L of H_2O_2 could almost completely remove 20 $\mu\text{mol/L}$ of BPA in solution in 20 min, the use of UV irradiation could decrease the concentration of Fe(III)-EDDS complex and H_2O_2 at least of one order of magnitude, which was used to effectively remove BPA and foreseeable to remove other organic chemicals. As the iron in the solution should be removed, photo-Fenton process will be more convenient for wastewater treatment and so much simpler. Furthermore, the use of UV irradiation with main wavelength at 365nm, which is a wavelength present in sunlight emission, makes the process possible under solar irradiation and so economic.

Moreover, in order to investigate the effect of UV irradiation on the $\bullet\text{OH}$ radical formation, in photo-Fenton systems, experiments with different numbers of lamps with main emission at 365 nm and without UV irradiation were performed. The results were shown in Figure D-32.

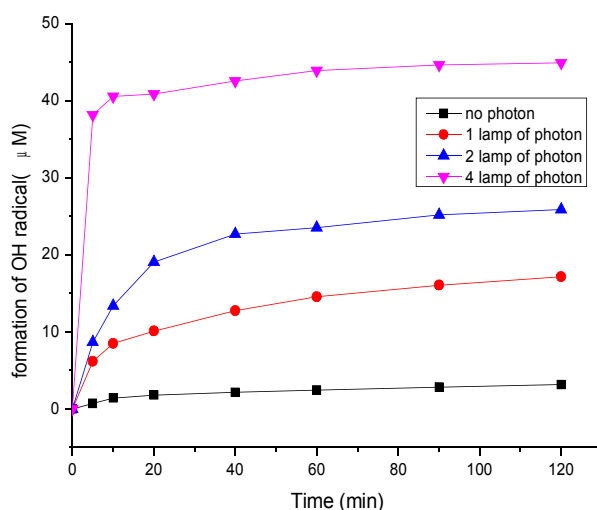


Figure D-32 Formation of $\bullet\text{OH}$ radical in photo-Fenton process with different numbers of lamps and without UV irradiation. Initial concentrations were 0.1 mmol/L Fe(III)-EDDS and 0.1 m mol/L H_2O_2 at pH 6.2.

It is observed that the efficiency of $\bullet\text{OH}$ radical formation in this photo-Fenton system enhances according with the higher number of lamps used. It can also be confirmed that the presence of light plays important role in the production of $\bullet\text{OH}$ radical. In the absence of light, the $\bullet\text{OH}$ radical formation could almost be neglected, which is consistent with comparison of BPA degradation between Fenton and photo-Fenton system in 0.1 mmol/L Fe(III)-EDDS and 0.1 mM H_2O_2 . So, this observation confirms that UV irradiation affected BPA degradation through enhancing the generation of $\bullet\text{OH}$ radical in the system. On the other hand, it is found that in the presence of UV irradiation, the generation of $\bullet\text{OH}$ radical was very fast in the first 5 min of the process and in the rest of the process this generation was very slow and almost stopped, which is also consistent with the BPA degradation that is very fast in the beginning and slow in the second step.

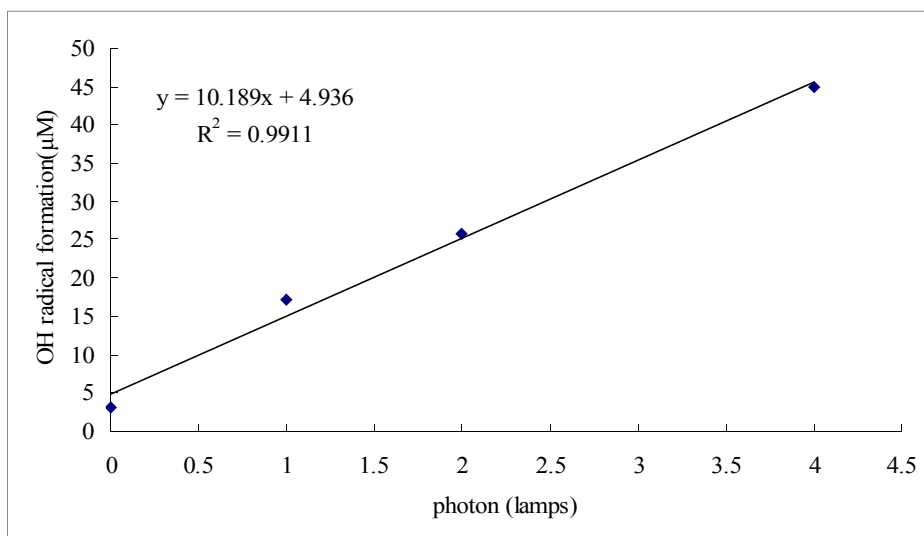


Figure D-33 •OH radical formation as a function of the number of lamps used in photo-Fenton system (0.1 mmol/L Fe(III)-EDDS and 0.1 mmol/L H₂O₂ at pH 6.2)

From the linear fit between •OH radical generation and the number of lamps used in photo-Fenton process shown in Figure D-33, it is found that the enhancement of •OH radical generation due to the increase of photon into the system followed a linear law.

D-3-4-8. Comparison with different organic ligands

Firstly, we compared the BPA degradation in photo-Fenton process in the presence of Fe(III)-EDDS complex and Fe(III)-EDTA complex. As it is known that EDDS is a structural isomer of EDTA, we would like to check if they have similar comportment and efficiency in photo-Fenton process. From the result showed in Figure D-34 it is found that both complexes could efficiently degrade BPA in photo-Fenton process. In the presence of Fe(III)-EDDS, the degradation rate was even higher. From the results for the redox potential detection, it is clear that the cyclic voltammogram of Fe(III)/Fe(II)-EDDS at pH = 6.2 is characterized by a quasi-reversibility with a half-wave potential ($E_{1/2}$) of 0.069 V/NHE. At the same pH, the $E_{1/2}$ value of Fe(III)/Fe(II)-EDTA (0.098 V/NHE) (0.096V/NHE at pH=7.2 and 25°C in previous work [311]) is obtained, which is slightly higher than that of Fe(III)/Fe(II)-EDDS. So, the higher degradation rate of BPA achieved in the presence of Fe(III)-EDDS could be attributed to the lower redox potential of

Fe(III)/Fe(II)-EDDS.

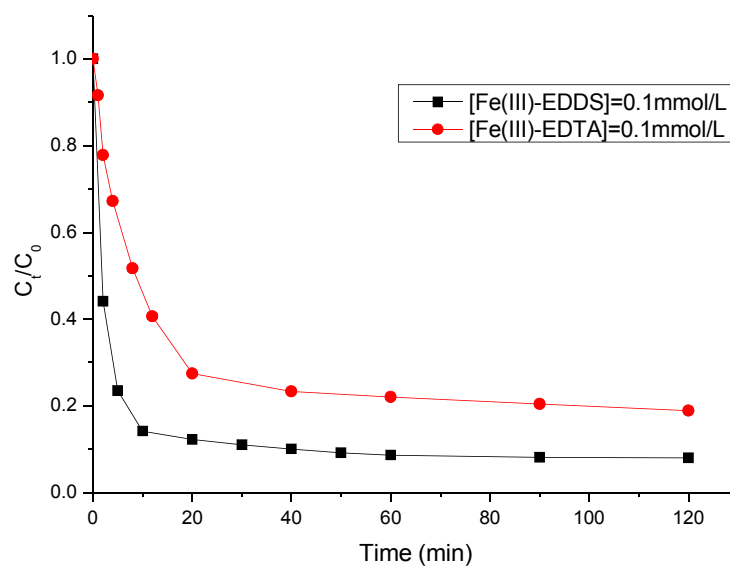
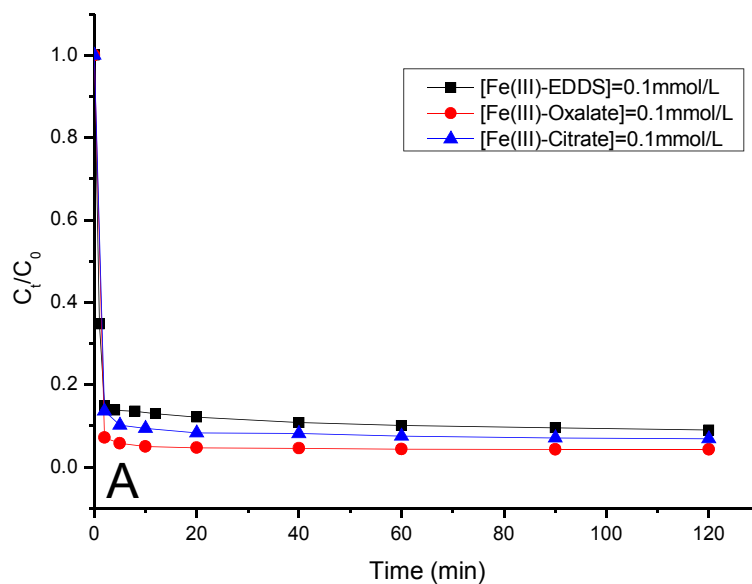


Figure D-34 BPA degradation comparison in the presence of Fe(III)-EDDS and Fe(III)-EDTA in 0.1 mmol/L H₂O₂ at pH 6.2



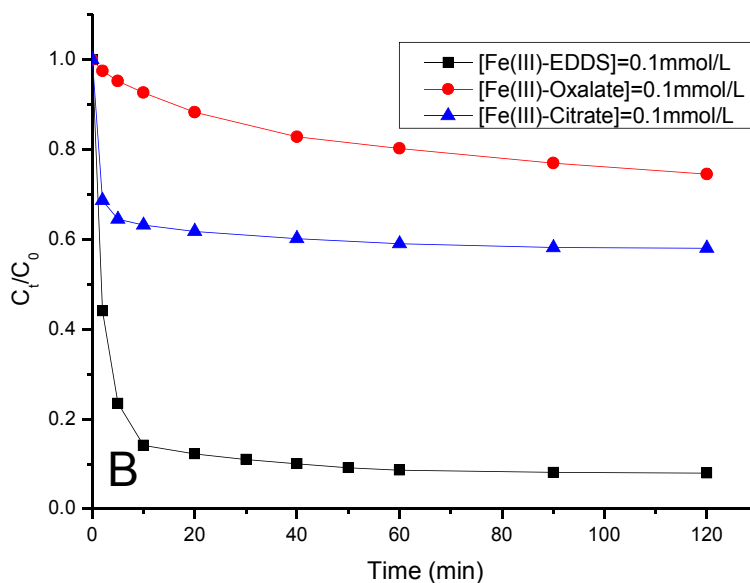


Figure D-35 BPA degradation comparison in the presence of different iron complexes in 0.1 mmol/L H_2O_2 at pH 3.7 for A and pH 6.2 for B.

As it is shown in Figure D-35 above, the positive effect of the Fe(III)-EDDS complex was compared, in terms of BPA degradation efficiency, with the other iron-complexes Fe(III)-oxalate and Fe(III)-citrate at pH = 3.7 and pH = 6.2. The result show that at pH = 3.7, the efficiency of different iron complexes including Fe(III)-citrate, Fe(III)-oxalate and Fe(III)-EDDS is almost the same, BPA in all these systems could be effectively degraded and very fast. Whereas at pH = 6.2, in the presence of Fe(III)-EDDS the BPA degradation rate is much higher than in the presence of other complexes. In order to better understand the differences among different iron complexes, the redox potentials of different Fe(III)/Fe(II)-complexes were also compared and can explain the differences among different systems. Comparing with E° for the free iron couple Fe(III)/Fe(II) (0.700 V/NHE), it is found that the $E_{1/2}$ value of Fe(III)/Fe(II)-EDDS is significantly lower, which makes the Fenton and photo-Fenton reaction more thermodynamically favourable in the presence of EDDS and can explain the higher efficiency of the Fe(III)-EDDS photo-Fenton process. From previous research, it is also found that the redox potential of Fe(III) /Fe(II)-citrate at pH = 7.0 and 25°C is 0.372 V/NHE [315], which is also much higher than that of Fe(III)/Fe(II)-EDDS at neutral pH condition. And the redox potential of Fe(III)/Fe(II)-oxalate reported in previous

research [101] is also much higher than that of Fe(III)/Fe(II)-EDDS. From all these results, it can be concluded that when the redox potential is lower, the efficiency of the system using iron complex is higher. Our results are consistent with the results from previous research showing that the addition of carboxylic acid as a complexing agent can reduce the redox potential of Fe(III)/Fe(II), and hence enhance the efficiency of the Fenton-like system.

D-3-4-9. Implication of $\text{HO}_2^\bullet/\text{O}_2^{\bullet-}$ and $^\bullet\text{OH}$ radicals in the photo-Fenton process

In order to determine the implication of $\text{HO}_2^\bullet/\text{O}_2^{\bullet-}$ radical in the photo-Fenton process, BPA degradation experiments with or without the addition of chloroform were carried out. Chloroform (CHCl_3) was used as scavenger of $\text{O}_2^{\bullet-}$. In fact, CHCl_3 reacts with a much higher second order rate constant with the superoxide radical anion $k_{\text{CHCl}_3, \text{O}_2^{\bullet-}} = 3 \times 10^{10} \text{ M}^{-1} \text{ s}^{-1}$ compared to hydroxyl radical $k_{\text{CHCl}_3, ^\bullet\text{OH}} = 5 \times 10^6 \text{ M}^{-1} \text{ s}^{-1}$ [302]. Referring the results observed in Fenton process, only one concentration of CHCl_3 (400 $\mu\text{mol/L}$) was used in photo-Fenton process. From the result shown in Figure D-36 it is found that the addition of 400 $\mu\text{mol/L}$ of CHCl_3 could partly inhibited the degradation of BPA in the photo-Fenton process. With CHCl_3 only about 76% of BPA was degraded whereas more than 90% of BPA was degraded without Chloroform. It means that the presence of $\text{HO}_2^\bullet/\text{O}_2^{\bullet-}$ radical devoted about 16% of BPA degradation in photo-Fenton process, which is quite different from the result observed in Fenton process.

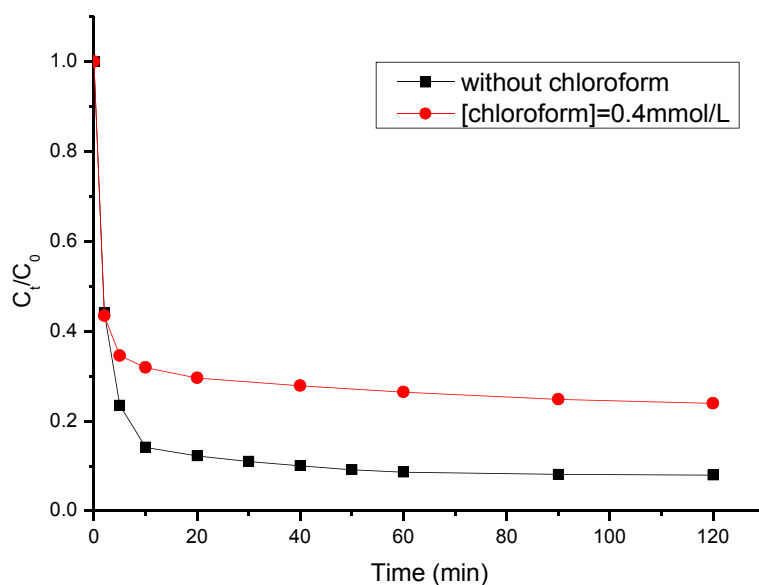


Figure D-36 Effect of chloroform on the degradation of BPA ([Fe(III)-EDDS] = 0.1 mmol/L, [H₂O₂] = 0.1 mmol/L, [BPA] = 20 μmol/L, pH = 6.2)

The implication of $\bullet\text{OH}$ radical was detected by the addition of 2-propanol. 2-propanol (

$k_{2\text{propanol},\bullet\text{OH}}=1.9 \times 10^9 \text{ M}^{-1}\text{s}^{-1}$ [302]) was used as $\bullet\text{OH}$ scavenger to check the effect on the

BPA degradation. Similarly, only one concentration of 2-propanol (2 mmol/L) was used referring the results before. The results shown in Figure D-37 indicated that the addition of 2-propanol obviously inhibited the degradation of BPA playing a competitive role toward the hydroxyl radical reactivity. At 2 mM of 2-propanol, the degradation of BPA was completely inhibited demonstrated that the degradation of BPA is mainly due to the reactivity with $\bullet\text{OH}$ radical.

Combining the results observed in the implication of $\text{HO}_2\bullet/\text{O}_2^{\bullet-}$ and $\bullet\text{OH}$ radicals, similar conclusion was achieved as their implication in Fenton process. $\bullet\text{OH}$ radical is the only one that attacks the molecules of BPA and induces its degradation, whereas the effect of $\text{HO}_2\bullet/\text{O}_2^{\bullet-}$ radical on BPA degradation affects the generation of $\bullet\text{OH}$ radical in this system. As it is preliminarily calculated, about 16% of $\bullet\text{OH}$ radical generation was attributed to the formation of $\text{HO}_2\bullet/\text{O}_2^{\bullet-}$ radical in photo-Fenton process, this percentage of contribution is quite small, and is different from the results in Fenton system that about 80% of $\bullet\text{OH}$

radical generation is related to $\text{HO}_2^\bullet/\text{O}_2^{\bullet-}$ radical. This could be explained by the photosensitivity of Fe(III) and Fe(III)-EDDS complex, which could induce the photogeneration of $^\bullet\text{OH}$ radical.

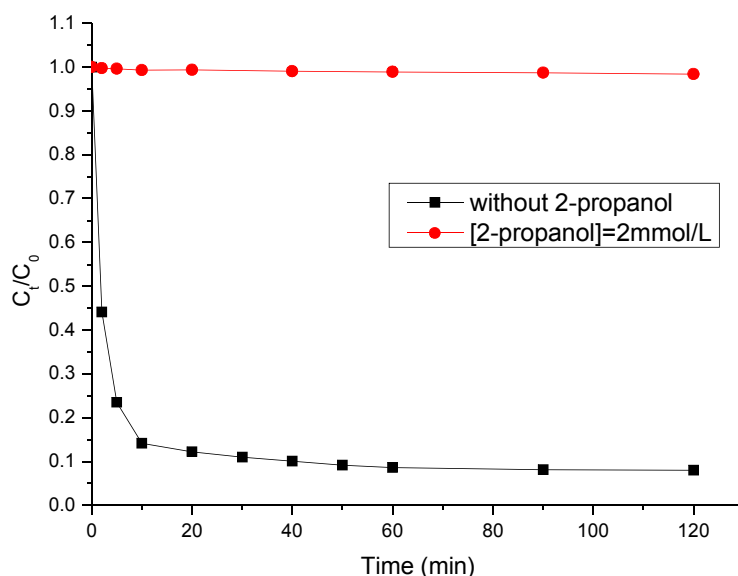


Figure D-37 Effect of 2-propanol on the degradation of BPA ([Fe(III)-EDDS] = 0.1 mmol/L, $[\text{H}_2\text{O}_2]$ = 0.1 mmol/L, [BPA] = 20 $\mu\text{mol/L}$, pH = 6.2)

D-3-5. Conclusion

From the evaluation of Fe(III)-EDDS complex effect on photo-Fenton process, it is found that Fe(III)-EDDS complex has very positive effect on both $^\bullet\text{OH}$ radical formation and BPA degradation at neutral pH. This is mainly due to the presence of EDDS that can stabilize Fe(III) in aqueous solution between pH 3 and 9, preventing its precipitation. In the experiments, the increase of H_2O_2 and Fe(III)-EDDS complex concentrations can enhance the degradation rate of BPA. However, when the concentrations of Fe(III)-EDDS and/or H_2O_2 are too high, a competition for the reactivity of $^\bullet\text{OH}$ is observed between BPA and Fe(III)-EDDS or H_2O_2 and so the degradation of BPA is lower. The experiments performed at different pHs demonstrated that BPA can be efficiently degraded in this photo-Fenton

system at acidic, neutral and alkaline pH, which means that the addition of EDDS can widen the applicable pH range of photo-Fenton system. The effect of oxygen was also determined and it was shown that oxygen is an important parameter for the oxidation of BPA.

From the results of $\cdot\text{OH}$ radical formation, it can be concluded that the addition of EDDS can enhance the production of $\cdot\text{OH}$ radical, and hence enhance the degradation of BPA. The very positive results of this research work are interesting for water treatment processes. They demonstrate the high efficiency of photo-Fenton process using Fe(III)-EDDS as iron source with lower complex and H_2O_2 concentrations in wider pH range, which is very encouraging for the application of the photo-Fenton process under neutral pH conditions encountered in natural aquatic environment.

D-4. BPA degradation in heterogeneous Fenton and photo-Fenton process

D-4-1. Heterogeneous Fenton process

D-4-1-1. Effect of EDDS on heterogeneous Fenton reaction

In previous research of our group, it can be concluded that the presence of EDDS can enhance the efficiency of homogeneous Fenton process. Base on this conclusion, addition of EDDS in heterogeneous Fenton process using goethite was taken into account. The experiments using self-made goethite as iron source in Fenton process to degrade BPA were conducted. EDDS was added as iron ligand to determine its role. The concentration of goethite we used was 0.1 g/L, the concentration of H_2O_2 used was 11.3 mmol/L, which gave a ratio of $[\text{Fe}^{3+}]$ and $[\text{H}_2\text{O}_2]$ at 1 to 10 in the suspension. The BPA concentration was 20 $\mu\text{mol/L}$, and the EDDS concentration added to the solution at pH 6.2 was 0.1 mmol/L, 0.25 mmol/L, 0.5 mmol/L and 1 mmol/L. When there is no EDDS in the reaction system, about 12% of BPA was degraded in 300 min, which means heterogeneous Fenton system is slow but workable in organic pollutant treatment at neutral pH (Figure D-38).

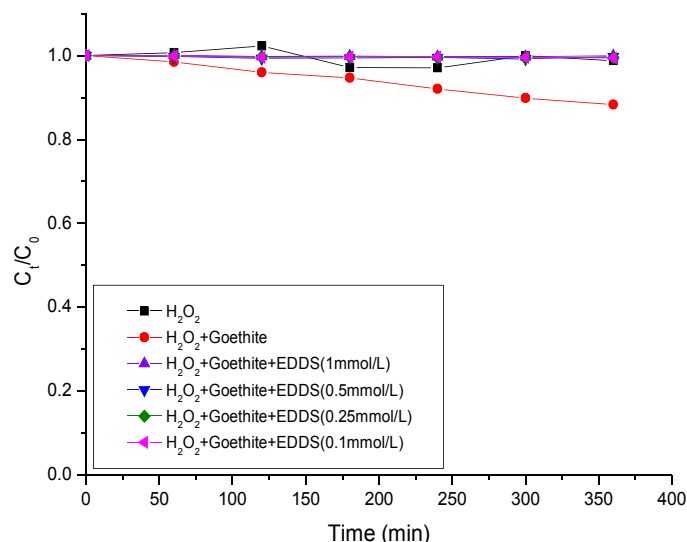


Figure D-38 BPA degradation in heterogeneous Fenton system with or without EDDS at pH 6.2, Initial concentrations were 20 $\mu\text{mol/L}$ BPA, 0.1 g/L goethite, 11.3 mmol/L H_2O_2 and different concentration of EDDS

However, from the results achieved in this part of experiments, which was shown in Figure D-38, almost no BPA degradation was achieved whatever the concentration of EDDS added, which is totally opposite to the result in homogeneous Fenton system where the presence of EDDS can effectively enhance the degradation of BPA. So, it is demonstrated that the addition of EDDS totally inhibited the degradation of BPA in the heterogeneous Fenton system at neutral pH. In order to better understand this phenomenon and explain this interesting result, several other experiments were carried out.

First of all, the same experiments at pH 3.7 were carried out in order to examine the effect of EDDS on heterogeneous Fenton system at acidic pH. In the heterogeneous Fenton system at pH 3.7, the degradation rate of BPA could reach 17% in 300 min (Figure D-39).

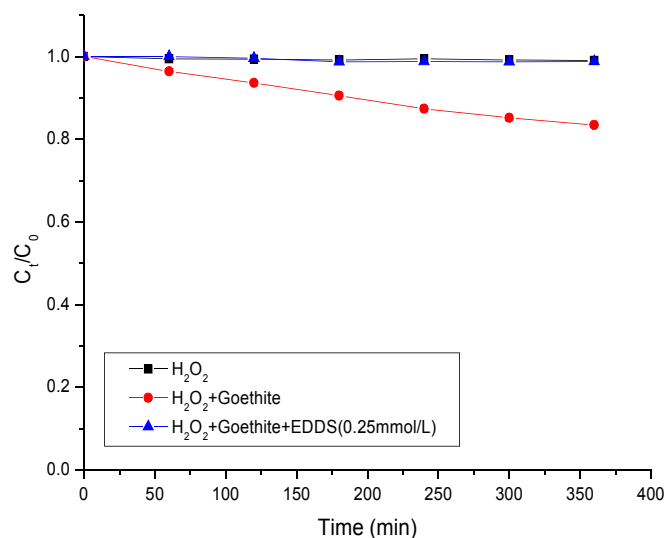


Figure D-39 BPA degradation in heterogeneous Fenton system with or without EDDS at pH 3.7,

Initial concentrations were 20 μM BPA, 0.1 g/L goethite, 11.3 mM H_2O_2 and 0.25 mM EDDS

However, when 0.25 mmol/L of EDDS was added into the suspension, as it is shown in Figure D-39, almost no BPA degradation was observed in the same degradation time period. This result proved that at acidic pH, the presence of EDDS also totally inhibited the Fenton process to degrade BPA. On the other hand, similar results were achieved at pH 8.7; the addition of EDDS totally inhibited the BPA degradation, which was not shown in the Figure. It means that in this concentration scale the addition of EDDS inhibited the process of BPA degradation in heterogeneous Fenton system at quite wide pH range.

Secondly, in order to examine the effect of EDDS on the iron leaching from the goethite solid to the liquid phase, the experiments in the dark with and without EDDS at pH 6.2 were conducted to detect the total iron concentration in the solution. From the result showed in Figure D-40 it is obvious that although the presence of 0.1 mmol/L EDDS enhances the total iron concentration in solution, the enhancement is not significant. The total iron concentration in both experiments was quite low, less than 2.5 $\mu\text{mol/L}$.

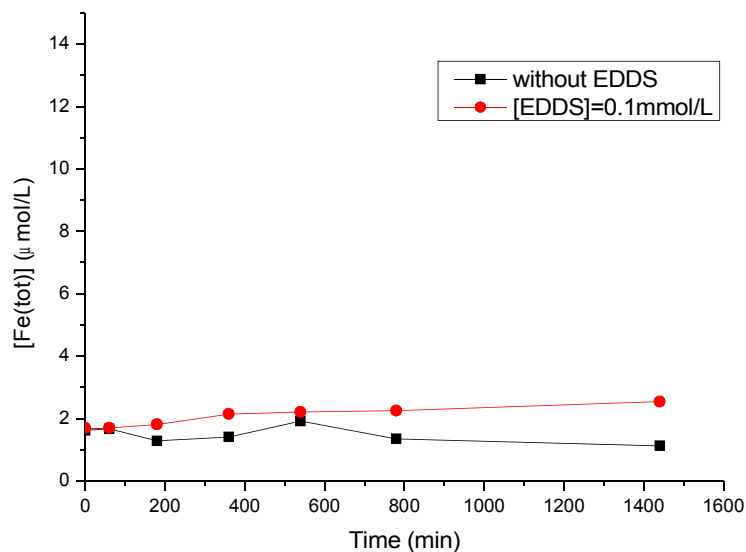


Figure D-40 Iron leaching in Fenton process with or without EDDS at pH 6.2. Initial concentrations were 20 μmol/L BPA, 0.1 g/L goethite and 0.1 mmol/L EDDS

This result firstly demonstrated that in this heterogeneous Fenton system the iron leaching was not so strong, as it is reported in previous research [230]. The Fenton process in this system mainly happens on both liquid phase and surface of solid, and the latter one was considered to be more important. Then, it can be concluded that the inhibition result from EDDS is not mainly due to the change of iron leaching, at least the presence of EDDS doesn't inhibit the iron leaching from goethite surface.

Eliminating the effect on iron leaching, there is another hypothesis that EDDS can be adsorbed strongly onto the goethite, which may block the active site of iron for H_2O_2 decomposition; hence the generation of $\cdot\text{OH}$ radical was inhibited. In order to verify this hypothesis, the experiments detecting the sorption of EDDS at different concentrations of EDDS (from 0.05 mmol/L to 2 mmol/L) onto goethite (0.1 g/L) were conducted.

From the result of the adsorption shown in Figure D-41, it can be seen that the sorption of EDDS onto the goethite was quite strong, which was consistent with the hypothesis we made before. So, we can make a preliminary conclusion that the inhibition of BPA degradation was related to the sorption of EDDS. At the same time, the sorption of BPA onto the goethite surface was determined (Figure D-42).

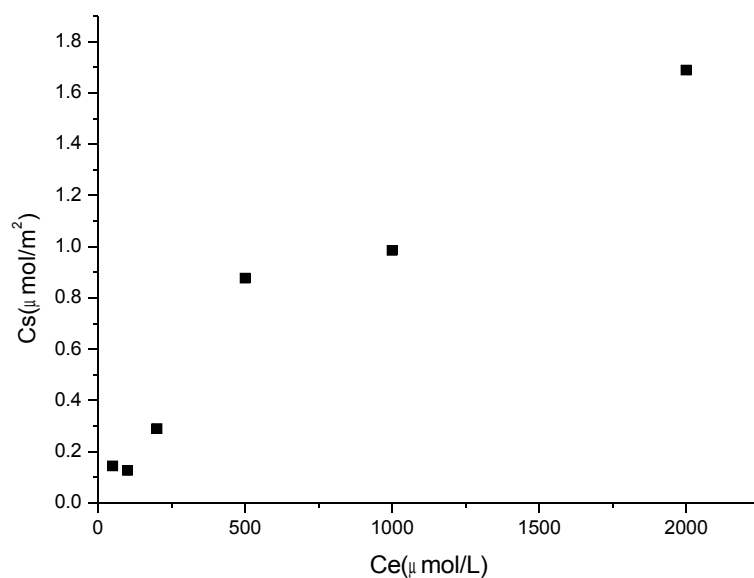


Figure D-41 Adsorption of EDDS onto goethite surface at pH 6.2. Initial goethite concentration was 0.1 g/L

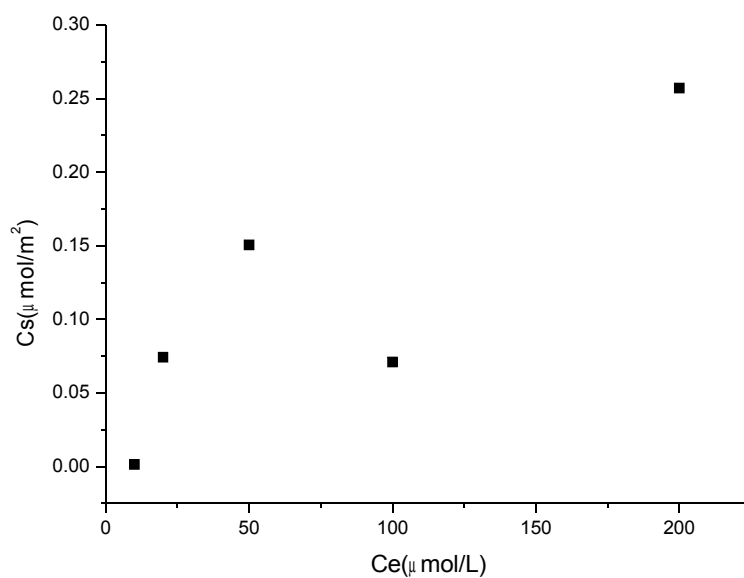
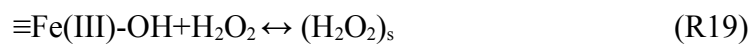
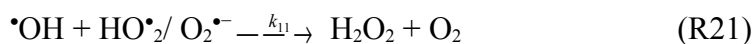


Figure D-42 Adsorption of BPA on to goethite surface at pH 6.2. Initial goethite concentration was 1 g/L





Then, in order to further determine the actual reason that results in the inhibition, the decomposition of H_2O_2 was also tested. However, from the results observed and shown in Figure D-43, the decomposition of H_2O_2 was almost the same whatever the systems. The decomposition of H_2O_2 showed unstable oscillation. Eliminating the uncertainty of detection method, this oscillation may be due to the adsorption/desorption of H_2O_2 onto goethite surface shown in reaction (R19), and the consumption/generation of H_2O_2 are shown in reaction (R20) and (R21). But there was not significant difference among different systems. So, it is still unknown if the generation of $\bullet\text{OH}$ radical is inhibited in presence of EDDS in this Fenton system.

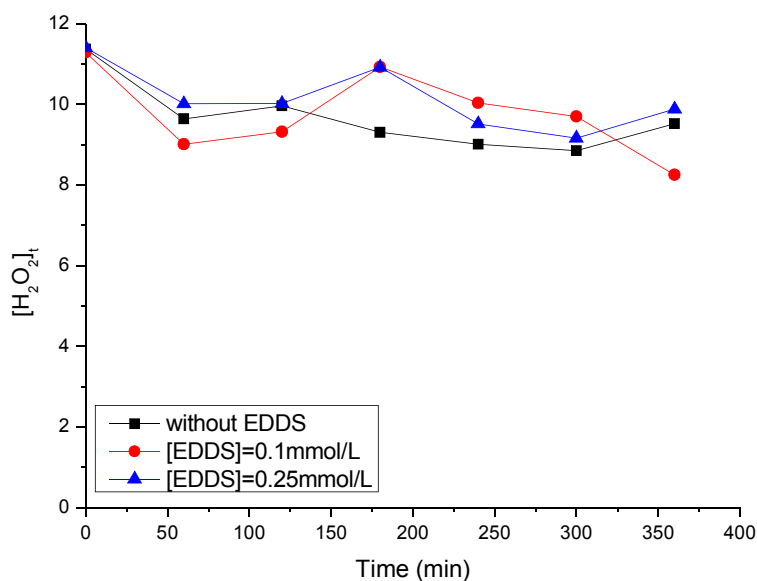


Figure D-43 H_2O_2 decomposition in Fenton system with or without EDDS at pH 6.2. Initial concentrations were 20 $\mu\text{mol/L}$ BPA, 0.1 g/L goethite, 11.3 mmol/L H_2O_2 and different concentration of EDDS

Finally, the $\bullet\text{OH}$ radical generation in this heterogeneous Fenton system was detected with

and without EDDS. The scavenger of $\cdot\text{OH}$ radical was Disodium terephthalate (TA) 1 mmol/L and the production 2-Hydroxyterephthalic acid (TAOH) due to the reaction between TA and $\cdot\text{OH}$ radical was detected. The concentration of TA used was high enough, making the reaction between $\cdot\text{OH}$ radical and other species negligible.

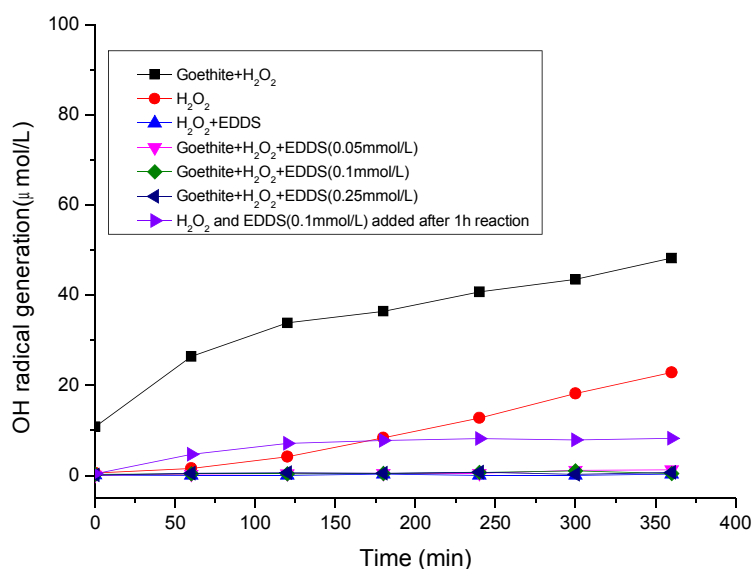


Figure D-44 OH radical formation process in Fenton process with or without EDDS at pH 6.2.

Initial concentrations were 1 mmol/L TA, 0.1 g/L goethite, 11.3 mmol/L H₂O₂ and different concentrations of EDDS

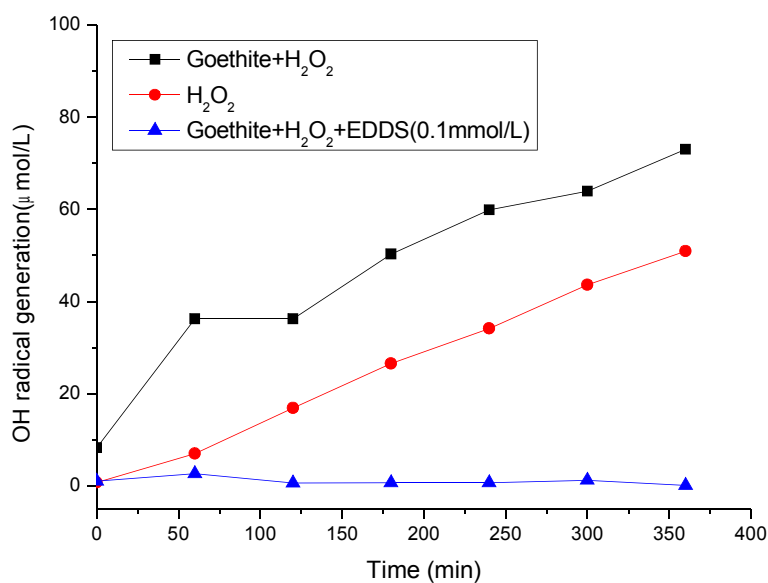


Figure D-45 OH radical formation process in Fenton process with or without EDDS at pH 4.5.

Initial concentrations were 1 mmol/L TA, 0.1 g/L goethite, 11.3 mmol/L H₂O₂ and 0.1 mmol/L EDDS

From the result presented in Figure D-44, it can be shown that the presence of goethite can actually result in the formation of $\bullet\text{OH}$ radical, comparing to the $\bullet\text{OH}$ radical generation in the presence of H₂O₂ alone, the $\bullet\text{OH}$ radical in Fenton system obviously enhanced from the very beginning. And when EDDS in different concentrations including 0.05 mmol/L, 0.1 mmol/L and 0.25 mmol/L, were added into the suspension at pH 6.2, the $\bullet\text{OH}$ radical production was almost totally inhibited. At the same time, at pH 6.2, another interesting experiment was carried out. In first 120 min of the experiment, there was only H₂O₂ and TA in the solution, it is found that the presence of H₂O₂ itself can also produce TAOH, which means that in this system $\bullet\text{OH}$ radical can be produced. However, when EDDS was added at the end of 120 min, after that, the production of $\bullet\text{OH}$ radical almost totally stopped. This interesting result further demonstrated that why the degradation of BPA was inhibited, the most possible reason is the presence of EDDS stopped the formation of $\bullet\text{OH}$ radical in this heterogeneous Fenton system, and hence stopped the degradation of BPA. Furthermore, there is possibility that EDDS could react with $\bullet\text{OH}$ radical or H₂O₂ directly. Comparing the reaction constant between $\bullet\text{OH}$ radical and BPA ($K_{(\bullet\text{OH},\text{BPA})} = 6.9 \times 10^9 \text{ M}^{-1}\text{S}^{-1}$) with that between $\bullet\text{OH}$ radical and EDDS ($K_{(\bullet\text{OH},\text{EDDS})} = 2 \times 10^8 \text{ M}^{-1}\text{S}^{-1}$ [46]), and knowing the concentration of BPA was 20 $\mu\text{mol/L}$, when the concentration of EDDS is 100 $\mu\text{mol/L}$, the pseudo-first order rate constants for BPA and EDDS are $1.38 \times 10^5 \text{ s}^{-1}$ and $2 \times 10^4 \text{ s}^{-1}$ respectively. Even in presence of 250 $\mu\text{mol/L}$ of EDDS, the pseudo-first order rate constant for EDDS is only $5 \times 10^4 \text{ s}^{-1}$, which is still not so significant comparing with that for BPA. As a result, the presence of EDDS theoretically could not trap large amount of $\bullet\text{OH}$ radical and could not inhibit the BPA degradation. At the same time, due to the high concentration of TA used as scavenger in $\bullet\text{OH}$ radical detection, the second reason is hard to explain the inhibition of $\bullet\text{OH}$ radical formation. Consequently, it is assumed that EDDS could prevent the formation of $\bullet\text{OH}$ radical from H₂O₂ decomposition directly. As it is observed from

experiments that the presence of EDDS didn't enhance the decomposition of H_2O_2 , hence in the condition that the H_2O_2 consumption is almost the same, this consumption of H_2O_2 in the absence of EDDS is due to the catalytic effect of goethite and could generate $\bullet\text{OH}$ radical, whereas this consumption of H_2O_2 in the presence of EDDS is still kept unknown clearly but may be related to the presence of EDDS, and the production of $\bullet\text{OH}$ radical was inhibited. Furthermore, the $\bullet\text{OH}$ radical detection at pH 4.5 showed similar trends that the presence of EDDS totally inhibited the generation of $\bullet\text{OH}$ radical (Figure D-45).

D-4-1-2. Effect of H_2O_2 concentration on this Fenton system in the presence of EDDS

In order to further confirm the inhibition of EDDS on this heterogeneous Fenton system, different concentration of H_2O_2 including 1.13 mmol/L (Figure D-46), 11.3 mmol/L (Figure D-39) and 113 mmol/L (Figure D-47) was tested in this system at pH 6.2.

Without EDDS, it is found that the increase of BPA degradation rate was consistent with the enhancement of H_2O_2 concentration. However, when EDDS was added into the suspension, the degradation of BPA was negligible whatever the concentration of H_2O_2 used. It means that whatever the concentration of H_2O_2 used in the system, there was Fenton process working for the degradation of BPA in the absence of EDDS, but when EDDS was added, the Fenton processes was completely stopped.

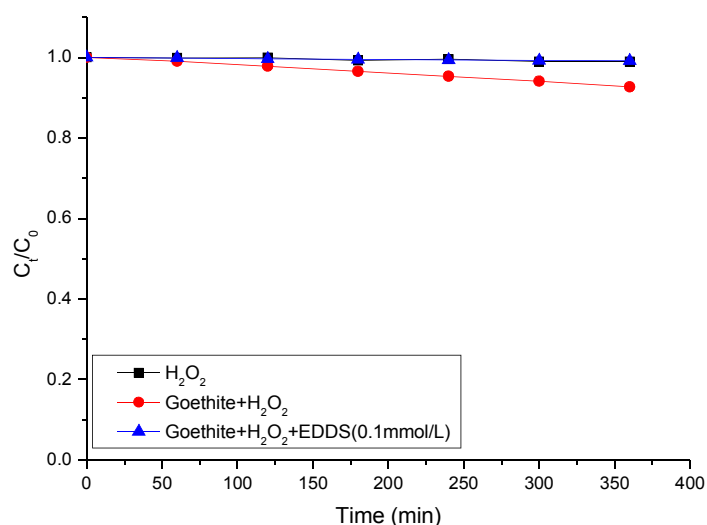


Figure D-46 BPA degradation in heterogeneous Fenton system with or without EDDS at pH 6.2.

Initial concentrations were 20 $\mu\text{mol/L}$ BPA, 0.1 g/L goethite, 1.13 mmol/L H_2O_2 and 0.1 mmol/L

EDDS

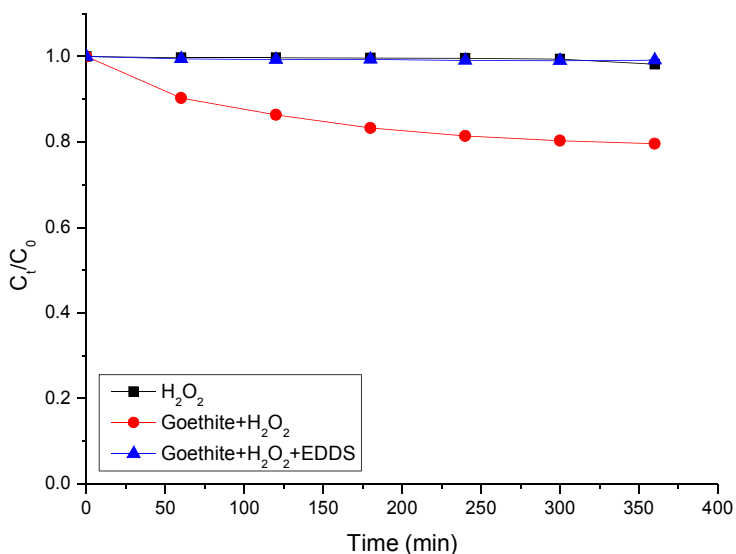


Figure D-47 BPA degradation in heterogeneous Fenton system with or without EDDS at pH 6.2.

Initial concentrations were 20 $\mu\text{mol/L}$ BPA, 0.1 g/L goethite, 113 mmol/L H_2O_2 and 0.1 mmol/L

EDDS

All of these results observed from the heterogeneous Fenton system indicate that the attempts of using EDDS in order to enhance the efficiency of this heterogeneous Fenton system are not favorable, since both BPA degradation and $\cdot\text{OH}$ radical formation were totally inhibited. To understand the mechanism of this inhibition in detail further investigations are necessary.

D-4-2. Heterogeneous photo-Fenton process

D-4-2-1. Effect of EDDS on the kinetic of heterogeneous photochemical system in the presence of goethite

In previous research of our group, it is found that EDDS can enhance the degradation of

organic compounds (E2) in heterogeneous photochemical process. In order to confirm this effect on BPA at neutral pH, the experiments of BPA photodegradation in the presence of fixed concentration of goethite (0.1 g/L) and different concentration of EDDS (0.05 mmol/L, 0.1 mmol/L, 0.25 mmol/L, 0.5 mmol/L and 1 mmol/L) at pH 6.2 were carried out. Irradiation was performed with polychromatic tubes emitting between 300 and 500 nm.

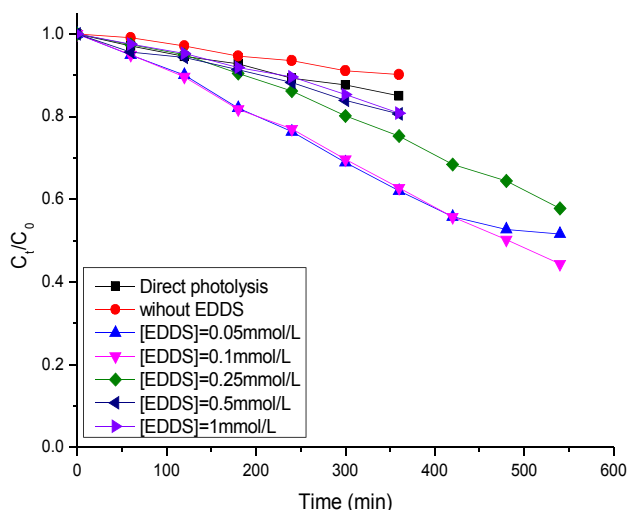


Figure D-48 Photodegradation of BPA in the presence of goethite with or without EDDS at pH 6.2. Initial concentrations were 20 μ mol/L BPA, 0.1 g/L goethite, and different concentration of EDDS

Firstly, as showed in Figure D-48, it is found that the direct photolysis of BPA was about 10% in 300 min, however, when goethite was added, the degradation rate was lower, which means that at pH 6.2, the presence of goethite itself could not help enhancing the BPA degradation due to its low iron leaching at neutral pH. On the other hand, there was screen effect because of the presence of solid in solution, and hence resulted in the lower absorption of UV light by BPA. When EDDS was added into the reaction system, the degradation of BPA was modified in different ways as a function of EDDS concentration used. The rate constants of BPA degradation as a function added EDDS concentration are presented Figure D-49.

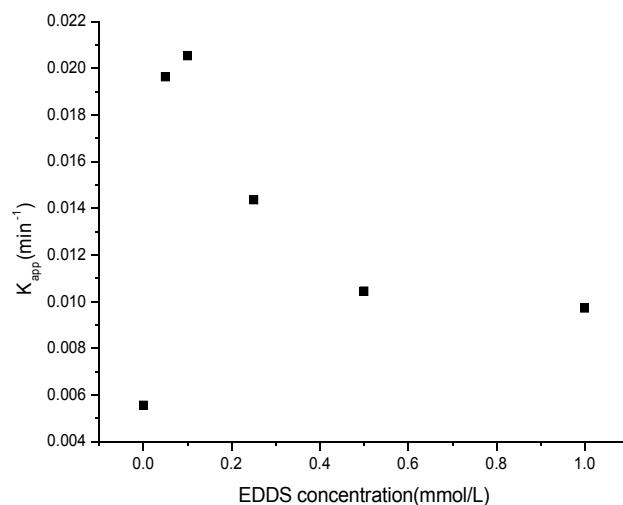


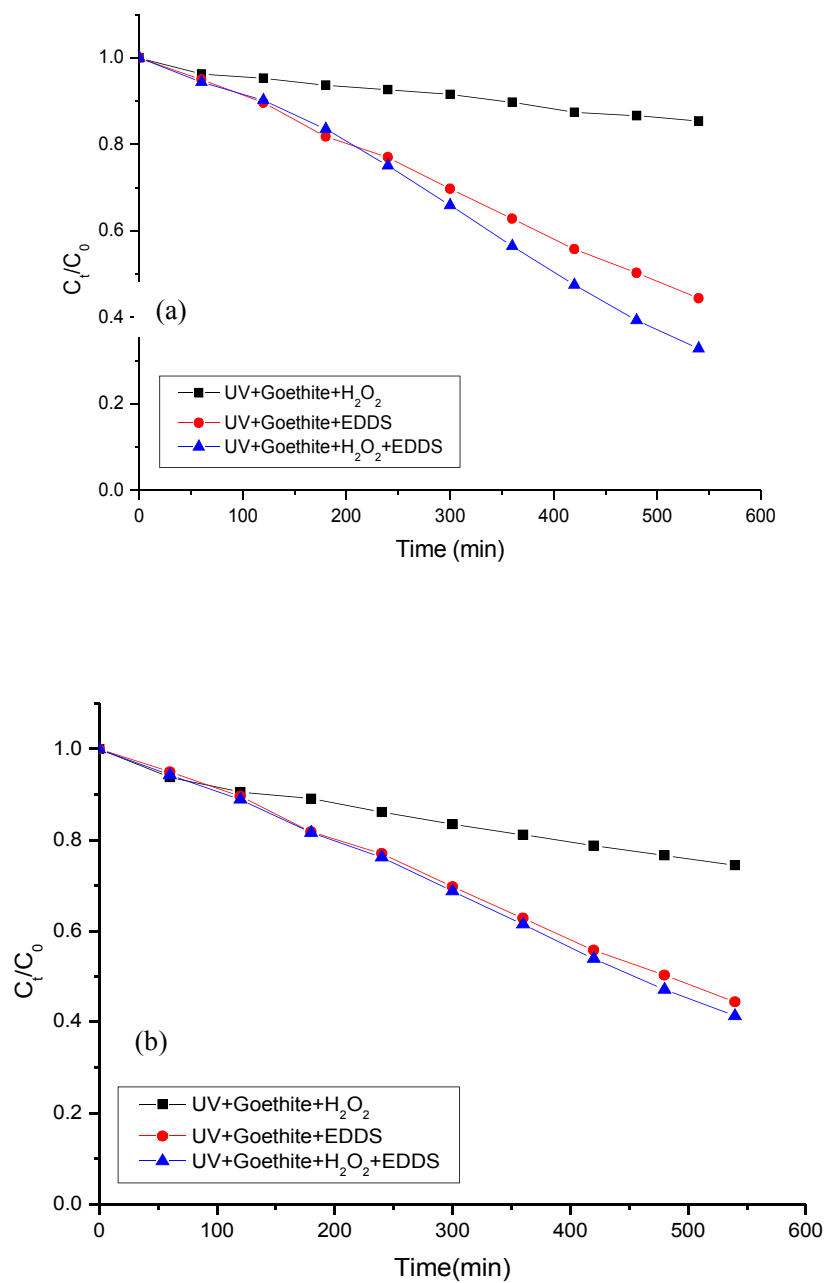
Figure D-49 Effect of EDDS concentration on the rate constant of BPA degradation

When the addition of EDDS was enhanced from 0.1 mmol/L to 1 mmol/L, the degradation rate of BPA was reduced. This inhibition of BPA degradation by high concentration of EDDS was firstly due to the strong adsorption of EDDS onto goethite which may block the interaction between BPA and the iron site of goethite, and secondly because of the competition for the reactivity of $\cdot\text{OH}$ radical between EDDS and BPA. When there was high concentration of EDDS in the solution, the $\cdot\text{OH}$ radical produced would react with EDDS firstly and hence the BPA degradation was inhibited. When 0.05 mmol/L of EDDS was added in the solution, the initial reaction rate constant of BPA was almost the same than with 0.1 mmol/L of EDDS. However, for longer irradiation time 400 min, the degradation in the presence of 0.05 mmol/L EDDS began to slow down and almost stopped at the time of 540 min, while the degradation in the presence of 0.1 mmol/L EDDS was still going on with the same reaction rate constant as before. This difference could be simply explained by the lack of EDDS in the process after a certain time of reaction.

D-4-2-2. Effect of goethite-EDDS complexation on the heterogeneous photo-Fenton process

In order to investigate the effect of EDDS on the heterogeneous photo-Fenton process,

experiments with different concentrations of H_2O_2 (0.1 mmol/L, 0.5 mmol/L and 1 mmol/L) in the presence of EDDS (0.1 mmol/L) were conducted.



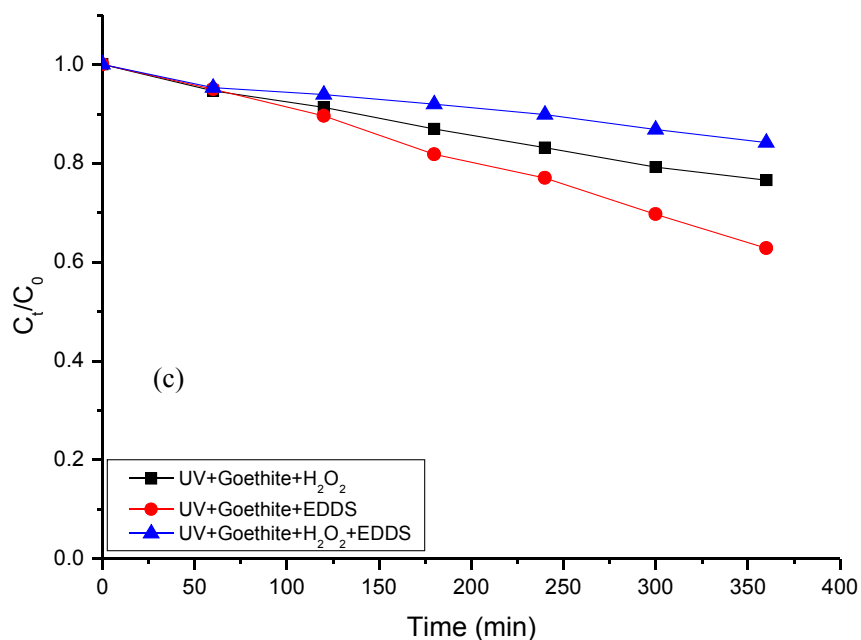
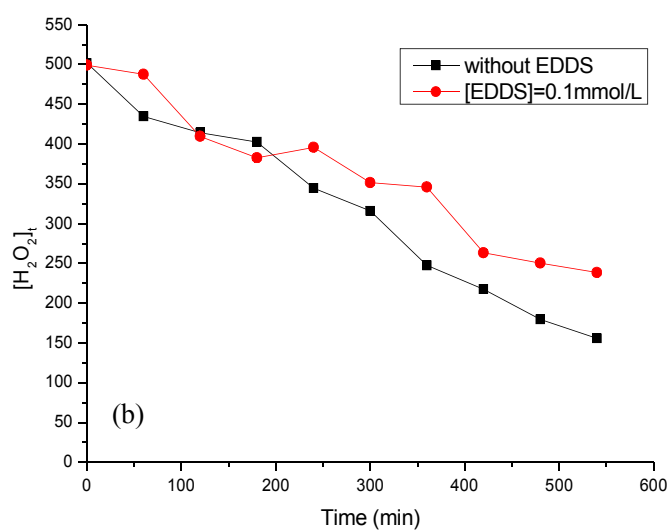
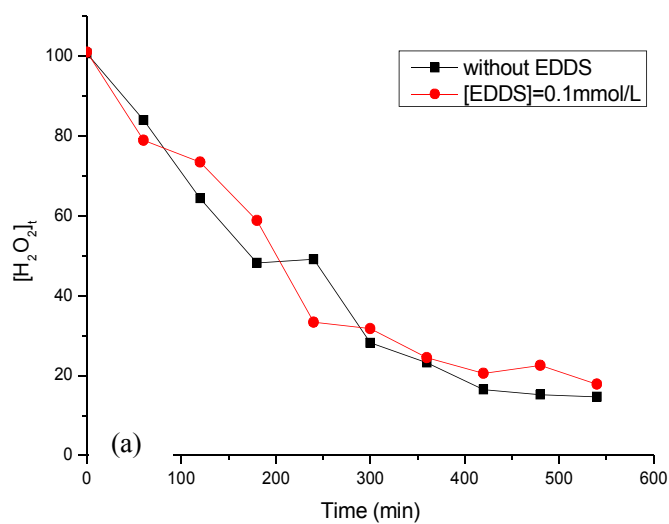


Figure D-50 BPA degradation in different systems including UV/goethite/EDDS, UV/goethite/H₂O₂ and UV/goethite/H₂O₂/EDDS. Initial concentrations were 20 μ mol/L BPA, 0.1 g/L goethite, 0.1 mmol/L EDDS and different concentration of H₂O₂ (0.1 mmol/L in a, 0.5 mmol/L in b and 1.13 mmol/L in c)

From the results observed (Figure D-50) in this part of experiments, interesting phenomenon was found that when different concentration of H₂O₂ was used, the effect of EDDS was totally different. Comparing the degradation process of BPA in three different systems which was shown in Figure D-50, including UV/goethite/H₂O₂, UV/goethite/EDDS and UV/goethite/H₂O₂/EDDS, it is found that in the case of 0.1 mmol/L of H₂O₂, the best BPA degradation was achieved in UV/goethite/H₂O₂/EDDS system. In this case, we obtain about 67.2% of BPA degradation in 540 min, higher than in both UV/goethite/H₂O₂ system (14.6%) and UV/goethite/EDDS system (55.6%). These results mean that when 0.1 mmol/L of H₂O₂ was added, the addition of EDDS increased the degradation of BPA. In the case of 0.5 mmol/L of H₂O₂, about 58.7% of BPA was degraded in UV/goethite/H₂O₂/EDDS system, which was higher than in UV/goethite/H₂O₂ system (25.6%), but almost the same than in UV/goethite/EDDS system (55.6%). However, in the case of 1.13 mmol/L of H₂O₂,

the degradation of BPA was much lower in UV/goethite/H₂O₂/EDDS system than in both UV/goethite/H₂O₂ system and UV/goethite/EDDS system, which indicated that at higher H₂O₂ concentration, the effect of EDDS was negative. It could be concluded that the positive effect of EDDS reduced when the concentration of H₂O₂ is higher. So, if we would like to add EDDS to increase the efficiency of the heterogeneous photo-Fenton system high H₂O₂ concentration could not be used.

In order to explain better this phenomenon, H₂O₂ concentration in the presence or absence of EDDS was detected.



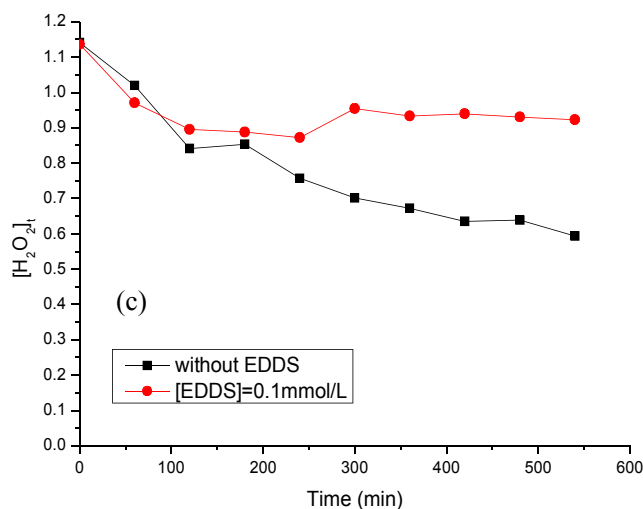


Figure D-51 H₂O₂ decomposition in photo-Fenton process with or without EDDS. Initial concentrations were 20 μ mol/L BPA, 0.1 g/L goethite, 0.1 mmol/L EDDS and different concentration of H₂O₂ (0.1 mmol/L in a, 0.5 mmol/L in b and 1.13 mmol/L in c)

From the results obtained in Figure D-51, it is found that in the case of 0.1 mmol/L of H₂O₂, the H₂O₂ decomposition didn't have significant difference in the presence or absence of EDDS. However, in the case of 0.5 mmol/L H₂O₂, the presence of EDDS slowed down the H₂O₂ decomposition a little bit. Furthermore, in the case of 1.13 mmol/L H₂O₂, the inhibition of H₂O₂ decomposition due to the presence of EDDS became more significant. This result was consistent with observed from previous research that the presence of EDDS will enhance the stability of H₂O₂ in the presence of aquifer materials [316]. According to this research, the largest H₂O₂ decomposition was observed in the presence of ferrous ions, whereas the presence of EDDS as chelant of iron largely decreases the decomposition of H₂O₂. It seems that in the case of higher H₂O₂ concentration, the presence of EDDS may slow down the decomposition of H₂O₂ much more significantly, and hence reduce the •OH radical production from H₂O₂ decomposition.

Moreover, in order to get some new information about the mechanism of BPA degradation enhancement in the presence of EDDS, an interesting experiment was conducted. First of all, 0.1 g/L of goethite and 0.1 mmol/L of EDDS was mixed together, and pH value in the suspension was adjusted to 6.2. Then, this suspension was kept in dark and stirring

magnetically for about 13 hours, after that, 20 $\mu\text{mol/L}$ of BPA and 0.1 mmol/L of H_2O_2 were added into the suspension, pH adjusted to 6.2 again, and the irradiation under UV light is started. In this BPA degradation process, it is found that BPA degradation was much faster than that in the irradiation process without time of stirring.

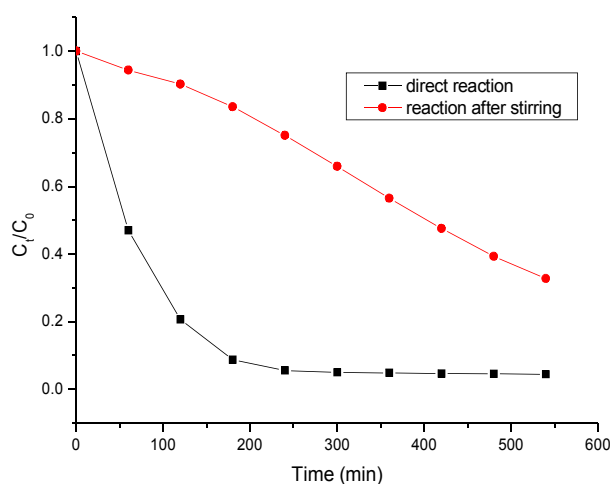


Figure D-52 0.1 g/L goethite and 0.1 mmol/L EDDS mixed together, stirring in the dark for 13h and then the mixture was used in BPA degradation in photo-Fenton system. Initial concentrations were 20 $\mu\text{mol/L}$ BPA, 0.1 g/L goethite, 0.1 mmol/L H_2O_2 and 0.1 mmol/L EDDS

The BPA degradation showed in Figure D-52 reached up to 90% in 180 min and then almost stopped, which means that the long time stirring period before irradiation had positive effect on the efficiency of photo-Fenton process. The result in Fenton process showed that the addition of EDDS had a little enhancement of iron leaching in water but not so obvious, so the degradation enhancement of BPA could be due to EDDS adsorption onto goethite except the enhance of iron leaching. The long time stirring make a stable equilibrium of EDDS adsorption onto goethite surface and it may complex with iron site on the surface. As it is known from previous research that under irradiation, Fe(III)-EDDS is easily photolyzed and the quantum yield of the $\cdot\text{OH}$ radical formation was higher at higher pH values in the range 3.0 - 9.0, which demonstrates that this complex is stable in aqueous solution at neutral pH and is photochemically efficient. The main conclusion of this part is that the complexation between iron and EDDS after a long time stirring both in aqueous

phase and goethite solid surface can enhance the efficiency of the whole photo-Fenton process.

D-4-2-3. Optimization of heterogeneous photo-Fenton system in the presence of EDDS

From the conclusion achieved on the above, it is found that at low H_2O_2 concentration, the addition of EDDS can considerably enhance the efficiency of heterogeneous photo-Fenton system. In order to increase the efficiency of the UV/goethite/ H_2O_2 /EDDS system, the effect of the goethite dosage, H_2O_2 and EDDS concentrations at different pHs was investigated.

I. Effect of goethite dosage

The experiments with a fixed concentration of EDDS (0.1 mmol/L), H_2O_2 (0.1 mmol/L), BPA (20 $\mu\text{mol/L}$) and using different goethite dosage: 0.01 g/L, 0.05 g/L, 0.1 g/L, 0.25 g/L, 0.35 g/L and 0.5 g/L, at pH 6.2 were conducted in order to investigate the effect of goethite dosage on the BPA degradation. From the results showed in Figure D-53 it can be concluded that for concentration ranging from 0.1 g/L up to 0.25 g/L, the degradation rate of BPA increases and the degradation rate reached about 80% in 540min when 0.25 g/L of goethite was used. However, increasing the dosage of goethite, the degradation rate of BPA decreases from about 65.9% to 62.0% in the case of 0.35 g/L and 0.5 g/L of goethite respectively. The enhancement of BPA degradation due to the addition of goethite can be explained by the increase of surface area, which may increase the interaction opportunity between iron side of goethite and other compounds such as H_2O_2 , EDDS and BPA, present in the solution. In same time, the number of photon onto the iron side could also be improved and hence the generation of $\cdot\text{OH}$ radical could increase. When the dosage of goethite increase up to 0.25 g/L the low BPA degradation could be explained by a negative effect of the solid goethite on the quantity of photons reaching the bulk of the irradiated solution.

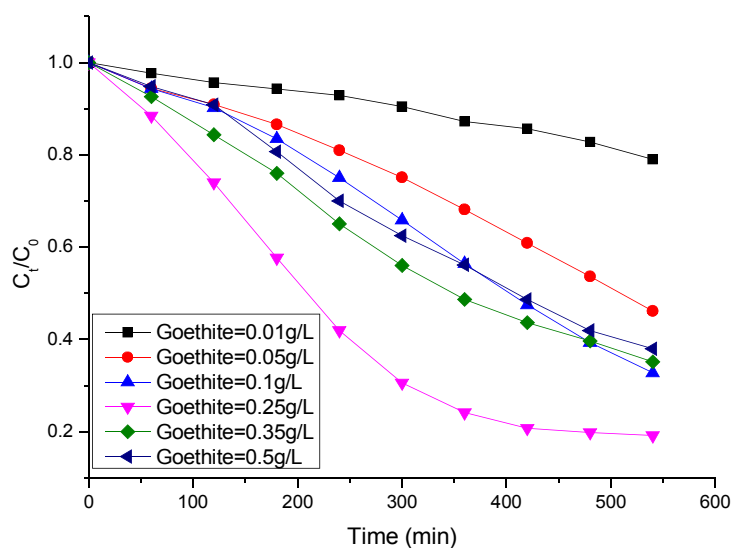


Figure D-53 BPA degradation in photo-Fenton process in the presence of different goethite dosage at pH 6.2, Initial concentrations were 20 $\mu\text{mol/L}$ BPA, 0.1 mmol/L H_2O_2 and 0.1 mmol/L EDDS

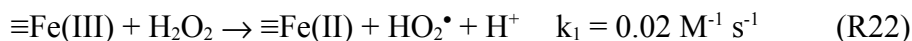
Table D-7 kinetic constant of BPA in different goethite dosage

Goethite dosage (g/L)	0.01	0.05	0.1	0.25	0.35	0.5
k_{app} (min^{-1})	0.0071	0.0185	0.0242	0.0466	0.0262	0.0244

II. Effect of H_2O_2 concentration

In previous research, it is found that when the concentration of H_2O_2 used in the system was higher than 1 mmol/L, the addition of EDDS play a negative effect in heterogeneous photo-Fenton system. It means that the H_2O_2 used in UV/goethite/ H_2O_2 /EDDS system can not be higher than 1 mmol/L. In order to determine the effect of H_2O_2 concentration on the BPA degradation the experiments with fixed goethite dosage (0.25 g/L), EDDS concentration (0.1 mmol/L), BPA concentration (20 $\mu\text{mol/L}$) and different H_2O_2 concentration: 0.05, 0.1, 0.2 and 0.5 mmol/L, at pH 6.2 were conducted. The results from the experiments above (Figure D-54) showed that when the H_2O_2 concentration increased from 0.05 mmol/L to 0.1 mmol/L, the degradation of BPA enhanced as expected, whereas the H_2O_2 concentration is higher, BPA degradation rate, as showed in Figure 16, strongly decreased. When 0.2

mmol/L and 0.5 mmol/L of H₂O₂ were used, only 43.2% and 25.8% of BPA degradation was achieved in 540 min. It is obviously that the increase of oxidant from 0.05 mmol/L to 0.1 mmol/L leads to the increase of BPA degradation rate, because an higher quantity of •OH radical is formed from reaction (R23) [117].



Where \equiv represents the surface of the catalyst goethite.

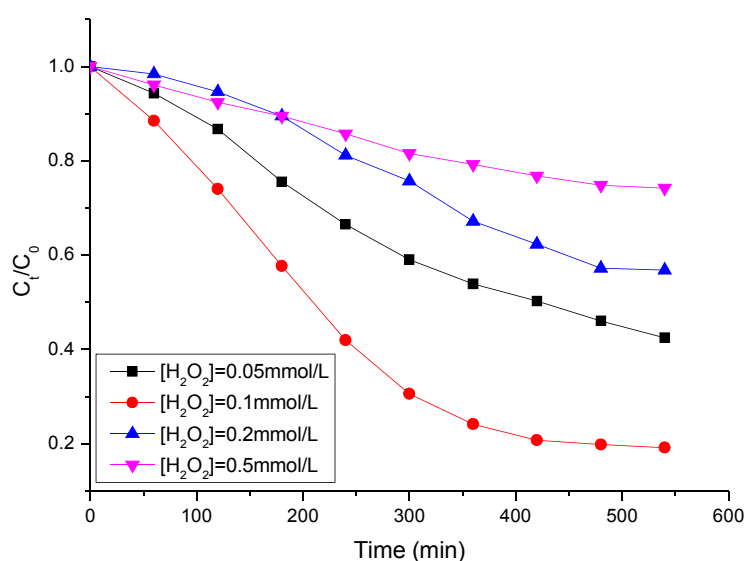


Figure D-54 BPA degradation in photo-Fenton process in the presence of different H₂O₂ concentration at pH 6.2, Initial concentrations were 20 μmol/L BPA, 0.25 g/L goethite and 0.1 mmol/L EDOS

Nevertheless, higher concentration of oxidant leads to a decrease of BPA degradation performance. As it is known, in Fenton process there is an optimum H₂O₂ concentration existing which can make the best efficiency. In traditional Fenton system, this appropriate H₂O₂ concentration can be easily explained by the fact that in the case of higher concentration, the excess amount of H₂O₂ can act as the scavenger of •OH radical via previously reported reaction (R5).

Whereas it is known from the result presented in Fe(III)-EDDS Fenton system research of our research group before that HO₂• radical can effect the generation of •OH radical but

their reactivity toward BPA could be neglected.

However, in our system, the optimum H_2O_2 concentration was much lower than traditional Fenton system, which is about 10 mmol/L. So except the scavenge effect of H_2O_2 , other influencing factors and especially the effect of EDDS must be taken into account. It is known from the previous research that EDDS was adsorbed onto goethite surface strongly, which may block the interaction between iron side of goethite and H_2O_2 , hence increase the scavenge effect to $\cdot\text{OH}$ radical.

Table D-8 kinetic constant of BPA in different H_2O_2 concentration

H_2O_2 (mmol/L)	0.05	0.1	0.2	0.5
k_{app} (min^{-1})	0.0236	0.0466	0.0168	0.0116

III. Effect of EDDS concentration

The results achieved in previous research showed that the addition of EDDS largely change the efficiency of heterogeneous photo-Fenton system. In order to better understand the effect of EDDS concentration, the experiments with fixed goethite dosage (0.25 g/L), H_2O_2 concentration (0.1 mmol/L), BPA concentration (20 $\mu\text{mol/L}$) and different EDDS concentration: 0.05, 0.1, 0.2 and 0.5 mmol/L, at pH 6.2 were conducted. The results reported in Figure D-55, showed that, when the concentration of EDDS increased from 0.05 mmol/L to 0.1 mmol/L, the degradation of BPA enhanced from 34.8% to 80.8%. On the contrary, when 0.05 mmol/L of EDDS were used, the degradation process of BPA suddenly stopped after about 360 min, which may be due to the totally consumption of EDDS in agreement with the result concerning the photochemical degradation of BPA in the presence of goethite-EDDS. The degradation after 540 min was about 64.5% and 45.7% in the presence of 0.2 mmol/L and 0.5 mmol/L of EDDS respectively.. This inhibition due in the presence of high EDDS concentration can be expressed by the following reasons: the first one is the strong adsorption of EDDS onto goethite surface, which may block the interaction between iron side of goethite and BPA/ H_2O_2 . When the concentration of EDDS gets higher, this negative effect gets stronger, leading to the decrease of BPA degradation.

The second reason could be attributed to the fact that EDDS can also react with $\bullet\text{OH}$ radical, when the concentration of EDDS gets higher, the competitive reaction between EDDS and BPA become more important decreasing, as consequence, the BPA degradation. At the same time, it is known that EDDS is photosensitive and it may adsorb the UV light and playing as screen decreasing the direct photolysis of H_2O_2 . It can be concluded from the results above that there is also optimum EDDS concentration in UV/goethite/ H_2O_2 /EDDS system, which can enhance the efficiency of heterogeneous photo-Fenton process.

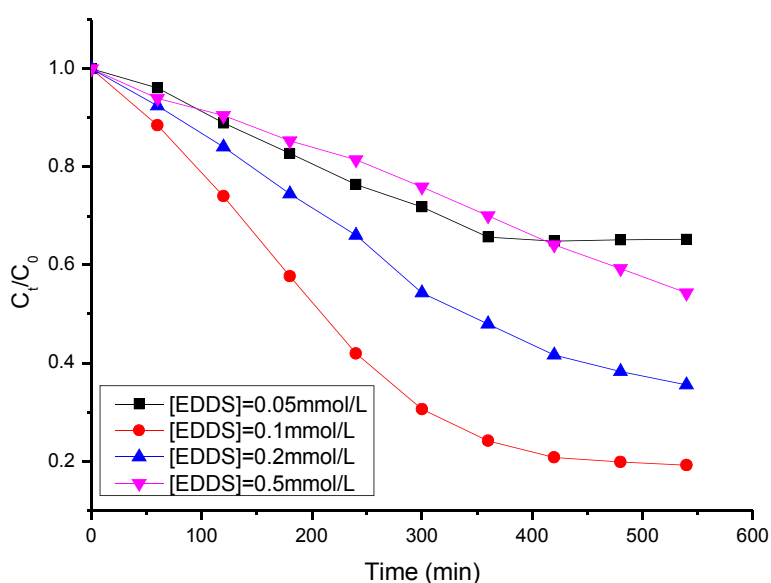


Figure D-55 BPA degradation in photo-Fenton process in the presence of different EDDS concentration at pH 6.2, Initial concentrations were 20 $\mu\text{mol/L}$ BPA, 0.25 g/L goethite and 0.1 mmol/L H_2O_2

Table D-9 kinetic constant of BPA in different EDDS concentration

EDDS (mmol/L)	0.05	0.1	0.2	0.5
k_{app} (min^{-1})	0.0190	0.0466	0.0290	0.0160

IV. Effect of pH value

It is known to all that Fenton or photo-Fenton process is affected by pH value of the

environment largely. Usually in traditional Fenton and photo-Fenton system, the best efficiency of the system is achieved at around pH 3. In order to investigate if the addition of EDDS changes the effect of pH, the experiments with fixed goethite dosage (0.25 g/L), H_2O_2 (0.1 mmol/L), EDDS (0.1 mmol/L) and BPA (20 $\mu\text{mol/L}$), at different pH value, of 3.7, 6.2 and 8.7, were conducted, It is observed from the results reported in Figure D-56 that the degradation of BPA at pH 3.7 and 8.7 was 45.0% and 41.2% respectively, which was almost the same but much lower than that at pH 6.2. This result was quite different with the result in traditional Fenton or photo-Fenton system. The kinetic constant of BPA at different pH also showed similar trends as the degradation rate.

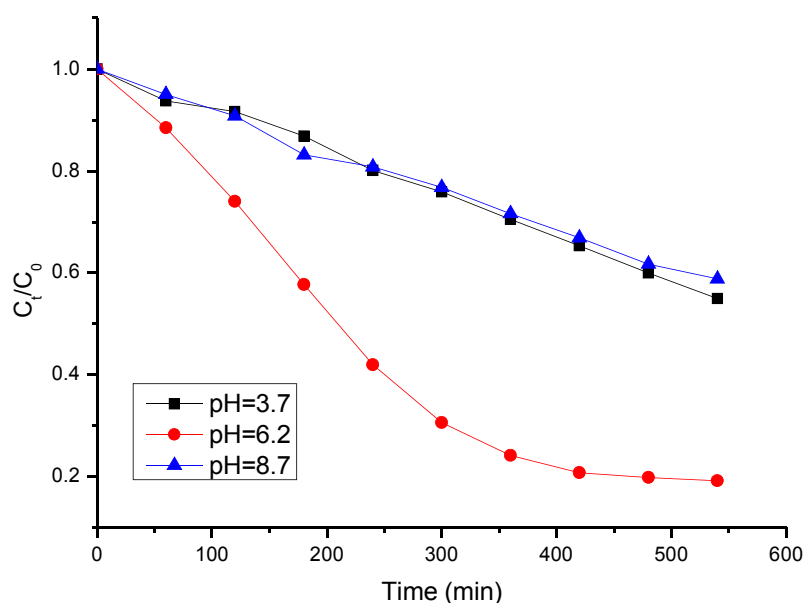
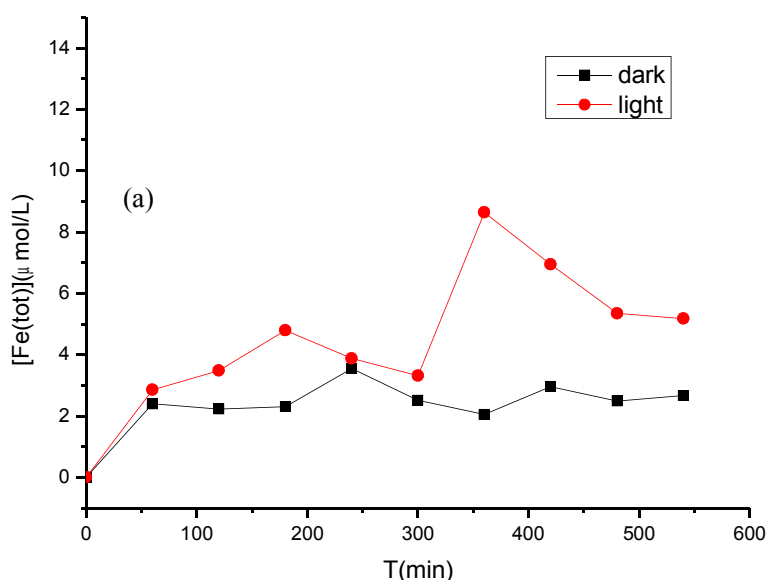


Figure D-56 BPA degradation in photo-Fenton process at different pH, Initial concentrations were 20 $\mu\text{mol/L}$ BPA, 0.25 g/L goethite, 0.1 mmol/L H_2O_2 and 0.1 mmol/L EDDS

Table D-10 kinetic constant of BPA at different pH

pH	3.7	6.2	8.7
k_{app} (min^{-1})	0.0164	0.0466	0.0158

In order to explain this observation, the iron leaching in the presence of EDDS with and without UV irradiation at pH 3.7, 6.2 and 8.7 respectively was detected. From the results shown in Figure D-57 it is observed that the iron leaching in the absence of UV light at pH 3.7, 6.2 and 8.7 was very low. In the presence of UV irradiation, the iron leaching was enhanced to varying degrees at these three pHs respectively. As expected at pH 3.7, the enhancement of iron leaching in the presence of UV irradiation was higher, especially after about 200 min where the maximum amount of iron leaching is about 13 $\mu\text{mol/L}$. However, this high value of the iron leaching at pH 3.7 didn't lead to higher efficiency in the BPA degradation. On the contrary, it is found that the efficiency of this heterogeneous photo-Fenton system in BPA degradation didn't have apparent relationship with the amount of iron leaching, which means that the reaction process of this heterogeneous photo-Fenton system primarily happens on the surface of goethite, other than the homogeneous photo-Fenton system in the solution. So we assumed that this gap at different pHs may be due to the difference in adsorption of EDDS onto goethite surface, which may strengthen interaction between EDDS and iron side of goethite.



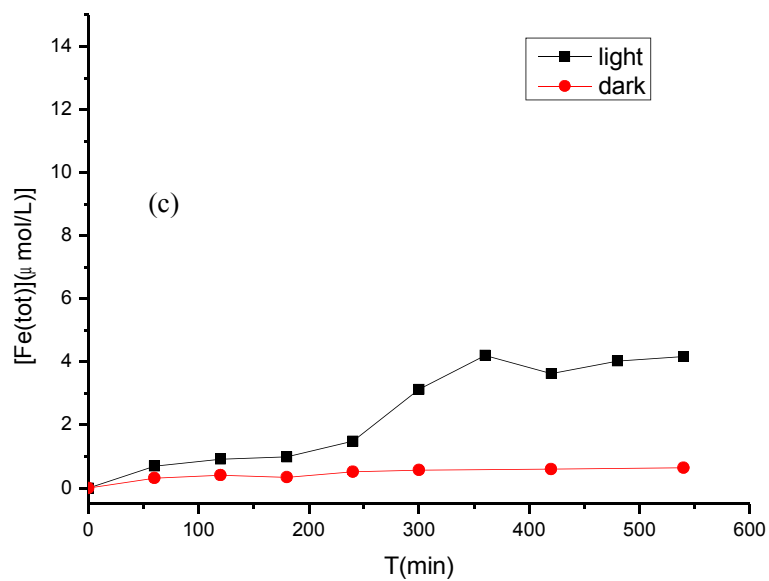
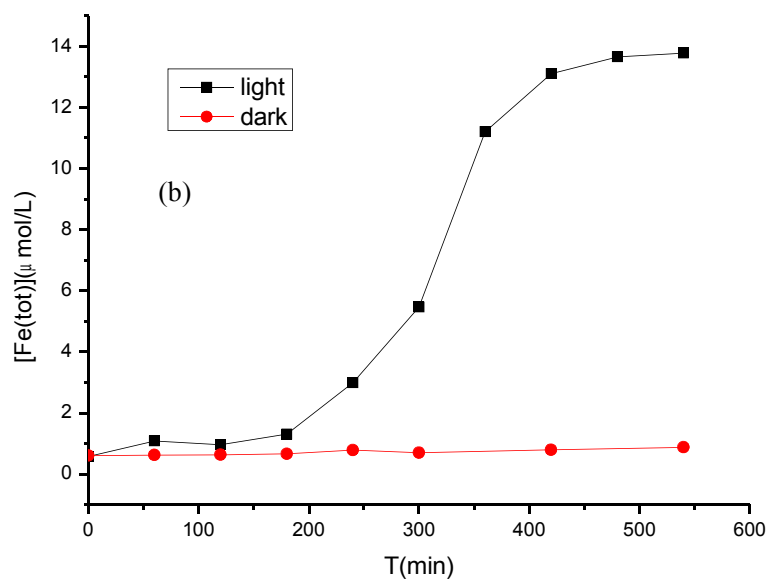


Figure D-57 iron leaching in the presence of EDDS with or without UV irradiation, pH 6.2 in a, pH 3.7 in b, pH 8.7 in c

Table D-11 Adsorption of EDDS in fixed concentration at different pH

pH	3.7	6.2	8.7
Cs($\mu\text{mol m}^{-2}$)	0.0145	0.1257	0.0269

In order to confirm this assumption, we detected the adsorption of EDDS onto goethite surface at different pHs. From the results achieved and showed in Table D-11, it is found that the highest adsorption of EDDS was achieved at pH 6.2, whereas the adsorption of EDDS at pH 3.7 and 8.7 respectively was much lower comparing with the adsorption at pH 6.2. And as it is known that for EDDS, $\text{pK}_1=2.4$, $\text{pK}_2=3.9$, $\text{pK}_3=6.8$, $\text{pK}_4=9.8$ in 25°C [84], the speciation of EDDS at pH 3.7, 6.2 and 8.7 is quite different due to different protonated degree of EDDS, hence this discrimination in adsorption could be attributed to a combination of pH-dependent speciation of EDDS, surface charge characteristics of goethite ($\text{PZC}\sim 9$). Such sorption behavior has also been observed for some organic acid complexation on oxide surfaces where the adsorption envelope typically showed maximum adsorption at a pH near the pK_a . And this discrimination of adsorption may effect the efficiency of this photo-Fenton system strongly.

V. Comparison of different systems

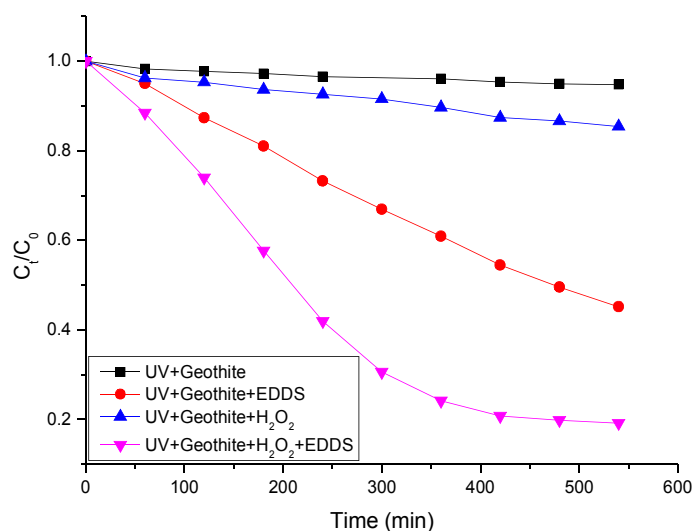


Figure D-58 BPA degradation comparison in different system in the optimum condition of photo-

Fenton system, Initial concentrations were 20 $\mu\text{mol/L}$ BPA, 0.25 g/L goethite, 0.1 mmol/L H_2O_2 and 0.1 mmol/L EDDS

In order to further confirm the positive effect of EDDS on the heterogeneous photo-Fenton process, the experiments of BPA (20 $\mu\text{mol/L}$) degradation in the following systems: UV/goethite, UV/goethite/EDDS, UV/goethite/ H_2O_2 and UV/goethite/ H_2O_2 /EDDS, in the presence of 0.25 g/L goethite, 0.1 mmol/L H_2O_2 and 0.1 mmol/L EDDS were conducted. From the results showed in Figure D-58 it the best BPA degradation was achieved in UV/goethite/ H_2O_2 /EDDS system, which confirmed again that the addition of EDDS could have positive effect on the heterogeneous photo-Fenton process.

D-4-3. Conclusion

All in all, we can concluded that in heterogeneous Fenton system using goethite, the presence of EDDS would totally inhibit the degradation of BPA and the generation of $\cdot\text{OH}$ radical at pH 6.2 and 3.7. From the results of EDDS adsorption onto goethite surface, iron leaching from goethite to liquid phase and decomposition of H_2O_2 , this inhibition could be expressed by the strong adsorption of EDDS onto the goethite surface, and hence the interaction between H_2O_2 and goethite was blocked.

In heterogeneous photo-Fenton system, the effect of EDDS on BPA degradation at pH 6.2 largely dependeds on the H_2O_2 initial concentration. When a low concentration of H_2O_2 was used, the addition of EDDS would enhance the efficiency of BPA degradation in the photo-Fenton system, whereas when the concentration of H_2O_2 increses, the positive effect weakened, and finally converted to negative effect while the concentration was higher than 1 mM. This effect could be preliminarily explained taking into account the interaction of EDDS with the H_2O_2 decomposition, which was achieved from the decomposition detection of H_2O_2 in photo-Fenton system with or without EDDS.

Finally, the optimum condition for BPA degradation in photo-Fenton process in the presence of EDDS was investigated and the variable effect including pH values, goethite dosage, H_2O_2 concentration and EDDS concentration was determined. The most effective

condition was achieved at pH 6.2 in the presence of 0.25 g/L goethite, 0.1 mmol/L H₂O₂ and 0.1 mmol/L EDDS was achieved, in this condition, about 80.8% of BPA was removed after 540min.

D-5. Products analysis in different systems

First of all, the direct photolysis of BPA was conducted as comparison with the photodegradation of BPA in homogeneous/heterogeneous Fenton and/or photo-Fenton systems. It is observed that excluding the impurities in the system, the only detectable chemical related with BPA in this system is the silylation product of BPA with the derivative BSTFA, which is in accord with the result of previous experiments that the direct photolysis was negligible.

The control experiment that without BPA was also conducted in order to determine the degradation products of EDDS and exclude the interference with the degradation products in the presence BPA. This result of is shown in Figure D-60. Since the degradation of EDDS in different systems doesn't have significant differences, we only represent one figure.

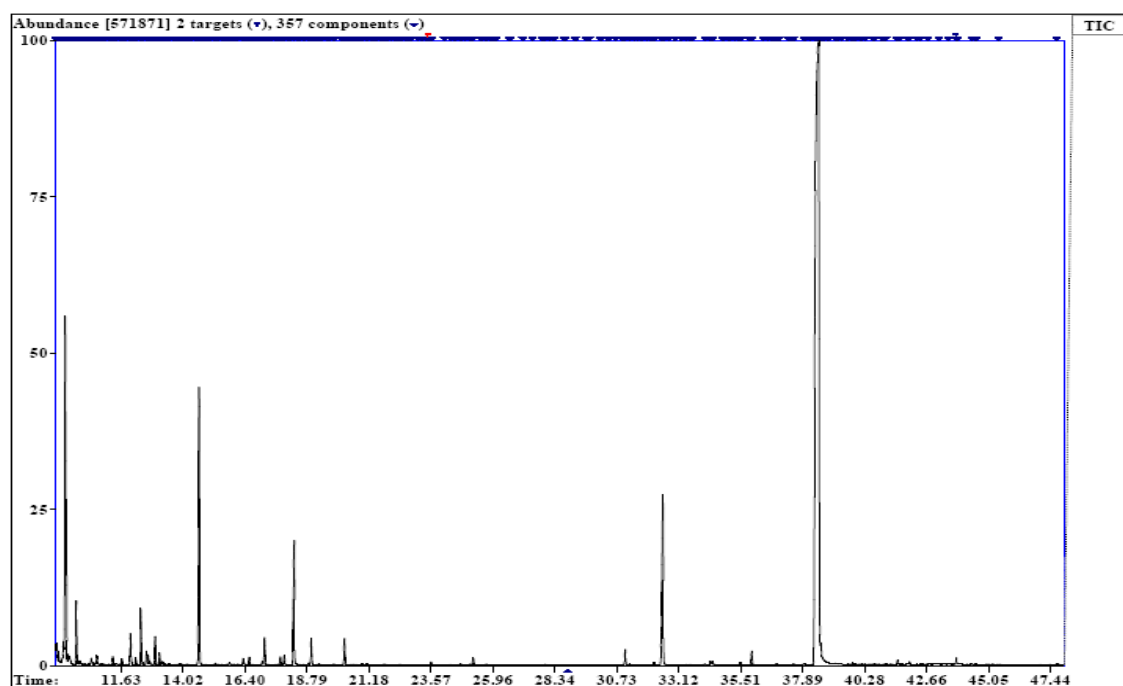


Figure D-59 GC–MS chromatograms of sample solution in direct photolysis of BPA

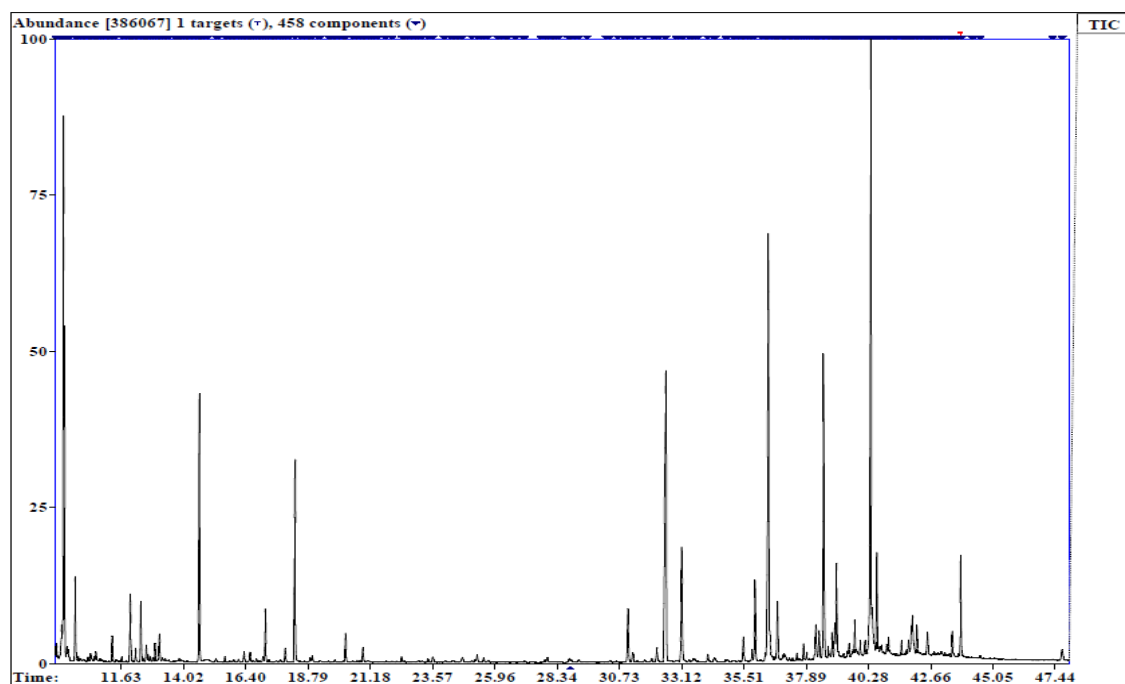


Figure D-60 GC–MS chromatograms of sample solution in degradation of EDDS

D-5-1. Product of BPA degradation analysis in homogeneous Fenton and photo-Fenton process

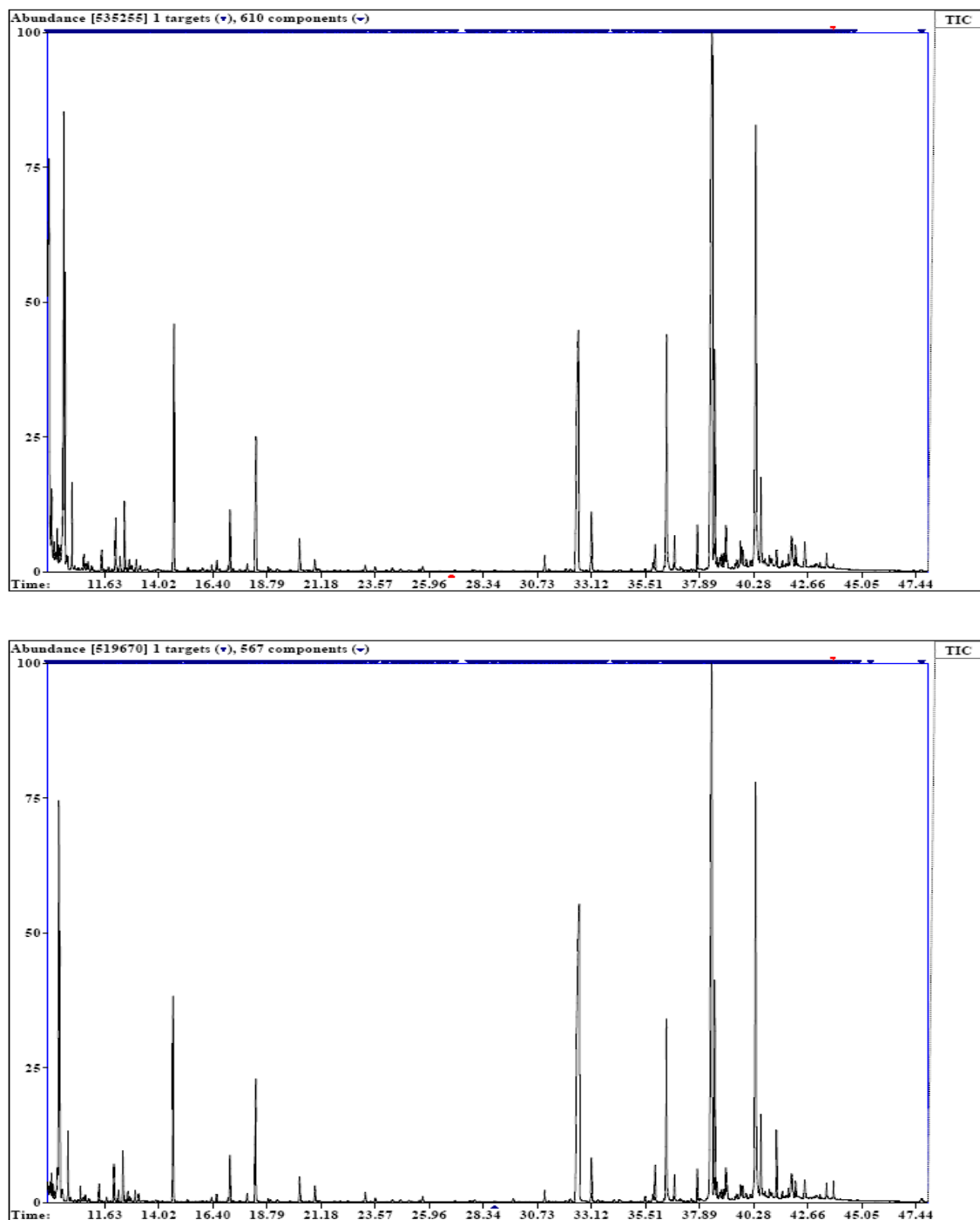
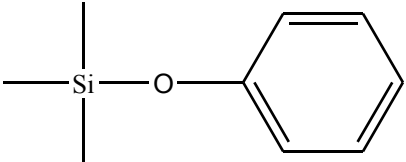
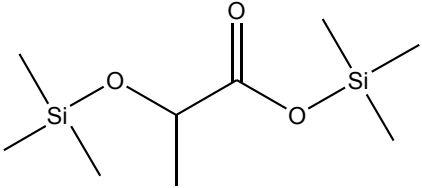
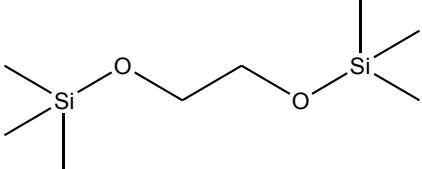
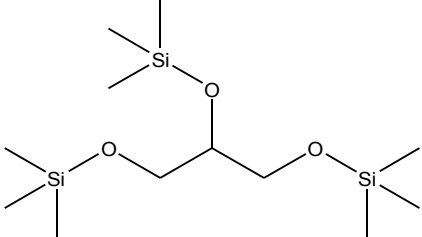
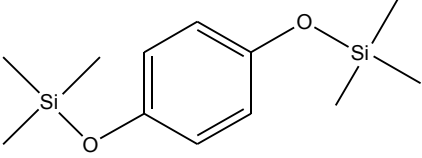
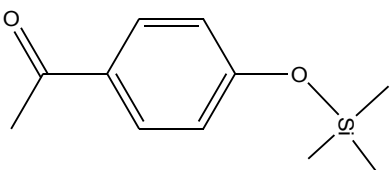
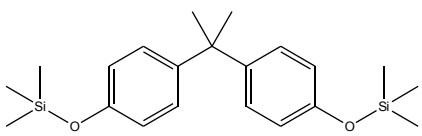


Figure D-61 GC–MS chromatograms of sample solution in heterogeneous Fenton process degradation of BPA (A as after 180min reaction, B as after 350min reaction)

The key products of BPA degradation in homogeneous Fenton and photo-Fenton system is shown in Table D-12.

Table D-12 Mass fragment ions (m/z) and relative abundance (%) of intermediates and BPA in

homogeneous Fenton process obtained from GC–MS spectra

Peak No.	Retention Time (min)	Detected ions, m/z (% abundance)	Name and Molecular weight (m/z)	Molecular structure
1	9.28	73(447), 75(205), 151(203)	trimethyl(phenoxy)silane 166	
2	12.76	147(999), 73(753), 117(691), 190(183), 191(175)	Trimethylsilyl 2-(trimethylsilyloxy)propanoate 234	
3	17.14	147(999), 73(374), 191(166), 148(151), 103(123)	1,2-bis(trimethylsilyloxy)ethane 206	
4	18.98	73(999), 147(958), 205(851), 117(383), 103(301)	1,2,3-tris(trimethylsilyloxy)propane 308	
5	22.03	239(999), 73(797), 254(710), 155(415), 44(353)	1,4-bis(trimethylsilyloxy)benzene 254	
6	23.61	193(999), 208(271), 194(153), 73(131), 152(113)	1-(4-(trimethylsilyloxy)phenyl)ethanone 208	
7	38.42	358(999), 357(999), 73(600), 372(495), 359(449)	2,2-bis(4-(trimethylsilyloxy)phenyl)propane 372	

The degradation products of BPA in homogeneous Fenton and photo-Fenton system were analyzed using GC-MS respectively. It is found from the results that there are no significant differences between Fenton and photo-Fenton system.

From the degradation product identification we can suggest that the first reaction step was

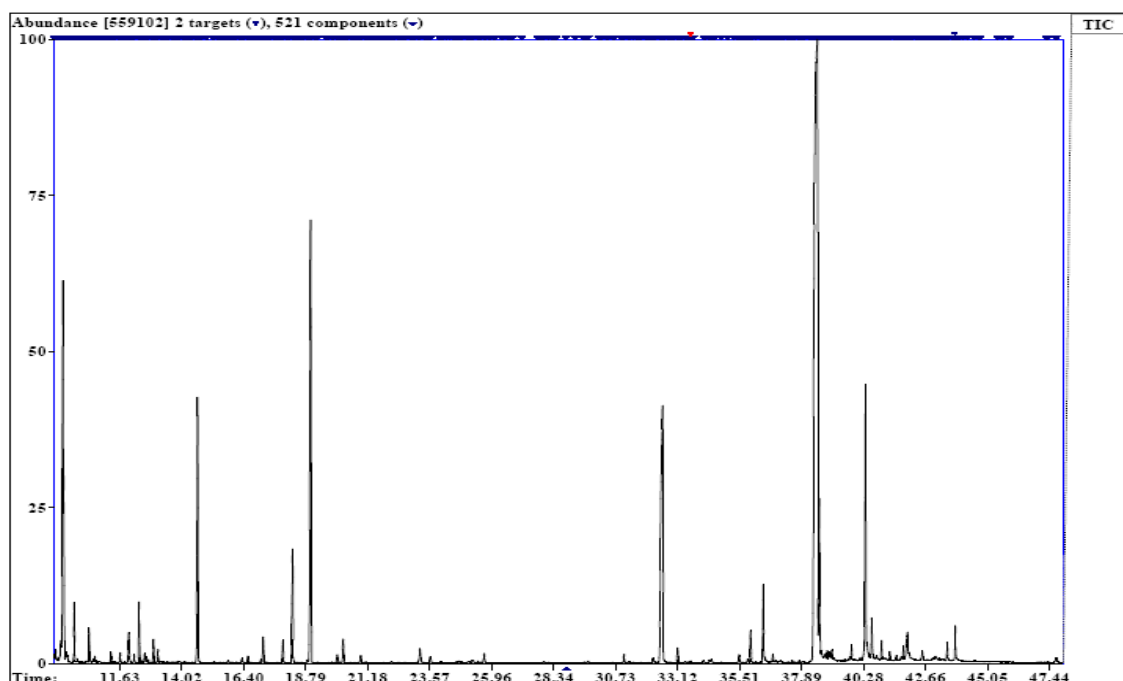
the cleavage of the two benzene rings followed by the oxidation leading to the formation of the benzene derived products. Next, the benzene ring was open due to the attack of $\bullet\text{OH}$ radicals producing the short chain organic compounds of low molecule weight like glycerol and glycol. Such compounds were further decomposed to the more simple organic acids and subsequent inorganic molecules such as CO_2 and H_2O . The proposed mechanism of BPA degradation was shown in Figure D-62.

In Figure D-62, the reactions represented by arrows with solid lines are detected from the experiments, whereas that represented by arrows with dashed lines are speculated through the experiment results and the related references [290, 322 and 323].

As it is seen in the proposed degradation scheme, firstly, BPA molecule was broken into phenoxyl and 4-isopropanolphenol radicals. The first one would form p-benzenediol and after, through the oxidation due to the $\bullet\text{OH}$ radical, glycol. Whereas the second one would be attacked by $\bullet\text{OH}$ radical and 4-(1-hydroxy-1-methyl-ethyl)-phenol could be formed. Successively two possible pathways could happen, the first is that isopropyl alkyl would disconnect from benzene ring, hence glycerol and p-benzenediol could be formed; the second possibility is that 4-(1,2-dihydroxypropan-2-yl)-phenol could be formed due to the attack of $\bullet\text{OH}$ radical, then this intermediate would be further oxidized to smaller molecules like methanol, 2-hydroxypropanoic acid and 1-(4-hydroxyphenyl)ethanone, finally further oxidation would take place like ring cleavage and finally simple molecule like CO_2 and H_2O would be formed.

In previous research, similar pathway of BPA degradation was also proposed. Katsumata et al [290] detected the BPA degradation products in traditional photo-Fenton processes and proposed the similar degradation pathway as described in our work. They reported that in the initial oxidation reaction, 4-isopropylphenol (IPP), *p*-hydroquinone (*p*-HQ), 4-(1-hydroxy-1-methyl-ethyl)-phenol (HMEP), and phenol are formed in the photocleavage of phenyl groups in BPA by attack of $\bullet\text{OH}$ radicals. After a sequence of reactions based on the one benzene ring products, an oxidative ring-opening reaction at the level of C–C bonds between adjacent hydroxyl or ketone groups was reported [322], leading to the formation of aliphatic compounds, such as HCOOH , CH_3COOH , and CH_3CHO , followed by production of CO_2 and H_2O . According to previously reported researches, the decomposition of phenol and *p*-benzenediol could produce ethanedioic acid through the intermediates of quinones [323].

D-5-2. Product of BPA degradation analysis in heterogeneous photo-Fenton process



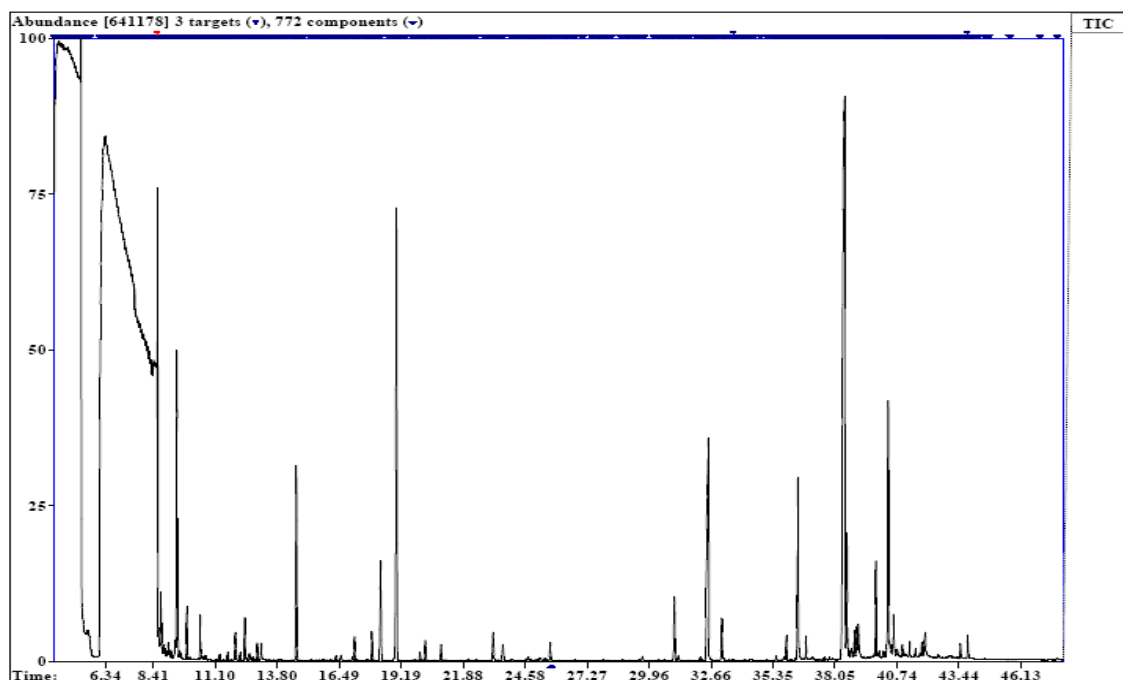
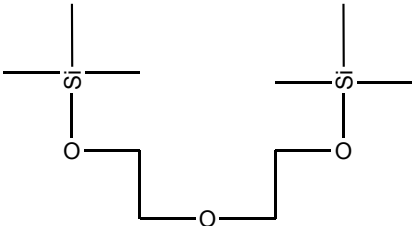
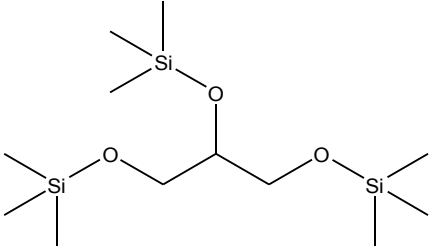
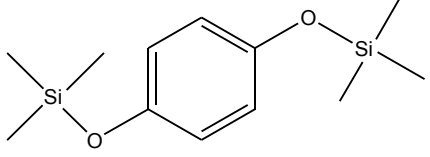
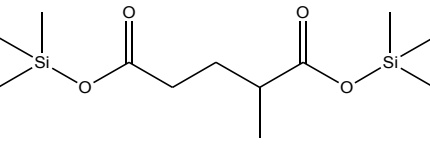
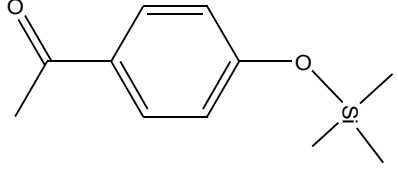
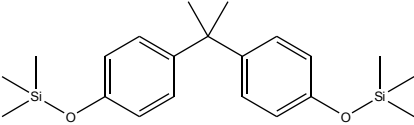


Figure D-63 GC–MS chromatograms of sample solution in heterogeneous photo-Fenton process degradation of BPA (A as after 240min reaction, B as after 540min reaction)

The main products of BPA degradation in heterogeneous photo-Fenton process is shown in Table D-13.

Table D-13 Mass fragment ions (m/z) and relative abundance (%) of intermediates and BPA in heterogeneous photo-Fenton process obtained from GC–MS spectra

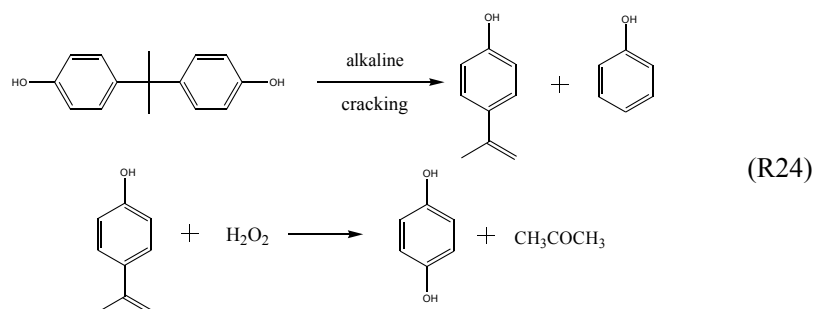
Peak No.	Retention Time (min)	Detected ions, m/z (% abundance)	Name and Molecular weight (m/z)	Molecular structure
1	9.28	73(447), 75(205), 151(203)	trimethyl(phenoxy)silane 166	
2	10.45	147(999), 73(374), 191(166), 148(151), 103(123)	1,2-bis(trimethylsilyl)oxyethane 206	

3	17.91	73(999), 117(580), 116(174), 147(174), 103(139)	Bis(2-(trimethylsilyloxy)ethyl) ether 250	
4	18.98	73(999), 147(958), 205(851), 117(383), 103(301)	1,2,3-tris(trimethylsilyloxy)propane 308	
5	22.03	239(999), 73(797), 254(710), 155(415), 44(353)	1,4-bis(trimethylsilyloxy)benzene 254	
6	22.46	147(999), 73(942), 75(565), 275(450), 44(321)	Bis(trimethylsilyloxy)2-methylpentanediol 290	
7	23.61	193(999), 208(271), 194(153), 73(131), 152(113)	1-(4-(trimethylsilyloxy)phenyl)ethanone 208	
8	38.42	358(999), 357(999), 73(600), 372(495), 359(449)	2,2-bis(4-(trimethylsilyloxy)phenyl)propane 372	

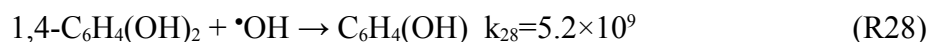
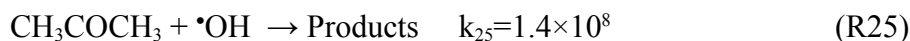
From the products detected, it is achieved that the separation of the two benzene rings of BPA molecule was also discovered in heterogeneous photo-Fenton process, since the products including one benzene ring were also found. Then all these chemicals were further oxidized and smaller organic molecules were formed such as 1,2,3-propanetriol.

The BPA degradation scheme in heterogeneous system is shown in Figure D-65 and it is found that the degradation pathway of BPA in heterogeneous system is similar to that in homogeneous system, except for glycerol and other intermediates such as p-benzenediol. Firstly, this accumulation of intermediates can be attributed to the lower $\bullet\text{OH}$ radicals

generation rate and to the terminal reaction of $\bullet\text{OH}$ radicals in heterogeneous system, which can limit the further oxidation of BPA and its degradation intermediates. Secondly, as it is shown, the intermediate 4-(1-hydroxy-1-methyl-ethyl)-phenol could be detected by $\bullet\text{OH}$ radicals and isopropyl radical cleavage from benzene ring and a series of intermediates such as acetone and prop-1-en-2-ol are formed, which could also be generated by following reaction:



In this heterogeneous system, the surface of iron oxide may play inductive effect on BPA or its phenolic intermediates and form surface complex through Fe(III) and phenolic group, hence inhibit the attack of $\bullet\text{OH}$ radicals to these intermediates. As results, the attack of $\bullet\text{OH}$ radicals focuses on acetone and prop-1-en-2-ol, and glycerine is produced. Thirdly, due to the low concentration of $\bullet\text{OH}$ radicals in the system, glycerine is not so easy to be further oxidized through the pathway shown in Figure D-64 and will accumulate in the system. In homogeneous system, however, $\bullet\text{OH}$ radicals can be produced in a large amount, so the intermediates can be easily further oxidized and seldom accumulate in the system, and H_2O_2 is also decomposed in a large extent, leading to the lower generation of acetone and/or prop-1-en-2-ol from the reaction (R24).



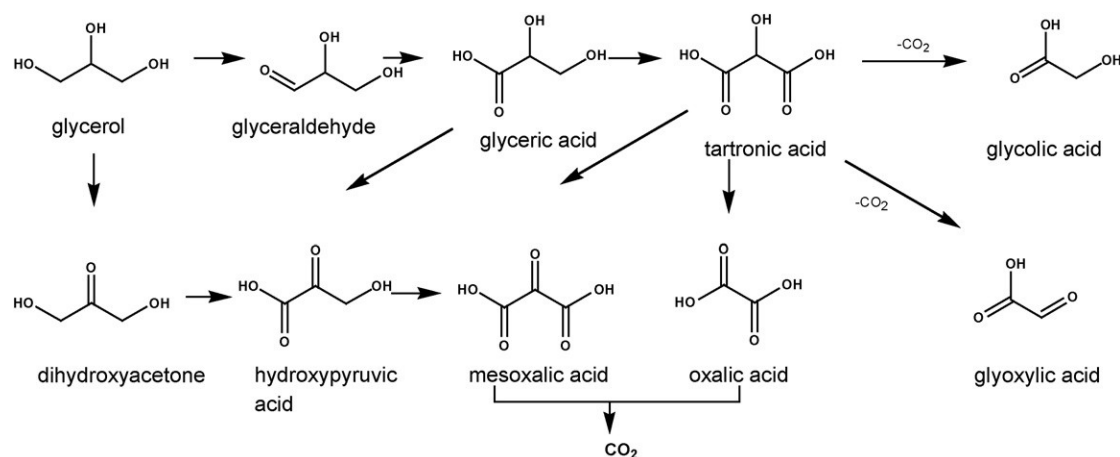
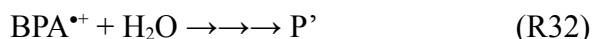
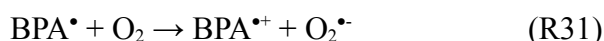


Figure D-64 oxidation pathway of glycerol in the presence of adequate •OH radicals [324]

Besides the similar pathway presented in homogeneous system, there are some supplements not presented in Figure D-65 in heterogeneous system. The long chain products produced from 2-methylpentanedioic acid and nonanedioic acid may be generated from the fracture of one or two benzene rings intermediates and oxidized by •OH radicals. Torres et al [310] reported that the UV irradiation can induce BPA degradation through photodecomposition or photooxidation as following reaction:



Zhou et al [325] reported the production of BPA-*o*-catechol in BPA degradation, which was analyzed by LC-MS. The two H atoms on the hydroxyl group of catechol are extracted by hydroxyl radicals in two separate steps producing BPA-semiquinone and BPA-*o*-quinone, respectively. According to Sorokin et al [326] the oxidation of BPA-*o*-quinone might undergo benzene ring cleavage to produce binary carboxylic acid up to mineralization. Although in our research BPA-*o*-quinone and BPA-semiquinone or BPA-*o*-quinone could not be detected, we could assume that the proposed pathway initiated by BPA-*o*-catechol took place, since long chain binary carboxylic acid such as 2-methylpentanedioic acid and nonanedioic acid was found in the system, which could be proposed to be generated from the benzene ring cleavage of BPA-semiquinone or BPA-*o*-quinone. And these long chain binary carboxylic acids would be further oxidized.



In Fact, in heterogeneous photo-Fenton system, the possible pathways of BPA degradation are much more complicated than in homogeneous system, since the reaction may take place both in liquid phase and on the surface of iron oxides, and the presence of EDDS may influence the whole pathway.

D-5-3. Conclusion

As it is achieved from above, the main pathway of BPA degradation in Fenton and photo-Fenton system is firstly the disconnection between two benzene rings, then the ring cleavage of benzene ring through some intermediates, and the intermediates such as glycol and glycerol was also found, finally some small molecule products are produced like CO₂ and H₂O. In homogeneous system, only one possible pathway of BPA degradation was proposed according to our research, whereas in heterogeneous photo-Fenton system, two possible pathways were proposed. More specific work on the BPA degradation pathway in our systems is needed in the future.

E. Conclusion

In this work, we tried to exam the effect of Fe(III)-EDDS in homogeneous and heterogeneous Fenton and photo-Fenton systems. The efficiency of BPA degradation and $\bullet\text{OH}$ radicals generation was detected respectively, and the effect of several variables such as pH values, H_2O_2 concentration, complex concentration and iron oxide dosage was checked.

First of all, the use of Fe(III)-EDDS complex as iron source in the Fenton process was detected. The main positive effect of Fe(III)-EDDS complex is the fact that Fe(III)-EDDS into Fenton reaction can extend and strongly improve the degradation of BPA at neutral and alkaline pH. The first important role of EDDS is the stabilization of Fe(III) in a large range of pH (3 to 9) preventing its precipitation. The increase of H_2O_2 and Fe(III)-EDDS concentrations leads to a higher efficiency of BPA degradation. However, beyond a certain concentration the competition of OH radical reactivity between BPA and H_2O_2 or Fe(III)-EDDS is detrimental for the efficiency of the process. The effect of oxygen was also determined and it was shown that oxygen is an important parameter for the oxidation of BPA. The experiments performed at different pH demonstrated that pH is an influent parameter. As a contrary, of a classical Fenton process using iron ions, the efficiency is much higher at near neutral and slightly basic pH than in acidic pH. This effect is due to the presence of $\text{HO}_2\bullet$ or $\text{O}_2^{\bullet-}$ as a function of pH ($\text{pK}_a = 4.86$). The formation and the role of two main radical species ($\bullet\text{OH}$ and $\text{HO}_2\bullet/\text{O}_2^{\bullet-}$) involved in such system were demonstrated. The hydroxyl radical is mainly responsible of organic compound (BPA) degradation but its formation is strongly dependant of the presence of superoxide radical anion ($\text{O}_2^{\bullet-}$). Indeed, the presence of this radical species accelerates the cycling between Fe(III) and Fe(II), avoid the decomposition of H_2O_2 for the reduction of Fe(III) species and so increase the production of $\bullet\text{OH}$ radical. For the first time, the results of this study demonstrate that the reduction of Fe(III)-EDDS by superoxide radical anion is a crucial reaction which govern the efficiency of the Fenton process involving iron complexes. These results are very

encouraging for the application of the Fenton process under conditions of pH closer natural conditions encountered in the environment.

Secondly, the effect of Fe(III)-EDDS complex in photo-Fenton process is evaluated. The main focus is on $\bullet\text{OH}$ radical formation and BPA degradation. It is found that Fe(III)-EDDS complex has significantly positive efficiency on both $\bullet\text{OH}$ radical formation and BPA degradation in photo-Fenton system at neutral pH. This is mainly due to the presence of EDDS that can stabilize Fe(III) in aqueous solution between pH 3-9, preventing its precipitation. In the experiments, the increase of H_2O_2 and Fe(III)-EDDS complex concentrations can enhance the degradation rate of BPA. However, when the concentrations of Fe(III)-EDDS and/or H_2O_2 are too high, a competition for the reactivity of $\bullet\text{OH}$ is observed between BPA and Fe(II)-EDDS or H_2O_2 and so degradation of BPA is lower. The experiments performed at different pHs demonstrated that BPA can be efficiently degraded in this photo-Fenton system at acidic, neutral and alkaline pH, which means that the addition of EDDS can widen the applicable pH range of photo-Fenton system. The effect of oxygen was also determined and it was shown that oxygen is an important parameter for the oxidation of BPA. From the results detecting $\bullet\text{OH}$ radical formation, it can be concluded that the addition of EDDS can enhance the production of $\bullet\text{OH}$ radical, and hence enhance the degradation of BPA. The very positive results of this research work are interesting for water treatment processes. They demonstrate the high efficiency of photo-Fenton process using Fe(III)-EDDS as iron source with lower complex and H_2O_2 concentrations in wider pH range, which is very encouraging for the application of the photo-Fenton process under neutral pH conditions encountered in natural aquatic environment.

Thirdly, the effect of EDDS on heterogeneous Fenton and photo-Fenton process was evaluated. It could be concluded that in heterogeneous Fenton system using goethite, the presence of EDDS would totally inhibit the degradation of BPA and the generation of $\bullet\text{OH}$ radical at pH 6.2 and 3.7. This inhibition could be expressed by the strong adsorption of EDDS onto the goethite surface, and hence the interaction between H_2O_2 and goethite was blocked. Then, in heterogeneous photo-Fenton system, the effect of EDDS on BPA degradation at pH 6.2 largely depended on the condition of H_2O_2 concentration. When low

concentration of H_2O_2 was used, the addition of EDDS would enhance the efficiency of BPA degradation in this photo-Fenton system, whereas when the concentration of H_2O_2 enhanced, the positive effect weakened, and finally converted to negative effect while the concentration was higher than 1mmol/L. This complicate effect could be preliminarily explained by the effect of EDDS on the H_2O_2 decomposition. The optimum condition for BPA degradation in photo-Fenton process in the presence of EDDS was investigated. And effective BPA degradation at pH 6.2 in the presence of 0.25g/L goethite, 0.1mmol/L H_2O_2 and 0.1 mmol/L EDDS was achieved.

Finally, the products of BPA degradation in homogeneous and heterogeneous systems were detected respectively. It is found that BPA degradation in homogeneous system was initiated from the disconnection between two benzene rings, then a sequence of reactions followed and the degradation of BPA achieved. Whereas in heterogeneous system, besides the same scheme in homogeneous system, there is another possible degradation pathway proposed.

Reference

- [1] F. Wu, N. Deng, Y. Zuo, 1999, Photochemical properties of ferricoxalate complexes and their effects on photodegradation of organic compounds in natural aqueous phase. *Advances in Environmental Science*, 7(2), 78-91. (Chinese version)
- [2] Y. Zuo, 1994, Light-induced oxidation of bisulfite-aldehyde adducts in real fog water. *Naturwissenschaften*, 81, 505-507.
- [3] A. Kotronarou, L. Sigg, 1993, Sulfur dioxide oxidation in atmospheric water: role of iron(II) and effect of ligands. *Environ. Sci. Technol.*, 27, 2725-2735.
- [4] J. W. Munger, D. J. Jacob, J. M. Waldman, M. R. Hoffmann, 1983, Fogwater chemistry in an urban atmosphere. *J. Geophys. Res.*, 88, 5109-5121.
- [5] S. Fuzzi, G. Orsi, G. Nardini, et al., 1988, Heterogeneous processes in the Po Valley radiation fog. *J. Geophys. Res.*, 93, 11141-11151.
- [6] A. G. Clark, M. Radojevic, 1987, Oxidation of SO₂ in rainwater and its role in acid rain chemistry. *Atmos. Environ.*, 21, 1115-1123.
- [7] F. Joos, U. Baltensperger, 1991, A field study on chemistry S(IV) oxidation rates and vertical transport during fog conditions. *Atmos. Environ.*, 25A, 217-230.
- [8] J. Hamilton-Taylor, M. Willis, 1990, A quantitative assessment of the sources and general dynamics of trace metals in a soft-water lake. *Limnol. Oceanogr.*, 35, 840-851.
- [9] U. Forstner, G. T. W. Wittmann, 1979, Metal pollution in the aquatic environment. Berlin; New York, Springer-Verlag.
- [10] R. Gachter, J. S. Meyer, A. Mares, 1988, Contribution of Bacteria to Release and Fixation of Phosphorus in Lake Sediments. *Limnol. Oceanogr.*, 33, 1542-1558.
- [11] K. Kawamura, A. Nissenbaum, 1992, High abundance of low molecular weight organic acids in hypersaline spring water associated with a salt diaper. *Org. Geochem.*, 18, 469-476.
- [12] T.E. Graedel, M.L. Mandich, C.J. Weschler, 1986, Kinetic Model Studies of Atmospheric Droplet Chemistry 2. Homogeneous Transition Metal Chemistry in Raindrops. *J. Geophys. Res.*, 91, 5205-5221.

- [13] Z. Yi, G. Zhuang, J. R. Brown, R. A. Duce, 1992, High-Performance Liquid Chromatographic Method for the Determination of Ultratrace Amounts of Iron(II) in Aerosols, Rainwater, and Seawater. *Anal. Chem.*, 64, 2826-2830.
- [14] L. J. Spokes, T. D. Jickells, 1996, Factors Controlling the Solubility of Aerosol Trace Metals in the Atmosphere and on Mixing into Seawater. *Aquatic Geochemistry*, 1, 355-374.
- [15] R. R. Haese, I. K. Wallmann, A. Dahmke, U. Kretzmann, I. P. J. Muller, H. D. Schulz, 1997, Iron species determination to investigate early diagenetic reactivity in marine sediments. *Geochim. Cosmochim. Acta*, 61, 63-72.
- [16] Z. Peng, 2008, Algae, Humic acid and Ferric Ions-induced Photodegradation of Phenolic Substances and the Mechanism. Ph.D thesis, Wuhan University. (Chinese version)
- [17] C. M. Flynn, 1984, Hydrolysis of inorganic iron(III) salts. *Chem. Rev.*, 84 (1), 31-41.
- [18] B.C. Faust, J. Hoigne, 1990, Photolysis of Fe (III)-hydroxy complexes as sources of OH radicals in clouds, fog and rain. *Atmos. Environ.*, 24, 79-89.
- [19] C.J. Weschler, M.L. Mandich, T.E. Graedel, 1986, Speciation, photosensitivity, and reactions of transition metal ions in atmospheric droplets. *J. Geophys. Res. D: Atmos.*, 91, 5189-5204.
- [20] E.M. Thurman, 1985, *Inorganic Geochemistry of Natural Waters*. Dr. W. Junk Martinus Nijhoff: Dordrecht, 88-295.
- [21] N. Deng, F. Wu, 2003, *Environmental Photochemistry*. Beijing: Chemical Industry Press. (Chinese Version)
- [22] W. Stumm, J.J. Morgan, 1981, *Aquatic Chemistry*, 2nd Edition. Wiley, New York.
- [23] T. Sinner, 1994, Mikroanalytische Charakterisierung atmosphärischer Proben mit besonderer Berücksichtigung der Bestimmung der verschiedenen Oxidationsstufen des Eisen. Doctoral thesis, Darmstadt.
- [24] M. Pourbaix, 1963, *Atlas d'équilibres électrochimiques*. Gauthier-Villars, Paris.
- [25] P. Warneck, 1988, *Chemistry of the Natural Atmosphere*. Academic Press, San Diego.
- [26] P. Hoffmann, A. N. Dedik, J. Ensling, S. Weinbruch, S. Weber, T. Sinner, P. Gütlich, H. M. Ortner, 1996, Speciation of Iron in Atmospheric Aerosol Sample. *J. Aerosol. Sci.*, 27 (2), 325-337.
- [27] C.F. Wells, M.A. Salam, 1966, Complex formation between Fe(II) and inorganic

anions. *Trans. Faraday. Soc.*, 63, 620.

[28] F.A. Cotton, G. Wilkinson, 1972, *Advanced Inorganic Chemistry*, 3rd Edition. Interscience Publishers, New York.

[29] P. Warneck, 1991, Chemical reactions in clouds. *Fresenius. J. Anal. Chem.*, 340, 585.

[30] H.J. Benkelberg, P. Warneck, 1995, Photodecomposition of iron (III) hydroxo and sulfato complexes in aqueous solution: wavelength dependence of OH and quantum yields. *J. Phys. Chem.*, 99, 5214–5221.

[31] G. Mailhot, M. Sarakha, B. Lavédrine, J. Cáceres, S. Malato, 2002, Fe(III)-solar light induced degradation of diethyl phthalate (DEP) in aqueous solutions. *Chemosphere*, 49, 525–535.

[32] P. Mazellier, G. Mailhot, M. Bolte, 1997, Photochemical behavior of the iron(III)/2,6-dimethylphenol system. *New. J. Chem.*, 21, 389–397.

[33] P. Mazellier, J. Jirkovsky, M. Bolte, 1997, Degradation of diuron photoinduced by iron(III) in aqueous solution. *Pestic. Sci.*, 49, 259-267.

[34] N. Brand, G. Mailhot, M. Bolte, 1997, Degradation and photodegradation of tetraacetythylenediamine (TAED) in the presence of iron (III) in aqueous solution. *Chemosphere*, 34, 2637-2648.

[35] N. Brand, G. Mailhot, M. Bolte, 1998, Degradation Photoinduced by Fe(III): Method of Alkylphenol Ethoxylates Removal in Water. *Environ. Sci. Technol.*, 32, 2715-2720.

[36] N. Brand, G. Mailhot, M. Bolte, 2000, The interaction “light, Fe(III)” as a tool for pollutant removal in aqueous solution: degradation of alcohol ethoxylates. *Chemosphere*, 40, 395-401.

[37] O. Bajt, G. Mailhot, M. Bolte, 2001, Degradation of dibutyl phthalate by homogeneous photocatalysis with Fe(III) in aqueous solution. *Appl. Catal. B: Environ.*, 33, 239-248.

[38] C. Catastini, M. Sarakha, G. Mailhot, M. Bolte, 2002, Iron (III) aquacomplexes as effective photocatalysts for the degradation of pesticides in homogeneous aqueous solutions. *Sci. Total Environ.*, 298, 219-228.

[39] H. Měšt'ánková, G. Mailhota, J. Pilichowskia, J. Krýsab, J. Jirkovskýc, M. Bolte, 2004, Mineralisation of Monuron photoinduced by Fe(III) in aqueous solution. *Chemosphere*, 57, 1307-1315.

- [40] E. M. Thurman, 1985, *Organic Geochemistry of Natural Waters*; Martinus Nijhoff, Dr. W. Junk Dordrecht, 88-92, 295-299.
- [41] E. M. Perdue, E. T. Gjessing, 1990, *Organic Acids in Aquatic Ecosystems*. Wiley: New York.
- [42] B.C. Faust, R.G. Zepp, 1993, Photochemistry of Aqueous Iron(III)-Polycarboxylate Complexes: Roles in the Chemistry of Atmospheric and Surface Waters. *Environ. Sci. Technol.*, 27, 2517-2522.
- [43] K. Kawamura, S. Steinberg, I.R. Kaplan, 1985, Capillary GC determination of short-chain dicarboxylic acids in rain, fog, and mist. *Int. J. Environ. Anal. Chem.*, 19, 175-188.
- [44] A. Plewka, T. Gnauk, E. Brüggemann, H. Herrmann, 2006, Biogenic contributions to the chemical composition of airborne particles in a coniferous forest in Germany. *Atmos. Environ.*, 40, 103-115.
- [45] A. Marinoni, P. Laj, K. Sellegri, G. Mailhot, 2004, Cloud chemistry at the Puy de Dôme: variability and relationships with environmental factors. *Atmos. Chem. Phys.*, 4, 715-728.
- [46] M. Löflund, A. Kasper-Giebl, B. Schuster, H. Giebl, R. Hitzenberger, H. Puxbaum, 2002, Formic, acetic, oxalic, malonic and succinic acid concentrations and their contribution to organic carbon in cloud water. *Atmos. Environ.*, 36, 1553-1558.
- [47] D. Panias, M. Taxiarchou, I. Paspaliaris, A. Kontopoulos, 1996, Mechanisms of dissolution of iron oxides in aqueous oxalic acid solutions. *Hydrometallurgy*, 42, 257-265.
- [48] R.B. Martin, 1986, Citrate binding of Al^{3+} and Fe^{3+} . *J. Inorg. Biochem.*, 28, 181-187.
- [49] J.L. Pierre, I. Gautier-Luneau, 2000, Iron and citric acid: A fuzzy chemistry of ubiquitous biological relevance. *Bio. Metals.*, 13, 91-96.
- [50] Y. Zuo, J. Holgne, 1992, Formation of Hydrogen Peroxide and Depletion of Oxalic Acid in Atmospheric Water by Photolysis of Iron(III)-Oxalato Complexes. *Environ. Sci. Technol.*, 26, 1014-1022.
- [51] S.M. Hyde, P.M. Wood, 1997, A mechanism for production of hydroxyl radicals by the brown-rot fungus *Coniophora puteana*: Fe(III) reduction by cellobiose dehydrogenase and Fe(II) oxidation at a distance from the hyphae. *Microbiology*, 143, 259-266.
- [52] H.B. Abrahamson, A.B. Rezvani, J.G. Brushmiller, 1994, Photochemical and

spectroscopic studies of complexes, of iron(III) with citric acid and other carboxylic acids. *Inorg. Chim. Acta*, 226, 117-127.

[53] Y. Zu, J. Hoigné, 1993, Evidence for photochemical formation of H₂O₂ and oxidation of SO₂ in authentic fog water. *Science*, 260, 071-73.

[54] F.Wu, 2003, Study on photodegradation of environmental endocrine disruptors in the Fe(III)-oxalate complexes system. Ph.D thesis, Wuhan University. (Chinese version)

[55] D.Zhou, F.Wu, N.Deng, 2004, Fe(III)-oxalate complexes induced photooxidation of diethylstilbestrol in water. *Chemosphere*, 57, 283-291.

[56] S.J. Hug, H.-U. Laubscher, 1997, Iron(III) Catalyzed Photochemical Reduction of Chromium(VI) by Oxalate and Citrate in Aqueous Solutions. *Environ Sci. Technol.* 31, 160-170.

[57] M. Bucheli-Witschel, T. Egli, 2001, Environmental fate and microbial degradation of aminopolycarboxylic acids. *FEMS Microbiol. Rev.*, 25, 69-106.

[58] A.C. Alder, H. Siegrist, W. Gujer, W. Giger, 1990, Behaviour of NTA and EDTA in biological wastewater treatment. *Water. Res.*, 24, 733-742.

[59] F.G. Kari, W. Giger, 1996, Speciation and fate of ethylenediaminetetraacetate (EDTA) in municipal wastewater treatment. *Water Res.*, 30, 122-134.

[60] A.C. Alder, H. Siegrist, K. Fent, T. Egli, E. Molnar, T. Poiger, C. Schaïner, W. Giger, 1997, The fate of organic pollutants in wastewater and sludge treatment: Significant processes and impact of compound properties. *Chimia*, 51, 922-928.

[61] K. Wolf, P.A. Gilbert, 1992, EDTA-ethylenediaminetetraacetic acid. In: *The Handbook of Environmental Chemistry*, Vol. 3 (Hutzinger, O., Ed.), 241-259. Springer, Berlin.

[62] R. Klopp, B. Patsch, 1994, Organische Komplexbildner in Abwasser, Oberflächenwasser und Trinkwasser, dargestellt am Beispiel der Ruhr. *Wasser Boden*, 8, 32-37.

[63] J.P. Houriet, 1996, NTA dans les eaux. *Cahier de l'environnement* 264. Office federal de l'environnement, des forets et du paysage (OFEFP), Bern.

[64] C.F. Bell, 1977, Principles and Applications of Metal Chelation. Clarendon Press, Oxford.

[65] G. Wilkinson, 1987, Comprehensive Coordination Chemistry. Pergamon Press,

Oxford.

- [66] T. Trott, R.W. Henwood, C.H. Langford, 1972, Sunlight photochemistry of ferric nitrilotriacetate complexes. *Environ. Sci. Technol.*, 6 (4), 367-368.
- [67] R.J. Stolzberg, D.N. Hume, 1975, Rapid formation of iminodiacetate from photochemical degradation of iron(III) nitrilotriacetate solutions. *Environ. Sci. Technol.*, 9 (7), 654-656.
- [68] R.L. Anderson, W.E. Bishop, R.L. Campbell, 1985, A review of the environmental and mammalian toxicology of nitrilotriacetic acid. *Crit. Rev. Toxicol.*, 15(1), 1-102.
- [69] P. Natarajan, J.F. Endicott, 1973, Photoredox behavior of transition metal-ethylenediaminetetraacetate complexes. A comparison of some group VIII metals. *J. Phys. Chem.*, 77, 2049-2054.
- [70] A. Svenson, L. Kaj, H. Bjorndal, 1989, Aqueous photolysis of the iron(III) complexes of NTA, EDTA and DTPA. *Chemosphere*, 18, 1805-1808.
- [71] R. Frank, H. Rau, 1989, Photochemical transformation in aqueous solution and possible environmental fate of ethylenediaminetetraacetic acid (EDTA). *Ecotox. Environ. Saf.*, 19, 55-63.
- [72] F.G. Kari, S. Hilger, S. Canonica, 1995, Determination of the reaction quantum yield for the photochemical degradation of Fe(III)-EDTA: Implications for the environmental fate of EDTA in surface waters. *Environ. Sci. Technol.*, 29, 1008-1017.
- [73] P. Kocot, A. Karocki, Z. Stasicka, 2006, Photochemistry of the Fe(III)-EDTA complexes A mechanistic study. *J. Photochem. Photobiol. A*, 179, 176-183.
- [74] E. Graf, J. R. Mahoney, R. G. Bryan, J. W. Eaton, 1984, Iron-catalyzed hydroxyl radical formation. Stringent requirement for free iron coordination site. *J. Biol. Chem.*, 259, 3620-3624.
- [75] B.H.J. Bielski, D.E. Cabelli, L.R. Arudi, A.B. Ross, 1985, Reactivity of HO₂/O₂-radicals in aqueous solution. *J. Phys. Chem. Ref. Data*, 14, 1041-1100.
- [76] C. E. Noradoun, C. S. Mekmaysy, R. M. Hutcheson, I. F. Cheng, 2005, Detoxification of malathion a chemical warfare agent analog using oxygen activation at room temperature and pressure. *Green Chem.*, 7, 426-430.
- [77] T. Zhou, Y. Li, F. Wong, X. Lu, 2008, Enhanced degradation of 2, 4-dichlorophenol by

ultrasound in a new Fenton like system (Fe/EDTA) at ambient circumstance. *Ultrason. Sonochem.*, 15, 782-790.

[78] C.E. Noradoun, M.D. Engelmann, M. McLaughlin, R. Hutcheson, K. Breen, A. Paszczynski, I.F. Cheng, 2003, Destruction of Chlorinated Phenols by Dioxygen Activation under Aqueous Room Temperature and Pressure Conditions. *Ind. Eng. Chem. Res.*, 42, 5024–5030.

[79] J.D. Englehardt, D.E. Meeroff, L. Echegoyen, Y. Deng, F.M. Raymo, T. Shibata, 2007, Oxidation of Aqueous EDTA and Associated Organics and Coprecipitation of Inorganics by Ambient Iron-Mediated Aeration. *Environ. Sci. Technol.*, 41, 270-276.

[80] S. Metsarinne, T. Tuhkanen, R. Aksela, 2001, Photodegradation of ethylenediaminetetraacetic acid (EDTA) and ethylenediamine disuccinic acid (EDDS) within natural UV radiation range. *Chemosphere*, 45, 949-955.

[81] Y.H. Dao, J. De Laat, 2011, Effect of some parameters on the rate of the catalysed decomposition of hydrogen peroxide by iron(III)-nitrilotriacetate in water. *Water Res.*, 45, 3309-3317.

[82] C. Lee, D.L. Sedlak, 2009, A novel homogeneous Fenton-like system with Fe(III)–phosphotungstate for oxidation of organic compounds at neutral pH values. *J. Mol. Catal. A: Chem.*, 311, 1-6.

[83] S. Tandy, A. Ammann, R. Schulin, B. Nowack, 2006, Biodegradation and speciation of residual SS-ethylenediaminedisuccinic acid (EDDS) in soil solution left after soil washing. *Environ. Poll.*, 142 (2), 191–199.

[84] D. Schowanek¹, T.C.J. Feijtel, C.M. Perkins, F.A. Hartman, T.W. Federle, R.J. Larson, 1997, Biodegradation of [S,S], [R,R] and mixed stereoisomers of Ethylene Diamine Disuccinic Acid (EDDS), a transition metal chelator. *Chemosphere*, 34, 2375–2391.

[85] P.C. Vandevivere, H. Saveyn, W. Verstraete, T.C. J. Feijtel, D.R. Schowanek, 2001, Biodegradation of Metal–[S,S]-EDDS Complexes. *Environ. Sci. Technol.*, 35 (9), 1765–1770.

[86] J.Li, 17 β -estradiol degradation photoinduced by iron complex, clay and iron oxide minerals: effect of the iron complexing agent ethylenediamine-n,n'-disuccinic acid. PhD thesis, no DU 1925, Université Blaise Pascal, Clermont-Ferrand (France).

- [87] V. Nagaraju, T. Goje, A.M. Crouch, 2007, Determination of Copper and Iron Using [S, S']-Ethylenediaminedisuccinic Acid as a Chelating Agent in Wood Pulp by Capillary Electrophoresis. *Anal. Sci.*, 23, 493-496.
- [88] L. Zhang, Z. Zhu, R. Zhang, C. Zheng, H. Zhang, Y. Qiu, J. Zhao, 2008, Extraction of copper from sewage sludge using biodegradable chelant EDDS. *J. Environ. Sci.* 20, 970-974.
- [89] Zhang C.B., Photodegradation of organic pollutants induced by iron-carboxylate complexes in aqueous solutions, PhD thesis, no DU 1925, Université Blaise Pascal, Clermont-Ferrand (France).
- [90] F. Pavelčík, J. Majer, 1978, The crystal and molecular structure of lithium [(S,S)-N,N'-ethylenediaminedisuccinato]cobaltate(III) trihydrate. *Acta Crystallogr. B*, 34, 3582–3585.
- [91] M. Oramaa, H. Hyvönena, H. Saarinen, R. Aksela, 2002, Complexation of [S,S] and mixed stereoisomers of N,N'-ethylenediaminedisuccinic acid (EDDS) with Fe(III), Cu(II), Zn(II) and Mn(II) ions in aqueous solution. *J. Chem. Soc., Dalton Trans.*, 4644-4648.
- [92] J. Li, G. Mailhot, F. Wu, N. Deng, 2010, Photochemical efficiency of Fe(III)-EDDS complex: OH radical production and 17 β -estradiol degradation. *J. Photochem. Photobiol., A* 212, 1-7.
- [93] R.M. Cornell, U. Schwertmann, 2003, The iron oxides: structure, properties, reactions, occurrences and uses. Wiley VCH.
- [94] http://minerals.usgs.gov/minerals/pubs/commodity/iron_oxide/
- [95] U. Schwertmann, R.M. Cornell, 1991, Iron oxides in the laboratory, V.C.H. Publisher, p137.
- [96] http://en.wikipedia.org/wiki/Iron_oxide#cite_note-cor-0
- [97] J.K. Leland, A. J. Bard, 1987, Photochemistry of colloidal semiconducting iron oxide polymorphs. *J. Phys. Chem.*, 91 (19), 5076–5083.
- [98] P. Mazellier, M. Bolte, 2000, Heterogeneous light-induced transformation of 2,6-dimethylphenol in aqueous suspensions containing goethite. *J. Photochem. Photobiol. A*, 132, 129-135.
- [99] A.G. B. Williams, M.M. Scherer, 2004, Spectroscopic Evidence for Fe(II)–Fe(III) Electron Transfer at the Iron Oxide–Water Interface. *Environ. Sci. Technol.*, 38, 4782–

4790.

- [100] W. Stumm, 1992, Chemistry of the solid-water interface, John Wiley and Sons: New York, 13-41.
- [101] H.H. Huang, M.C. Lu, J.N. Chen, 2001, Catalytic Decomposition of Hydrogen Peroxide and 2-chlorophenol with iron oxides. Water Res., 35, 2291–2299.
- [102] <http://en.wikipedia.org/wiki/Goethite>
- [103] C.S. Hurlbut, K. Cornelis, 1985, Manual of Mineralogy (20th ed.). Wiley.
- [104] <http://www.galleries.com/minerals/oxides/goethite/goethite.htm>
- [105] <http://webmineral.com/data/Goethite.shtml>
- [106] <http://www.mindat.org/min-1719.html>
- [107] M. Kosmulski, 1997, Attempt to determine pristine points of zero charge of Nb₂O₅, Ta₂O₅ and HfO₂. Langmuir, 13, 6315-6320.
- [108] M. Kosmulski, 2001, Chemical Properties of Material Surfaces. Marcel Dekker, New York.
- [109] G.A. Parks, 1965, The isoelectric points of solid oxides, solid hydroxides, and aqueous hydroxo complex systems. Chem. Rev., 65, 177-198.
- [110] T. Hiemstra, J.C.M. de Wit, W.H. van Riemsdijk, 1989, Multisite proton adsorption modeling at the solid/solution interface of (hydr)oxides: a new approach. II. Application to various important (hydr)oxides. J. Colloid Interf. Sci., 133, 105-117.
- [111] K. Parida, J. Das, 1996, Studies on Ferric Oxide Hydroxides: II. Structural Properties of Goethite Samples (α -FeOOH) Prepared by Homogeneous Precipitation from Fe(NO₃)₃ Solution in the Presence of Sulfate Ions. J. Colloid Interface Sci., 178, 586-593.
- [112] C. Domingo, R. Rodríguez-Clemente, 1993, Nature and reactivity of intermediates in the auto-oxidation of iron (II) in aqueous acid media. Solid State Ionics, 59, 187-195.
- [113] H. Dong, R.K. Kukkadapu, J.K. Fredrickson, J.M. Zachara, D.W. Kennedy, H.M. Kostandarithes, 2003, Microbial Reduction of Structural Fe(III) in Illite and Goethite. Environ. Sci. Technol., 37 (7), 1268–1276.
- [114] B. Nowack, L. Sigg, 1996, Adsorption of EDTA and metal-EDTA complexes onto goethite. J. Colloid Interface Sci., 177, 106-121.
- [115] B.A. Manning, S.E. Fendorf, S. Goldberg, 1998, Surface Structures and Stability of

Arsenic(III) on Goethite: Spectroscopic Evidence for Inner-Sphere Complexes. *Environ. Sci. Technol.*, 32 (16), 2383-2388.

[116] J.G. Wiederhold, S.M. Kraemer, N. Teutsch, P.M. Borer, A.N. Halliday, R. Kretzschmar, 2006, Iron Isotope Fractionation during Proton-Promoted, Ligand-Controlled, and Reductive Dissolution of Goethite. *Environ. Sci. Technol.*, 40, 3787-3793.

[117] S.S. Lin, M.D. Gurol, 1998, Catalytic Decomposition of Hydrogen Peroxide on Iron Oxide: Kinetics, Mechanism, and Implications. *Environ. Sci. Technol.*, 32, 1417-1423.

[118] E.G. Garrido-Ramírez, B.K.G Theng, M.L. Mora, 2010, Clays and oxide minerals as catalysts and nanocatalysts in Fenton-like reactions — A review. *Applied Clay Sci.*, 47, 182-192.

[119] J. X. Ravikumar, M. D. Gurol, 1994, Chemical oxidation of chlorinated organics by hydrogen peroxide in the presence of sand. *Environ. Sci. Technol.*, 28, 394-400.

[120] S. H. Kong, R. J. Watts, J. H. Choi, 1998, Treatment of petroleum-contaminated soils using iron mineral catalyzed hydrogen peroxide. *Chemosphere*, 37, 1473-1482.

[121] R. L. Valentine, H. C. A. Wang, 1998, Iron oxide surface catalyzed oxidation of quinoline by hydrogen peroxide. *J. Environ. Eng.*, 124, 31-38.

[122] D.M. Sherman, 2005, Electronic structures of iron(III) and manganese(IV) (hydr)oxide minerals: Thermodynamics of photochemical reductive dissolution in aquatic environments. *Geoch. Cosmochim. Acta*, 69, 3249-3255.

[123] M. A. Blesa, A. E. Regazzoni, A. J. G. Maroto, 1988, Reactions of Metal Oxides with Aqueous Solutions. *Mater. Sci. Forum*, 29, 31-98.

[124] M. I. Litter, E.C. Baumgartner, G.A. Urrutia, M.A. Blesa, 1991, Photodissolution of iron oxides. 3. Interplay of photochemical and thermal processes in maghemite/carboxylic acid systems. *Environ. Sci. Technol.*, 25, 1907-1913.

[125] B. Sulzberger, 1990, Photoredox reactions at hydrous metal oxide surfaces: A surface coordination chemistry approach, in W. Stumm, Ed., *Aquatic Chemical Kinetics*, Wiley, New York, 401-429.

[126] B. Sulzberger, D. Suter, C. Siffert, S. Banwart, W. Stumm, 1989, Dissolution of Fe(III)(hydr) oxides in natural waters; laboratory assessment on the kinetics controlled by surface coordination. *Mar. Chem.* 28, 127-144.

- [127] E. B. Borghi, A. E. Regazzoni, A. J. G. Maroto, M. A. J. Blesa, 1989, Reductive dissolution of magnetite by solutions containing EDTA and FeII. *Colloid Interface Sci.* 130, 299-310.
- [128] B.C. Faust, M.R. Hoffmann, 1986, Photoinduced Reductive Dissolution of α -Fe₂O₃ by Bisulfite. *Environ. Sci. Technol.*, 20, 943-948.
- [129] R. M. Cornell, P. W. Schindler, 1987, Photochemical dissolution of Goethite in acid/oxalate solution. *Clays Clay Miner.*, 35, 347-352.
- [130] F. Wu, N. Deng, 2000, Photochemistry of hydrolytic iron (III) species and photoinduced degradation of organic compounds. A minireview. *Chemosphere*, 41, 1137-1147.
- [131] B. Gu, J. Schmitt, Z. Chen, L. Liang, J.F. McCarthy, 1994, Adsorption and desorption of natural organic matter on iron oxide: mechanisms and models. *Environ. Sci. Technol.*, 28 (1), 38-46.
- [132] K. Noren, J.S. Loring, J.R. Bargar, P. Persson, 2009, Adsorption Mechanisms of EDTA at the Water-Iron Oxide Interface: Implications for Dissolution. *J. Phys. Chem.*, 113, 7762-7771.
- [133] C. Pulgarin, J. Kiwi, 1995, Iron Oxide-Mediated Degradation, Photodegradation, and Biodegradation of Aminophenols. *Langmuir*, 11, 519-526.
- [134] S.O. Pehkonen, R.L. Siefert, M.R. Hoffmann, 1995, Photoreduction of Iron Oxyhydroxides and the Photooxidation of Halogenated Acetic Acids. *Environ. Sci. Technol.*, 29, 1215-1222.
- [135] J. Lei, C. Liu, F. Li, X. Li, S. Zhou, T. Liu, M. Gu, Q. Wu, 2006, Photodegradation of orange I in the heterogeneous iron oxide-oxalate complex system under UVA irradiation. *J. Hazard. Mater.*, 137, 1016-1024.
- [136] F.B. Li, X.Z. Li, X.M. Li, T.X. Liu, J. Dong, 2007, Heterogeneous photodegradation of bisphenol A with iron oxides and oxalate in aqueous solution. *J. Colloid Interf Sci.*, 311, 481-490.
- [137] P.Mazellier, B. Sulzberger, 2001, Diuron Degradation in Irradiated, Heterogeneous Iron/Oxalate Systems: The Rate-Determining Step. *Environ. Sci. Technol.*, 35, 3314-3320.
- [138] M.A. Fox, M.T. Dulay, 1993, Heterogeneous photocatalysis. *Chem. Rev.*, 93, 341-

351.

- [139] P.R. Gogate, S. Mujumdar, A.B. Pandit, 2002, A sonophotochemical reactor for the removal of formic acid from wastewater. *Ind. Eng. Chem. Res.*, 41, 3370-3378.
- [140] W.H. Glaze, F. Beltran, T. Tuhkanen, J.W. Kang, 1992. Chemical models of advanced oxidation processes. *Water. Pollut. Res.J. Can.*, 27, 23.
- [141] C. von Sonntag, 1996, Degradation of aromatics by advanced oxidation processes in water remediation: some basic considerations. *J. Water Supply Res. Tech.*, 45, 84-91.
- [142] J. Hoigne, 1997, Inter-calibration of OH radical sources and water quality parameters. *Water Sci. Technol.*, 35, 1-8.
- [143] J.J. Wu, M. Muruganandham, S.H. Chen, 2007, Degradation of DMSO by ozone-based advanced oxidation processes. *J. Hazard. Mater.*, 149, 218-225.
- [144] N.C. Shang, Y.H. Chen, H.W. Ma, C.W. Lee, C.H. Chang, Y.H. Yu, C.H. Lee. 2007, Oxidation of methyl methacrylate from semiconductor wastewater by O₃ and O₃/UV processes *J. Hazard. Mater.*, 147, 307-312
- [145] S. Irmak, O. Erbatur, A. Akgerman. 2005, Degradation of 17 β -estradiol and bisphenol A in aqueous medium by using ozone and ozone/UV techniques. *J. Hazard. Mater.*, 126, 54-62
- [146] S.N. Frank, A.J. Bard. 1977, Heterogeneous photocatalytic oxidation of cyanide and sulfite in aqueous solutions at semiconductor powders. *J. Phys. Chem.*, 81, 1484–1488
- [147] K. Tanaka, R.C.R. Calanag, T. Hisanaga. 1999, Photocatalyzed degradation of lignin on TiO₂. *J. Mol. Catal.*, 138, 287-294
- [148] J. Dzenzel, J. Theurich, D.W. Bahnemann, 1999, Formation of Nitroaromatic Compounds in Advanced Oxidation Processes: Photolysis versus Photocatalysis. *Environ. Sci. Technol.*, 33, 294-300
- [149] R. Andreozzi, V. Caprio, A. Insola, R. Marotta. 2000, The oxidation of metol (N-methyl-p-aminophenol) in aqueous solution by UV/H₂O₂ photolysis. *Water Res*, 34, 463-472
- [150] A. Lopez, B. Anna, M. Giuseppe, K. John, 2003, Kinetic investigation on UV and UV/H₂O₂ degradations of pharmaceutical intermediates in aqueous solution. *J. Photochem. Photobiol.*, 156, 121-126

- [151] D. Vogna, R. Marotta, R. Andreozzi, A. Napolitano, M. d'Ischia, 2004, Kinetic and chemical assessment of the UV/H₂O₂ treatment of antiepileptic drug carbamazepine. *Chemosphere*, 54, 497-505
- [152] Z.M. Li, P.J. Shea, S.D. Comfort, 1998, Nitrotoluene destruction by UV-catalyzed fenton oxidation. *Chemosphere*, 36, 1849-1865.
- [153] K. Lin, D. Yuan, M. Chen, Y. Deng, 2004, Kinetics and Products of Photo-Fenton Degradation of Triazophos, *J. Agric. Food Chem.*, 52, 7614-7620.
- [154] H. Kušić, N. Koprivanac, A.L. Božić, I. Selanec, 2006, Photo-assisted Fenton type processes for the degradation of phenol: A kinetic study. *J. Hazard. Mater.*, 136, 632-644.
- [155] J. Anotai, M.C. Lu, P. Chewprecha, 2006, Kinetics of aniline degradation by Fenton and electro-Fenton processes. *Water Res.*, 40 (9), 1841-1847
- [156] Wang-Ping Ting, Ming-Chun Lu, Yao-Hui Huang. 2009, Kinetics of 2,6-dimethylaniline degradation by electro-Fenton process. *J. Hazard. Mater.*, 161 (2-3), 1484-1490
- [157] N. Oturan, M. Zhou, M.A. Oturan, 2010, Metomyl Degradation by Electro-Fenton and Electro-Fenton-Like Processes: A Kinetics Study of the Effect of the Nature and Concentration of Some Transition Metal Ions As Catalyst. *J. Phys. Chem. A*, 114, 10605-10611
- [158] I. Peternel, N. Koprivanac, H. Kusic, 2006, UV-based processes for reactive azo dye mineralization. *Water Res.*, 40, 525-532
- [159] F. Han, V. Subba R. Kambala, M. Srinivasan, D. Rajarathnam, R. Naidu, 2009, Tailored titanium dioxide photocatalysts for the degradation of organic dyes in wastewater treatment: A review. *Appl. Catal. A: General*, 359, 25-40
- [160] E. Rosales, O. Iglesias, M. Pazos, M.A. Sanromán, 2012, Decolourisation of dyes under electro-Fenton process using Fe alginate gel beads. *J. Hazard. Mater.*, In Press
- [161] S.B. Abdelmelek, J. Greaves, K.P. Ishida, W.J. Cooper, W. Song, 2010, Removal of Pharmaceutical and Personal Care Products from Reverse Osmosis Retentate Using Advanced Oxidation Processes. *Environ. Sci. Technol.*, 45, 3665–3671
- [162] H. Shemer, Y. K. Kunukcu, K. G. Linden. 2006, Degradation of the pharmaceutical Metronidazole via UV, Fenton and photo-Fenton processes. *Chemosphere*, 63, 69-76

- [163] V. Homem, L. Santos. 2011, Degradation and removal methods of antibiotics from aqueous matrices – A review. *J. Environ. Manag.*, 92 , 2304-2347
- [164] I. Oller, S. Malato, J.A. Sánchez-Pérez, M.I. Maldonado, R. Gassó, 2007, Detoxification of wastewater containing five common pesticides by solar AOPs–biological coupled system. *Catal. Today*. 129, 69-78
- [165] E. Evgenidou, K. Fytianos. 2002, Photodegradation of Triazine Herbicides in Aqueous Solutions and Natural Waters. *J. Agric. Food Chem.* 50, 6423-6427
- [166] I. K. Konstantinou, T. M. Sakellarides, V. A. Sakkas, T. A. Albanis. 2001, Photocatalytic Degradation of Selected s-Triazine Herbicides and Organophosphorus Insecticides over Aqueous TiO₂ Suspensions. *Environ. Sci. Technol.*, 35, 398-405.
- [167] E.M.R. Rocha, V.J.P. Vilar, A. Fonseca, Isabel Saraiva, Rui A.R. Boaventura. 2011, Landfill leachate treatment by solar-driven AOPs. *Sol. Energy*, 85, 46-56
- [168] J.P. Scott, D.F.Ollis, 1995, Integration of chemical and biological oxidation processes for water treatment: review and recommendations. *Environ. Prog.*, 14, 88-103
- [169] J.P. Scott, D.F. Ollis, 1996, Engineering models of combined chemical and biological processes. *J. Environ. Eng.*, 122, 1110-1114.
- [170] J.P. Scott, D.F. Ollis. 1997, Integration of chemical and biological oxidation processes for water treatment: II. Recent illustrations and experiences. *J. Adv. Oxid. Tech.*, 2, 374-381.
- [171] I. Oller, S. Malato, J.A. Sánchez-Pérez, 2011, Combination of Advanced Oxidation Processes and biological treatments for wastewater decontamination—A review. *Sci.Total Environ.*, 409, 4141-4166.
- [172] C. Minero, E. Pelizzetti, S. Malato, J. Blanco, 1993, Large solar plant photocatalytic water decontamination: Degradation of pentachlorophenol. *Chemosphere*, 26, 2103-2119.
- [173] D. Bahnemann, 2004, Photocatalytic water treatment: solar energy application. *Sol. Energy.*, 77, 445-459.
- [174] S. Malato, J. Blanco, A. Vidal, C. Richter, 2002, Photocatalysis with solar energy at a pilot-plant scale: an overview. *Appl. Catal. B: Environ.*, 37, 1-15.
- [175] M.E.T. Sillanpää, T.A. Kurniawan, W. Lo, 2011, Degradation of chelating agents in aqueous solution using advanced oxidation process (AOP). *Chemosphere*, 83, 1443-1460.

- [176] R. Venkatadri, R.W. Peters, 1993, Chemical oxidation technology: ultraviolet light/hydrogen peroxide, Fenton's reagent and titanium dioxide-assisted photocatalysis. *Hazard. Waste Hazard.*, 10, 107-149.
- [177] B.H.J. Bielski, D.E. Cabelli, R.L. Arudi, A. Ross, 1985, Reactivity of HO_2/O_2 -radicals in aqueous solutions. *J. Phys. Chem. Ref. Data*, 14, 1041-1100.
- [178] W.Z. Tang, 2004, *Physico-chemical Treatment of Hazardous Wastes*. CRC Press, London.
- [179] H. Christensen, K. Sehested, H. Corfitzen, 1982, Reactions of hydroxyl radicals with hydrogen peroxide at ambient and elevated temperatures. *J. Phys. Chem.*, 86, 1588-1590.
- [180] M. Muruganandham, M. Swaminathan, 2004, Photochemical oxidation of reactive azo dye with UV- H_2O_2 process. *Dyes and Pigments*, 62 (3), 269-275.
- [181] M. Neamtu, I. Siminiceanu, A. Yediler, A. Kettrup, 2002, Kinetics of decolorization and mineralization of reactive azo dyes in aqueous solution by the UV/ H_2O_2 oxidation. *Dyes Pigments*, 53, 93-99.
- [182] R. Andreozzi, V. Caprio, A. Insola, R. Marotta, 1999, Advanced oxidation processes (AOP) for water purification and recovery. *Catal. Today*, 53, 51-59.
- [183] B. Langlais, D.A. Reckhow, D.R. Brink, 1991, *Ozone in Water Treatment: Application and Engineering*. CRC Press, London.
- [184] F.J. Beltrán, J.F.G. Araya, I. Giráldez, F.J. Masa, 2006, Kinetics of activated carbon promoted ozonation of succinic acid in water. *Ind. Eng. Chem. Res.*, 45, 3015-3021.
- [185] K. Yu, G.W.M. Lee, 2007, Decomposition of gas-phase toluene by the combination of ozone and photocatalytic oxidation process (TiO_2/UV , $\text{TiO}_2/\text{UV}/\text{O}_3$, and UV/O_3). *Appl. Catal. B: Environ.*, 75, 29-38.
- [186] Y. Shen, Y. Ku, 1999, Treatment of gas-phase volatile organic compounds (VOCs) by the UV/O_3 process. *Chemosphere*, 38, 1855-1866.
- [187] Y. Kua, W. Sua, Y. Shen, 1996, Decomposition of phenols in aqueous solution by a UV/O_3 process. *Ozone: Science & Engineering: J. Int. Ozone Assoc.*, 18, 443-460.
- [188] H. Shu, M. Chang, 2005, Decolorization effects of six azo dyes by O_3 , UV/O_3 and $\text{UV}/\text{H}_2\text{O}_2$ processes. *Dyes Pigments* 63, 25-31.
- [189] M.R. Hoffmann, S.T. Martin, W. Choi, D.W. Bahneman, 1995, *Environmental*

Applications of Semiconductor Photocatalysis. Chem. Rev., 95, 69–96.

[190] K. Vinodgopal, S. Hotchandani, V. Kamat, 1993, Electrochemically assisted photocatalysis. TiO₂ particulate film electrodes for photocatalytic degradation of 4-chlorophenol. J. Phys. Chem., 97, 9040-9044.

[191] K. Vinodgopal, V. Kamat, 1996, Combine electrochemistry with photocatalysis. Chem. Tech., 26, 19-23.

[192] J.M. Kesselman, N.S. Lewis, M.R. Hoffmann, 1997, Photoelectrochemical degradation of 4-chlorocatechol at electrodes: comparison between sorption and photoreactivity. Environ. Sci. Technol., 31, 2298-2302.

[193] J.A. Byrne, B.R. Eggins, W. Byers, N.M.D. Brown, 1999, Photoelectrochemical cell for the combined photocatalytic oxidation organic pollutants and the recovery of metals from wastewaters. Appl. Catal. B: Environ., 20, L85-L89.

[194] T. An, X. Zhu, Y. Xiong, 2002, Feasibility study of photoelectrochemical degradation of methylene blue with three-dimensional electrode-photocatalytic reactor. Chemosphere, 46, 897-903.

[195] K. Vinodgopal, U. Stafford, K.A. Gray, P.V. Kamat, 1994, Electrochemically Assisted Photocatalysis. 2. The Role of Oxygen and Reaction Intermediates in the Degradation of 4-Chlorophenol on Immobilized TiO₂ Particulate Films. J. Phys. Chem., 98, 6797-6803.

[196] C. Lee, J. Yoon, 2004, Temperature dependence of hydroxyl radical formation in the $h\nu/\text{Fe}^{3+}/\text{H}_2\text{O}_2$ and $\text{Fe}^{3+}/\text{H}_2\text{O}_2$ systems. Chemosphere, 56, 923-924.

[197] R.F.P. Nogueira, A.G. Trovó, M.R.A. da Silva, R.D. Villa, M.C. de Oliveira, 2007, Fundamentos e aplicações ambientais dos processos Fenton e foto-Fenton. Quim. Nova. 30, 400-408.

[198] E.G. Garrido-Ramírez, B.K.G Theng, M.L. Mora, 2010, Clays and oxide minerals as catalysts and nanocatalysts in Fenton-like reactions-A review. Appl. Clay Sci., 47, 182-192.

[199] J.D. Laats, H. Gallard, 1999, Catalytic Decomposition of Hydrogen Peroxide by Fe(III) in Homogeneous Aqueous Solution: Mechanism and Kinetic Modeling. Environ. Sci. Technol., 33 (16), 2726-2732.

[200] E. Neyens, J. Baeyens, 2003, A review of classic Fenton's peroxidation as an advanced oxidation technique, J. Hazard. Mater., B98, 33-50.

- [201] K. Wu, Y. Xie, J. Zhao, H. Hidaka, 1999, Photo-Fenton degradation of a dye under visible light irradiation. *J. Mol. Catal. A: Chemical*, 144, 77-84.
- [202] E. Neyens, J. Baeyens, 2003, A review of classic Fenton's peroxidation as an advanced oxidation technique. *J. Hazard. Mater.*, 98, 33-50.
- [203] H.J.H. Fenton, 1894, Oxidation of tartaric acid in the presence of iron. *Chem. Soc. J. Lond.*, 65, 899-910.
- [204] C.P. Huang, C. Dong, Z. Tang, 1993, Advanced chemical oxidation: its present role and potential future in hazardous waste treatment, *Waste Manag.*, 13, 361-377.
- [205] J.J. Pignatello, 1992, Dark and photoassisted Fe^{3+} -catalyzed degradation of chlorophenoxy herbicides by hydrogen peroxide. *Environ. Sci. Technol.*, 26, 944-951.
- [206] S.M. Arnold, W.J. Hickey, R.F. Harris, 1995, Degradation of atrazine by Fenton's reagent: condition optimization and product quantification. *Environ. Sci. Technol.*, 29, 2083-2089.
- [207] B.D. Lee, M. Iso, M. Hosomo, 2001, Prediction of Fenton oxidation positions in polycyclic aromatic hydrocarbons by Frontier electron density. *Chemosphere*, 42, 431-435.
- [208] K.H. Chan, W. Chu, 2005, Model applications and mechanism study on the degradation of atrazine by Fenton's system. *J. Hazard. Mater.*, 118, 227-237.
- [209] A.L. Barros, T.M. Pizzolato, E. Carissimi, I.A.H. Schneider, 2006, Decolorizing dye wastewater from the agate industry with Fenton oxidation process. *Miner. Eng.*, 19, 87-90.
- [210] Y. Deng, J.D. Englehardt, 2006, Treatment of landfill leachate by the Fenton process. *Water Res.*, 40, 3683-3694.
- [211] Y. Deng, 2007, Physical and oxidative removal of organics during Fenton treatment of mature municipal landfill leachate. *J. Hazard. Mater.*, 146, 334-340.
- [212] Y. Li, Y. Lu, X. Zhu, 2006, Photo-Fenton discoloration of the azo dye X-3B over pillared bentonites containing iron. *J. Hazard. Mater.*, 132, 196-201.
- [213] L. Núñez, J.A. García-Hortal, F. Torrades, 2007, Study of kinetic parameters related to the decolourization and mineralization of reactive dyes from textile dyeing using Fenton and photo-Fenton processes. *Dyes Pigm.*, 75, 647-652.
- [214] I.S. Oliveira, L. Viana, C. Verona, F.V.L. Vargas, A.C.M. Nunes, M. Pires, 2007, Alkydic resin wastewaters treatment by Fenton and photo-Fenton processes. *J. Hazard.*

Mater., 146, 564-568.

[215] E.M. Siedlecka, A. Wieckowska, P. Stepnowski, 2007, Influence of inorganic ions on MTBE degradation by Fenton's reagent. *J. Hazard. Mater.*, 147, 497-502.

[216] E. Ferrarese, G. Andreottola, I.A. Oprea, 2008, Remediation of PAH-contaminated sediments by chemical oxidation. *J. Hazard. Mater.*, 152, 128-139.

[217] R.G. Zepp, B.C. Faust, J. Hoigne, 1992, Hydroxyl radical formation in aqueous reactions (pH 3-8) of iron(II) with hydrogen peroxide: the photo-Fenton reaction. *Environ. Sci. Technol.*, 26, 313-319.

[218] R. Bauer, H. Fallmann, 1997, The Photo-Fenton Oxidation - A cheap and efficient wastewater treatment method. *Res. Chem. Intermediat.*, 23, 341-354.

[219] S.J. Hug, L. Canonica, M. Wegelin, 2001, Solar Oxidation and Removal of Arsenic at Circumneutral pH in Iron Containing Waters. *Environ. Sci. Technol.*, 35, 2114-2121.

[220] H. Katsumata, S. Kaneco, T. Suzuki, K. Ohta, Y. Yobiko, 2006, Photo-Fenton degradation of alachlor in the presence of citrate solution. *J. Photochem. Photobiol. A*, 180, 38-45.

[221] M.R.A. Silva, A.G. Trovó, R.F.P. Nogueira, 2007, Degradation of the herbicide tebuthiuron using solar photo-Fenton process and ferric citrate complex at circumneutral pH. *J. Photochem. Photobiol. A*, 191, 187-192.

[222] Y. Sun, J.J. Pignatello, 1992, Chemical Treatment of Pesticide Wastes. Evaluation of Fe(III) Chelates for Catalytic Hydrogen Peroxide Oxidation of 2,4-D at Circumneutral pH. *J. Agric. Food Chem.*, 40, 322-327.

[223] C. Fan, L. Tsui, M. Liao, 2011, Parathion degradation and its intermediate formation by Fenton process in neutral environment. *Chemosphere*, 82, 229-236.

[224] G.M.S. ElShafei, F.Z. Yehia, O.I.H. Dimitry, A.M. Badawi, G. Eshaq, 2010, Degradation of nitrobenzene at near neutral pH using Fe^{2+} -glutamate complex as a homogeneous Fenton catalyst. *Appl. Catal. B: Environ.*, 99, 242-247.

[225] Y. Lee, W. Lee, 2010, Degradation of trichloroethylene by Fe(II) chelated with cross-linked chitosan in a modified Fenton reaction. *J. Hazard. Mater.*, 178, 187-193.

[226] C. Lee, D.L. Sedlak, 2009, A novel homogeneous Fenton-like system with Fe(III)-phosphotungstate for oxidation of organic compounds at neutral pH values. *J. Mol. Catal.*,

311, 1-6.

- [227] E. Lipczynska-Kochany, J. Kochany, 2008, Effect of humic substances on the Fenton treatment of wastewater at acidic and neutral pH. *Chemosphere*, 73, 745-750.
- [228] S. Caudo, G. Centi, C. Genovese, S. Perathoner, 2007, Copper- and iron-pillared clay catalysts for the WHPCO of model and real wastewater streams from olive oil milling production. *Appl. Catal. B: Environ.* 70, 437-446.
- [229] M. Cheng, W. Song, W. Ma, C. Chen, J. Zhao, J. Lin, H. Zhu, 2008, Catalytic activity of iron species in layered clays for photodegradation of organic dyes under visible irradiation. *Appl. Catal. B: Environ.*, 77, 355-363.
- [230] J. He, W.H. Ma, J.J. He, J.C. Zhao, J.C. Yu, 2002, Photooxidation of azo dye in aqueous dispersions of $\text{H}_2\text{O}_2/\alpha\text{-FeOOH}$. *Appl. Catal. B: Environ.*, 39, 211-220.
- [231] S. Lin, M.D. Gurol, 1998, Catalytic Decomposition of Hydrogen Peroxide on Iron Oxide: Kinetics, Mechanism, and Implications. *Environ. Sci. Technol.*, 32, 1417-1423.
- [232] C.M. Flynn, 1984, Hydrolysis of inorganic iron (III) salts. *Chem. Rev.*, 84, 31-41.
- [233] Y. Dong, H. Fujii, M.P. Hendrich, R.A. Leising, G. Pan, C.R. Randall, E.C. Wilkinson, Y. Zang, L. Que, 1995, A High-Valent Nonheme Iron Intermediate. Structure and Properties of $[\text{Fe}_2(\mu\text{-O})_2(5\text{-Me-TPA})_2](\text{ClO}_4)_3$. *J. Am. Chem. Soc.*, 117, 2778-2792.
- [234] S. Rahhal, H.W. Richter, 1988, Reduction of hydrogen peroxide by the ferrous iron chelate of diethylenetriamine- N,N,N',N'',N'' -pentaacetate. *J. Am. Chem. Soc.*, 110, 3126-3133.
- [235] B. Meunier, 1992, Metalloporphyrins as versatile catalysts for oxidation reactions and oxidative DNA cleavage. *Chem. Rev.*, 92, 1411-1456.
- [236] P. Baldrian, V. Merhautová, J. Gabriel, F. Nerud, P. Stopka, M. Hrubý, M.J. Benes, 2006, Decolorization of synthetic dyes by hydrogen peroxide with heterogeneous catalysis by mixed iron oxides. *Appl. Catal. B: Environ.*, 66, 258-264.
- [237] K. Hanna, T. Kone, G. Medjahdi, 2008, Synthesis of the mixed oxides of iron and quartz and their catalytic activities for the Fenton-like oxidation. *Catal. Commun.*, 9, 955-959.
- [238] M.J. Liou, M.C. Lu, 2008, Catalytic degradation of explosives with goethite and hydrogen peroxide. *J. Hazard. Mater.*, 151, 540-546.

- [239] R. Matta, K. Hanna, S. Chiron, 2007, Fenton-like oxidation of 2, 4, 6-trinitrotoluene using different iron minerals. *Sci. Total Environ.*, 385, 242-251.
- [240] H.H. Huang, M.C. Lu, J.N. Chen, 2001, Catalytic decomposition of hydrogen peroxide and 2-chlorophenol with iron oxides. *Water Res.*, 35, 2291-2299.
- [241] M.C. Lu, J.N. Chen, H.H. Huang, 2002, Role of goethite dissolution in the oxidation of 2-chlorophenol with hydrogen peroxide. *Chemosphere*, 46, 131-136.
- [242] S. Chou, C. Huang, 1999, Application of a supported iron oxyhydroxide catalyst in oxidation of benzoic acid by hydrogen peroxide. *Chemosphere*, 38, 2719-2731.
- [243] R. Andreozzi, V. Caprio, R. Marotta, 2002, Oxidation of 3, 4-dihydroxybenzoic acid by means of hydrogen peroxide in aqueous goethite slurry. *Water Res.*, 36, 2761-2768.
- [244] S.H. Kong, R.J. Watts, J.H. Choi, 1998, Treatment of petroleum-contaminated soils using iron mineral catalyzed hydrogen peroxide. *Chemosphere* 37, 1473-1482.
- [245] C.K.J. Yeh, C.Y. Hsu, C.H. Chiu, K.L. Huang, 2008, Reaction efficiencies and rate constants for the goethite-catalyzed Fenton-like reaction of NAPL-form aromatic hydrocarbons and chloroethylenes. *J. Hazard. Mater.*, 151, 562-569.
- [246] J.C. Barreiro, M.D. Capelato, L. Martin-Neto, H.C.B. Hansen, 2007, Oxidative decomposition of atrazine by a Fenton-like reaction in a H_2O_2 /ferrihydrite system. *Water Res.*, 41, 55-62.
- [247] R. Andreozzi, A. D'Apuzzo, R. Marotta, 2002, Oxidation of aromatic substrates in water/goethite slurry by means of hydrogen peroxide. *Water Res.*, 36, 4691-4698.
- [248] J.J. Wu, M. Muruganandham, J.S. Yang, S.S. Lin, 2006, Oxidation of DMSO on goethite catalyst in the presence of H_2O_2 at neutral pH. *Catal. Commun.*, 7, 901-906.
- [249] F. Martínez, G. Calleja, J.A. Melero, R. Molina, 2007, Iron species incorporated over different silica supports for the heterogeneous photo-Fenton oxidation of phenol. *Appl. Catal. B: Environ.*, 70, 452-460.
- [250] J. He, X. Tao, W. Ma, J. Zhao, 2002, Heterogeneous Photo-Fenton Degradation of an Azo Dye in Aqueous H_2O_2 /Iron Oxide Dispersions at Neutral pHs. *Chem. Lett.*, 31, 86-87.
- [251] J. Feng, X. Hu, P. Yue, 2003, Degradation of Azo-dye Orange II by a Photoassisted Fenton Reaction Using a Novel Composite of Iron Oxide and Silicate Nanoparticles as a Catalyst. *Ind. Eng. Chem. Res.*, 42, 2058-2066.

- [252] C. Hsueha, Y. Huanga, C. Wangb, C. Chen, 2006, Photoassisted fenton degradation of nonbiodegradable azo-dye (Reactive Black 5) over a novel supported iron oxide catalyst at neutral pH. *J. Mol. Cat. A: Chemical*, 245, 78-86.
- [253] Y. Zhao, J. Hu, 2008, Photo-Fenton degradation of 17 β -estradiol in presence of α -FeOOHR and H₂O₂. *Appl. Catal. B: Environ.*, 78, 250-258.
- [254] S. Shin, H. Yoon, J. Jang, 2008, Polymer-encapsulated iron oxide nanoparticles as highly efficient Fenton catalysts. *Catal. Comm.*, 10, 178-182.
- [255] A. Cuzzola, M. Bernini, P. Salvadori, 2002, A preliminary study on iron species as heterogeneous catalysts for the degradation of linear alkylbenzene sulphonic acids by H₂O₂. *Appl. Catal. B: Environ*, 36, 231-237.
- [256] C.L. Hsueh, Y.H. Huang, C.Y. Chen, 2006, Novel activated alumina-supported iron oxide-composite as a heterogeneous catalyst for photooxidative degradation of reactive black 5. *J. Hazard. Mater.*, 129, 228-233.
- [257] M. I. Pariente, F. Martinez, J.A. Melero, J.A. Botas, T. Velegraki, N.P. Xekoukoulotakis, D. Mantzavinos, 2008, Heterogeneous photo-Fenton oxidation of benzoic acid in water: Effect of operating conditions, reaction by-products and coupling with biological treatment. *Appl. Catal. B: Environ.*, 85, 24-32.
- [258] R. Kavlock, 1999, Overview of endocrine disruptor research activity in the United States. *Chemosphere*, 39, 1227-1236.
- [259] T. Colborn, D. Dumanoski, J.P. Myers, 1996, *Our Stolen Future*. Plume/Penguin Book: New York.
- [260] United States Environmental Protection Agency (USEPA). 1997, Special report on environmental endocrine disruption: an effects assessment and analysis. Washington, DC: Office of Research and Development, EPA/630/R-96/012, 6.
- [261] W. Kelce, C. Stone, S. Laws, L. Gray, J. Kemppainen, E. Wilson, 1995, Persistent DDT metabolite p,p'-DDE is a potent androgen receptor antagonist. *Nature*, 375, 581-585.
- [262] H. Bertold, S. Martin, 1999, Detecting estrogens in food and the environment. *Nature Biotechnol.*, 17, 1162-1163.
- [263] S. Lorenz, 2003, Toxicology-E.U. Shifts Endocrine Disrupter Research into Overdrive. *Science*, 300, 1069-1069.

- [264] K. Jocelyn, 2007, Endocrine disruptors: Controversy Continues after Panel Rules on Bisphenol A. *Science*, 317, 884-885.
- [265] T.H. Hutchinson, R. Brown, K.E. Brugger, P.M. Campbell, M. Holt, R. Lange, P. McCahon, L.J. Tattersfield, 2000, Egmond R.V. Ecological risk assessment of endocrine disruptors. *Environ. Health Persp.*, 108, 1007-1014.
- [266] Z.Q. Zeng, T. Shan, Y. Tong, S.H. Lam, Z.Y. Gong, 2005, Development of Estrogen-Responsive Transgenic Medaka for Environmental Monitoring of Endocrine Disruptors. *Environ. Sci. Technol.*, 39, 9001-9008.
- [267] J.P. Giesy, K. Hilscherova, P.D. Jones, K. Kannan, M. Machala, 2002, Cell bioassays for detections of aryl hydrocarbon (AhR) and estrogen receptor (ER) mediated activity in environmental samples. *Mar. Pollut. Bull.*, 45, 3-16.
- [268] J. Bourguignon, et al, 2009, Environmental Endocrine-Disrupting Chemicals (EDCs). The Hormone Foundation.
- [269] L. Ze-hua, K. Yoshinori, M. Satoshi, 2009, Removal mechanisms for endocrine disrupting compounds (EDCs) in wastewater treatment-physical means, biodegradation, and chemical advanced oxidation: A review. *Sci. Total Environ.*, 407, 731-748.
- [270] <http://en.wikipedia.org/wiki/Bisphenol>
- [271] T. Zincke, 1905, Mittheilungen aus dem chemischen Laboratorium der Universitat Marburg. *Justus Liebigs Annals Chemie*, 343, 75-99.
- [272] <http://www.bisphenol-a.org/about/bpa-info/bpa-synthesis.html>
- [273] C.A. Staples, P.B. Dom, G.M. Klecka, S.T. O'Block, L.R. Harris, 1998, A review of the environmental fate, effects, and exposures of bisphenol A. *Chemosphere*, 36, 2149-2173.
- [274] G. Matsumoto, R. Isbiwatari, T. Hayna. 1977, Gas Chromatographic-Mass Spectrometric Identification of Phenols and Aromatic Acids in River Waters. *Water Res.*, 11, 693-698.
- [275] H. Fromme, T. Küchler, T. Otto, K. Pilz, J. Müller, A. Wenzel, 2002, Occurrence of phthalates and bisphenol A and F in the environment. *Water Res.*, 36 (6), 1429-1438.
- [276] T. Yamamoto, A. Yasuhara, 1999, Quantities of bisphenol a leached from plastic waste samples. *Chemosphere*, 38 (11), 2569-2576.

- [277] T. Kamiura, Y. Tajima, T. Nakahara, 1997, Determination of bisphenol A in air, J. Environ. Chem, 7, 275-279 (In Japanese).
- [278] D. Bing, Z. Peng-yi, Z. Zu-ling, Y. Gang, 2004, Preliminary Investigation on Endocrine Disrupting Chemicals in a Sewage Treatment Plant of Beijing. Environ. Sci., 25, 114-116.
- [279] H. C. Alexander, D. C. Dill, L. W. Smith, P. D. Guiney, P. B. Dorn, 1988, Bisphenol A: Acute Aquatic Toxicity. Environ. Toxicol. Chem., 7, 19-26.
- [280] P. Sohoni, C. R. Tyler, K. Hurd, J. Caunter, M. Hethridge, T. Williams, C. Woods, M. Evans, R. Toy, M. Gargas, J. P. Sumpter, 2001, Reproductive effects of long-term exposure to bisphenol A in the fathead minnow (*Pimephales promelas*). Environ. Sci. Technol., 35, 2917-2925.
- [281] J. E. Caunter, 2000, Bisphenol A: Multigeneration Study with Fathead Minnow (*Pimephales promelas*), Brixham, Devon, UK: Brixham Environmental Laboratory, Zeneca, Ltd.. Report No. BL6878/B.91.
- [282] J.A. Brotons, M.F. Olea-Serrano, M. Villalobos, V. Pedraza, N. Olea, 1995, Xenoestrogens released from lacquer coatings in food cans, Environ. Health Perspect., 103, 608-612.
- [283] J. Ashby, R.W. Tennant, 1988, Chemical structure, Salmonella mutagenicity and extent of carcinogenicity as indicators of genotoxic carcinogenesis among 222 chemicals tested in rodents by the U.S. NCI/NTP, Mutat. Res. Genet. Tox., 204, 17-115.
- [284] S. Suarez, R. Sueiro, J. Garrido, 2000, Genotoxicity of the coating lacquer on food cans, bisphenol A diglycidyl ether (BADGE), its hydrolysis products and a chlorohydrin of BADGE, Mutat. Res. Genet. Tox. En., 470, 221-228.
- [285] T. Tanaka, K. Yamada, T. Tonosaki, T. Konishi, H. Goto, M. Taniguchi, 2000, Enzymatic degradation of alkylphenols, Bisphenol A, synthetic estrogen, and phthalic ester. Water Sci. Technol., 42, 89-95.
- [286] F.B. Li, X.Z. Li, C.S. Liu, X.M. Li, T.X. Liu, 2007, Effect of oxalate on photodegradation of Bisphenol A at the interface of different iron oxides, Ind. Eng. Chem. Res., 46, 781-787.
- [287] F.B. Li, X.Z. Li, C.S. Liu, T.X. Liu, 2007, Effect of alumina on photocatalytic activity

- of iron oxides for bisphenol A degradation, *J. Hazard. Mater.*, 149, 199-207.
- [288] R.A. Torres, G. Sarantakos, E. Combet, C. Petrier, C. Pulgarin, 2008, Sequential helio-photo-Fenton and sonication processes for the treatment of bisphenol A, *J. Photochem. Photobiol., A*, 199, 197-203.
- [289] I. Ioan, S. Wilson, E. Lundanes, 2007, A. Neculai, Comparison of Fenton and sono-Fenton bisphenol A degradation, *J. Hazard. Mater.*, 142, 559-563.
- [290] H. Katsumata, S. Kawabe, S. Kaneco, T. Suzuki, K. Ohta, 2004, Degradation of bisphenol A in water by the photo-Fenton reaction. *J. Photochem. Photobiol., A*, 162, 297-305.
- [291] G. Wang, F. Wu, X. Zhang, M. Luo, N. Deng, 2006, Enhanced TiO_2 photocatalytic degradation of bisphenol A by β -cyclodextrin in suspended solutions, *J. Photochem. Photobiol., A*, 179, 49-56.
- [292] I. Gultekin, N.H. Ince, 2007, Synthetic endocrine disruptors in the environment and water remediation by advanced oxidation processes, *J. Environ. Manage.*, 85, 816-832.
- [293] U. Schwertmann, R.M. Cornell, 2000, *Iron Oxides in the Laboratory: Preparation and Characterization*. Wiley-VCH, New York.
- [294] D. Dulin, T. Mill, 1982, Development and evaluation of sunlight actinometers. *Environ. Sci. Technol.*, 16, 815-820.
- [295] G.A. Parks, P.L. de Bruyn, 1962, The zero point of charge of oxides. *J. Phys. Chem.*, 66, 967-973.
- [296] L.L. Stookey, 1970, Ferrozine: a new spectrophotometric reagent for iron. *Anal. Chem.*, 42, 779-781.
- [297] E. Viollier, P.W. Inglett, K. Hunter, A.N. Roychoudhury, P. Van Cappellen, 2000, The ferrozine method revisited: Fe(II)/Fe(III) determination in natural waters. *Appl. Geochem.*, 15, 785-790.
- [298] A. L. Lamus, G. L. Kok, S. N. Gitlin, J. A. Lind, 1985, Automated Fluorometric Method for Hydrogen Peroxide in Atmospheric Precipitation. *Anal. Chem.*, 57, 917-922.
- [299] G. G. Guilbault, P. J. Brignac, M. Juneau, 1968, Substrates for the fluorometric determination of oxidative enzymes. *Anal. Chem.*, 40, 1256-1263.
- [300] G. L. Kok, K. Thompson, A. L. Lazrus, S. E. McLaren, 1986, Derivatization

Technique for the Determination of Peroxides in Precipitation. *Anal. Chem.*, 58, 1192-1194.

[301] L. Carlos, D. Fabbri, A.L. Capparelli, A.B. Prevot, E. Pramauro, F.S.G. Einschlag, 2008, Intermediate distributions and primary yields of phenolic products in nitrobenzene degradation by Fenton's reagent, *Chemosphere*, 72, 952-958.

[302] G.V. Buxton, C.L. Greenstock, W.P. Helman, A.B. Ross, 1998, Critical review of rate constants for reactions of hydrated electrons, hydrogen atoms and hydroxyl radicals ($\bullet\text{OH}/\bullet\text{O}^-$) in aqueous solution, *J. Phys. Chem. Ref. Data*, 17, 513-886.

[303] D.O. Martire, P. Caregnato, J. Furlong, P. Allegreti, M.C. Gonzalez, 2002, Kinetic study of the reactions of oxoiron(IV) with aromatic substrates in aqueous solutions. *Int. J. Chem. Kinet.*, 34, 488-494.

[304] X. Fang, G. Mark, C. von Sonntag, 1996, OH radical formation by ultrasound in aqueous solutions. Part I. The chemistry underlying the terephthalate dosimeter, *Ultrason. Sonochem.* 3, 57-63.

[305] J.C. Barreto, G.S. Smith, N.H.P. Strobel, P.A. McQuillan, T.A. Miller, 1995, Terephthalic acid: A dosimeter for the detection of hydroxyl radicals in vitro, *Life Sci.*, 56, 89-96.

[306] K.R. Millington, L.J. Kirschenbaum, 2002, Detection of hydroxyl radicals in photoirradiated wool, cotton, nylon and polyester fabrics using a fluorescent probe, *Color. Technol.*, 118, 6-14.

[307] C. Luo, Z. Shen, X. Li, 2005, Enhanced phytoextraction of Cu, Pb, Zn and Cd with EDTA and EDDS. *Chemosphere*, 59, 1-11.

[308] K. Hanna, C. Carteret, 2007, Sorption of 1-hydroxy-2-naphthoic acid to goethite, lepidocrocite and ferrihydrite: Batch experiments and infrared study. *Chemosphere*, 70, 178-186.

[309] X. Xue, K. Hanna, C. Despas, F. Wu, N. Deng, 2009, Effect of chelating agent on the oxidation rate of PCP in the magnetite/ H_2O_2 system at neutral pH. *J. Mol. Catal. A: Chem.*, 311, 29-35.

[310] R.A. Torres, C. Pétrier, E. Combet, F. Moulet, C. Pulgarin, 2006, Bisphenol A mineralization by integrated ultrasound-UV-iron (II) treatment. *Environ. Sci. Technol.*, 41, 297-302.

- [311] G.G. Jayson, B.J. Parsons, A.J. Swallow, 1973, Oxidation of ferrous ions by perhydroxyl radicals. *J. Chem. Soc. Faraday Trans.*, 169, 236-242.
- [312] J.D. Rush, B.H.J. Bielski, 1985, Pulse radiolytic studies of the reactions of HO_2/O_2^- with Fe(II)/Fe(III) ions. The reactivity of HO_2/O_2^- with ferric ions and its implication on the occurrence of the Haber-Weiss reaction. *J. Phys. Chem.*, 89, 5062-5066.
- [313] W.G. Rothschild, A.O. Allen, 1958, Studies in the radiolysis of ferrous sulfate solutions. III. Air-free solutions at higher pH. *Radiat. Res.*, 8, 101-110.
- [314] H. Gallard, J. De Laat, B. Legube, 1999, Spectrophotometric study of the formation of iron (III)-hydroperoxy complexes in homogeneous aqueous solutions. *Water Res.*, 33, 2929-2936.
- [315] B. Thamdrup, 2000, Bacterial manganese and iron reduction in aquatic sediments, in: *Advances in Microbial Ecology* vol 16, Kluwer Academic/Plenum Publishers, New York, 41-84.
- [316] X.Xu, N.R. Thomson, 2007, An evaluation of the greenchelantEDDS to enhance the stability of hydrogenperoxide in the presence of aquifersolids. *Chemosphere*, 69, 755-762.
- [317] B. Prélôt, et al, 2003, Morphology and surface heterogeneities in synthetic goethites. *Colloid Interf. Sci.*, 261, 244-254.
- [318] F. Haber, J. Weiss, 1934, The catalytic decomposition of hydrogen peroxide by iron salts. *Proc. R. Soc. London, A* 147, 332-351.
- [319] J. L. Pierre, M. Fontecave, 1999, Iron and activated oxygen species in biology: The basic chemistry. *BioMetals*, 12, 195-199.
- [320] J. M. Gutteridge, L. Maitt, L. Poyer, 1990, Superoxide dismutase and Fenton chemistry. Reaction of ferric-EDTA complex and ferric-bipyridyl complex with hydrogen peroxide without the apparent formation of iron(II). *Biochem. J.*, 269, 169-174.
- [321] B. G. Kwon, E. Kim, J. H. Lee, 2009, Pentachlorophenol decomposition by electron beam process enhanced in the presence of Fe(III)-EDTA . *Chemosphere*, 74, 1335-1339.
- [322] N. Watanabe, S. Horikoshi, H. Kawaba, Y. Sugis, J. Zhao, H. Hidaka, 2003, Photodegradation mechanism for bisphenol A at the $\text{TiO}_2/\text{H}_2\text{O}$ interfaces. *Chemosphere*, 52, 851-859.
- [323] C. Catrinescu, C. Teodosiu, M. Macoveanu, J. Mieke-Brendle, R. Le Dred, 2003,

Catalytic wet peroxide oxidation of phenol over Fe-exchanged pillared beidellite. *Water Res.* 37, 1154-1160.

[324] S. Demirel, K. Lehnert, M. Lucas, P. Claus, 2007, Use of renewables for the production of chemicals: Glycerol oxidation over carbon supported gold catalysts. *Appl. Catal. B: Environ.*, 70, 637-643.

[325] D. Zhou, F. Wu, N. Deng, W. Xiang, 2004, Photooxidation of bisphenolA (BPA) in water in the presence of ferric and carboxylatesalts. *Water Res.*, 38, 4107-4116.

[326] A. Sorokin, L. Fraisse, A. Rabion, B. Meunier, 1997, Metallophthalocyanine-catalyzed oxidation of catechols by H_2O_2 and its surrogates. *J. Mol. Catal. A: Chem.*, 117, 103–114

Papers Published

1. **Huang Wenyu**, Wang Beibei, Guo Li, Wu Feng, Deng Nansheng. Photochemical Processes and the Related Advanced Oxidation Technology: a Minireview. Fresen. Environ. Bull. 2009, 18(12): 2259-2267. (SCI)
2. **Wenyu Huang**, Marcello Brigante, Feng Wu, Khalil Hanna, Gilles Mailhot. Development of a new homogenous Photo-Fenton process using Fe(III)-EDDS complexes, Journal of Photochemistry and Photobiology A: Chemistry, 2012. (SCI) (Accepted)
3. **Wenyu Huang**, Marcello Brigante, Feng Wu, Khalil Hanna, Gilles Mailhot. Homogeneous fenton and photofenton processes: impact of iron complexing agent on the reactive species formation. 12th European Meeting on Environmental Chemistry, 2011, France: Clermont-Ferrand, P52.
4. Gilles Mailhot, **Wenyu Huang**, Marcello Brigante, Feng Wu, Khalil Hanna. Development of New Fenton and Photo-Fenton Processes Using Fe(III)-EDDS Complex. 7th European Meeting on Solar Chemistry and Photocatalysis - Environmental Applications, 2012, Portugal: Oporto. (Accepted)
5. **Wenyu Huang**, Marcello Brigante, Feng Wu, Khalil Hanna, Gilles Mailhot. Effect of Ethylenediamine-N,N'-disuccinic acid on heterogeneous Fenton and photo-Fenton processes: optimization of parameters for Bisphenol A degradation. Environmental Science and Pollution Research (SCI) (under review)
6. Danna Zhou, **Wenyu Huang**, Feng Wu, Chaoqun Han, Yin Chen. Photodegradation of chloromycetin in aqueous solutions: kinetics and influencing factors. Reaction Kinetics, Mechanisms and Catalysis. 2010, 100(1): 45-53. (SCI)
7. Cong Ren, Hong Peng, **Wenyu Huang**, Yajie Wang, Feng Wu. Speciation of inorganic As(V)/As(III) in water and soils by hydride generation-atomic fluorescence spectrometry. Fresen. Environ. Bull. 20(4a): 2011. (SCI)
8. Guo Li, Wang Beibei, **Huang Wenyu**, Wu Feng, Huang Jin. Photocatalytic degradation of diphenolic acid in the Presence of beta-Cyclodextrin under UV Light. 2009 International Conference on Environmental Science and Information Application Technology (2009 EI)
9. Guo Li, Wang Beibei, **Huang Wenyu**, Wu Feng, Yiming Li. Adsorption and photodecomposition of diphenolic acid in alpha- or beta-cyclodextrins and TiO₂ suspensions. 2009 Symposium on Photonics and Optoelectronics (SOPO 2009) (2009EI)

Titre français :

Procédés de Fenton et photo-Fenton homogène et hétérogène : Impact d'un agent complexant du fer, l'acide éthylènediamine-N,N'-disuccinique (EDDS).

Résumé français:

Dans cette étude nous avons utilisé le bisphénol A (BPA) comme polluant modèle pour analyser l'efficacité des différents processus de Fenton et photo-Fenton mis en place. Dans un premier temps nous avons étudié le processus de Fenton en présence du complexe Fe(III)-EDDS utilisé comme source de fer. Différents paramètres physico-chimiques (concentrations en H_2O_2 , Fe(III)-EDDS, O_2 et le pH) ont été testés afin d'optimiser l'efficacité du système en termes de dégradation du BPA. Parallèlement, le même type d'étude a été menée en présence de lumière (de 300 à 450 nm) afin d'étudier le processus de photo-Fenton. Dans les 2 cas nous avons mis en évidence un effet du pH peu commun puisque la dégradation de BPA est plus rapide et importante plus le pH est élevé dans une gamme allant de 3,0 à 9,0. Dans le but de comprendre le mécanisme mis en jeu des expériences d'inhibition de radicaux ($\bullet OH$ et $HO_2\bullet/O_2\bullet^-$) ont été réalisées. Une des conclusions importantes de ce travail est que dans les deux systèmes le complexe Fe(III)-EDDS joue un rôle très positif pour la dégradation du BPA. De plus, nous avons également montré que ces processus étaient très efficaces pour des pH proche de la neutralité et faiblement basiques. La comparaison avec d'autres complexant du fer (EDTA, citrate, oxalate) montre qu'en présence du complexe Fe(III)-EDDS nous obtenons l'efficacité la plus importante. Ce résultat et le fait que les processus soient très efficaces à pH neutre ou faiblement basiques montrent que le complexe Fe(III)-EDDS est vraiment une source de fer très prometteuse dans les processus de Fenton et photo-Fenton. Dans une troisième partie nous avons regardé l'effet d'EDDS dans un système hétérogène en présence de Goethite comme source de fer. Dans ce chapitre il a été mis en évidence que l'EDDS inhibe le processus de Fenton, EDDS s'adsorbe fortement à la surface et limite la réactivité de H_2O_2 avec la surface de la Goethite. Par contre dans le processus de photo-Fenton, EDDS augmente l'efficacité de dégradation du BPA à pH proche de la neutralité et à faible concentration en H_2O_2 .

Mots clés :

Traitement des eaux ; Fenton ; Photo-Fenton ; EDDS ; BPA ; Goethite ; Photodégradation, radicaux.

Titre anglais:

Homogeneous and heterogeneous Fenton and photo-Fenton processes: Impact of iron complexing agent Ethylenediamine-N,N'-disuccinic acid (EDDS)

Résumé anglais:

In this study we used the bisphenol A (BPA) as a model pollutant to analyse the efficiency of the Fenton and photo-Fenton processes. In the first part of the thesis, we studied the Fenton process in the presence of the complex Fe(III)-EDDS used as iron source. Different physico-chemical parameters (concentrations of H_2O_2 , Fe(III)-EDDS, O_2 and pH) were tested with the goal to optimized the efficiency of the system in terms of BPA degradation. In the same time, the same kind of experiments were performed in the presence of light (emission from 300 to 450 nm) to study the photo-Fenton process. In the two cases (Fenton and photo-Fenton), we observed a strong and not usual pH effect. Indeed, the degradation of BPA is faster and more important when the pH is higher in the range between 3.0 and 9.0. To understand the mechanisms involved in such processes, some inhibition experiments of radicals ($\bullet OH$ and

$\text{HO}_2^\bullet/\text{O}_2^{\bullet-}$) were performed. One of the most important conclusion of this research work is that the Fe(III)-EDDS complex plays a very positive role for the degradation of BPA. Moreover, in the presence of Fe(III)-EDDS the Fenton and photo-Fenton processes are very efficient in neutral and slightly basic pH. The comparison with other iron complexes (EDTA, citrate, oxalate) shows that in the presence of Fe(III)-EDDS complex we obtained the better efficiency for the degradation of BPA. This result and the fact that Fe(III)-EDDS is efficient until pH 9.0 show that Fe(III)-EDDS complex is really a promising iron source for the Fenton and photo-Fenton processes. In a third part, we studied the effect of EDDS in a heterogeneous system in the presence of Goethite as an iron source. In this chapter, we demonstrated that the presence of EDDS is detrimental for the Fenton process and leads to an inhibition of the process. In fact, EDDS is strongly adsorbed at the surface of the Goethite and avoid the reactivity of H_2O_2 at the Goethite surface. On the contrary, in the photo-Fenton process EDDS increases the efficiency of the BPA degradatoion for pHs near 7.0 and at low H_2O_2 concentrations.

Key words:

Water treatment; Fenton; Photo-Fenton; EDDS; BPA; Goethite; Photodegradation, radical species.